South Puget Sound Water Quality Study

Phase 1

October 2002

Publication No. 02-03-021
printed on recycled paper

Publication Information

This report is available on the Department of Ecology home page on the World Wide Web at http://www.ecy.wa.gov/biblio/0203021.html

For a printed copy of this report, contact:

Department of Ecology Publications Distributions Office
Address: PO Box 47600, Olympia WA 98504-7600
E-mail: ecypub@ecy.wa.gov
Phone: (360) 407-7472

Ask for publication number 02-03-021.

.

South Puget Sound Water Quality Study

Phase 1

by
Storrs "Skip" L. Albertson, Karol Erickson, Jan A. Newton, Greg Pelletier, Rick A. Reynolds, and Mindy Roberts

Environmental Assessment Program
Olympia, Washington 98504-7710

October 2002

Waterbody Numbers
WA-13-0010, WA-13-0020, WA-13-0030
WA-14-0010, WA-14-0020, WA-14-0050
WA-14-0100, WA-14-0110

Publication No. 02-03-021

printed on recycled paper

Table of Contents

Appendices

List of Figures

List of Figures (cont.)

List of Figures (cont.)

List of Tables

Abstract

Increasing development around South Puget Sound, defined as the basin south of The Narrows near Tacoma, may adversely affect marine water quality through elevated point and nonpoint source loading of nutrients. Although individual sources may not have a measurable influence, their combined impact could lead to significant water quality degradation, such as reduced dissolved oxygen concentrations, reduced water clarity, altered species composition, and formation of algal scums.

South Puget Sound's complex morphology contributes to slow flushing rates, which limits the ability of the basin to dilute and exchange with the Pacific Ocean. Several inlets have high productivity and low near-bottom dissolved oxygen. Many studies have concluded that South Sound is particularly susceptible to water quality problems. South Puget Sound marine waterbody segments have been identified as impaired through the federal Clean Water Act Section 303(d) list for dissolved oxygen, fecal coliform bacteria, and other variables.

The *South Puget Sound Water Quality Study* offers the opportunity to quantitatively assess existing and potential future water quality. It is divided into two phases:

- Phase 1, described in this report, includes analysis of historical data, data collection, experimental measurements, and initial development of coupled three-dimensional hydrodynamic and water quality models of South Puget Sound.
- Phase 2, as recommended herein, will refine the models and fill in gaps in understanding necessary to evaluate future conditions and recommend management strategies.

This Phase 1 study found that South Puget Sound is sensitive to nutrient addition, confirming the potential for serious water quality degradation due to increased nutrient loads. Both point and nonpoint sources contribute significantly. Modeled near-bottom dissolved oxygen is most sensitive to the sediment model constituents. Case, Carr, and Budd inlets appear to have the lowest dissolved oxygen levels observed within South Puget Sound, and may be the most sensitive to increased nutrient loads.

Acknowledgments

Funding for the South Puget Sound Nutrient Study was provided by the U.S. Environmental Protection Agency through the National Nutrient Strategy Program (October 1998) and the SWAT Program (July 1998), as well as the Washington State Department of Ecology Emerging Fund (July 1998).

The authors wish to express their gratitude to Ecology personnel who participated in the fieldwork, sample analyses, and data processing: Julia Bos, Kara Nakata, and John Summers. In addition, numerous volunteers from the Department of Ecology and the University of Washington (UW) donated time and effort to assist in sample collection. Captain Ray McQuinn of the *R/V Clifford Barnes* provided a safe and enjoyable sampling platform. Nutrient and salinity analyses were conducted by Katherine Krogslund at the UW School of Oceanography Marine Chemistry Laboratory.

Watershed flow and load estimates would not have been possible without the extensive data collection networks of the U.S. Geological Survey, Thurston County, Department of Ecology, and the Bremerton-Kitsap County Health District. The Budd Inlet study conducted by the Lacey, Olympia, Tumwater, Thurston County Partnership (LOTT) and its consultants was instrumental in developing fine-scale information in an area of critical interest.

The authors would like to thank Hal Mofjeld for his input on Puget Sound tides, as well as Jody Klymak and Ren-Chieh Lien of the UW Applied Physics Lab for their harmonic analysis program based on Foreman (1978).

Finally, the authors would like to thank John Yearsley of the U.S. Environmental Protection Agency for his comprehensive review of this report, as well as Pete Dowty of the Puget Sound Water Quality Action Team, Hal Mofjeld of Pacific Marine Environmental Laboratory, and Randy Shuman of the King County Department of Natural Resources for providing reviews of individual chapters.

Executive Summary

The Washington State Department of Ecology (Ecology) is concerned that increasing development around South Puget Sound, defined as the basin south of The Narrows near Tacoma (Figure ES-1), may adversely affect South Sound water quality through elevated point and nonpoint source loading of nutrients. Although individual sources may not have a measurable influence, their combined impact could lead to a significant degradation of water quality.

Eutrophication of a waterbody refers to the process in which elevated nutrient levels result in excessive primary production by the plant community, potentially leading to a number of deleterious consequences:

- Reduction in dissolved oxygen concentrations as increasing amounts of organic material are produced and decomposed within the water column.
- Reduction in water clarity, limiting the light available for subsurface organisms.
- Altered species composition, including a shift towards predominance of undesirable forms (e.g., toxic phytoplankton blooms or anaerobic bacteria), or disruptions in the normal food web.
- Formation of mats and surface scums, which may interfere with recreation, reduce light availability, or produce objectionable odors.

The sensitivity to, or cumulative effects of, increased nutrient loading in South Puget Sound urgently deserves further attention and quantitative assessment. Several attributes of South Puget Sound suggest that this region may be susceptible to the effects of eutrophication. Physical characteristics of the South Puget Sound basin, such as its distance from the Strait of Juan de Fuca (source of incoming Pacific Ocean water) and its complex morphology with a high number of blind-end inlets, contribute to long water residence times and slow flushing rates. This limits the ability of the basin to dilute and exchange inputs of nutrients and pollutants with the Pacific Ocean. Several inlets have high measured rates of primary production, and experiments have shown an enhancement in these rates with the addition of nutrients. Concomitantly, near-bottom dissolved oxygen (DO) concentrations have been observed to be low during the end of the growing season. Further increases in productivity, stimulated by nutrient addition, may further decrease dissolved oxygen concentrations in the water column to levels harmful to benthic and pelagic organisms.

Cultural eutrophication refers to eutrophication stimulated by anthropogenic nutrient inputs, both point and nonpoint sources. The extensive shorelines around the South Puget Sound inlets attract significant residential development, which has increased considerably in the last two decades. Development in Pierce, Mason, Thurston, and Kitsap counties is expected to continue at a rapid pace. Increased development contributes higher point and nonpoint source pollution loads, as higher populations produce more wastewater and development converts more undeveloped land to residential lawns.

Many studies have previously concluded that South Puget Sound is susceptible to water quality problems due to reduced circulation (Cokelet and Stewart, 1985; URS, 1985; URS, 1986a; WRE, 1975) and shows signs of nutrient sensitivity (Rensel and PTI, 1991; Harrison et al., 1994). Ecology's assessment of marine water quality throughout Washington State, as part of the Puget Sound Ambient Monitoring Program (PSAMP), showed similar results (Newton et al., 1997; Newton et al., 1998). Analysis of the long-term PSAMP monitoring data from 1990-1997 indicated that sensitivity to nutrient addition was particularly evident in the South Puget Sound area (Figure ES-2). This analysis, based on several water quality indicators (e.g., stratification, lack of surface nutrients in summer, and low DO), confirmed that physical and chemical attributes of this basin result in a higher sensitivity to impacts from eutrophication, relative to most of the other Puget Sound basins.

Washington State has developed water quality standards to protect the beneficial uses of both freshwater and marine waterbodies. South Puget Sound includes 17 marine segments; several segments presently do not meet water quality standards for such parameters as dissolved oxygen, fecal coliform bacteria, and various toxic substances, as shown in Table ES-1. Appendix A describes the changes in impaired waterbodies between the 1996 and 1998 303(d) lists as well as the reasons for changes in listing status. The sources of these impairments are believed to be nonpoint sources, natural sources, recreational activities, municipal point sources, and industrial point sources. Much of South Puget Sound, however, has not been studied sufficiently to determine all areas not meeting water quality standards.

Table ES-1. Impaired waterbodies from the 1996 and 1998 Section 303(d) lists.

Waterbody Segment Number	Waterbody Name	Parameters Exceeding Standards (1996)	Parameters Exceeding Standards (1998)
WA-13-0010	Henderson Inlet	Fecal Coliform	Fecal Coliform, Dissolved Oxygen
WA-13-0020	Budd Inlet (outer)	Fecal Coliform, Total Nitrogen, pH	Dissolved Oxygen, pH
WA-13-0030	Budd Inlet (inner)	Fecal Coliform, Dissolved Oxygen, Total Nitrogen, pH, and a number of toxic substances	Dissolved Oxygen, pH, and a number of toxic substances
WA-14-0010	Squaxin, Peale, and Pickering Passages	pH	Dissolved Oxygen, pH
WA-14-0020	Eld Inlet	Fecal Coliform	(not listed)
WA-14-0050	Shelton Harbor (inner)	Fecal Coliform	Fecal Coliform
WA-14-0100	Hammersley Inlet	Fecal Coliform	Fecal Coliform
WA-14-0110	Oakland Bay	Fecal Coliform, Dissolved Oxygen	Fecal Coliform

Section 303(d) of the federal Clean Water Act requires states to develop total maximum daily loads (TMDLs) for waterbodies not meeting designated uses under technology-based pollutant controls. The capacity of South Puget Sound to assimilate the pollutant loads has not been quantified. Given that the South Sound already experiences impaired water quality and that

development is expected to continue, cultural eutrophication may increase, contributing to further water quality degradation.

This *South Puget Sound Water Quality Study* offers the first opportunity to assess the existing water quality in further detail and to evaluate the cumulative impacts of the various point and nonpoint source loads on existing water quality. The primary goals of this study are to (1) assess the hydrodynamics and current water quality status of the South Puget Sound basin, and (2) develop computer models to simulate existing and future conditions in order to explore the links between loads and water quality at a finer resolution than is possible with the most extensive data collection programs.

Study objectives include the following:

- Identify areas within South Puget Sound where nutrients limit phytoplankton growth (e.g., areas susceptible to eutrophication and its impacts).
- Assess the flushing and nutrient cycling rates in South Puget Sound inlets and bays.
- Estimate existing point and nonpoint source pollutant loads to South Puget Sound.
- Develop three-dimensional hydrodynamic and water quality models to evaluate the capacity of South Puget Sound to assimilate existing and future pollutant loads and still meet water quality standards.

Given the limited availability of widespread data and need for understanding highly site-specific processes, the project was divided into two phases.

1. Phase 1, described in the present report, includes data collection and analysis of historical data, as well as development of initial hydrodynamic and water quality models of South Puget Sound. Phase 1 project components include oceanographic field studies to supplement the limited data available for South Puget Sound, watershed and point source pollutant load estimates, as well as hydrodynamic and water quality model development and initial calibration.

2. Phase 2 will address several data needs and will refine the models based on the results of Phase 1 and future data collection programs. Ultimately the effort will establish load and wasteload allocations based on the TMDL for South Puget Sound.

Oceanographic Field Studies

Limited historical data indicate that phytoplankton communities in many South Puget Sound areas are highly productive and sensitive to nutrient addition, resulting in low dissolved oxygen levels in bottom waters. The data show a high degree of variability in time and space. Ecology and the University of Washington have conducted seven data-collection cruises since 1994 to assess the seasonal variability of parameters related to water quality and phytoplankton growth in the South Sound. Phase 1 of the *South Puget Sound Water Quality Study* partially funded six cruises in 1998-2000 to examine hydrographic and biological characteristics, and to provide data for model input, calibration, and validation.

Water column stratification, due to the combined effects of temperature and salinity, strongly influences water quality. The intensity and persistence of stratification governs the vertical transport of nutrients, affects the amount of light available for phytoplankton growth, and controls aeration of deeper water by limiting atmospheric gas exchange. Freshwater inflows contribute to the significant spatial variability in salinity and stratification intensity. During winter months, stratification remains relatively strong throughout South Puget Sound due to high salinity gradients induced by precipitation and resulting river discharge. Transects along the length of Carr and Case inlets suggest that this water column stratification can persist throughout much of the year. Where stratification persists into the spring and summer, conditions favorable to phytoplankton growth result in a depletion of inorganic nutrients at the surface and a drawdown of dissolved oxygen in bottom waters. Figure ES-3 presents the spatial patterns in near-bottom dissolved oxygen concentrations from the 1998-99 cruises. While the lowest dissolved oxygen concentrations were recorded in Budd Inlet, Carr and Case inlets also show significant drawdown of near-bottom dissolved oxygen concentrations.

Nutrients (nitrogen and phosphorus) and light are essential for phytoplankton growth. Typically nitrogen or light limits primary production in marine systems. In the winter, light availability primarily limits phytoplankton growth. When sufficient light is available for photosynthesis, inorganic nitrogen may limit additional phytoplankton growth. Deep ocean waters, and freshwater inflows to a lesser extent, are rich in dissolved inorganic nitrogen (DIN) components (nitrate and ammonia).

While surface DIN concentrations remain constant in the winter months, levels decline during the spring and summer. These depletions coincide with increases in chlorophyll *a* fluorescence (a measure of phytoplankton abundance), as shown in Figure ES-4. Chlorophyll concentrations are lowest in the near-surface waters where DIN is depleted, and in the bottom waters where light limits productivity. Highest concentrations of chlorophyll exist where both light and DIN are available. Plots of nitrate vs. orthophosphate indicate that nitrogen, rather than phosphorus, limits growth in Carr Inlet at certain times of the year, and likely in other areas of South Puget Sound. Nutrient-addition experiments confirm that additional nutrients in the growing season could increase phytoplankton growth in areas such as Carr Inlet. Data available from discrete cruise measurements did not determine the factors responsible for the ephemeral and non-repetitive nature of algal blooms.

Carr, Case, and Budd inlets appear most susceptible to effects from eutrophication. While smaller, shallower inlets show nutrient sensitivity at times, they are generally well-mixed by tides and thus strong oxygen gradients do not appear. However, loads of other substances (e.g., fecal coliform bacteria) are of concern due to the slow flushing rates of some of these inlets.

Point and Nonpoint Source Load Estimates

The hydrodynamic and water quality models require daily flows and loads from nonpoint sources, point sources, and atmospheric sources to simulate seasonal variations in South Puget Sound water quality. The parameters of interest include nutrients, fecal coliform bacteria,

oxygen demand, total suspended solids, dissolved oxygen, and organic carbon. The NPDES permit system provides monitoring data for some point sources. Atmospheric loads are estimated from the National Atmospheric Deposition Program, National Trends Network, and a supplementary station operated by the U.S. Geological Survey (USGS).

Historical monitoring data provide the basis for nonpoint source load estimates. USGS developed the regression-based approach (Cohn et al., 1992) and applied a proprietary model to the major rivers of Puget Sound (Embrey and Inkpen, 1998), including the Deschutes, Nisqually, and Puyallup rivers. However, watershed loads from smaller tributaries and direct inflows govern the response of smaller inlets and bays of South Puget Sound. Continuous or discrete flow monitoring and water quality monitoring data cover nearly 90% of the land area within the model domain. Site-specific multiple linear regression coefficients provide daily concentrations based on discharge and season. Loads are calculated from estimated concentrations and flows. Where limited or no monitoring data are available, regression coefficients from a nearby watershed of similar size and land use are used.

Loads normalized by relative contributions to South Puget Sound identify not only the largest loads but the most densely distributed loads. The load is the proportion of total pollutant load produced by a watershed normalized by the proportion of watershed area represented. Therefore, watersheds with normalized loads >1.0 produce loads higher than the average from the entire South Puget Sound watershed. Figure ES-5 presents these normalized loads for nitrite/nitrate and ammonia, two of the most important parameters to productivity. While some watersheds produce both high ammonia and nitrite/nitrate loads, others produce one or the other, and these sources do not necessarily coincide.

Overall, point and watershed-based nonpoint sources dominate atmospheric loads by two orders of magnitude. The larger point source and nonpoint source loads of dissolved inorganic nitrogen are of similar magnitude, as evident in Figure ES-6. While point sources contribute 2% of the inflows to South Puget Sound, they contribute 30 to 50% of the nutrient load but only 0.2% of the fecal coliform load.

Hydrodynamic Model

Representing the complex structure and response of South Puget Sound requires a three-dimensional model. Based on an extensive review of hydrodynamic and contaminant transport computer models (West Consultants, 1996), the Environmental Fluid Dynamics Code (EFDC) model was selected as the best choice for South Puget Sound. EFDC offers a public-domain platform that simulates hydrodynamics, salinity, temperature, nutrient cycling, two phytoplankton groups, sediment transport, sediment diagenesis, and other conservative and non-conservative substances. EFDC solves the three-dimensional equations of motion for a free-surface, variable-density fluid. Grid size varies in a curvilinear orthogonal coordinate system but averages 630 m by 630 m in the present application. Figure ES-7 presents the South Puget Sound grid, which includes 1,906 cells. Each of the four layers represents one-quarter of the water depth at mean lower low water (MLLW).

Hydrodynamic model inputs include tidal forcing at the model boundary at Alki Point, freshwater inflows, solar radiation, wind, and other meteorological data. Figure ES-8 compares model output sea surface elevations against measured data from four of ten tidal monitoring stations operated by various agencies and institutions. While the model largely represents sea surface elevations and physical processes well, no domain-wide tidal current data exist, a more sensitive indicator of model accuracy. Comparing model output with limited velocity data from Budd Inlet (Aura Nova Consultants et al., 1998) indicates that the model represents velocity magnitude and direction in Budd Inlet reasonably well. Overall, the model represents tidal forcing, wind effects, and hydrodynamic responses appropriately.

The hydrodynamic portion of the model also simulates the density structure through variations in temperature and salinity. Comparing model output to measured data in Budd Inlet without additional calibration indicates that while EFDC represents seasonal variations well, magnitudes are not adequately represented. For example, the model overpredicts temperature by approximately 3°C, resulting in less dense water than actual conditions. However, the model also overpredicts salinity, resulting in denser water than actual conditions. While the two trends offset impacts to the density stratification, thermodynamic processes must be represented better.

Water Quality Model

The water quality components of the EFDC model simulate the concentration of dissolved oxygen in response to phytoplankton primary production, oxidation of organic material, and sediment flux. Mass transport, chemical transformation, and biological processes are based on the output from the hydrodynamic model, tidal boundary conditions, point and nonpoint source flows and loads, and meteorological data.

EFDC includes numerous state variables that must be calibrated to the conditions of South Puget Sound, yet little information exists for some of the variables and coefficients. Thus, values from similar studies in Budd Inlet and the Chesapeake Bay system are applied to the entire model domain. Because Budd Inlet offers the most extensive data set for model calibration (Aura Nova Consultants et al., 1998), the sub-grid is evaluated independently.

The roughly calibrated model represents the seasonal pattern of increasing chlorophyll from April to September coupled with decreasing dissolved inorganic nitrogen, representing nutrient food sources. During this period, lower water column dissolved oxygen concentrations decline. While the model represents Budd Inlet reasonably well (Figure ES-9), the model over-predicts the dissolved oxygen in other areas such as Dana Passage (Figure ES-10). The Budd Inlet results are most sensitive to sediment oxygen demand, settling rates of phytoplankton and particulate organic matter, as well as algal metabolism, growth, and predation rates. However, no field studies are available that would aid in calibrating individual processes. Ongoing research by Ecology and the University of Washington may improve the understanding and quantify these processes. Limited model runs of the entire model domain indicate that the model sufficiently represents the observed conditions in the surface layer. The model also represents bottom layer conditions sufficiently, but based on limited data.

Conclusions and Recommendations

Phase 1 Conclusions

- Based on field observations and experimental measurements, South Puget Sound appears to be sensitive to nutrient addition. This report confirms the potential for serious water quality degradation due to increased nutrient loads.

- Case, Carr, and Budd inlets appear to have the lowest dissolved oxygen levels within South Puget Sound, and may be the most sensitive areas to increased nutrient loads. Whereas Budd Inlet has been studied in detail, additional focus on Case and Carr inlets is warranted.

- While point sources discharging directly to South Puget Sound contribute 2% of the total inflows, point sources contribute 30% of the dissolved inorganic nitrogen load and 54% of the total phosphorus load. Fecal coliform loads from watershed inflows are two orders of magnitude greater than point sources.

- Water quality modeling shows that dissolved oxygen is more sensitive to nutrient-driven processes than direct biochemical oxygen demand (BOD) loading.

- A coupled hydrodynamic and water quality model has been successfully developed for South Puget Sound that can be applied to evaluate the sensitivity of dissolved oxygen levels to increased nutrient loading. However, the model requires further refinement and testing before the results can be used for management decisions. Additional monitoring data will be needed for model calibration and verification.

Recommendations and Approach for Phase 2

To help define the next steps, Ecology should establish a South Puget Sound project advisory group, with representatives from other agencies and groups with an interest in South Puget Sound water quality.

Ecology should conduct Phase 2 of the *South Puget Sound Water Quality Study* to address several data needs and to calibrate the hydrodynamic and water quality models to the entire South Sound. Specific observational studies include the following:

- Conduct annual marine monitoring in the fall to document dissolved oxygen levels during the critical period and to establish a long-term dataset.

- Improve understanding of temporal and spatial variability in South Puget Sound, i.e., using the high-frequency CISNet profiling mooring operated by Ecology and UW, and using remote sensing of phytoplankton.

- Evaluate cross-channel spatial variation in selected inlets.

- Measure current velocities in key locations to improve the understanding of physical flushing in South Puget Sound and its inlets. Current velocities will also provide data for direct calibration of the hydrodynamic model.

- Update watershed load estimates to reflect more recent data collection, and include a range of hydrologic conditions.

- Conduct limited water quality monitoring in tributaries to Carr and Case inlets.

- Conduct limited field investigations for water quality model parameters, such as algal growth rates.

Both the hydrodynamic and water quality models need refinement, testing, and further calibration. Specific modeling needs include the following:

- Focus hydrodynamic model calibration efforts on appropriate bottom friction as well as thermodynamic processes, which will impact the water quality cycles.

- Calibrate water quality model state variables to South Puget Sound conditions.

- Assess the impacts of non-anthropogenic processes, such as climate or oceanic variation.

- Use the calibrated hydrodynamic and water quality model to evaluate the response of South Puget Sound to increased nutrient loads.

Model sensitivity should be assessed, and the model should be used to allocate loads and wasteloads for the development of TMDLs, if needed.

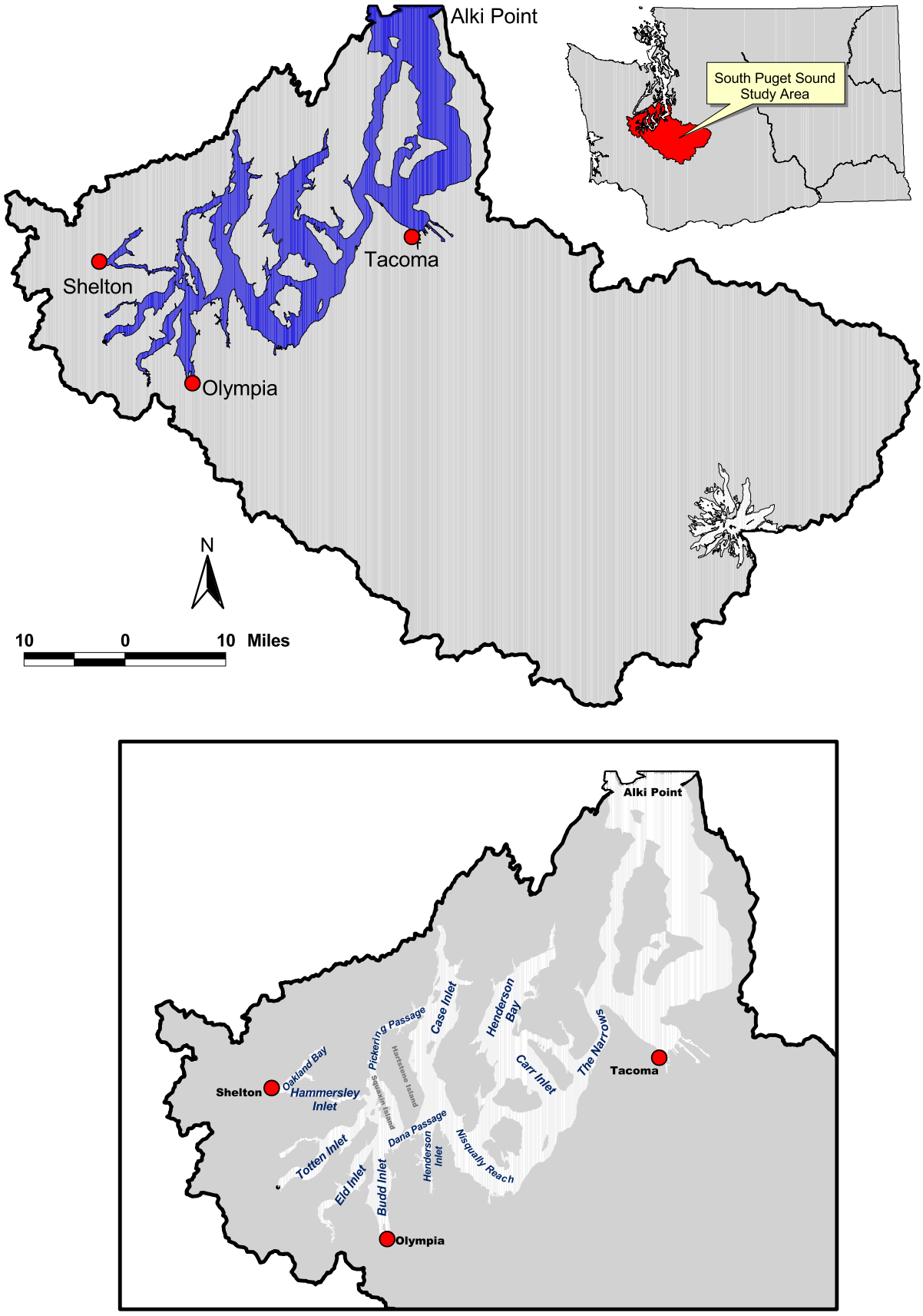

Figure ES-1. South Puget Sound study area.

This page is purposely blank for duplex printing

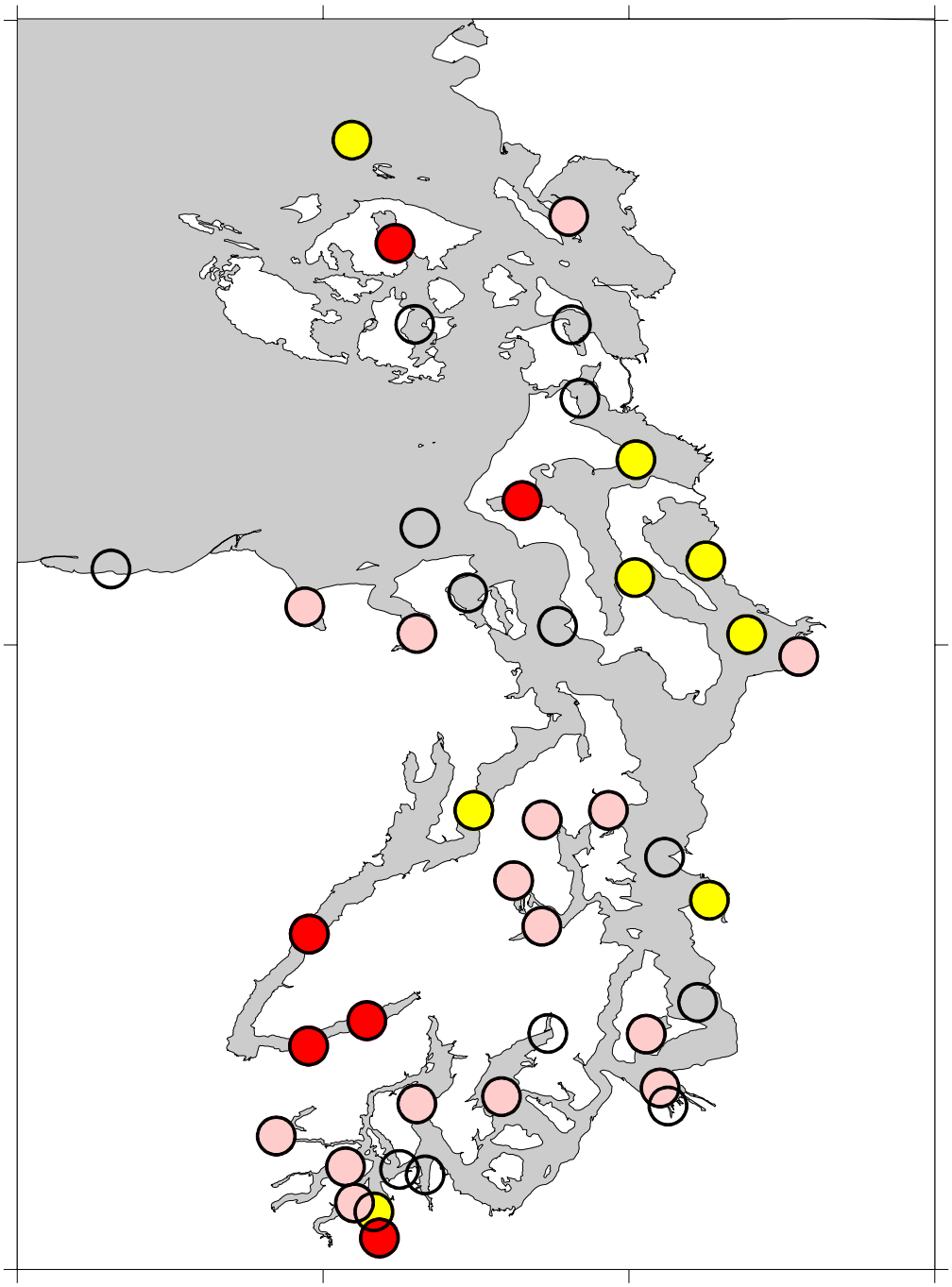

Figure ES-2. Ecology's Marine Waters Monitoring stations exhibiting either low dissolved oxygen concentrations (*red:* hypoxia <= 3 mg/L; *yellow:* biological stress level <= 5 mg/L) or sensitivity to impacts from eutrophication based upon physical and chemical characteristics *(pink)*. Stations assessed but with neither condition are also shown (*clear*).

The graphic is a compilation of monthly Ecology-PSAMP data for water years (WY) 1990-1997. Not all stations were monitored in all years, so classification was based on the occurrence of a condition within one or more years. Prior to WY 1990, data are not comparable due to refinements and changes in analytical and sampling techniques.

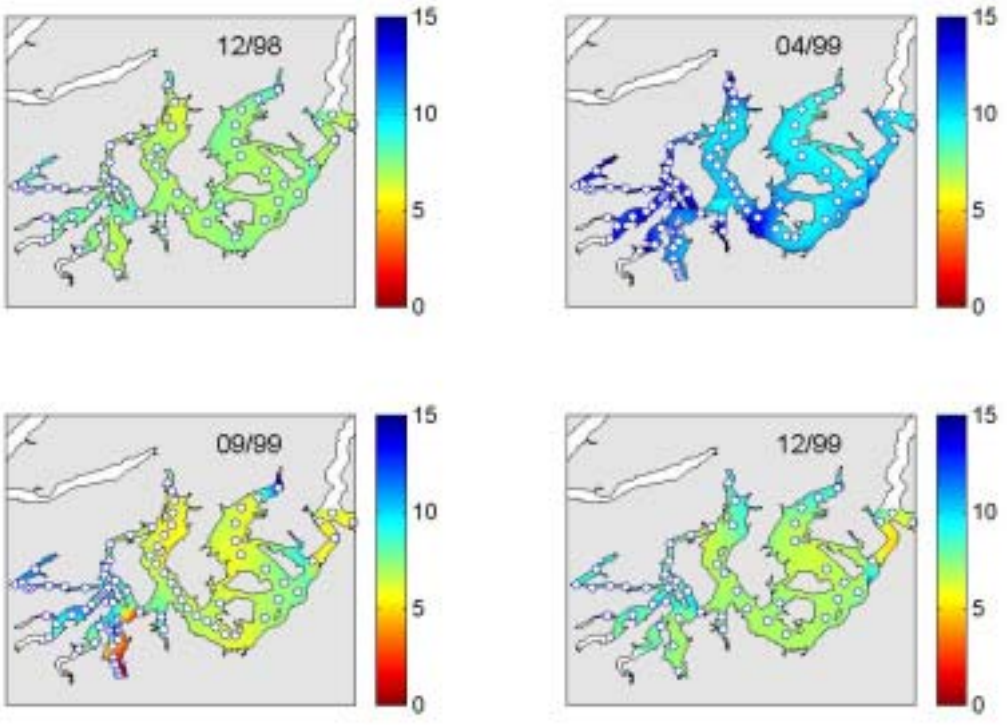

Figure ES-3. Dissolved oxygen concentration (mg/L) in near-bottom waters at different times of the year.

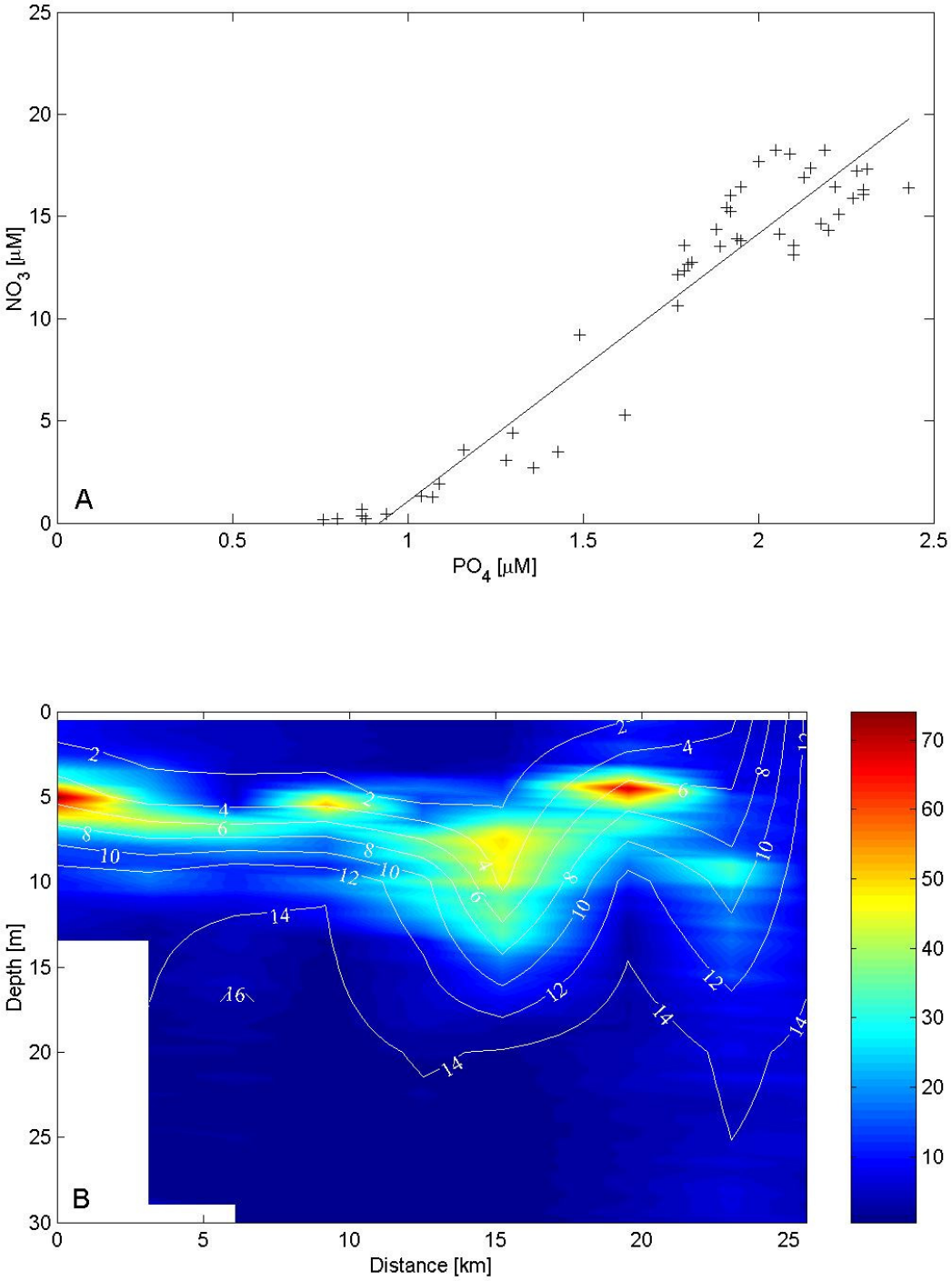

Figure ES-4. Measurements in Carr Inlet during September 1997.

A: Scatter plot of nitrate vs. phosphate concentrations from discrete water samples. The line represents a best-fit regression of the relationship for phosphate concentrations greater than 1 µM.

B: False color plot illustrating the distribution of chlorophyll *a* fluorescence (relative units) as a function of distance from the northern head of the inlet (Station 75). Overlaid are contours of nitrate concentration (µM).

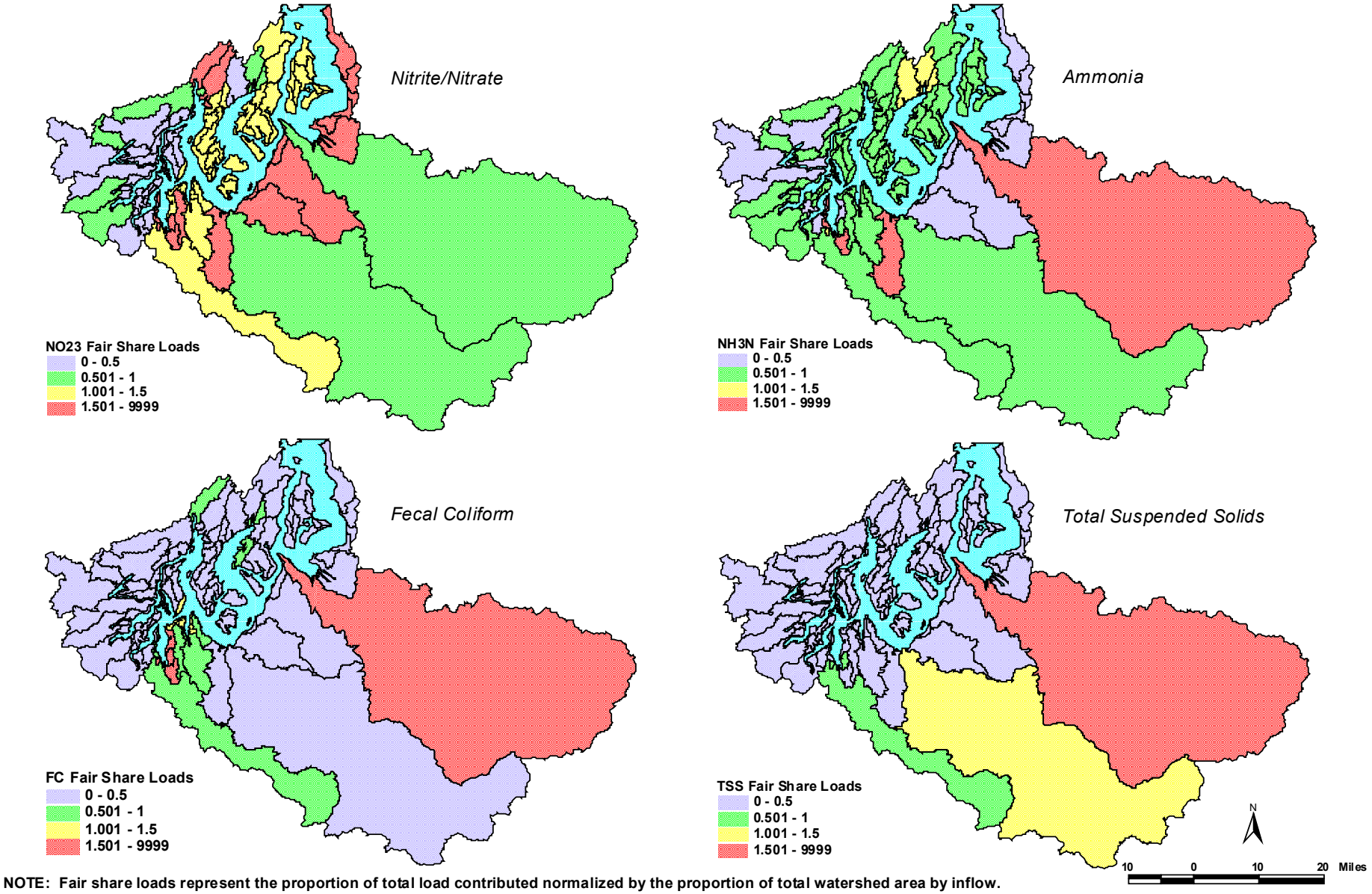

NOTE: Fair share loads represent the proportion of total load contributed normalized by the proportion of total watershed area by inflow.

Figure ES-5. South Puget Sound normalized loads for nitrite/nitrate, ammonia, fecal coliform, and TSS.

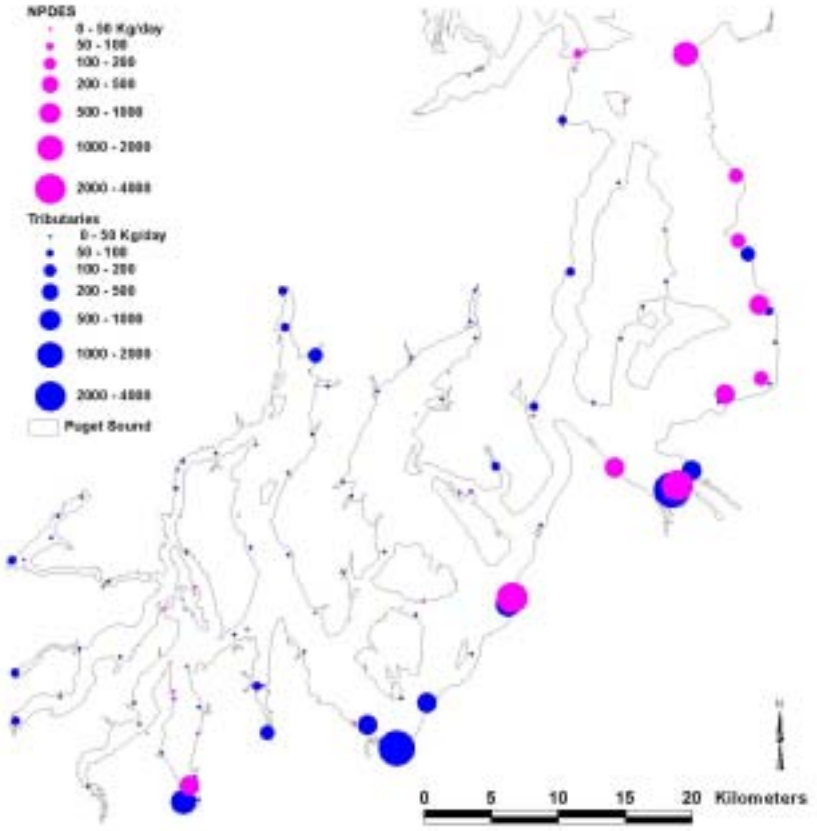

Figure ES-6. Annual DIN loads from watershed and point sources.

.

This page is purposely blank for duplex printing

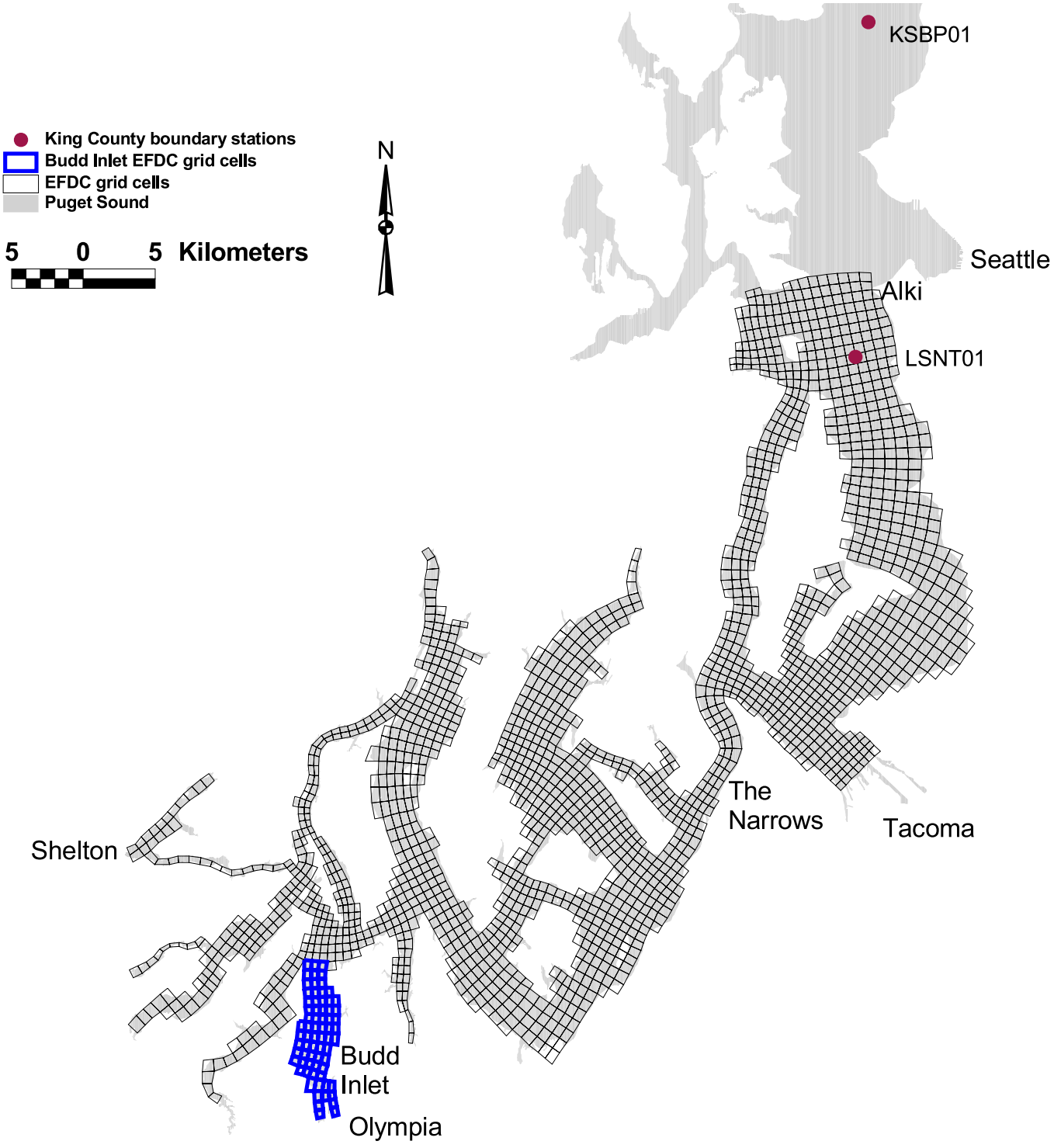

Figure ES-7. Computational grid for the South Puget Sound Model.

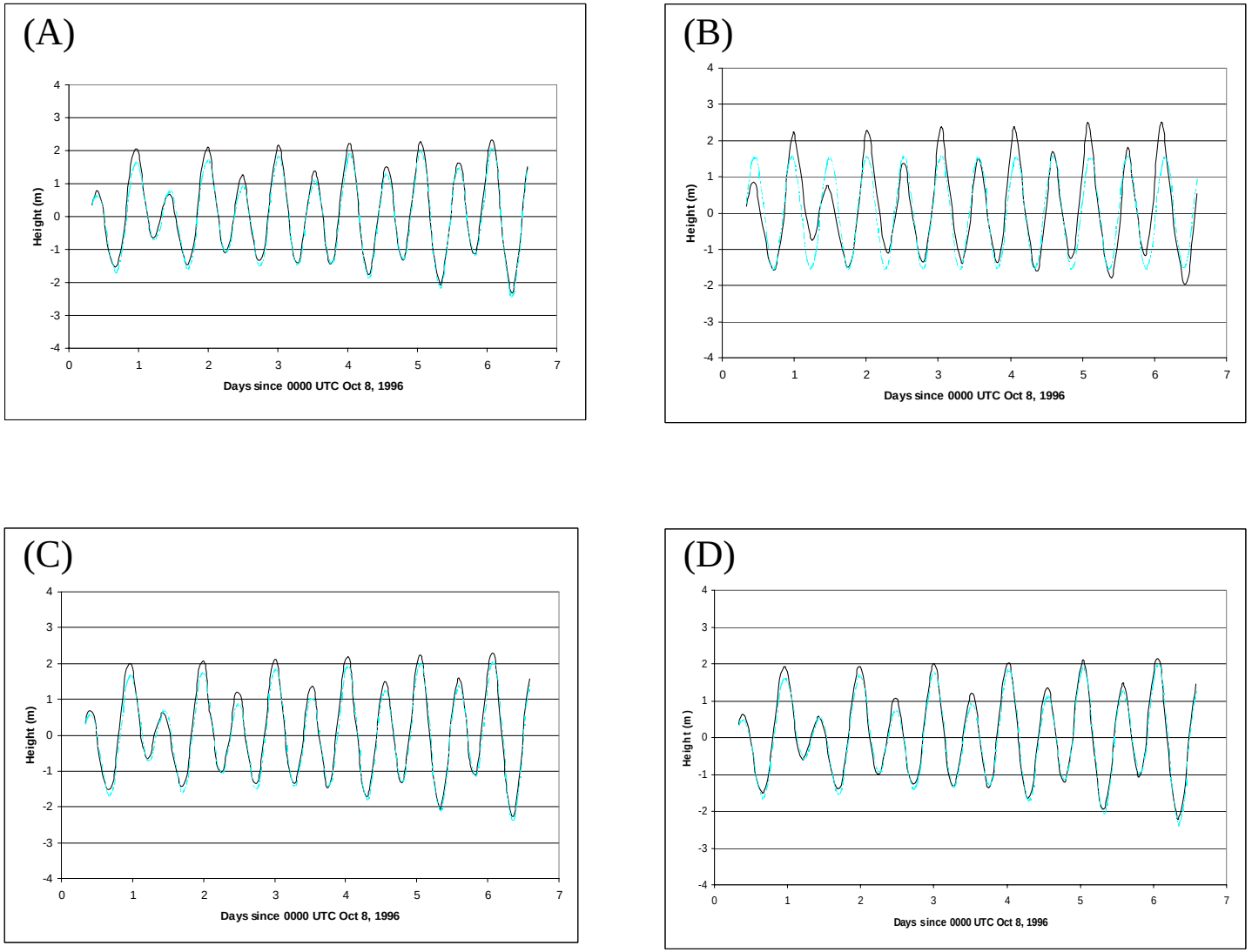

Figure ES-8. Time series for observed tides with no wind (light gray lines) with model output (solid black lines) at (A) Budd Inlet (6969), (B) Oakland Bay, Shelton (0178), (C) Port of Allyn in Case Inlet (6281) and (D) Carr Inlet (6451).

Due to the short duration of the time series at Oakland Bay (1 week), only an M2 constituent is typically available, which is responsible for the large discrepancy.

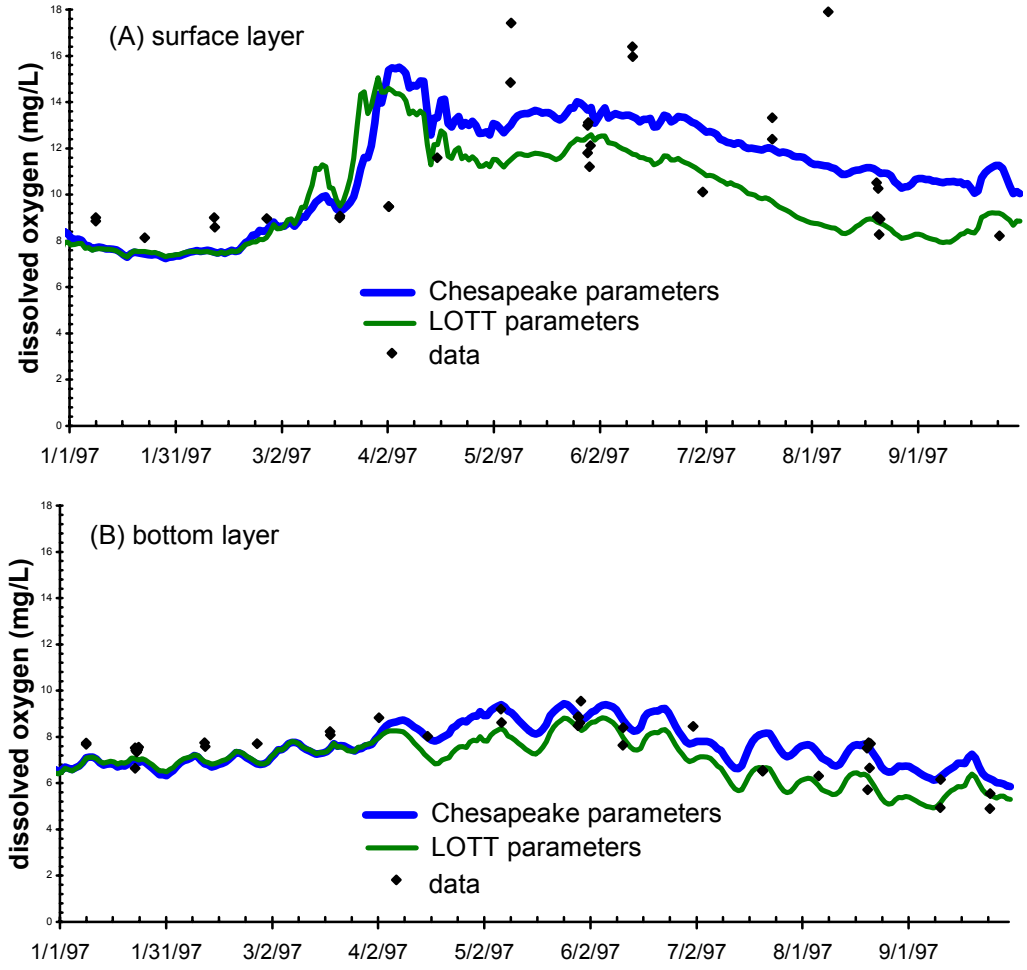

Figure ES-9. Model output dissolved oxygen concentrations (solid lines) compared with monitoring data (diamonds) for (A) the surface and (B) the bottom layer in central Budd Inlet (station BUD005).

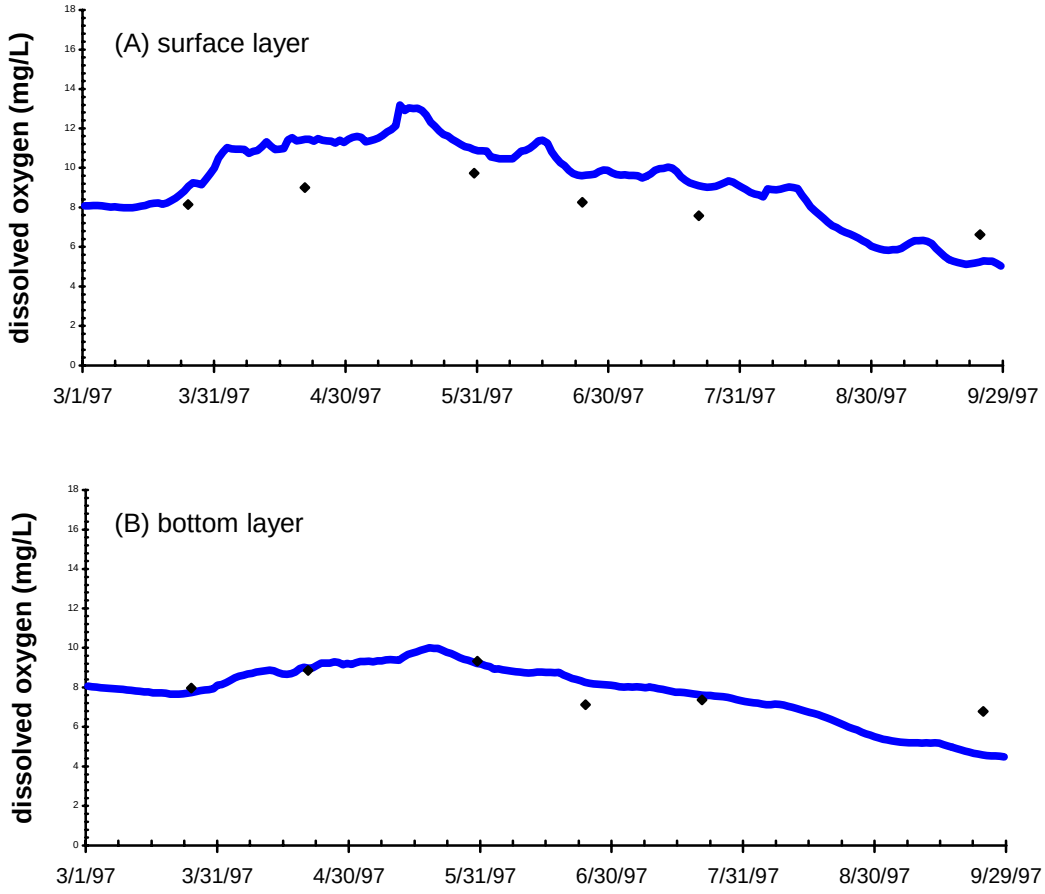

Figure ES-10. Model output dissolved oxygen concentrations (solid lines) compared with monitoring data (diamonds) for (A) the surface and (B) the bottom layer in Dana Passage (station DNA001).

1. Introduction

South Puget Sound is not subject to the rapid flushing of the deeper waters of northern Puget Sound, and includes many blind-end inlets with sluggish circulation. Newton et al. (1997) assessed dissolved oxygen concentrations at locations throughout Puget Sound and suggested that depletion of bottom dissolved oxygen concentrations can be exacerbated in areas that have strong density stratification (e.g., in areas with freshwater input), high production due to inhibited mixing, and oxidation of sunken organic material (i.e., dead phytoplankton). Eutrophication will likely have the greatest impact in South Sound areas where flushing is low, where strong density stratification occurs, and where phytoplankton growth may be nutrient limited, such as in bays and inlets. Increases in nutrient loads can accelerate the eutrophication process. Like many other western Washington locations, the South Puget Sound watershed receives significant development pressure.

The purpose of the *South Puget Sound Water Quality Study* is to evaluate the impacts of nutrient loading on phytoplankton growth and associated changes in dissolved oxygen (DO) concentrations. Project components include oceanographic field studies to supplement the limited data available for South Puget Sound, estimates of watershed and point source pollutant loads, and hydrodynamic and water quality model development and initial calibration.

Problem Statement

The Washington State Department of Ecology (Ecology) Southwest Regional Office expressed concern about nonpoint and point source nutrient loading to the southern portion of Puget Sound, located south of The Narrows near Tacoma. Past and future growth around this region may cause adverse effects on water quality due to increased eutrophication. The Southwest Regional Office requested that the Environmental Assessment Program evaluate the ability of South Puget Sound to assimilate nutrients, and if needed, recommend point source waste load allocations and nonpoint source load allocations for controlling nutrients.

Figure 1-1 presents the study area, which includes all of Puget Sound south of Alki Point. The area between Alki Point and The Narrows was added to the study area as a transition region between the seaward boundary and the main area of interest south of The Narrows. Findings for the entire study area will be useful, although the area in the vicinity of Alki will be most sensitive to the assumed boundary condition.

Background

Hydrographically, South Puget Sound is very different from the main basin of Puget Sound. Physical characteristics of the South Puget Sound basin, such as its distance from the Strait of Juan de Fuca (source of incoming Pacific Ocean water) and its complex morphology with a high number of blind-end inlets, lead to long residence times and slow flushing rates. As a result of the shallower depths and longer residence times, land-derived nutrients are not diluted or transported out of the South Puget Sound basin as much as occurs in the deeper, more tidally

mixed areas of central Puget Sound. Biologically, South Sound is also different from other regions within Puget Sound. Because of the slow flushing time and physical stability of the water column, many of the inlets and bays are exceptionally productive. For example, despite a water column of about 10 meters, the annual depth-integrated primary production in Budd Inlet is actually higher than the 110-meter water column in Dabob Bay. The geomorphology of South Sound is also different than the deep, open basins of central and northern Puget Sound. The hydrological, biological, and geomorphological attributes of the South Puget Sound region make it susceptible to adverse effects from eutrophication.

South Puget Sound is divided into numerous inlets, which results in a high shoreline-to-water volume ratio. Extensive shorelines and the rural nature of the upland and lowland areas around these inlets attract significant residential development. In the past decade, many of the stream corridors and shorelines in the area have experienced considerable growth. In 1990, Thurston County ranked as the third fastest growing county in Washington with a population increase of nearly 30% since 1980 (personal communication, Thurston County Planning Council, 1996). In addition, many recreational farms now exist in the watersheds. The recreational farms are typically less than 20 acres in size and consist of several large animals (e.g., horses, cows, and llamas). Development is expected to continue at a high rate in the counties contributing to South Sound (i.e., Thurston, Mason, and Pierce Counties). As a result of increases in human activities, nutrient loading to South Puget Sound likely exceeds past loads and will likely increase in the future.

Eutrophication caused by increased nutrient concentrations can lead to water quality problems such as excessive algal blooms with resulting low dissolved oxygen in the bottom waters. Other impacts from eutrophication are less well known, but concerns exist about the impact of human caused nutrient loading on the prevalence of harmful algal blooms (e.g., Paralytic Shellfish Poisoning [PSP] and Amnesiac Shellfish Poisoning). The first known outbreak of PSP in South Sound was recorded in November 1997. The PSP outbreak resulted in closure of commercial shellfish growing areas to harvest in several South Sound inlets. More recently, in August of 2000 an outbreak of PSP in Carr Inlet afflicted seven people who had eaten mussels there. One person required extensive hospitalization and treatment on a respirator. PSP events are thought to be increasing in frequency and extending farther south into South Puget Sound than previously reported, including first-ever reported blooms in Totten and Eld inlets in summer 2001 (Olympian, 2001).

Over the last few years, unexplained mortalities have occurred at marine salmon net-pen facilities located in South Sound. The most recent fish loss was in October 1997 in pens located east of Squaxin Island. The pens are owned and operated by the Department of Fish and Wildlife. They reported losses of 90% of their three-year-old Chinook brood fish. Other salmon net pens located southeast of Hartstene Island reported large fish losses in May and October of 1994, and also in the fall and winter of 1996. After a number of studies, the cause of these fish kills still has not been determined.

Numerous factors control nutrient enrichment, eutrophication, and oxygen depletion. Nutrient loads from atmospheric deposition, tributary inflows, point source discharges, nonpoint source inputs, and sediment-water exchange determine the inputs to South Puget Sound. Hydrodynamic

characteristics, such as tides, stratification, mixing, and freshwater inflows govern transport of nutrients and other parameters. Photosynthesis characteristics and processes such as light availability (season, depth), temperature, growth, death, respiration, settling, and other phytoplankton kinetics determine nutrient transformations and oxygen depletion.

Excessive nutrient inputs can accelerate the eutrophication process and affect water quality in several ways:

- Increase the algal growth and cause shifts in community structure, leading to the predominance of undesirable forms (e.g., toxic phytoplankton blooms).
- Alter the balance between phytoplankton, zooplankton, fish, and shellfish that may result in an unusually high accumulation rate of organic matter on bottom sediments, which may depress bottom oxygen concentrations.
- Change the aerobic bacteria populations to anaerobic sulfate-reducing bacteria, that can increase the water column levels of hydrogen sulfide, which may lead to further community structure changes.
- Affect recreational activities due to objectionable odors, and unsightly algal mats.

Concerns about eutrophication impacts are not new to South Sound. Conditions in Budd Inlet have been studied actively since the 1980s. Due to degraded water quality, the Lacey, Olympia, Tumwater, Thurston County (LOTT) wastewater treatment plant was required to upgrade the facility to remove nitrogen from its effluent. The upgrade, implemented in 1994, clearly was associated with a significant reduction in the concentration of nitrogenous nutrients in the water-column (Eisner and Newton, 1997). However, because of expected growth in the region, the LOTT partners initiated a multi-million dollar Budd Inlet Study to determine if the inlet can accommodate additional nutrient loading during winter. The study has had technical input from scientists from private, governmental, and academic institutions. A report summarizing the findings of the study was published in 1998 (Aura Nova Consultants et al.). The Budd Inlet study reinforced the importance of accurate hydrography, sediment nutrient cycling, applying an appropriate water quality model, and parameter dynamics (tidal, weather, and runoff related forcing mechanisms) in understanding water quality processes.

Other studies have previously concluded that South Puget Sound is susceptible to water quality problems due to reduced circulation (Cokelet and Stewart, 1985; URS, 1985; URS, 1986a; WRE, 1975) and shows signs of nutrient sensitivity (Rensel and PTI, 1991; Harrison et al., 1994). Ecology's assessment of marine water quality throughout Washington State, as part of the Puget Sound Ambient Monitoring Program (PSAMP), showed similar results (Newton et al., 1997; Newton et al., 1998). Analysis of the long-term PSAMP monitoring data from 1990-1997 indicated that sensitivity to nutrient addition was particularly evident in the South Puget Sound area (Figure ES-2). This analysis, based on several water quality indicators (e.g., stratification, lack of surface nutrients in summer, and low DO), confirmed that physical and chemical attributes of this basin result in a higher sensitivity to impacts from eutrophication, relative to most of the other Puget Sound basins.

Despite this conclusion, the current status of water quality is somewhat difficult to assess, owing to lack of a lengthy historical record[1]. Also natural processes, such as inputs of nutrients from oceanic upwelling intrusions, can mimic cultural eutrophication. The natural dissolved oxygen concentrations in many of South Puget Sound waters are sometimes lower than the criteria because upwelled Pacific Ocean water flowing into the Puget Sound can have naturally low dissolved oxygen. It is thus critically important to distinguish this natural variability from human-induced changes.

Several studies have included development of models of various levels of complexity to predict circulation and water quality within southern Puget Sound. WRE (1975) developed a link-node hydrodynamic model of southern Puget Sound combined with a vertically averaged eutrophication model of water quality. The WRE model was able to simulate seasonal patterns of vertically-averaged water quality fairly well. However, the assumption of vertically mixed conditions for the water quality model was recognized by WRE as a major limitation because of the pronounced stratification of dissolved oxygen and salinity in the inner inlets.

URS (1986a) applied a simple model of circulation and flushing that was based on a tidal prism calculation and the mass balance of water and salt to estimate the potential dilution of wastewater in various regions of southern Puget Sound. URS (1986b) developed a more detailed 2-dimensional (width-averaged), vertically stratified hydrodynamic model combined with a eutrophication model of water quality of Budd Inlet to estimate the assimilative capacity for nutrient loading with respect to depletion of dissolved oxygen in the bottom layer of the inner inlet.

The study by URS (1986a and 1986b) recognized that simple tidal prism and salt budget models were insufficient to estimate assimilative capacity and predict water quality changes. URS (1986b) and LOTT (1998) recognized that the more complex 2-dimensional model that was developed by URS (1986b) still lacked the ability to describe the important and complex hydrodynamics, spatial variations, and water quality processes that are necessary to quantify the relationship between increasing nutrient loading and depletion of dissolved oxygen in critical areas of Budd Inlet.

One of the main goals of the present study is to begin the development of a tool for evaluating the response of dissolved oxygen and other water quality variables to nutrient loading in southern Puget Sound, including Budd Inlet and the other similar stratified and spatially complex inlets. Therefore, a 3-dimensional model of hydrodynamics, combined with a state-of-the-art eutrophication model of water quality was considered to be a necessary component of the study. The EFDC model was selected in consideration of the recognized need for a 3-dimensional model for southern Puget Sound, and also based on a rigorous review of available models that was conducted by King County for selection of a model for a similar purpose to describe Elliot Bay in central Puget Sound (WEST, 1996).

[1] The best historical database for Puget Sound was compiled by Collias et al. (1974) for 1952-1966. However, South Puget Sound data were only collected from Case and Carr inlets. Additionally, this database does not contain nitrogenous nutrient data or phytoplankton chlorophyll measurements. Data collected by Ecology from 1973-1989 are available for relatively few stations in South Puget Sound.

Beneficial Uses and Water Quality Impairment

South Puget Sound comprises 17 marine waterbodies of Washington State. Each of these waterbodies is classified by water use and water quality criteria as either Class AA, A, or B in Chapter 173-201A of the Washington Administrative Code (Washington State, 1997). These classes stipulate the type of water use and the water quality criteria that apply to each waterbody. For example, any Class AA water "is expected to markedly and uniformly exceed the requirements for all or substantially all uses."

The characteristic uses for marine classes include fish and shellfish migration, rearing, spawning, and harvesting; wildlife habitat; recreation; and commerce and navigation. The water quality criteria for marine classes specify numeric limits for fecal coliform bacteria, dissolved oxygen, temperature, pH, turbidity, deleterious material concentrations (e.g., toxic or radioactive substances), and narrative criteria for aesthetic values. The aesthetic values of Class AA and A waters "shall not be impaired by the presence of materials or their effects, excluding those of natural origin, which offend the senses of sight, smell, touch, or taste."

Table 1-1 lists the South Puget Sound waterbodies that are listed as impaired under Section 303(d) of the Clean Water Act. Appendix A describes the changes in impaired waterbodies between the 1996 and 1998 303(d) lists and the reasons for changes in listing status. Fecal coliform bacteria levels exceed the criterion in all of these waters, and dissolved oxygen does not meet water quality criteria in some. The sources of these impairments are believed to be nonpoint sources, natural sources, recreational activities, municipal point sources, and industrial point sources. Although these listings are based on water quality data, most of South Sound has not been sufficiently studied to determine all possible areas that may violate the water quality criteria for dissolved oxygen. The areas needing additional study include many of South Puget Sound bays and inlets, which are most susceptible to eutrophication and other impacts of pollution.

Table 1-1. Impaired waterbodies from the 1996 and 1998 Section 303(d) lists.

Waterbody Segment Number	Waterbody Name	Parameters Exceeding Standards (1996)	Parameters Exceeding Standards (1998)
WA-13-0010	Henderson Inlet	Fecal Coliform	Fecal Coliform, Dissolved Oxygen
WA-13-0020	Budd Inlet (outer)	Fecal Coliform, Total Nitrogen, pH	Dissolved Oxygen, pH
WA-13-0030	Budd Inlet (inner)	Fecal Coliform, Dissolved Oxygen, Total Nitrogen, pH, and a number of toxic substances	Dissolved Oxygen, pH, and a number of toxic substances
WA-14-0010	Squaxin, Peale, and Pickering Passages	pH	Dissolved Oxygen, pH
WA-14-0020	Eld Inlet	Fecal Coliform	(not listed)
WA-14-0050	Shelton Harbor (inner)	Fecal Coliform	Fecal Coliform
WA-14-0100	Hammersley Inlet	Fecal Coliform	Fecal Coliform
WA-14-0110	Oakland Bay	Fecal Coliform, Dissolved Oxygen	Fecal Coliform

Section 303(d) of the Clean Water Act requires states to develop total maximum daily loads (TMDLs) for waterbodies not meeting designated uses under technology-based pollutant controls. Since no site-specific or numeric nutrient criteria exist for Puget Sound, criteria must be developed to protect the designated uses and water quality standards. For South Puget Sound, Ecology may develop site-specific nutrient criteria based on the impact of measured nutrient concentrations (or loads) on endpoint indicators such as dissolved oxygen concentrations.

The marine water quality standards for dissolved oxygen vary according to the classification of a waterbody. Waterbody Classes AA, A, and B are required to have dissolved oxygen concentrations which exceed 7.0, 6.0, and 5.0 mg/L, respectively. In addition, the following applies to all waterbodies: "[w]hen natural conditions, such as upwelling, occur, causing the dissolved oxygen to be depressed near or below the criterion, natural dissolved oxygen levels may be degraded by up to 0.2 mg/L by human-caused activities." Many of the bays and inlets in the region have periods, primarily in late summer, when oxygen concentrations drop below the criteria.

Project Goals and Objectives

The capacity of South Puget Sound to assimilate pollutants from its drainage basins is not well understood. The primary goals of this project are to understand the hydrodynamics and current water quality and to develop a computer model to simulate various hydrodynamics and water quality scenarios. If needed, another goal of the project will be to establish load allocations for waterbodies not meeting standards.

Specific objectives to support the goals include the following:

- Identify areas in South Puget Sound where the phytoplankton are naturally nutrient limited and thus susceptible to nutrient loading.
- Assess the flushing and cycling rates in the inlets and bays in South Sound and variations due to seasonal dynamics.
- Develop a three-dimensional hydrodynamic and water quality model to evaluate the capacity of South Puget Sound to assimilate loads from point and nonpoint sources of nutrients and biochemical oxygen demand (BOD) and to meet water quality criteria for dissolved oxygen.
- Gather available data and conduct limited hydrodynamic and water quality sampling investigations for calibrating and confirming the results of the 3-D model.
- Develop methods or models to predict loading of nutrients, BOD, and other pollutants. Determine the nutrient, BOD, and other pollutant loads to South Puget Sound from watershed sources, including tributaries and nearshore areas.
- Determine the nutrient, BOD, and other pollutant loads to South Puget Sound from point sources (i.e., NPDES permitted discharges).

Given the limited availability of widespread data and need for understanding highly site-specific processes, the project was divided into phases. The first phase, described in the present report, includes some data collection and analysis of historical data, as well as development of initial hydrodynamic and water quality models of South Puget Sound.

Ecology recognizes that this project is of interest to, and has the potential to affect, a large number of parties. Therefore before moving into Phase 2 of the technical work, we plan to establish a collaborative approach for refining and applying this tool to address water quality issues. One of the first steps will be to establish an advisory group for the project, with representatives from other agencies and groups with an interest in South Puget Sound water quality.

Phase 2 will refine the models based on the results of the first phase, future data collection programs, and advice from the advisory committee. If needed, an eventual outcome would be wasteload allocations and load allocations based on water quality modeling of past, current, and future nutrient and BOD loading scenarios.

Technical Approach

The approach to the *South Puget Sound Water Quality Study* is to use existing information to the extent possible and focus resources on monitoring marine water quality. Data are used to understand the water quality processes of South Puget Sound as well as parameterize the hydrodynamic and water quality models. The models can be used to improve understanding of the responses of South Puget Sound to various forcing mechanisms representing current and future conditions.

Data Collection and Load Estimates

South Puget Sound's physical characteristics suggest a susceptibility to eutrophication, and limited historical data indicate a dissolved oxygen deficit in the bottom waters. Seven marine monitoring cruises have been conducted since 1994, four of which were funded by the present project. The purpose of the cruises was to describe seasonal variability of hydrographic, chemical, and biological characteristics.

Loads to South Puget Sound come from atmospheric, point and nonpoint terrestrial sources, and the Pacific Ocean. While monitoring data exist to quantify atmospheric and point sources, nonpoint source loads were developed using a regression-based approach to predict watershed inflow concentrations as a function of discharge and season.

Section 2 describes the marine monitoring efforts. Section 3 discusses the methods for estimating watershed loads and compares watershed, atmospheric and point source loads to South Puget Sound.

Modeling

Ecology selected the Environmental Fluid Dynamics Code (EFDC) model to simulate the hydrodynamics and water quality of South Puget Sound. The model was selected based on a 1996 review funded by King County to evaluate the ability of over a dozen hydrodynamic and contaminant transport computer models to simulate the complex conditions of Puget Sound (West Consultants, Inc., 1996). In the review conducted by West Consultants, Inc., the EFDC model was described as follows:

> *"EFDC is a single code that incorporates hydrodynamics, salinity, temperature, dye, cohesive and non-cohesive sediments, toxicants, and water quality state variable transport. It is a three-dimensional model that uses a curvilinear-orthogonal grid in the horizontal, and a sigma (or stretched) transformation in the vertical. It uses a finite volume-finite difference formulation to ensure conservation of mass. The model has been applied to 22 sites to date."*

The EFDC model represents the best choice of existing models to apply to South Puget Sound for several reasons. EFDC has the same or similar hydrodynamic capabilities of the Princeton Ocean Model being applied to Puget Sound by the University of Washington School of Oceanography, which will provide opportunities for collaboration. The model can represent watershed inflows and has been modified to simulate nearshore areas, including wetting and drying processes. In addition to salinity and thermal transport, EFDC can simulate sediment transport and the transport of equilibrium-partitioning toxic contaminants in water and sediments. Finally, the model can simulate nutrient cycling through 20 state variables for simulating water column eutrophication and 26 state variables for simulating sediment biogeochemical processes. These characteristics provide the framework for addressing the current concern about nutrient loading, but also provide options for applying the model to other water quality or toxic parameters.

Section 4 describes the simulation of South Puget Sound hydrodynamics, while Section 5 describes the water quality model application. Section 6 provides a summary and lists recommendations for future study.

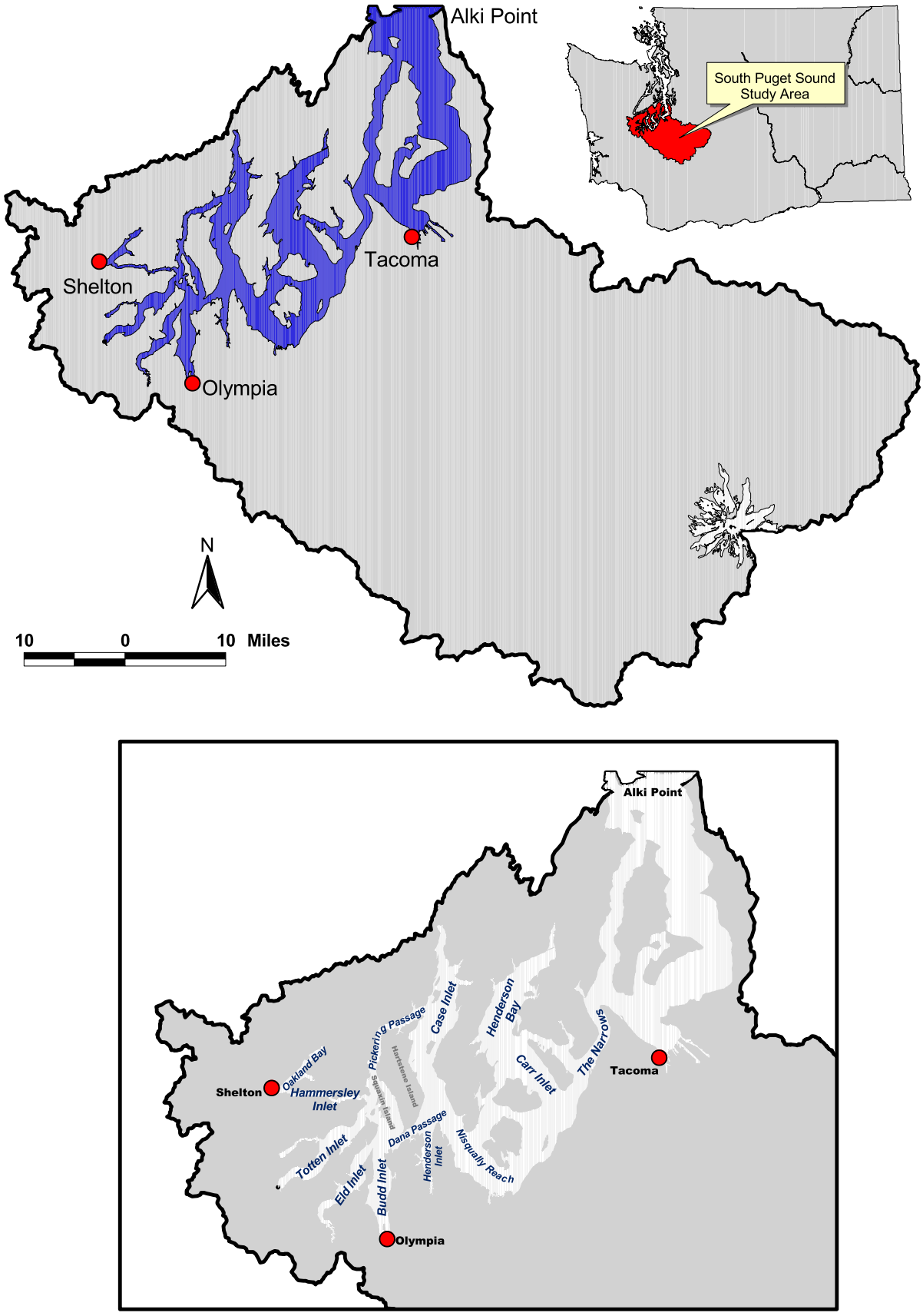

Figure 1-1. South Puget Sound study area.

This page is purposely blank for duplex printing

2. Oceanographic Field Studies in South Puget Sound

by J.A. Newton and R.A. Reynolds

Introduction

Impetus for a study on nutrient sensitivity of South Puget Sound was, in part, provided by recent assessments of water quality in greater Puget Sound that showed a high percentage of sites sensitive to eutrophication were focused in the South Puget Sound basin (Figure 2-1). Sensitive sites were identified from long-term marine waters monitoring data for 1990-1997, collected monthly by the Ecology's Environmental Assessment Program as part of the Puget Sound Ambient Monitoring Program (PSAMP). Five indicators were developed for this analysis, to identify a location's susceptibility to impacts from eutrophication (Newton et al., 1997; Newton et al., 1998):

- Persistence of density stratification.
- Presence of low dissolved oxygen concentrations.
- Occurrence of high concentrations of fecal coliform bacteria (indicating potential sewage or animal waste contamination).
- Occurrence of high concentrations of ammonium (indicating possible human or animal sewage sources).
- Depleted dissolved inorganic nitrogen (DIN; nitrate + nitrite + ammonium) for consecutive months during the phytoplankton growing season.

Results of this assessment are consistent with South Puget Sound's physical characteristics that suggest sensitivity to eutrophication, including relatively shallow depths, slow flushing time, physical stability of the water column, and high shoreline to water surface ratio. These features, coupled with the high projected human population growth in the counties surrounding South Puget Sound, argue for close monitoring of this basin's water quality.

However, long-term water quality data for South Puget Sound are relatively sparse. The best historical database for Puget Sound was compiled by Collias et al. (1974) for 1952-1966. However, South Puget Sound data were only collected from Case and Carr inlets. Additionally, this database does not contain nitrogenous nutrient data or phytoplankton chlorophyll measurements. Historically, Ecology's monthly monitoring data included only three stations in South Sound (Budd Inlet, Oakland Bay, and Dana Passage). Two additional stations, Gordon Point and Nisqually Reach, were added in 1997. The limited monitoring data available from South Puget Sound show a high degree of variability in water quality properties, both in time and space.

Intensive studies that have measured water properties at temporal and spatial scales smaller than those represented in the monitoring program have been conducted in only one area of South Puget Sound. Several studies focused on Budd Inlet (URS, 1986b; Tetra Tech, 1988; Eisner et al., 1994; Eisner and Newton, 1997; Newton et al, 1998; Aura Nova Consultants et al., 1998), primarily to assess water quality impacts from wastewater treatment plant discharges from the Lacey-Olympia-Tumwater-Thurston County facility. These studies confirmed that phytoplankton in Budd Inlet have a strong sensitivity to nutrient addition. The studies also showed that water properties vary significantly within Budd Inlet on time scales of weeks to days. Monthly observations grossly undersample the bloom dynamics of phytoplankton, which can change on the order of days. Stations closer to shore often have different oxygen, nutrient and chlorophyll content than those in the center of the bay or inlet, where regular monitoring typically occurs. Thus, while the monitoring data are useful as screening tools, these data do not provide adequate coverage of the inherent variation in both time and space of water quality properties.

Thus, increased spatial and temporal characterization of water properties is necessary to improve the evaluation of water quality sensitivity in South Puget Sound, and will enhance the utility of modeling the South Sound. A series of cruises throughout the South Puget Sound basin were conducted to partially fulfill this goal. The objectives of these cruises were to achieve the following:

- Provide data for initialization, calibration, and verification of the hydrodynamic model (Section 4) and the water quality model (Section 5).
- Characterize spatial and temporal patterns of basic water quality variables within South Puget Sound.
- Experimentally assess factors controlling phytoplankton production.
- Identify regions within South Puget Sound that potentially are sensitive to the effects of eutrophication.

The cruises were intended to improve our understanding of spatial variation within South Puget Sound on a seasonal basis, and were conducted in all four seasons (December, April, July, and September). The data obtained in these surveys provide snapshots of the variation in water properties at 80 stations throughout the basin at a given time.

As a complement to these surveys, a fixed monitoring station in Carr Inlet, operated through collaboration between the University of Washington (UW) and Ecology, provides valuable insight into high-frequency temporal variations. This study, a Coastal Intensive Site Network project, funded by EPA, NOAA, and NASA, uses a moored sensor package that autonomously profiles the entire water column four times a day and relays the data to shore. These data have been available since June 2000. Although these data will not be described in detail here, initial observations are used to enhance our emerging understanding of South Puget Sound water quality dynamics.

Methods

Field Surveys

Table 2-1 lists eight field surveys completed in South Puget Sound and analyzed as part of Phase 1. The research vessel *Clifford A. Barnes*, operated by the UW, was used to conduct surveys over a 3- to 5-day period. UW funded[2] cruises in December 1994 and September 1997. In partnership with UW, Ecology undertook several additional cruises at 3- to 5-month intervals to assess seasonal variability (winter, spring, fall, winter) during 1998 to 2000 under Phase 1 of the present study. This report will focus primarily on results of the Phase 1 1998-9 surveys, which allow examination of hydrographic and biological characteristics over a contiguous yearly cycle.

Table 2-1. Field studies in South Puget Sound as part of the South Puget Sound Study Phase 1. All surveys were conducted using the *R/V Clifford A. Barnes* operated by the University of Washington.

Year	Dates	Cruise ID
1994	December 14-15	9412B549
1997	September 3-5	9709B613
1998	December 14-17	9812B646
1999	April 20-23	9904B652
1999	September 20-23	9909B664
1999	December 13-16	9912B675
2000	July 10-14	0007B692
2000	September 25-29	0009B697

Beginning in December 1998, surveys monitored a grid of 80 sampling locations in the South Puget Sound basin (Figure 2-2 and Table 2-2). These sites include historical stations sampled by Ecology's Marine Waters Monitoring Program (http:// www.ecy.wa.gov/programs/eap/mar_wat/mwm_intr.html) and the UW (Collias et al. 1974), as well as several new sites added to enhance spatial coverage.

[2] Donation of ship time and PRISM (Puget Sound Regional Synthesis Model, http://www.prism.washington.edu/) funds for sample analyses.

Table 2-2. Location and identification of nominal stations sampled during project-related fieldwork. Historical station names used by Ecology (Eco), the University of Washington (UW), or the Lacey, Olympia, Tumwater, Thurston County Partnership (LOTT) are provided.

Station ID	Historical Station ID	Lat (˚N)	Long (˚W)
1	HND002 (Eco)	47.130	122.830
2	HND001 (Eco)	47.152	122.833
3	DNA001 (Eco)	47.162	122.870
4	BI5 (Eco/Lott)	47.052	122.907
5	BI4 (Eco/Lott)	47.060	122.908
6	BA2 (Eco/Lott)	47.072	122.914
7	BB2 (Eco/Lott)	47.083	122.916
8	BC3 (Eco/Lott)	47.102	122.917
9	BD2 (Eco/Lott)	47.114	122.908
10	BE1 (Eco/Lott)	47.129	122.909
11	BE2 (Eco/Lott)	47.130	122.915
12	BE3 (Eco/Lott)	47.129	122.921
13	BF2 (Eco/Lott)	47.145	122.910
14	BG2 (Eco/Lott)	47.151	122.908
15	465 (UW)	47.137	122.938
16	ELD001 (Eco)	47.107	122.948
17	ELD002 (Eco)	47.097	122.975
18	Ehope (New)	47.177	122.917
19	454 (UW)	47.180	122.930
20	Whope (New)	47.188	122.937
21	472 (UW)	47.173	122.953
22	TOT001 (Eco)	47.165	122.963
23	473 (UW)	47.157	122.987
24	476 (UW)	47.153	123.030
25	474 (UW)	47.140	123.013
26	475 (UW)	47.117	123.027
27	Nhope (New)	47.193	122.933
28	456 (UW)	47.203	122.925
29	480 (UW)	47.203	122.963
30	481 (UW)	47.205	123.000
31	482 (UW)	47.207	123.027
32	483 (UW)	47.203	123.057
33	484 (UW)	47.203	123.063
34	485 (UW)	47.208	123.083
35	486 (UW)	47.212	123.073
36	488 (UW)	47.235	123.050
37	457 (UW)	47.227	122.932
38	Squax1 (New)	47.215	122.912
39	455 (UW)	47.197	122.892
40	PK2 (New)	47.238	122.928

Station ID	Historical Station ID	Lat (˚N)	Long (˚W)
41	458 (UW)	47.250	122.923
42	459 (UW)	47.278	122.922
43	PK1 (New)	47.293	122.887
44	438 (UW)	47.307	122.850
45	437 (UW)	47.383	122.822
46	CS34 (Eco)	47.368	122.815
47	434 (UW)	47.353	122.810
48	CS32 (Eco)	47.332	122.813
49	436 (UW)	47.310	122.815
50	CS29 (Eco)	47.293	122.828
51	CS28 (Eco)	47.275	122.840
52	433 (UW)	47.258	122.853
53	CS26 (Eco)	47.243	122.842
54	432 (UW)	47.228	122.828
55	CS24 (Eco)	47.212	122.817
56	431 (UW)	47.197	122.807
57	CS21 (Eco)	47.182	122.798
58	407 (UW)	47.167	122.788
59	CS19 (Eco)	47.153	122.772
60	408 (UW)	47.175	122.733
61	CS18 (Eco)	47.145	122.755
62	CS17 (Eco)	47.135	122.740
63	CS16 (Eco)	47.122	122.723
64	406 (UW)	47.120	122.707
65	NSQ003 (Eco)	47.150	122.655
66	405 (UW)	47.183	122.633
67	404 (UW)	47.195	122.598
68	411 (UW)	47.212	122.622
69	413 (UW)	47.235	122.653
70	416 (UW)	47.260	122.697
71	419 (UW)	47.283	122.707
72	420 (UW)	47.313	122.707
73	421 (UW)	47.340	122.695
74	422 (UW)	47.358	122.667
75	423 (UW)	47.375	122.633
76	403 (UW)	47.248	122.573
77	402 (UW)	47.288	122.537
78	401 (UW)	47.317	122.560
79	324 (UW)	47.332	122.540
80	323 (UW)	47.315	122.503

Measurement Protocols

The sampling and analysis protocols used in this project were those in use by Ecology's Environmental Monitoring and Trends Section for its Marine Water Monitoring program (Newton et al., 1998). All protocols used are in compliance with the USEPA Puget Sound Estuary Program Standard Protocols (PSEP, 1997).

Two types of data were obtained: *in situ* measurements (using a sensor deployed in the field) and discrete samples (collected in a sampling vessel for subsequent analyses in a laboratory). *In situ* data, binned every 0.5 meter, include conductivity, temperature, pressure, water density, dissolved oxygen, light transmission, chlorophyll *a* fluorescence, photosynthetically active radiation (PAR). Secchi disk depth was determined at all stations occupied during daylight hours. Discrete samples at several depths within the water column were analyzed for salinity, dissolved oxygen, phytoplankton pigments, nutrients, phytoplankton species, and plankton biomass.

Table 2-3 lists *in situ* sensors and manufacturer. At each station, a conductivity-temperature-depth (CTD) unit was lowered through the water column to generate a depth profile. Sensors were equilibrated just below the sea surface, before the unit was lowered at a steady rate to a few meters above the sea bed and raised back to the sea surface. Data were averaged in 0.5-m vertical length bins and the downcast data were processed using manufacturer's software (Sea-Bird Electronics SEASOFT; versions used were those current for each sampling year).

Table 2-3. *In situ* sensors used for South Puget Sound surveys.

Parameter	Manufacturer
Conductivity (used to calculate salinity)	Sea-Bird Electronics®
Temperature	Sea-Bird Electronics®
Pressure (used to calculate depth)	Sea-Bird Electronics®
Density	(calculated from salinity and temperature)
Dissolved oxygen (DO)	Yellow Springs International® and Beckman®
Light transmission	Sea-Tech®
Chlorophyll *a* fluorescence	Sea-Tech®
Photosynthetically active radiation[3] (PAR)	LiCor®

In addition, at all daylight stations a Secchi disk was lowered to the depth of its disappearance and that depth recorded. This depth was then used in standard equations (Poole and Atkins, 1929) to determine the light extinction coefficient and the euphotic zone depth (e.g., Newton et al., 1998).

Accompanying the depth profiles, discrete samples of salinity, dissolved oxygen (DO), and phytoplankton pigments (chlorophyll *a* and phaeopigments) were obtained as check samples for salinity and as calibration samples for DO and chlorophyll *a* for the *in situ* sensors. Salinity, DO,

[3] Integrated light intensity over the spectral region 400 to 700 nm, which is of greatest importance to primary productivity.

and pigments were sampled using a rosette of Niskin bottles around the CTD, closed remotely at the desired depth. Sampling procedures for these parameters followed Ecology protocols (Janzen, 1992; Newton et al., 1998).

UW's state-accredited School of Oceanography Marine Chemistry Laboratory analyzed salinity using the state-of-the-art Guildline Instruments, Inc. Autosal® salinometer with standard seawater as a reference. Analysis followed the UNESCO (1994) protocol. Results for salinity were recorded as PSU (practical salinity units), which are generally equivalent to parts per thousand.

The titration of DO in seawater used the Carpenter method with a Beckmann Dosimat® microburet (Carpenter, 1964). This method is a refinement over the standard Winkler titrations, offering increased precision and accuracy for marine water samples. Samples were drawn into clean glass iodine flasks through tubing to minimize turbulence. The sample was fixed with $MnCl_2$ and NaI-NaOH-azide, inverted to mix, and stored out of direct light or heat. After a second mixing, H_2SO_4 was added prior to analysis and samples were titrated with sodium thiosulfate. This analysis was conducted onboard the ship within 48 hrs of sample collection. The equations in Strickland and Parsons (1968) were used to calculate DO in mg/L.

Fluorometric determination of chlorophyll *a* and phaeopigments was conducted using a Turner model 10 fluorometer and the standard acidification method of Lorenzen (1966). Seawater was filtered onto Whatman GF/F filters, the filter immersed in 90% acetone, and extracted in a dark freezer (to prevent photo-oxidation). The extract was sonicated to promote chloroplast lysis, centrifuged to remove cell and filter debris, and decanted into a cuvette for determination of fluorescence before and after addition of 2 drops 1N HCl. This analysis was conducted onboard the ship; samples were held in a freezer and analyzed within 48 hrs of collection. The equations of Lorenzen (1966) were used to calculate chlorophyll *a* and phaeopigments in µg/L.

Other discrete marine samples were obtained for parameters for which there were no *in situ* sensors. These include inorganic nutrient concentrations, phytoplankton production, and plankton biomass.

Seawater samples for dissolved nutrients were filtered through 0.45-µm cellulose filters in the field at the time of collection. The filtrate was dispensed into acid-washed, deionized water-rinsed bottles and frozen immediately onboard the ship. The Marine Chemistry Laboratory analyzed frozen dissolved nutrient samples while Ecology monitored QC data and procedures. Nutrient concentrations (µmoles/L = µM) were determined for nitrate, nitrite, ammonium, silicate, and orthophosphate.[4]

Phytoplankton primary production was estimated from standard ^{14}C uptake experiments (Steeman-Neilson, 1952) following more recent protocols of Barber (1992). Some of the precautions regarding trace metal contamination and toxicity (Fitzwater et al., 1982) were followed, including contamination of stock, acid cleaning and rinsing of incubation bottles, and

[4] Conversion to mg/L can be determined as: $\text{mg/L} = \frac{\mu M}{\mu\text{mole}} \times \frac{14.01\mu g}{1000\mu g} \times \frac{mg}{}$

use of silicone tubing/o-rings on Niskin bottles. Samples for phytoplankton production were collected from six depths at specified light levels within the euphotic zone (100%, 50%, 25%, 12.5%, 6.25%, and 1.6% surface irradiance), as determined from Secchi disk calculations.

Samples were obtained with clean Niskin bottles and dispensed into clean, acid-washed polycarbonate bottles. Sample bottles were inoculated with sodium bicarbonate ($NaH^{14}CO_3$) stock of a known activity. Replicate bottles were incubated in screened bags to mimic the light level at which samples were obtained and one bottle was incubated in the dark. At each depth, two sets of bottles were used for ambient and nutrient-spiked (nitrogen and phosphorus addition) treatments. Incubation was on-deck in a running seawater incubator for 24 h. At the conclusion of incubation, the sample was filtered, acidified to eliminate aqueous ^{14}C activity, and placed in scintillation vials filled with 10 mL EcoLume® scintillation fluor. At the beginning of the incubation, samples for abiotic uptake and adsorption (T_o) were inoculated, filtered immediately, and treated as above. From the T_o samples, 1-mL aliquots were removed and injected into a scintillation vial with fluor to determine the total activity added to sample bottles. The specific activity in the scintillation vials was counted using a Beckmann Liquid Scintillation Counter. Disintegrations per minute (DPMs) were converted to photosynthetic carbon uptake (primary production) in mg-C m^{-3} d^{-1} using standard equations (Strickland and Parsons, 1968).

Although no samples have been analyzed, samples for plankton biomass and species composition were taken following UNESCO (Hasle, 1978) protocols. At each productivity station, samples of plankton were collected in glass jars and preserved with 1% formalin. No funding was provided for analysis of these samples; however, if phytoplankton species abundance is desired, the samples will be retained for two years.

Data Reduction, Review, and Reporting

Digital data obtained using the CTD were logged internally, downloaded to a field laptop computer, processed, and stored in both raw and processed forms. Multiple backups were archived in paper and digital form. Software used in processing CTD data was the most recent version of SEASOFT® supplied by the CTD manufacturer, Sea-Bird Electronics, Inc. New software versions were tested for differences from calculated values and any changes noted in database documentation.

Graphics depicting the spatial distribution of measured parameters (both plan views and vertical cross-sections) were created by extrapolating data obtained at discrete stations, using custom-written gridding and interpolation routines created in MATLAB® (The MathWorks). Caution should be exercised in interpreting the graphical representation of data between actual sampling stations, particularly in regions of strong gradients where artifacts arising from interpolation may be significant.

Data from lab instruments were maintained on printed sheets in notebooks. Sheets were copied and one copy filed with the CTD data from each survey. The originals are maintained in the notebooks stored at Ecology. Raw data from the hard copy sheets were transcribed into standard template Microsoft Excel® spreadsheets that have transformation equations entered. Units were

recorded in all spreadsheets and data sheets, and are accounted for in all calculations. The data spreadsheet was then saved under a different file name. Calculations are checked for accuracy using previous known data.

Newton et al. (1998) describe data archiving procedures in more detail. Data are compiled into a Microsoft Access® database, following the format already in use by Ecology's Marine Waters Monitoring Unit.

Quality Control Procedures

Quality assurance procedures and objectives for these cruises followed those in the Quality Assurance Project Proposal written for similar marine studies in Puget Sound by Newton et al. (1998).

CTD sensors were evaluated monthly for blank (zero) and standard (or known) readings when possible for conductivity, temperature, DO, light transmission, and pH. Voltage readings for the CTD fluorescence and PAR sensors were verified for blanks under dark conditions. Failure to meet these criteria prevents use of the sensors until servicing. The data obtained from the CTD were processed using the manufacturer's software, then the processed data are checked for accuracy in values and coefficients. Failure to obtain 100% agreement results in a complete re-processing.

Laboratory instruments were also checked for blank and standard readings. The DO titration was subjected to three standard determinations and one blank determination, following published protocols (Strickland and Parsons, 1968). Analysis was not conducted unless two of the three standard values agreed within 0.002 mL and the blank determination was less than 0.010 mL. A blank reading for the lab fluorometer was determined using a 90% acetone sample that was required to read below 0.5 fluorescence units (FU). Due to the stability of the fluorometer, standards were not run, but every 6 to 8 months the instrument was calibrated against a dilution series of known concentrations of chlorophyll *a*, as determined by spectrophotometric analysis. Drift in instrument response between calibrations was extremely low. The PAR sensor was checked for zero readings (dark) and reasonable output at the time of use. Failure to obtain reasonable values from either the fluorometer or PAR sensor prevented further analysis.

Instruments owned by the UW Marine Chemistry Laboratory (salinometer, nutrient auto-analyzer) have prescribed QC check procedures that were followed by the lab personnel. Results of the checks for the samples from this project were made available to Ecology. The liquid scintillation counter was first run with blank and standard ^{14}C vials. The values for these vials were verified before proceeding with sample vial counts.

Preventative maintenance was routinely performed on all instruments, as indicated in Newton et al. (1998). All meters were maintained in accordance with the manufacturer's recommendations. Critical equipment and supplies are listed on a check-sheet and are the responsibility of the field personnel.

Results and Discussion

Water Temperature, Salinity, and Vertical Stratification

Water temperature and salinity strongly influence physical, chemical, and biological processes which directly impact water quality. These characteristics are determined locally by atmospheric heating and cooling, evaporation and precipitation, and by more remote processes such as the advection of Pacific Ocean water and riverine input. These processes all have strong seasonal variability in the Pacific Northwest region, and these patterns are reflected in the seasonal hydrography of South Puget Sound.

Stratification, which refers to the horizontal layering of water masses resulting from density differences, is an important physical characteristic influencing water quality. Temperature, salinity, and pressure are the principal determinants of water density, and thus vertical gradients in these characteristics determine the degree of vertical stratification. Water density increases with decreasing temperature and increasing salinity. Highly stratified water columns require large amounts of external energy in the form of wind and tides to mix, thus limiting the vertical exchange between layers. The intensity and persistence of stratification has important implications for water quality by influencing vertical transport of nutrients or pollutants, affecting the average amount of light available for phytoplankton growth, and controlling aeration of deeper waters by restricting mixing of oxygen-rich surface waters downwards.

Within Puget Sound, stratification is often determined by salinity gradients resulting from riverine freshwater input. In addition to large tributaries such as the Puyallup, Nisqually, and Deschutes rivers, a number of smaller creeks drain into various locations around South Puget Sound (see Section 3) leading to considerable spatial variability in salinity and stratification intensity.

Seasonal and spatial patterns

Surface waters of South Puget Sound, defined in this report as the 0.5 meter depth bin, exhibit significant seasonal trends in both temperature and salinity (Table 2-4). Surface water temperatures were coldest in the two December surveys and exhibit the smallest range of spatial variability (Figure 2-3). Surface temperatures increased only slightly by the April survey, most noticeably in small shallow inlets such as Hammersley, Totten, and Eld inlets. Average surface temperature increased to 15.2°C by September and had the greatest range of variation of all surveys, with the highest temperatures again observed in the smaller inlets and cooler temperatures occurring within and south of The Narrows near Tacoma. The latter observation likely results from vertical entrainment to the surface of deep water entering from the main basin of Puget Sound as it passes through The Narrows.

Table 2-4. Temperature and salinity characteristics of surface (0.5-meter depth bin) water from South Puget Sound surveys. Temperature is reported in units of degrees Celsius, salinity in PSU (practical salinity units). The coefficient of variation (CV, in percent) is provided within the parentheses.

	Surface Temperature [ºC]		Surface Salinity [PSU]	
Survey	Range	Mean (CV)	Range	Mean (CV)
Dec-98	8.2 – 10.6	9.5 (6.5)	13.6-29.8	25.5 (14.1)
Apr-99	8.9 – 11.8	10.1 (7.7)	22.1-28.4	26.6 (4.8)
Sep-99	11.9 – 18.4	15.2 (8.6)	26.9-29.9	28.8 (26.9)
Dec-99	7.1 – 10.0	9.2 (6.4)	14.9-29.3	26.0 (28.0)

Surface salinity values vary more than twofold throughout the year, ranging from 13.6 to 29.9 practical salinity units (PSU)[5]. In contrast to temperature, the greatest variability in surface salinity occurs in December (Figure 2-4), coincident with the period of peak flows for many of the rivers feeding into South Sound. Freshest values were observed during this period, primarily near regions of high river flow such as the Nisqually Delta, the northern head of Case Inlet, and Hammersley Inlet. Surface salinity values increased through summer and were relatively uniform throughout the study region by the September survey.

In estuaries with significant freshwater input such as Puget Sound, variations in salinity generally have the greatest influence on determining patterns in water density. For convenience, water density is often expressed in terms of sigma-*t* (σ_t) [6]. An indicator of the degree of water column stratification, $\Delta\sigma_t$, was calculated as the arithmetic difference between the surface layer (0.5 m depth bin) density and the near-bottom layer (defined in this report as within 5 m of the bottom) density. Larger differences in values between these two layers indicate a more strongly stratified water column, thus requiring greater wind or tidal energy to initiate mixing. In regions of low energy, persistent stratification of the water column can effectively isolate deeper waters from the surface layer.

During winter months, stratification is relatively strong throughout South Puget Sound as a result of large vertical gradients in salinity maintained by high precipitation and resulting river flow (Figure 2-5). One notable exception to this trend is the area immediately around The Narrows, a region of strong currents. Following the winter months, stratification intensity in general appears to decrease as freshwater inputs lessen and salinity gradients are reduced. Nevertheless, several regions in South Sound appear to maintain measurable stratification throughout this time period, most notably in Carr, Case, and Budd inlets, and in the immediate vicinity of the Nisqually River. These areas still have significant inputs of freshwater from adjacent rivers, although flows are reduced compared to winter values.

[5] Oceanographers express salinity in terms of practical salinity units (PSU), which is roughly equivalent to parts per thousand.

[6] Sigma-*t* is calculated from water density; σ_t = density (kg m^{-3}) –1000.

Transects of vertical distributions

Transects conducted along the length of Carr and Case inlets suggest that water column stratification can persist throughout much of the year (Figures 2-6 and 2-7), primarily maintained by vertical gradients in salinity. In December, temperature is generally uniform both horizontally and vertically; freshwater input at both northern and southern ends of these inlets result in strong salinity and density gradients. These gradients weaken towards the middle of these inlets, resulting in a deeper surface layer. Following the cold wet months of winter, these inlets are colder and fresher in April and the depth of the surface layer decreases; this pattern is more pronounced in Carr Inlet. Water temperature and salinity increased overall by September, and steep vertical gradients in both parameters appear to maintain density stratification of the upper 10 to 20 meters of the water column until overturning occurs in late fall.

The consequences of stratification are evident in the seasonal and spatial distributions of water column properties such as dissolved oxygen, inorganic nutrients, and phytoplankton biomass. Regions where stratification is persistent throughout much of the spring and summer are more favorable for phytoplankton growth and accumulation in the surface layers, resulting in depletion of inorganic nutrients at the surface and a drawdown of dissolved oxygen in underlying waters.

Dissolved Oxygen

Concentrations of dissolved oxygen reflect the net balance of oxygen sources (atmospheric and photosynthetic input), losses (consumption through chemical oxidation and biological respiration), and physical advection. Stratification isolates bottom waters from atmospheric gas exchange, and these layers may become depleted in oxygen over time as oxygen is consumed. During the phytoplankton growing season (spring and summer), this problem is exacerbated as stratification also stimulates the photosynthetic production of organic matter by maintaining phytoplankton cells within well lit surface waters; when this material sinks into deeper layers, its decomposition consumes large amounts of oxygen. Concentrations of dissolved oxygen below 5 mg/L are generally considered the level at which marine biota begin to experience oxygen stress, with concentrations below 3 mg/L having detrimental effects on the health of many organisms.

Seasonal and spatial patterns

Figure 2-8 depicts spatial patterns in near-bottom concentrations of dissolved oxygen obtained from the 1998-9 cruises. The data in this figure depict oxygen concentrations measured at the deepest portion of the water column sampled with the CTD (conductivity-temperature-depth profiler) at a particular station, usually within 5 m of the actual bottom, and thus can be considered as representative of the bottom layer of the water column. The bottom depth varies considerably among stations, ranging from greater than 100 m in some areas to less than 3 m at the head of small inlets. Because sharp gradients in oxygen concentrations often are observed at the sediment-water interface, these data should not be considered indicative of concentrations likely to be experienced by organisms dwelling within the benthos.

For both December surveys, values of dissolved oxygen near the bottom show little spatial variation, averaging around 7.5 mg/L. These concentrations had increased by the April survey, with measurements typically greater than 10 mg/L and approaching or exceeding saturation values. This contrasts markedly with the September surveys, where dissolved oxygen generally decreases throughout the Sound and depletion is observed in some areas. Lowest values were observed in Budd Inlet, where four stations recorded dissolved oxygen concentrations less than 3 mg/L. These observations are consistent with previous studies in this inlet (Eisner et al., 1994; Eisner and Newton, 1997). Of particular interest, however, is the observation that large portions of both Carr and Case inlets show significant drawdown of near bottom dissolved oxygen concentrations (Figure 2-9), with values approaching 5 mg/L. This suggests that these areas would be particularly susceptible to increased loading of organic material.

Transects of vertical distributions

Transect data from Carr and Case inlets confirm that September concentrations of dissolved oxygen have steep vertical gradients with values decreasing near the bottom. The influence of photosynthetic production of oxygen is evident in surface layers in both April and September. Dissolved oxygen concentrations become uniform throughout the water column in December.

Dissolved Nutrients

During periods of the year when sufficient light is available for photosynthesis, the availability of inorganic nitrogen can become a growth-limiting factor for phytoplankton growth in Puget Sound. Waters of Puget Sound are naturally high in dissolved inorganic nitrogen sources such as nitrate, owing to the large annual input from deep Pacific Ocean waters entering the Strait of Juan de Fuca, and to a lesser extent terrestrial contributions through rivers and streams. Depletion of nitrogen has been observed only in surface waters with persistent stratification throughout the growing season, where phytoplankton populations may draw down nitrogen concentrations to levels approaching zero.

Seasonal and spatial patterns

High concentrations of nitrate in surface waters were observed throughout the Sound during December (Figure 2-12), exceeding concentrations of 15 μM (0.93 mg/L). Nitrate in surface waters decreases considerably throughout much of the Sound by April (values < 0.5 μM or <0.03 mg/L) and this depletion is even more widespread in September.

Transects of vertical distributions

Transects depicting the vertical distribution of nitrate and ammonium in Carr and Case inlets illustrate the seasonal drawdown of nitrogen in surface waters (Figures 2-11 and 2-12, respectively). During winter high concentrations of nitrate and low concentrations of ammonium persist throughout the entire water column. By summer, surface nitrate is depleted (likely due to uptake by phytoplankton), while bottom ammonia is enriched (likely due to nutrient regeneration).

Phytoplankton Biomass and Productivity

Chlorophyll *a* is a major light-harvesting pigment common to nearly all photosynthetic organisms, and is commonly used as a proxy for algal biomass in aquatic ecosystems. It is also a fluorescent molecule, which allows the vertical distribution to be measured at high resolution with *in situ* instruments. Although a convenient indicator of phytoplankton populations, chlorophyll *a* amounts per cell can vary markedly among species or in response to growth conditions (e.g., light or nutrient availability), and therefore cannot be directly converted to other common measures of biomass, such as numbers of cells.

Phytoplankton concentrations vary markedly on short temporal and spatial scales as environmental conditions change, and reflect the balance between growth of the population and losses due to advection, herbivory, and cell death or sinking. Regions with rapid accumulation of phytoplankton biomass, known as blooms, result when favorable environmental conditions allow growth rates to exceed loss rates. Growth rates depend upon the availability of sufficient light energy to drive photosynthesis, availability of nutrients for incorporation into biomass, and the stability of water column to maintain cells within the well lit surface layer.

Seasonality and spatial distribution of chlorophyll *a*

Blooms, generally ephemeral in nature, last on the order of a few to several days; thus, field surveys provide only a snapshot in time of a continually varying process. During winter months, light availability limits phytoplankton growth and chlorophyll *a* concentrations are uniformly low throughout the entire South Puget Sound (Figure 2-13). During both April and September cruises, high concentrations (chlorophyll *a* > 40 µg/L) were observed in surface waters, but these blooms are highly localized phenomenon. Transects of Carr and Case Inlet show that these blooms have restricted horizontal and vertical distributions even within an inlet (Figure 2-14).

Seasonality and spatial distribution of primary production

Data from the five cruises from December 1998 to July 2000 exhibit a typical seasonal pattern of ambient levels of phytoplankton primary production integrated over the euphotic zone. April had the highest values (around 6000 mg-C m^{-2} d^{-1}), reflecting the spring bloom, while July and September had moderate values (around 3000 mg-C m^{-2} d^{-1}) and December had very low values (~30 mg-C m^{-2} d^{-1}), reflecting light limitation and cold temperatures (Figure 2-15). These values are similar for those reported in Budd Inlet (Newton et al., 1998) and are relatively high when compared to other estuaries, suggesting that South Puget Sound is very productive.

Spring (April) integrated productivity values at all South Puget Sound stations were quite similar, ranging from 5,100 to 6,400 mg-C m^{-2} d^{-1}. Spatial variation increased during the summer months (July and September) with ranges from 2,300 to 4,300 and 2,100 to 5,200 mg-C m^{-2} d^{-1}, respectively. During both of these months, primary production in Carr Inlet was the smallest or next to smallest relative to the other four stations (Figure 2-15), implying a possible growth limitation in this inlet.

Nutrient limitation of production

To assess whether nutrients stimulate primary production, primary productivity determinations were conducted on water samples using two experimental treatments: one set of water samples were measured with no additional treatment to represent ambient conditions, while a second set received additions of nitrogen and phosphorus, simulating nutrient enrichment from humans. If phytoplankton are not affected by the addition of nutrients, then another factor (e.g., sunlight or mixing) controls production rates. Lack of phytoplankton stimulation would indicate that increased loading from humans likely will not impact phytoplankton production and consequent bottom-water oxygen deficits. However, if production is stimulated by added nutrients, more carbon will be produced, which will ultimately consume more oxygen as the organic material sinks and decomposes.

The nutrient-addition experiments conducted in South Puget Sound show significant increases in primary productivity (Figure 2-16). As shown by carbon fixation rates in the surface bottles, where the nutrient stimulation was maximal, this increase was largest in summer, variable in spring, and absent in winter. This pattern reflects the availability of surface nitrogenous nutrients measured. The net amount of carbon production increase from the addition of nutrients (i.e., the arithmetic difference between the spike and ambient treatments) was as high as 1,500 mg-C m^{-3} d^{-1} in the surface water and 4,500 mg-C m^{-2} d^{-1} integrated over the entire euphotic zone.

A seasonal time series of the change in nutrient-stimulated production, expressed as a percent of the ambient (naturally-occurring) production, shows strong evidence for nutrient sensitivity in South Sound (Figure 2-17). During the latter half of the growing season (July to September), Carr Inlet shows the highest percentage increase, indicating that nutrients strongly limit phytoplankton growth. Thus, Carr Inlet has a strong potential to be affected by increased nutrient loads. Future studies should determine whether this amount of additional carbon production could result in reduced water quality from oxygen depletion. The amount of carbon that would be produced during eutrophication of Carr Inlet could be calculated, and the resulting near-bottom dissolved oxygen concentrations could be modeled to assess the significance of this impact on oxygen levels and water quality.

While the spike additions in these experiments added both nitrogen and phosphorus, evidence suggests that nitrogen is the limiting nutrient, as is typical for marine systems and has been documented for Budd Inlet (Eisner and Newton, 1997). A plot of nitrate versus orthophosphate in Carr Inlet (Figure 2-18A) shows a typical Redfield ratio between the elements (about 16:1). As nitrate goes to zero, excess orthophosphate is still found. Results are consistent with historical patterns, where surface waters had measurable phosphorous concentrations while nitrate, nitrite, and ammonium were below detection levels. Further evidence of nitrogen control of phytoplankton is shown by the strong overlap in chlorophyll *a* fluorescence with that of nitrate contours in the water column of Carr Inlet during the growing season (Figure 2-18B).

Temporal Variation

It is important to note that the observations of water quality and dynamics of the nutrient-phytoplankton-oxygen interactions in this report are based on snapshot views afforded by single

visits to a station in a given month. This snapshot view is being used to offer a representative view of a given season; however, there may be inherent bias in our interpretation for a given seasonal view due to the non-representativeness of a single day for a season. For instance, the variation shown in chlorophyll patterns is quite strong in July and September, yet the variation in water properties that should determine phytoplankton biomass (e.g., stratification, nutrients, light penetration) is not as strong. The ability to demonstrate how local conditions influence blooms is quite low. Clearly there are mechanisms responsible for the chlorophyll variation, but discerning these will require field observations on a time scale of days to hours, which is the lifetime of phytoplankton cells.

Ecology's collaboration with the University of Washington (CISNet project) on the innovative deployment of a profiling mooring with sensors to monitor water quality properties will improve substantially the ability to interpret variation in nutrient, phytoplankton, and oxygen dynamics. Figure 2-19 provides examples of the initial data collected by this unit, which provides vertical profiles of the water column multiple times daily. The data capture seasonal patterns, such as summertime trends of increasing salinity and decreasing oxygen with time. Also evident is significant small-scale variation at smaller temporal scales; the mechanisms responsible for this variation are presently being investigated as part of this project.

Summary and Conclusions

Stratification intensity and persistence are quite variable in South Puget Sound. Salinity gradients, as well as seasonal temperature increases, are evident in some areas (for example, Budd, Carr, and Case inlets), leading to persistent or seasonal stratification of large areas of South Puget Sound. Stratification in other areas is weak, owing to strong tidal mixing in some of the shallower inlets (for example, Hammersley and Totten inlets and Dana Passage).

Some inlets that are replete with nutrients at the beginning of the growing season show a surface depletion of nitrogenous nutrients by the early spring that last through late summer. This indicates the significant utilization of nutrients by phytoplankton when light is available for photosynthesis.

Discrete measurements of chlorophyll *a* at bloom concentrations (15-60 µg/L) often accompany the spatial and temporal depletion of surface nitrate. The location of such blooms are random and non-repetitive, indicating the strong ephemeral nature of these events. The data obtained from occasional surveys are insufficient to elucidate the principal factors responsible for producing a bloom in one place and not in another location.

Low concentrations of dissolved oxygen in bottom-water samples were observed during late summer, reaching the threshold of biological stress (5 mg/L) in Carr and Case inlets and exceeding the threshold in Budd Inlet (2 mg/L).

Phytoplankton productivity can be limited by nitrogen availability during the growing season. Nutrient addition substantially enhanced measured rates of primary production, especially in late summer.

The above observations indicate that areas within South Puget Sound are sensitive to increased nutrient loadings and consequent eutrophication. The strongest water quality concerns in regards to eutrophication appear to be in Carr, Case, and Budd inlets. While other smaller inlets do exhibit nutrient sensitivity at times, these are generally well-mixed by tides so that strong oxygen gradients do not appear.

The South Puget Sound system is sensitive to the addition of nutrients. The heightened sensitivity of some locations in South Sound, relative to other locations, may have implications for planning and permitting discharges. Nutrient sensitivity should be taken into account not only for local but also for basin-wide considerations.

This field assessment still includes a number of unknowns. First, data collection may not have captured baseline conditions, since South Puget Sound already may be affected by nutrient enrichment. Without extensive, long-term historical data there is no way to determine whether phytoplankton blooms are more frequent or larger than 40 years ago. Second, while the study has focused on quantitative impacts on phytoplankton and oxygen concentrations from nutrient addition, the study has not addressed how the species composition of the phytoplankton community might be altered, which has implications to upper trophic levels. Unfortunately, no easy methods exist and scientific understanding of this issue is lacking.

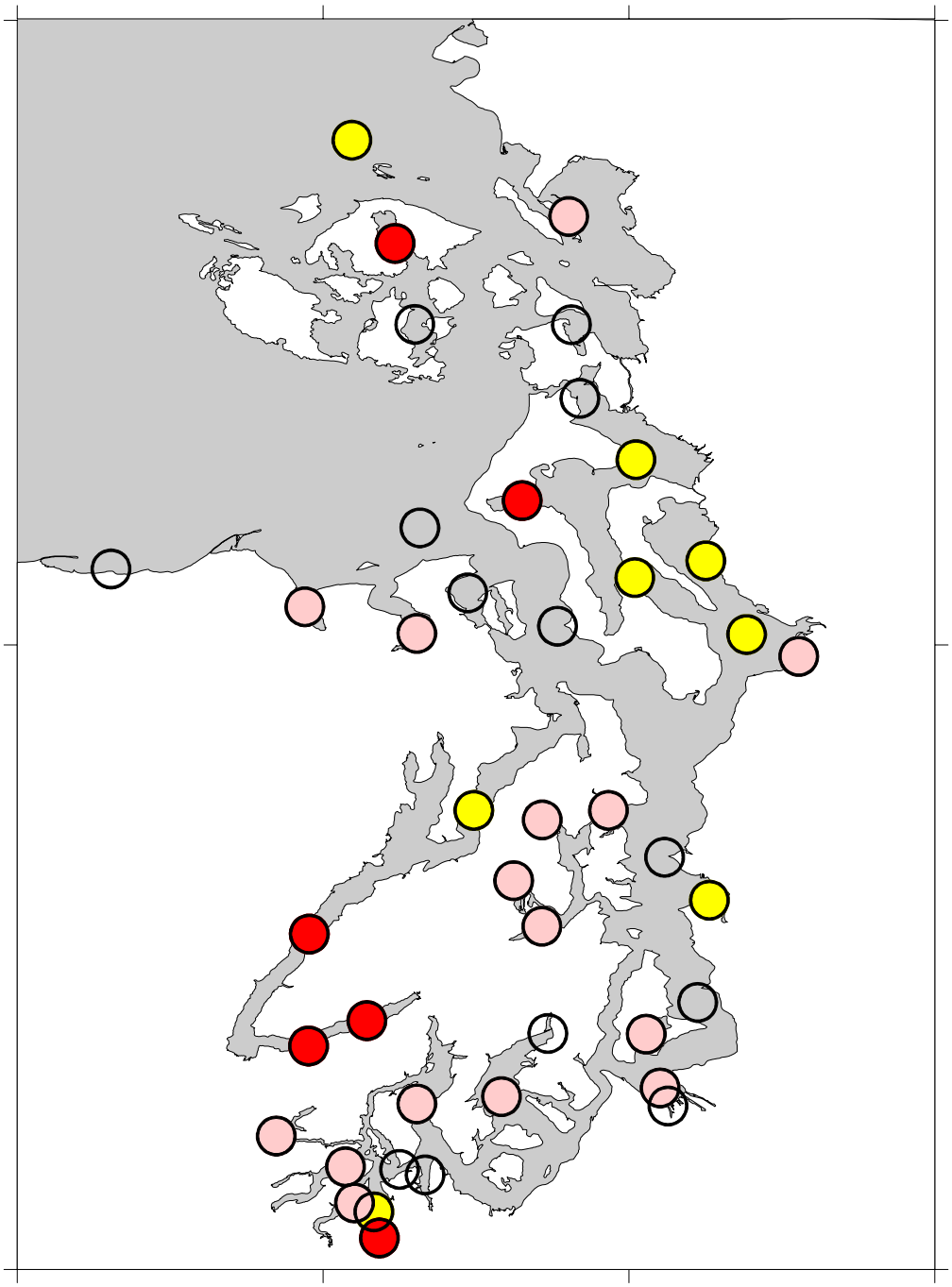

Figure 2-1. Ecology's Marine Waters Monitoring stations exhibiting either low dissolved oxygen concentrations (*red:* hypoxia <= 3 mg/L; *yellow:* biological stress level <= 5 mg/L) or sensitivity to impacts from eutrophication based upon physical and chemical characteristics *(pink)*. Stations assessed but with neither condition are also shown (*clear*).

The graphic is a compilation of monthly Ecology-PSAMP data for water years (WY) 1990-1997. Not all stations were monitored in all years, so classification was based on the occurrence of a condition within one or more years. Prior to WY 1990, data are not comparable due to refinements and changes in analytical and sampling techniques.

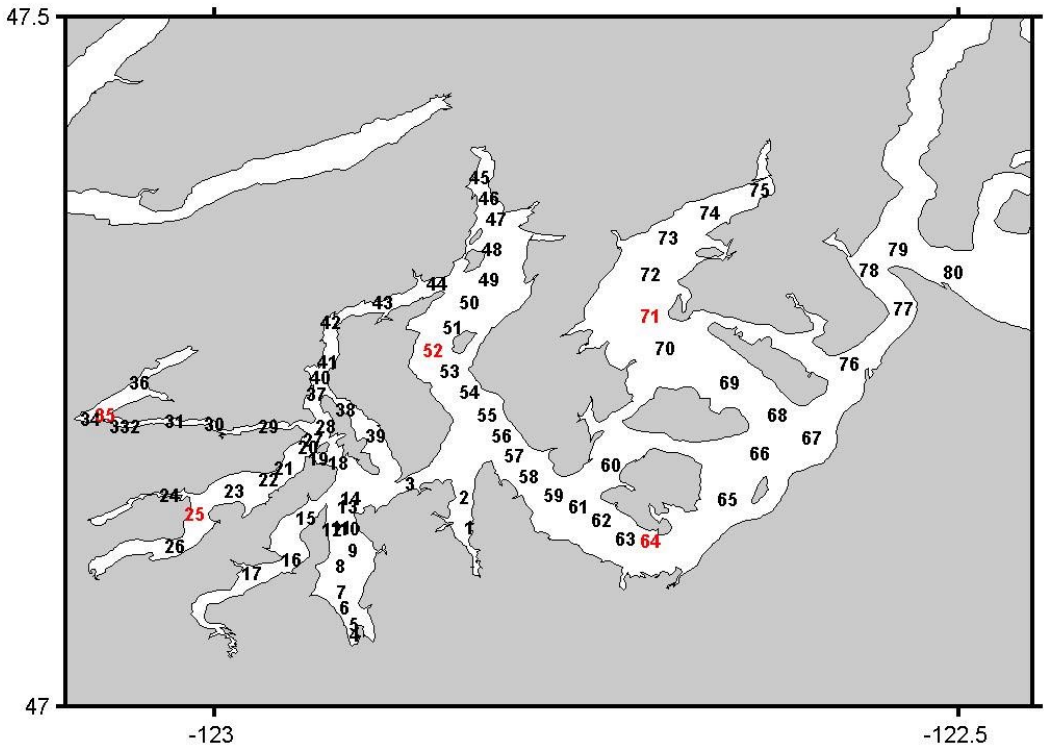

Figure 2-2. Station locations for South Puget Sound Study field surveys. Red numbers indicate stations where primary productivity experiments were conducted.

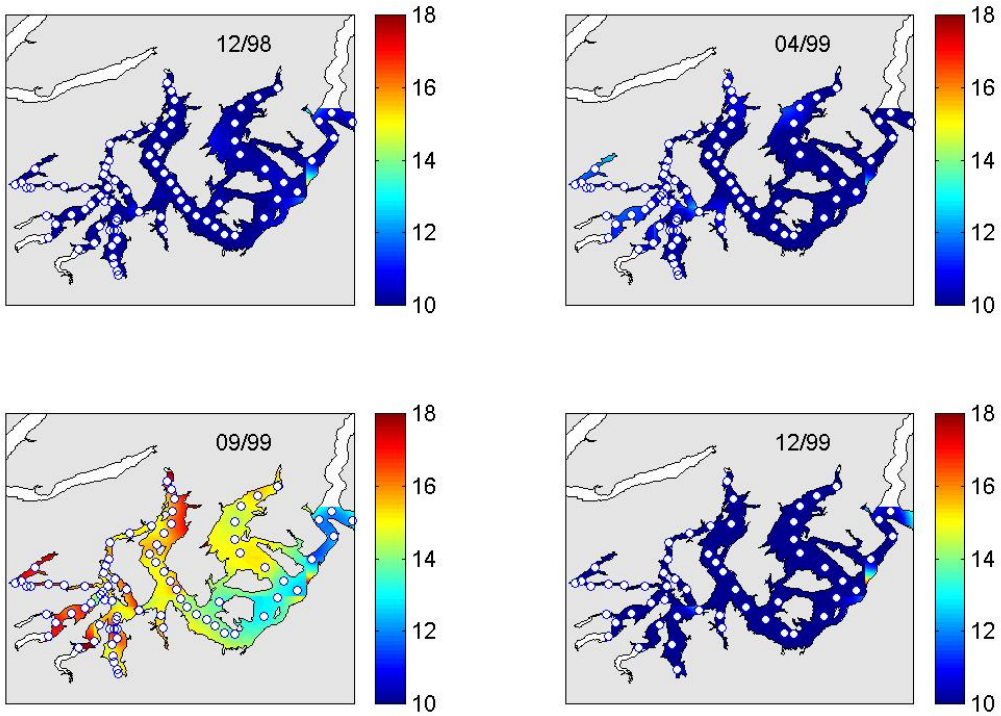

Figure 2-3. Distribution of sea surface temperatures (°C, 0.5m depth bin) determined from field surveys.

White circles indicate sampling locations from which data were obtained and used to interpolate between stations.

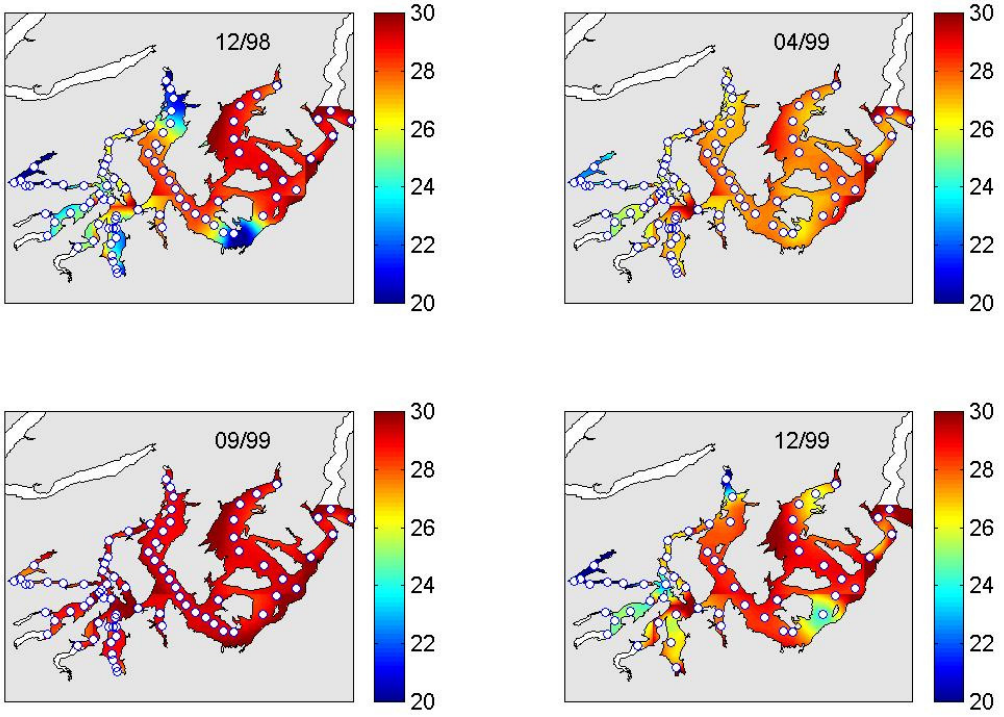

Figure 2-4. Distribution of sea surface salinity (PSU) determined from field surveys.

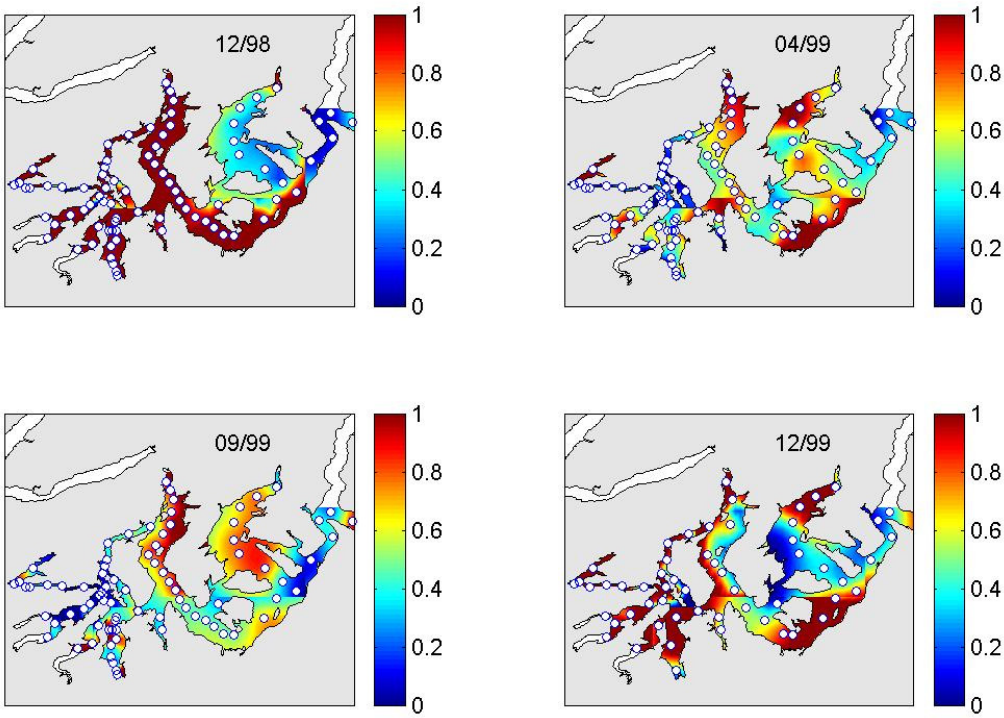

Figure 2-5. Stratification intensity as estimated by the arithmetic difference in sigma-*t* ($\Delta\sigma_t$) between the surface and near-bottom (within 5 meters of the bottom) layers of the water column.

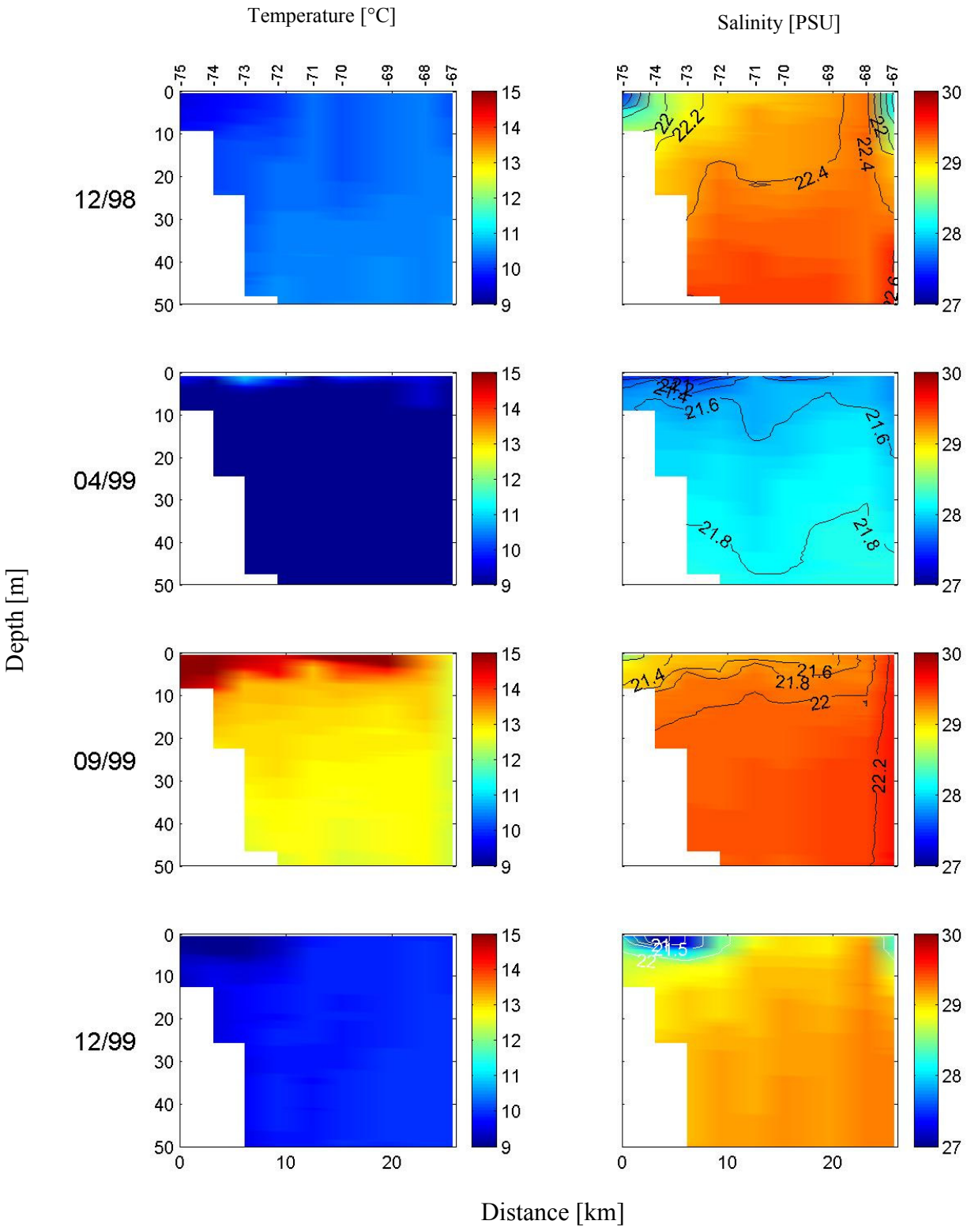

Figure 2-6. Vertical distributions of temperature (left panels), salinity (right panels, false color), and σ_t (right panels, contour lines) along Carr Inlet. Station numbers are indicated at the top of the uppermost figures.

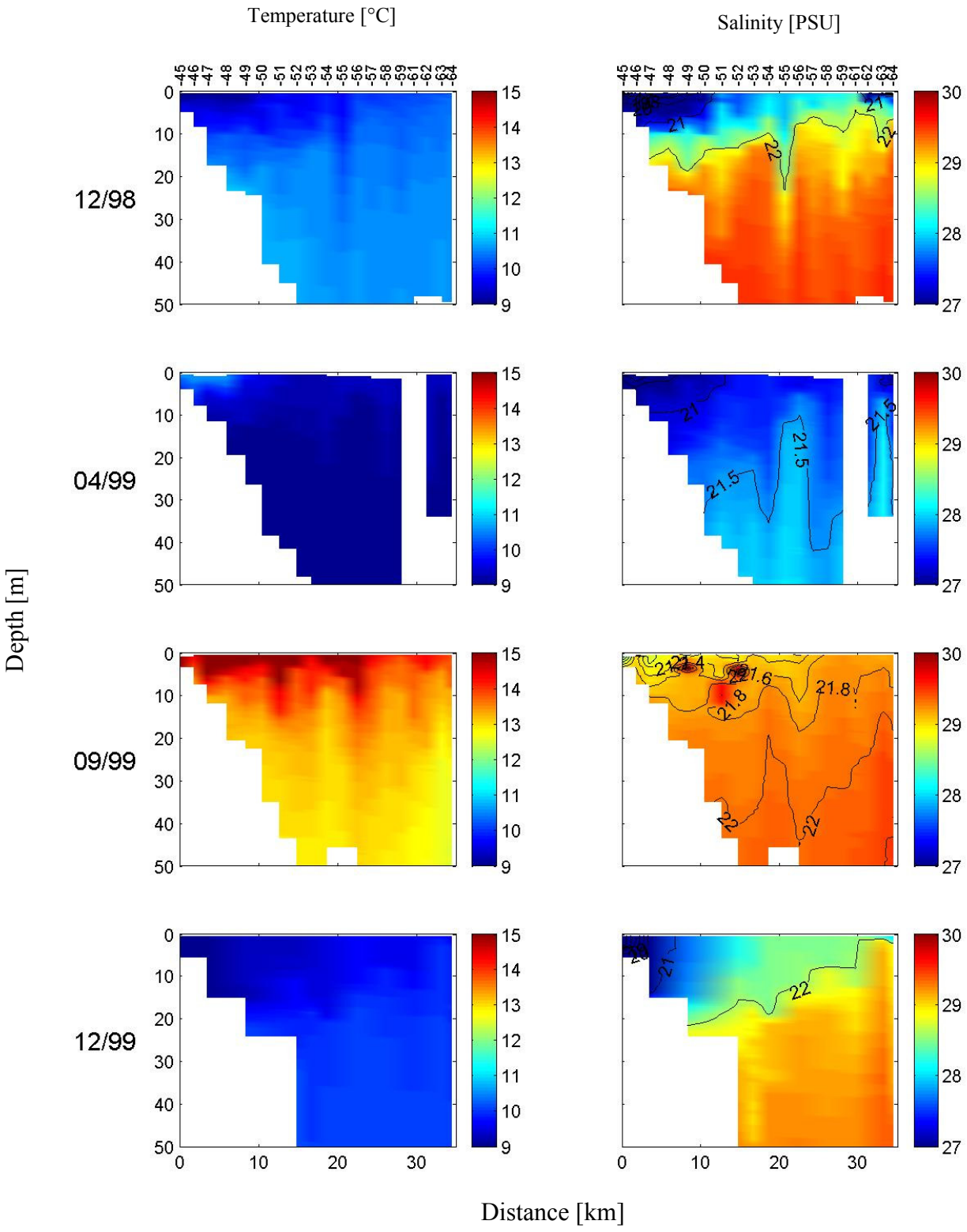

Figure 2-7. Vertical distributions of temperature (left panels), salinity (right panels, false color), and σ_t (right panels, contour lines) along Case Inlet. Station numbers are indicated at the top of the uppermost figures.

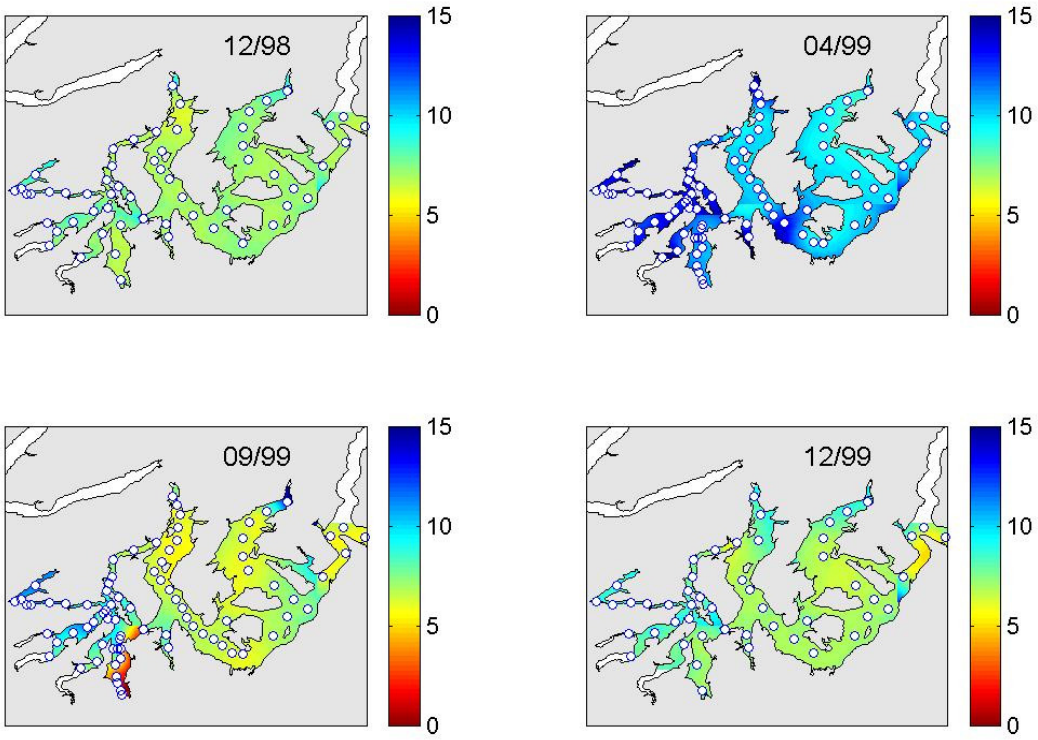

Figure 2-8. Dissolved oxygen concentration (mg/L) in near-bottom waters at different times of the year.

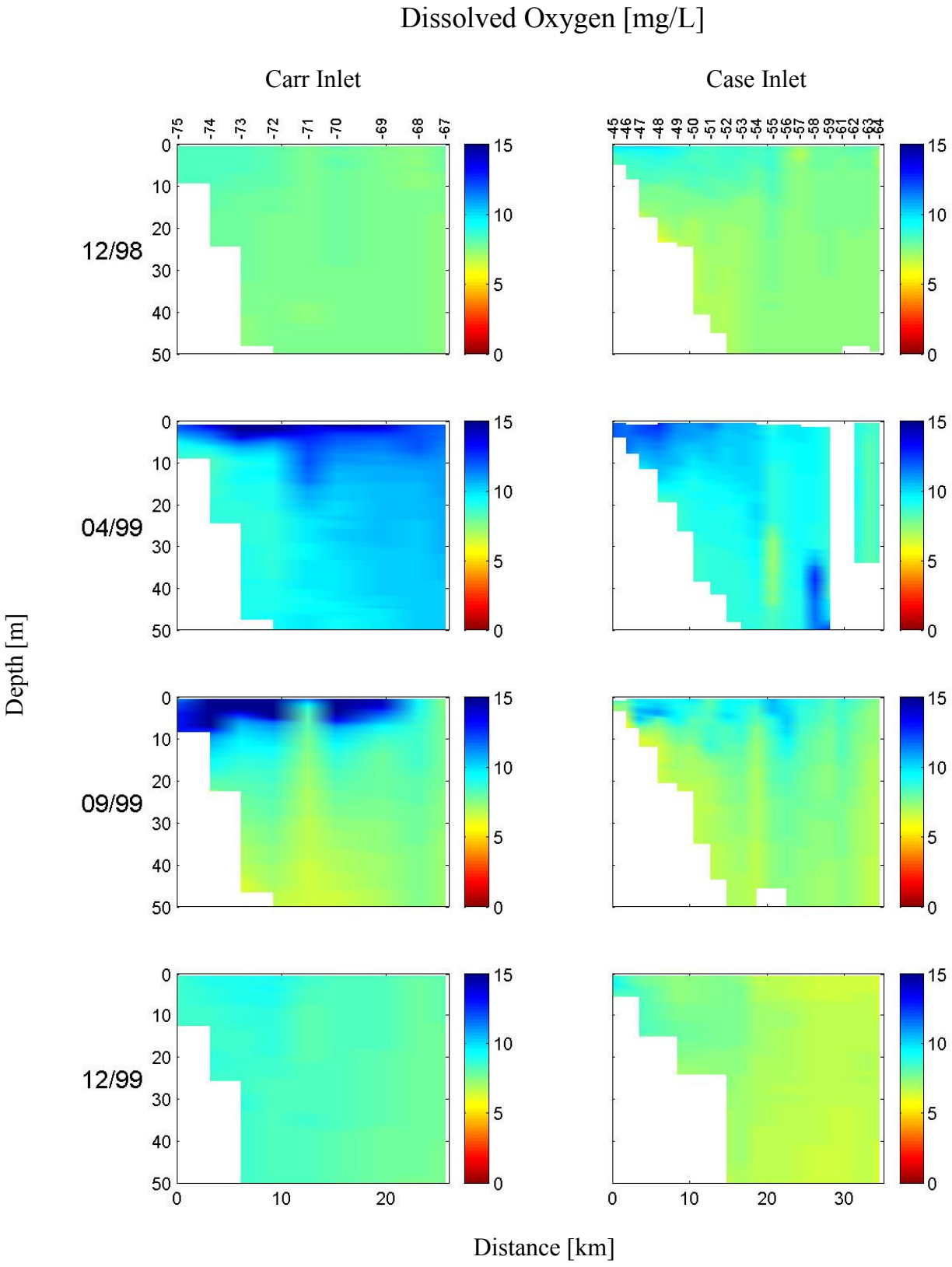

Figure 2-9. Dissolved oxygen concentrations (mg/L) along Carr Inlet (left panels) and Case Inlet (right panels). Station numbers are indicated at the top of the uppermost figures.

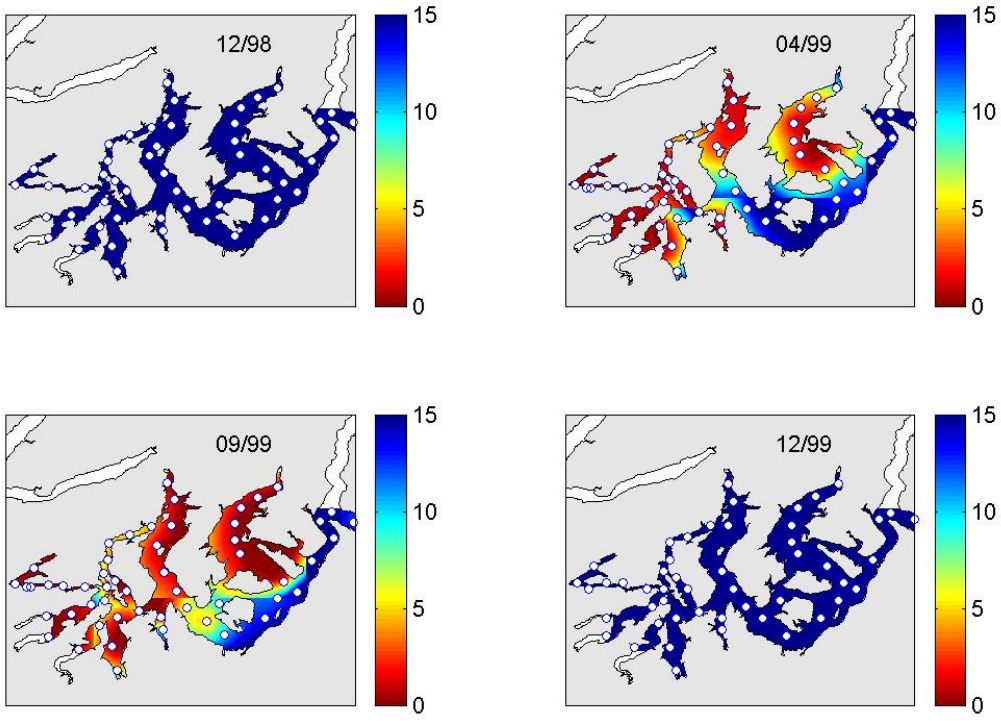

Figure 2-10. Distribution of surface nitrate concentration (μM) determined from field surveys.

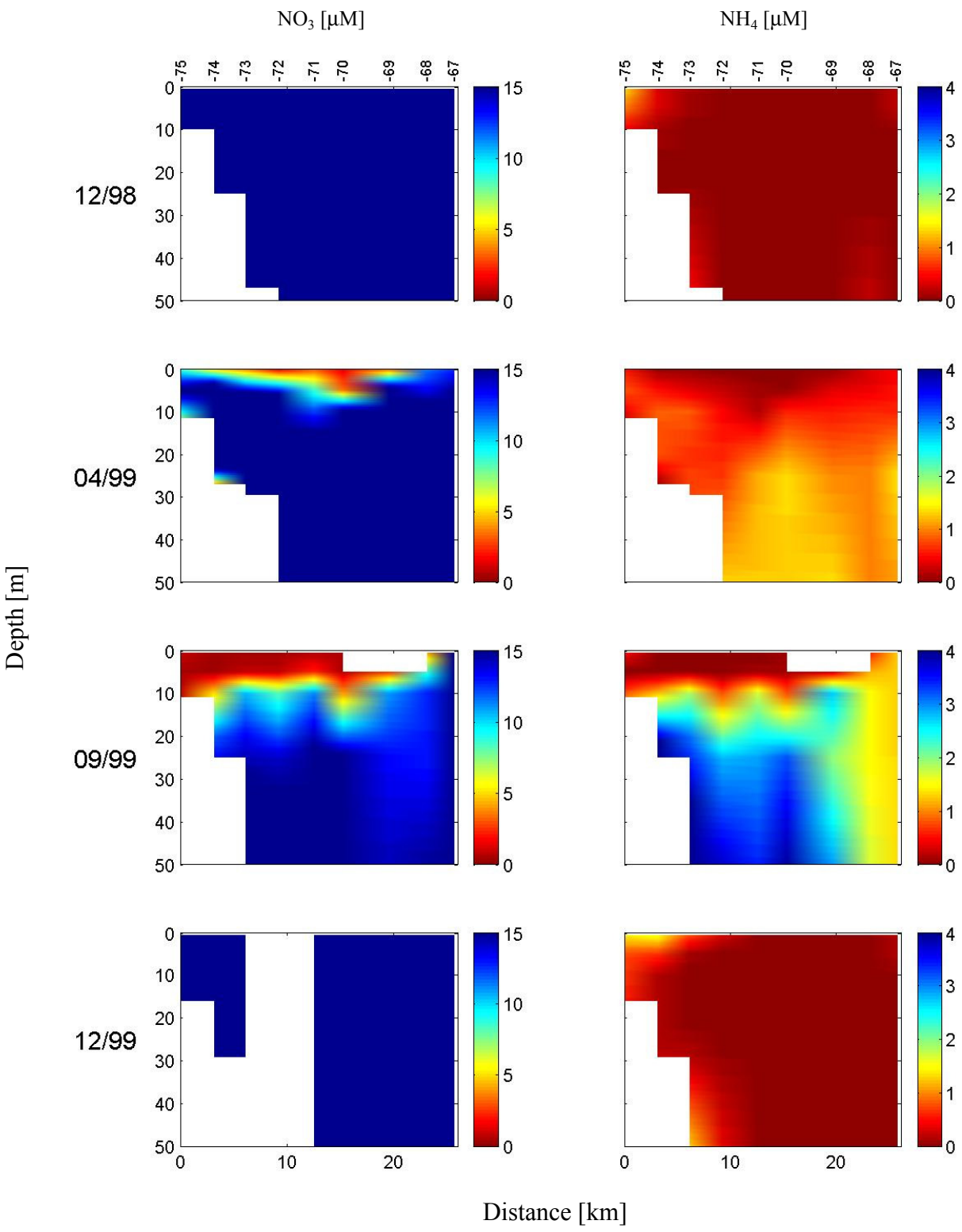

Figure 2-11. Distributions of nitrate (left panels) and ammonium (right panels) in Carr Inlet. Station numbers are indicated at the top of the uppermost figures.

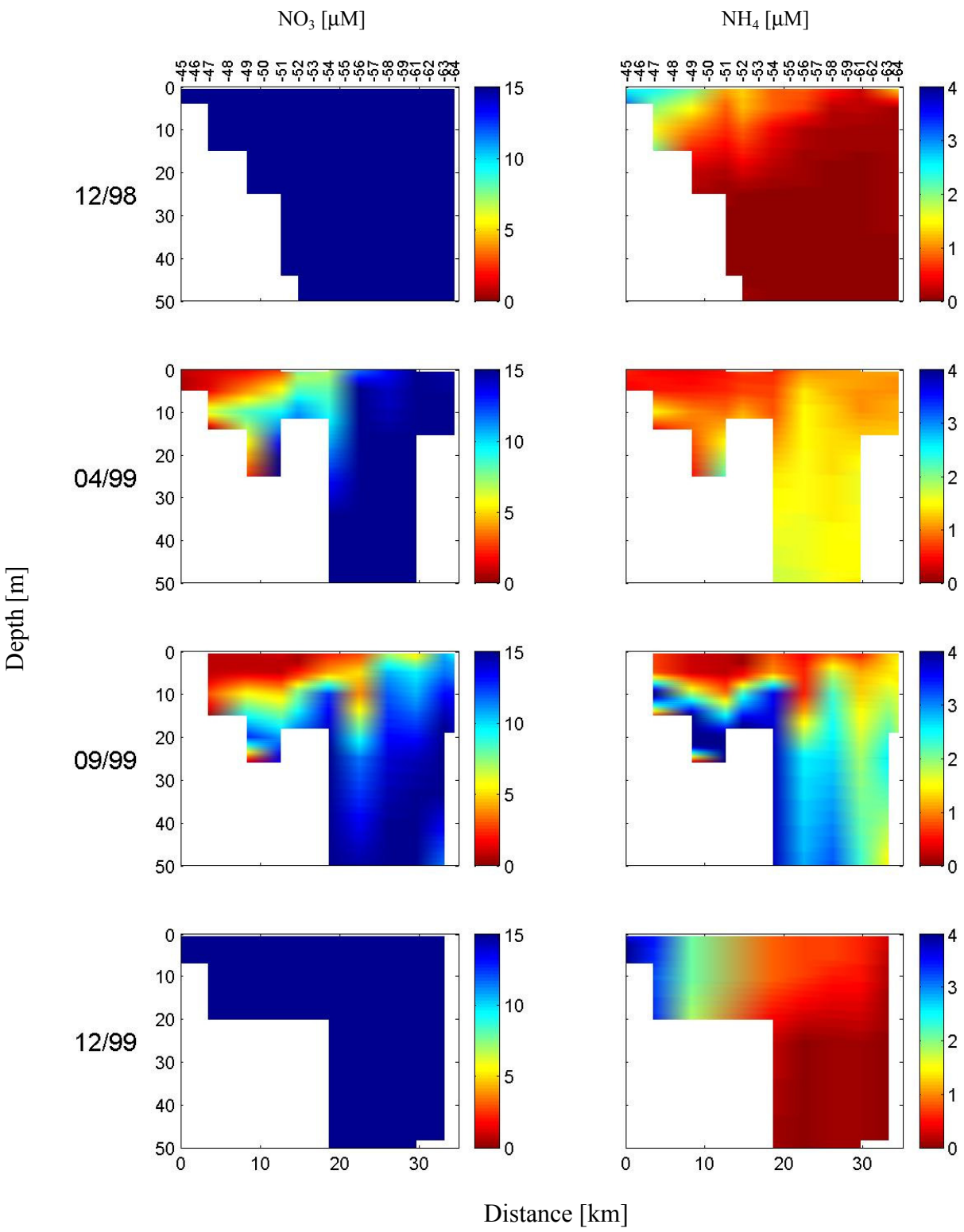

Figure 2-12. Distributions of nitrate (left panels) and ammonium (right panels) in Case Inlet. Station numbers are indicated at the top of the uppermost figures.

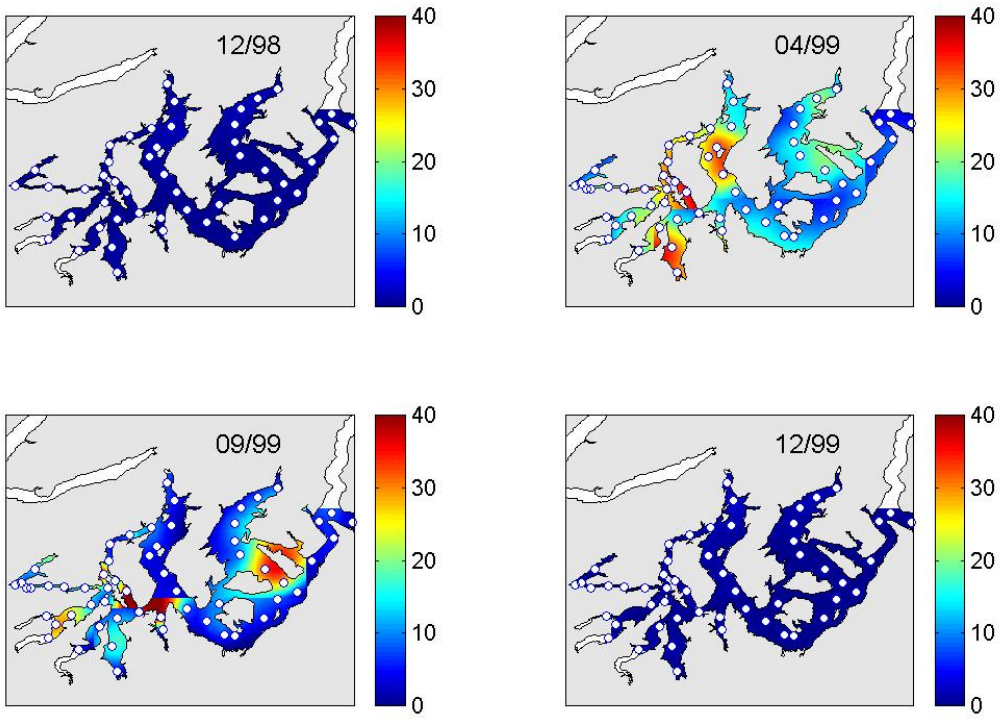

Figure 2-13. Distribution of surface chlorophyll *a* concentration (µg/L) determined from cruises.

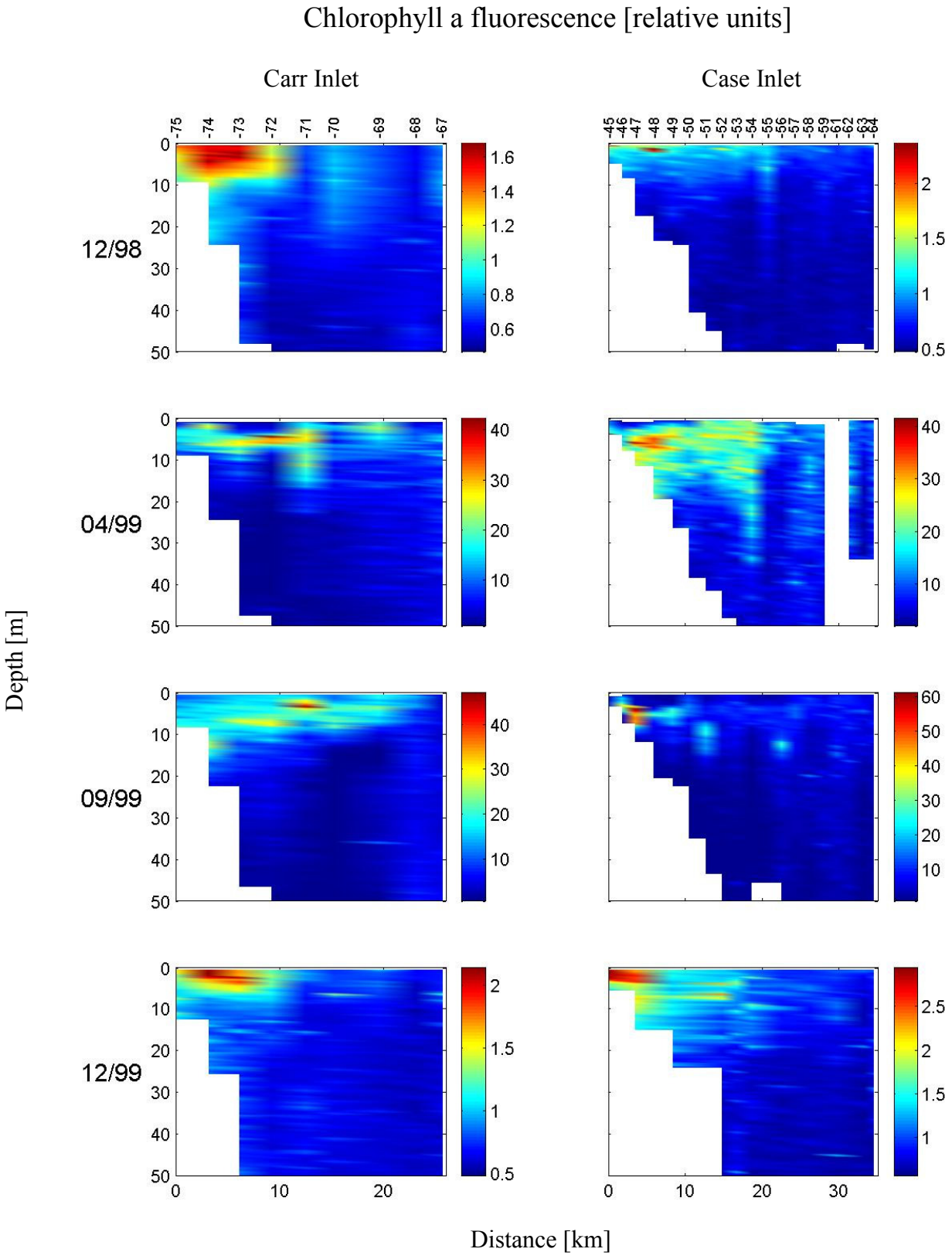

Figure 2-14. Chlorophyll *a* fluorescence, an indicator of phytoplankton concentration, in Carr Inlet (left panels) and Case Inlet (right panels). Station numbers are indicated at the top of the uppermost figures. Note that the color scales vary considerably among panels.

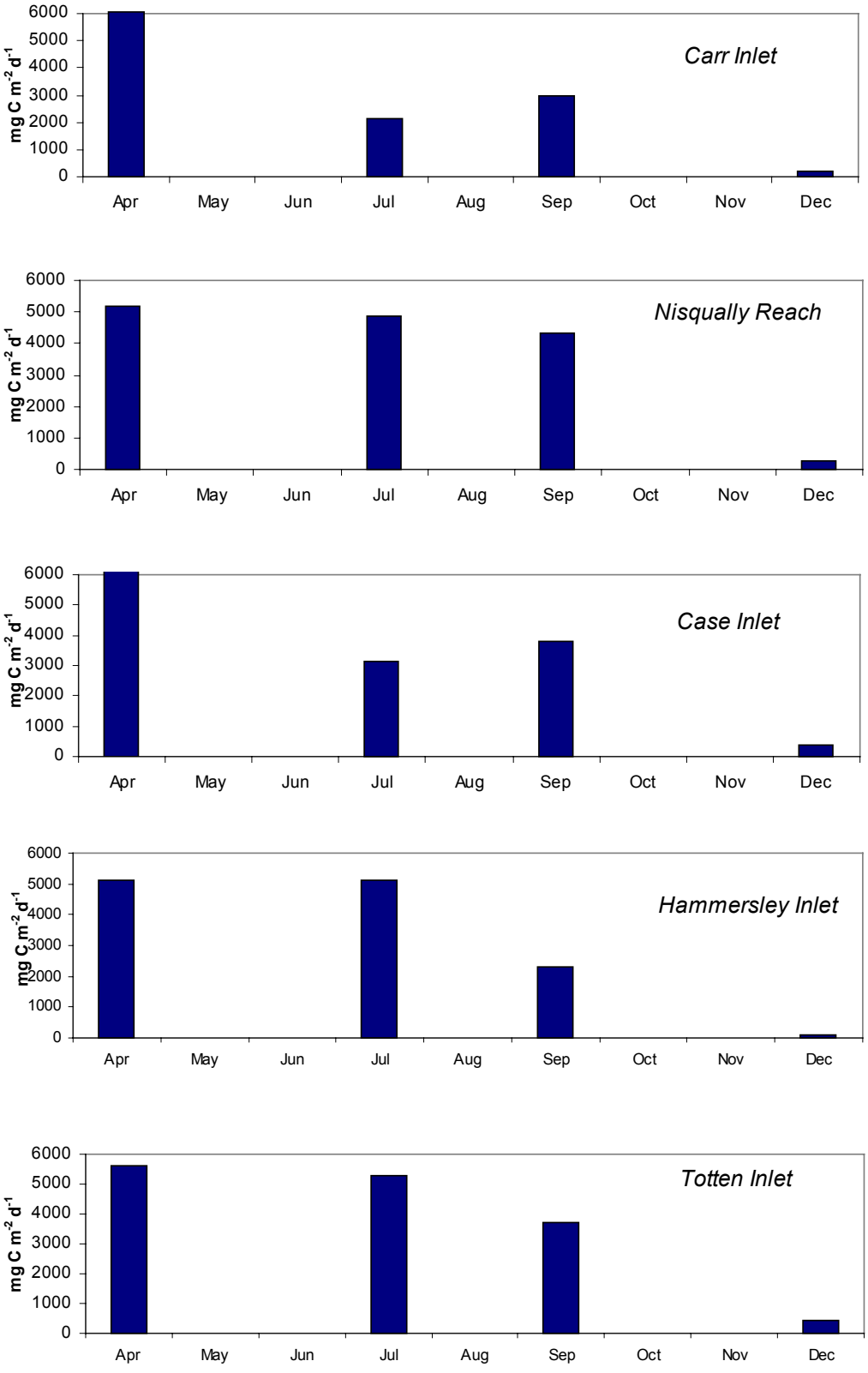

Figure 2-15. Seasonal levels of ambient primary production vertically integrated over the euphotic zone. Data shown are April 1999, July 2000, September 1999, and December 1999.

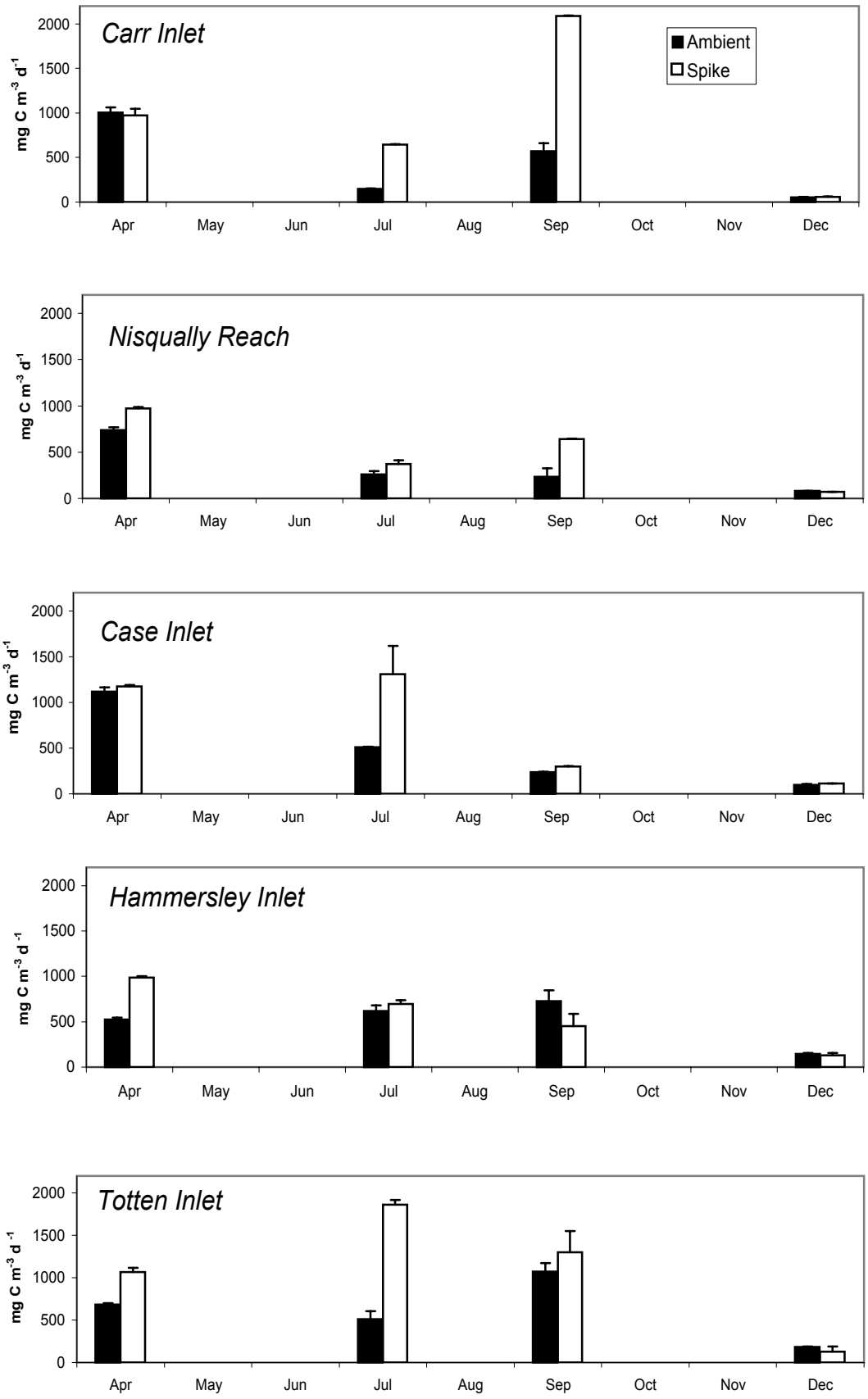

Figure 2-16. Seasonal view of primary productivity rates in natural (Ambient) and nutrient-enhanced (Spike) surface seawater samples. Data shown are April 1999, July 2000, September 1999, and December 1999. The December data were multiplied by 10 in order to be legible. Error bars represent 1 standard deviation as determined from replicate samples.

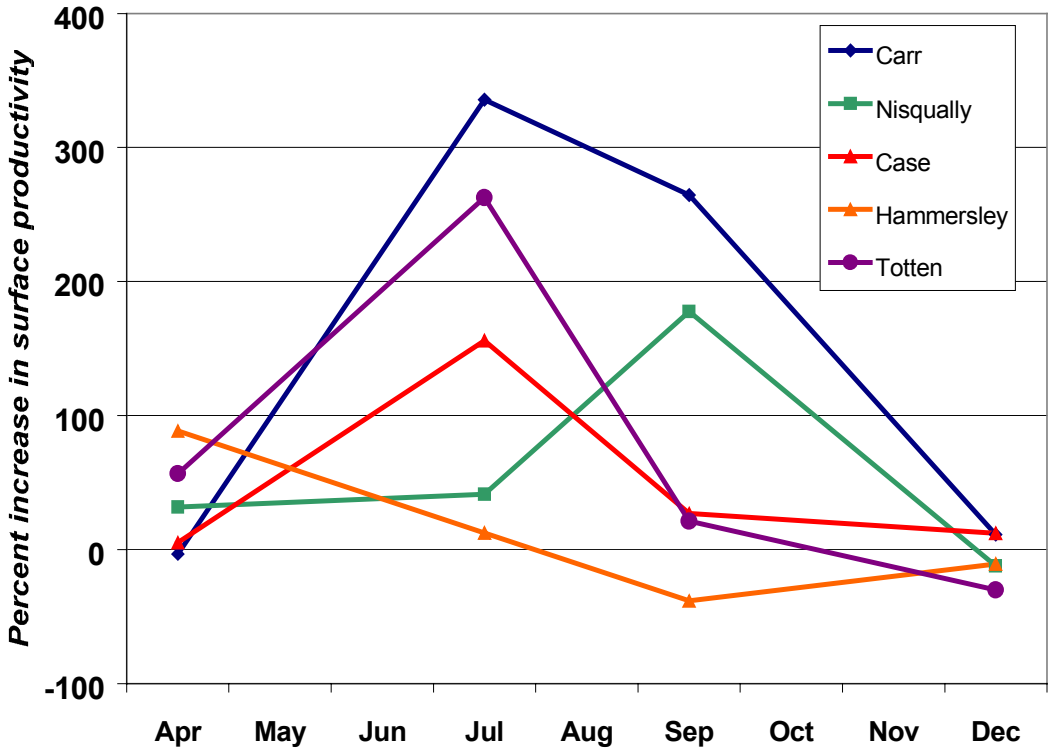

Figure 2-17. The percent increase in surface primary productivity due to an added nutrient spike for experiments conducted in April 1999, July 2000, September and December 1999.

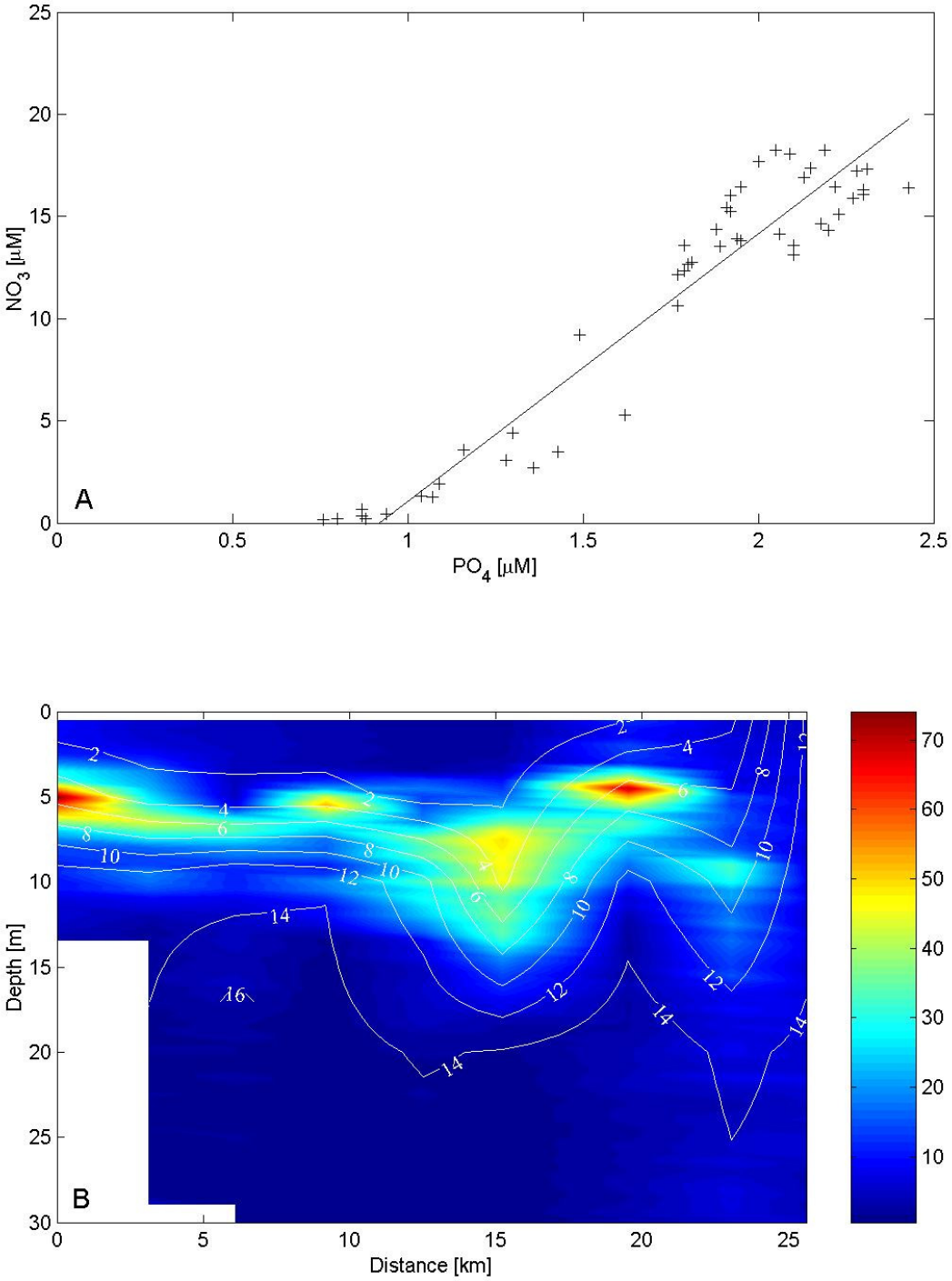

Figure 2-18. Measurements in Carr Inlet during September 1997.

A: Scatter plot of nitrate vs. phosphate concentrations from discrete water samples. The line represents a best-fit regression of the relationship for phosphate concentrations greater than 1 µM.

B: False color plot illustrating the distribution of chlorophyll *a* fluorescence (relative units) as a function of distance from the northern head of the inlet (Station 75). Overlaid are contours of nitrate concentration (µM).

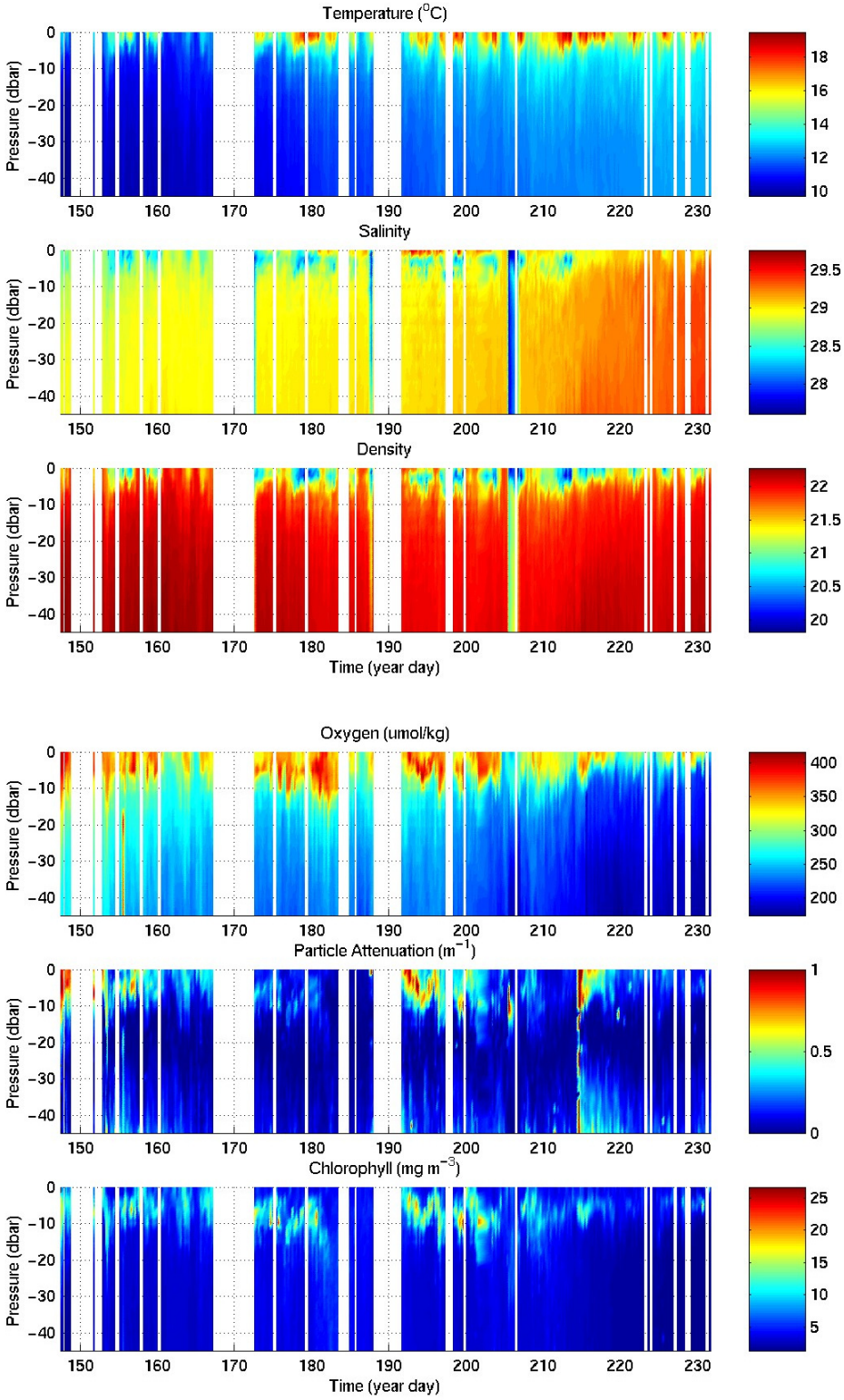

Figure 2-19. Water column data from UW-Ecology CISNet profiling mooring located in Carr Inlet. Preliminary data courtesy of J. Dunne, UW.

This page is purposely blank for duplex printing

3. Watershed and Point Source Loads

by M.L. Roberts and G. Pelletier

Introduction

The water quality model described in Section 5 simulates numerous water quality processes, including primary production, oxidation of organic material, and sediment-water interactions. In addition to marine and meteorological forcing parameters such as tides and solar radiation, the model requires freshwater inflows from the watershed and direct point source and atmospheric loads. Point sources that discharge to freshwater are included in watershed load estimates.

One option for estimating watershed inflows involves the development of a watershed-loading model for South Puget Sound. However, the effort would require significant resources and time and would need to be calibrated against monitoring data. Under the National Water Quality Assessment (NAWQA) program, the U.S. Geological Survey (USGS) estimated nutrient loads in major rivers tributary to the Puget Sound Basin for the period 1980-93 (Embrey and Inkpen, 1998), based on available historical data. Within the South Puget Sound study area, Embrey and Inkpen estimated annual loads of inorganic nitrogen (nitrite, nitrate, and ammonia) and total phosphorus for the Deschutes, Nisqually, and Puyallup rivers. However, the study did not include smaller tributaries or direct inflows, which are less important at the scale of the Puget Sound Basin. Yet, these inflows may impact the smaller bays and arms of South Puget Sound significantly.

The regression-based approach used by USGS was applied to 71 watersheds tributary to South Puget Sound to estimate daily loads. The 71 watersheds were selected to represent major and minor inflows. Direct inflows were included as discrete shoreline inflow points located approximately every two miles. Figure 3-1 presents the watershed boundaries and the inflow locations. Parameters of interest include nitrite/nitrate (NO23), ammonia (NH3), organic nitrogen (OrgN), orthophosphate (OP), organic phosphorus (OrgP), total phosphorus (TP), fecal coliform bacteria (FC), total suspended solids (TSS), dissolved oxygen (DO), oxygen demand, and organic carbon[7].

Methods

Watershed flow and load estimates were based on existing information, and very limited additional monitoring was conducted. Figure 3-2 presents the locations of existing monitoring stations, drawing from various efforts of the USGS; Washington State Department of Ecology (Ecology); Thurston County; Lacey, Olympia, Tumwater, Thurston County (LOTT) Budd Inlet study; and Bremerton-Kitsap County Health District.

[7] The water quality model requires organic nitrogen (calculated as total nitrogen minus inorganic nitrogen), organic phosphorus and organic carbon partitioned into dissolved and particulate forms, with particulate further divided into labile and refractory. No monitoring data were available to estimate these partitions for South Puget Sound, and literature-based estimates of 0.5 dissolved, 0.2 refractory particulate and 0.3 labile particulate proportions of organic constituents were used, based on water quality studies elsewhere (Tetra Tech, 1999).

Continuous flow gaging covers approximately 66% of the model domain land area and discrete measurements at the time of historical data collection cover an additional 23%. In addition, discrete water quality monitoring covers approximately 89% of the model domain land area (Figure 3-3). The four major river basins (Puyallup River, Nisqually River, Deschutes River and Chambers/Clover Creek) represent 2,000 mi^2 (5,200 km^2), or 71% of the total land area in the model, and have long-term data sets available.

Daily loads were estimated for the model calibration period of September 1996 through October 1997. The period of calibration represents above-average precipitation and river discharge. Because discharge was 20 to 35% higher than average (Table 3-1) for the period of interest, loads will be higher for the calibration period than for a typical hydrologic year.

Table 3-1. Discharge characteristics for the calibration period.

	Deschutes	Nisqually	Puyallup
Average Flow (cfs) for Period of Record	408	1,318	3,318
Average Flow (cfs) for Calibration Period	542	1,775	4,009
% Increase over Long-term Average	33%	35%	21%

Watershed Flows

Continuously gaged stations were used to estimate flows for watersheds with only discrete flow measurements, drawing from watersheds of similar size, land use, and proximity. The continuous flow record was normalized by tributary area and average annual rainfall[8] and scaled by the area and rainfall of the target watershed. Available discrete measurements verified the appropriateness of the approach. The same approach was used for direct inflows and other watersheds with no flow measurements.

Watershed Loads

Multiple-regression model coefficients represented conditions specific to each watershed for each parameter. The premise of the regression approach is that parameter concentrations can be predicted based on other parameters, such as flow and the time of year. For example, total suspended solids concentration tends to increase with increasing flow, due to the scouring action of high flows. Nitrite/nitrate tends to vary seasonally due to primary productivity and senescent cycles in riparian and wetland vegetation.

The multiple linear regression equation used for South Puget Sound loads is given by

$$\log(c) = b_o + b_1 \log(Q/A) + b_2 \log(Q/A)^2 + b_3 \sin(2\pi f_y) + b_4 \cos(2\pi f_y) + b_5 \sin(4\pi f_y) + b_6 \cos(4\pi f_y),$$

[8] A statewide grid of precipitation was developed by Washington Department of Natural Resources, Forest Practices Division in 1991.

where c is parameter concentration (mg/L or #/100 mL), Q is discharge (m^3/s), A is area tributary to the monitored location (km^2), f_y is year fraction (dimensionless, varies from 0 to 1), and b_i are the best-fit coefficients calculated for each data set. The regressions were carried out as logarithms of concentration and flow, given the order-of-magnitude variability in the source data. The flow terms can be based on discharge or area-normalized discharge, Q/A. For single stations, using Q/A has no effect on the regressions. However, in a limited number of cases, data from two adjacent systems with similar conditions were combined to provide a site-specific model appropriate for either (e.g., Mill, Deer, and Cranberry creeks into Hammersley Inlet), and using Q/A allows the data sets to be combined.

A simple SYSTAT® (SPSS Inc. ©1997, standard version 7.0.1 for Windows) code provided the regression coefficients and appropriate statistical parameters, following the approach[9] presented in Cohn et al. (1989). Residuals plots were examined for heteroscedasticity and adjusted R-squared was used to evaluate model fit. The smearing adjustment of Cohn et al. (1992) corrected for bias due to retransformation from log space. Initial regressions produced several outliers (studentized residual > 3.0). These data points tend to be associated with extreme flow events, obvious errors in the data sets, or an apparently different population. Outliers with studentized residuals greater than 3.0 were removed from the data set because of the likely errors and differences in the populations.

Where more than one organization collected data at or near the same location, data sets were reviewed for consistency and merged, since the regression approach improves with larger data sets. Long data sets were truncated, and only the most recent decade of data used.

Data collection programs used for the regressions relied on regular intervals for sampling, which reduces some sampling bias. Because the programs did not necessarily catch the largest flows, the regression model extrapolates patterns to higher flows, potentially producing significant sources of error. This type of error is more likely for parameters like fecal coliform bacteria and total suspended solids, which respond strongly to high flows. The maximum concentration recorded in the monitoring data was used to cap predicted concentration to minimize error due to the extrapolation.

Inflows with Monitoring Data

Of the 71 watersheds tributary to South Puget Sound, 23 watersheds have sufficient monitoring data available to calculate the regression coefficients. Initially all non-detects were assigned a value equal to the detection limit. The site-specific regression coefficients provided daily concentrations from daily flows. Daily loads were calculated from the estimated concentration and average daily flow for each of the parameters of interest for the period September 1996 through October 1997. The continuous daily load estimates were compared against discrete measured data to verify appropriateness of the model. In one case (ammonia from the Nisqually River), the high proportion of non-detects and representation as equal to the detection limit influenced the regression coefficients such that concentrations were overpredicted. Ammonia

[9] The proprietary USGS software Estimator uses the same approach to estimate daily loads from discrete water quality data.

non-detects in the Nisqually River were assigned a value of half the detection limit; new regression coefficients provided a better fit to the measured data.

Monitoring stations may not occur directly at the mouth of each watershed. To account for the loads from the ungaged proportion of the watershed, predicted flows were scaled by differences in watershed area and average annual precipitation. The scaled flows were multiplied by the predicted concentration to develop load estimates of the entire area.

Inflows with Limited or No Monitoring Data

An index water quality station, selected based on size, geographic proximity, and land use characteristics, provided a basis for estimating loads for areas with limited or no monitoring data. Where several were available, regression coefficients from each station were used with the estimated daily average flows at the site to predict concentrations and loads. The station producing the best overall fit with the set of monitoring data was used, rather than different index stations for different parameters. The approach is reasonable given the regional nature of the analysis. Six of the 71 watersheds have limited data that were insufficient for a site-specific regression but that could be used to check the appropriateness of an index station.

While all of the large and moderate inflows to South Puget Sound have at least some water quality data available, many of the small inflows or direct inflows have no data. The station providing the best fit to nearby monitored streams was used as an index for the small, unmonitored inflows. The remaining 42 watersheds have no site-specific data, although they represent only 11% of the model domain. Most of the ungaged watersheds are under 6 mi^2 (16 km^2) with the largest at 34 mi^2 (88 km^2).

Direct Point Source Loads

For model calibration, a time series of loads for the October 1996 through September 1997 simulation period was developed for nutrients, biochemical oxygen demand (BOD), dissolved oxygen, and fecal coliform bacteria for the point sources using Ecology's NPDES Daily Monitoring Report database[10]. Ammonia, nitrate, and total phosphorus were reported for some facilities, but not all. Also, facilities generally do not measure organic carbon. Therefore, a method was developed to estimate the various species of nitrogen, phosphorus, and carbon that were needed by the EFDC model from the data available in the DMR reports. Detailed data from plants in Washington were used to estimate ratios between nutrient forms where they were readily available (e.g., Heffner, 1992; Pelletier, 1994). Detailed monitoring data from plants in Pennsylvania and Delaware were evaluated to determine typical ratios between various nutrient species (Tetra Tech, 1999). Also, Lung (1993) and Metcalf and Eddy (1991) have summarized typical ratios between nutrient forms from nation-wide data and typical effluent concentrations. Table 3-2 presents the estimated ratios between forms of BOD, carbon, and nutrients along with assumed default concentrations in the absence of site-specific monitoring.

[10] Because EPA issues permits for the Fort Lewis Solo Point wastewater treatment plant discharge, the facility was not included in the first phase, but will be included in the following work.

Table 3-2. Assumptions for estimating loads from NPDES discharges

Parameter*	Default Conversion Factor**	Pulp and Paper Conversion Factor***	Default Concentration for Municipal Effluent if Not Measured (mg/L)
$CBOD_5/BOD_5$	0.67	1.00	
$CBOD_U/CBOD_5$	2.84	6.40	
$CBOD_U$/DOC	2.67		
RPOC/DOC	0.50		
LPOC/DOC	0.50		
RPOP/Total P	0.02		
LPOP/Total P	0.02		
DOP/Total P	0.04		
PTO4/Total P	0.92		
RPON/ORGN	0.25		
LPON/ORGN	0.25		
DON/ORGN	0.50		
Total-N/NH3	2.42		
NO2+NO3/NH3	0.87		
COD/BOD5	9.6		
Organic Nitrogen			8
Ammonia Nitrogen			22
Nitrite/Nitrate			1
Total Phosphorus			8

* See Section 5 for parameter explanations.
** Tetra Tech (1999)
*** Pelletier (1997)

Nutrient loads from fish net pens were estimated based on the reported quantity of feed that was applied and estimated conversion factors that were derived after Rensel (1999). Table 3-3 presents the estimated distribution of feed elements from commercial fish farm net pens and Table 3-4 details discharges.

Atmospheric Loads

Atmospheric loading of nitrogen, phosphorus, and carbon from wet and dry deposition was estimated as the rate of mass loading per unit area. Embrey and Inkpen (1998) reported atmospheric loading as 0.001 to 0.002 g/m^2/day of total nitrogen and 0.0001 to 0.0002 g/m^2/day of total phosphorus, based on data collected at stations operated by the National Trends Network of the National Atmospheric Deposition Program and a supplementary station operated by USGS. The mid-range estimates of 0.0015 g/m^2/day of total nitrogen and 0.00015 g/m^2/day of total phosphorus were used for modeling.

Table 3-3. Distribution of feed elements from a generalized commercial fish farm.

	Bulk	Total C	Total N	Total P
Assumptions				
Consumed food/bulk weight	95%			
Wasted food/bulk weight	5%			
Amount/bulk weight		44%	7.1%	1.0%
Respired CO2/consumed carbon		50%		
Harvested/consumed food		20%	50%	30.2%
Dissolved excretion (urine)/consumed food		0.0%	38%	22%
Settleable excretion (feces)/consumed food		30%	13%	48%
Applied Food Content				
Consumed food/applied food		42%	6.8%	0.95%
Wasted food/applied food	2.6%	2.2%	0.4%	0.05%
Settleable excretion/applied food	13.8%	12.5%	0.8%	0.5%
Dissolved excretion/applied food	2.7%	0.0%	2.5%	0.2%
Total discharge/applied food	19.2%	14.7%	1.2%	0.5%

Table 3-4. Waste fractions of applied food.

	C	N	P	RPOC	LPOC	DOC	RPOP	LPOP	DOP	TPO4	RPON	LPON	DON	NH4	NO23
Settleable/buried fraction of waste	67%	67%	67%												
Dissolved organic fraction of settleable waste	33%	33%	33%												
Fractionation of organic portion				25%	25%	50%	25%	25%	50%		25%	25%	50%		
Fraction of excreted dissolved									50%	50%			33%	33%	33%
Discharge/applied food				1.2%	1.2%	2.4%	0.04%	0.04%	0.19%	0.1%	0.1%	0.1%	1.0%	0.8%	0.8%

Results and Discussion

Watershed Inflow Concentrations and Regressions

Figure 3-4 compares the predicted and measured loads for the Puyallup River for nitrite/nitrate and ammonia during the period of calculation. The regression was based on data from 1991 to 1997 but only the year of interest for model calibration is presented. The flow and seasonal parameters explain 78% of the nitrite/nitrate concentration variability, but only 23% of the ammonia concentration variability. However, the predicted loads follow the measured loads well, even for ammonia. Thus, although the statistical parameters would suggest a poor fit for

the concentration, the variability in the flow exceeds the variability in the concentration, and the loads still match reasonably well. These findings are consistent with Cohn et al. (1992) and Embrey and Inkpen (1998), which found that while the regression model may account for 10 to 50% of the variability in concentration, the overall load model provides satisfactory results, even where the model does not explain most of the variability in concentration. Figure 3-5 compares measured with predicted loads for the Puyallup River data set. While dissolved oxygen and nitrite/nitrate show reasonable agreement, fecal coliform bacteria, TSS, and phosphorus show significant scatter. The adjusted R^2 values varied widely, with generally the highest values achieved for dissolved oxygen and nitrite/nitrate (median adjusted $R^2 = 0.6$ to 0.7) and the lowest values for fecal coliform bacteria and ammonia (median adjusted $R^2 = 0.3$).

Two watersheds tributary to Colvos Passage originally were believed to have no site-specific data, and loads were estimated based on a nearby index station. Afterwards, the Bremerton-Kitsap County Health District provided flow, dissolved oxygen, fecal coliform bacteria, and total suspended solids data, which were compared with regression-based estimates. Figure 3-6 illustrates that the approach provides reasonable flow and load estimates for these sites.

Watershed Loads

The regression coefficients for the various watersheds were used to calculate daily pollutant loads for the water quality model. However, the loads generated are also of interest from a watershed standpoint, particularly in comparing among watersheds. Watershed loads were summarized two ways: (1) total load to the Sound, and (2) load normalized by relative contribution to the Sound.

Figure 3-7 summarizes the annual average daily watershed flows and loads to South Puget Sound based on the regions identified in Figure 3-8. While the Puyallup River occupies 35% of the South Puget Sound watershed area and contributes 43% of the average annual inflow, the river contributes significantly greater proportions of the ammonia and fecal coliform loads.

While the load magnitudes are important to identify the largest contributors to South Puget Sound, comparisons among watersheds are limited to the size of the watershed as a general proxy, since the larger watersheds tend to contribute the larger flows and loads. However, should loads need to be reduced to achieve water quality standards within Puget Sound, load per unit area may be a better indicator of the most densely distributed sources.

For example, McAllister Creek watershed contributes approximately 280 kg/d of nitrite/nitrate and occupies about 42 mi^2 (109 km^2). The total South Sound tributary area is approximately 2,800 mi^2 (7,300 km^2) and produces an estimated 9,700 kg/d (sum of 71 watershed contributions) of nitrite/nitrate. McAllister Creek contributes 2.8% of the total load, but occupies 1.5% of the watershed area. The normalized load is the load proportion divided by the area proportion, or 1.9. In other words, the McAllister Creek watershed contributes 1.9 times the average areal nitrite/nitrate load compared with the overall South Puget Sound watershed, since normalized loads above 1.0 are higher than average.

Normalized loads include variations due to discharge. Thus, watersheds with higher-than-average discharge may have higher-than-average loads. Figure 3-9 presents the normalized discharge for South Puget Sound. Watersheds are coded by the proportion of discharge normalized by the proportion of watershed area. Because the Deschutes, Nisqually, and Puyallup rivers represent 67% of the watershed area, they control the domain-wide average discharge. The resulting normalized discharges are only slightly greater than one; therefore, differences in discharge will not bias normalized loads significantly in the three largest watersheds. The northern and western regions have lower-than-average discharge, which is consistent with the annual rainfall contours shown in Figure 3-10. Thus, the normalized loads tend to be lower than average in the northern and western watersheds when compared to the entire project area.

Figure 3-11 presents the normalized loads for nitrite/nitrate, ammonia, fecal coliform bacteria, and TSS. The urban areas of Chambers/Clover Creek and areas tributary to Budd Inlet produce nitrite/nitrate normalized loads >1.5, indicating loads are 50% higher than the average. Other regions with elevated nitrite/nitrate are Woodard Creek (tributary to Henderson Inlet), McAllister Creek, and Rocky and Coulter Creek (tributary to Case Inlet). Normalized loads for the direct inflows north of Tacoma are based on the Chambers/Clover Creek results, because of the extensive development in both areas. Sequalitchew Creek also appears to contribute relatively high levels of nitrite/nitrate, based on limited sampling in 1999. Of the three major inflows, the Deschutes River contributes the highest nitrite/nitrate load normalized by tributary area.

Sources of ammonia appear distinct from sources of nitrite/nitrate. The Puyallup River contributes the highest ammonia load in magnitude, but McAllister Creek and two small tributaries to Budd Inlet (Butler Creek and Moxlie Creek) contribute higher normalized ammonia loads. Minter, Burley, and Purdy creeks, tributary to Carr Inlet, contribute ammonia loads.

The Puyallup River dominates the fecal coliform load to South Puget Sound. Several tributaries to Budd Inlet also contribute high area-normalized loads: Gull Harbor, Ellis/Mission Creeks, Moxlie/Indian Creeks, and Schneider Creek. Thus, Budd Inlet and Commencement Bay receive the highest normalized fecal coliform loads of the South Puget Sound region.

Total suspended solids loads are proportional to the discharge from the watersheds, with the Puyallup River contributing the highest normalized TSS load, followed by the Nisqually and Deschutes rivers. The three largest watersheds produce the greatest discharges and receive the highest annual average rainfall in the headwaters (Figure 3-10).

Figure 3-12 presents the normalized loads for orthophosphate, total phosphorus, organic phosphorus, and organic carbon. Sources of orthophosphate do not coincide with significant sources of total phosphorus. The greatest normalized loads of orthophosphate are Ellis/Mission Creeks, Schneider Creek, and Moxlie/Indian Creeks, tributary to Budd Inlet; Rocky/Coulter Creeks, tributary to Case Inlet; Burley Creek, tributary to Carr Inlet; and McAllister Creek. Schneider and Burley creeks are also significant sources of total phosphorus, in addition to the Puyallup River. The Puyallup River provides the highest area-normalized organic phosphorus load to South Puget Sound.

Few organic carbon data were available beyond the Budd Inlet study (Aura Nova Consultants et al., 1998) and the Puyallup River (USGS, 2000). Only the Schneider Creek watershed in Budd Inlet produced elevated normalized loads.

Comparison with USGS Puyallup River Load Estimates

A recent USGS study estimated nutrient loads from major rivers around Puget Sound, including the Puyallup, Nisqually, and Deschutes rivers in South Puget Sound (Embrey and Inkpen, 1998). Table 3-5 compares the results of the USGS study for the period 1980-1993 with results from the present study for October 1996 through September 1997. Average daily flows were significantly higher for the present study and account for most of the differences between load estimates. When normalized by average flow during the periods of analysis, the differences between Puyallup River the two estimates of inorganic nitrogen and total phosphorus loads were 2% and 13% relative percent difference, respectively. Because the relationship between concentration and flow is nonlinear, flow differences have secondary effects on load estimates.

Table 3-5. Comparison of Puyallup River load estimates between studies.

Parameter	USGS (1980 – 1993)	Present Study (Oct. 1996 – Sept. 1997)	
Total Phosphorus	340 tons/year	1,338 kg/d	538 tons/year
Ammonia		338 kg/d	136 tons/year
Nitrite/Nitrate		3,014 kg/d	1,213 tons/year
Inorganic Nitrogen	950 tons/year	3,352 kg/d	1,349 tons/year

Direct Point Source Loads

A summary of the average annual flows and loads of nutrients and fecal coliform bacteria from point sources discharging directly to South Puget Sound is presented in Table 3-6. The largest NPDES point source discharges to South Puget Sound include Simpson Tacoma Kraft and municipal wastewater discharges from Tacoma Central No. 1, Chambers Creek, LOTT, and King County Metro Alki. Overall, direct point sources contribute over 7,000 kg/d total nitrogen and over 3,000 kg/d total phosphorus to South Puget Sound. While Simpson Tacoma Kraft contributes a high proportion of the TOC load, nitrogen and phosphorus loads are comparable to a moderate municipal wastewater treatment plant. Metro Alki contributes 60% of the point source fecal coliform load to South Puget Sound.

Table 3-6. Estimated annual average loads from NPDES discharges[11] to South Puget Sound during the calibration period (October 1996 through September 1997).

Name	Flow (m^3/s)	TOC (kg/d)	TON (kg/d)	TOP (kg/d)	DIN (kg/d)	N (kg/d)	P (kg/d)	FC (#/d)
Municipal								
Tacoma Central No. 1	1.23	2351	850	68	1196	2046	850	6.88E+10
Chambers Creek	0.68	727	473	38	1237	1710	473	1.11E+10
LOTT	0.59	442	71	33	323	394	409	1.69E+10
Metro Alki[12]	0.43	3796	299	24	518	817	299	1.67E+12
Tacoma North No. 3	0.25	523	170	14	254	424	170	2.13E+10
Midway	0.21	427	147	12	219	367	147	4.85E+10
Lakehaven Lakota	0.21	465	143	11	213	357	143	3.31E+09
Miller Creek	0.17	236	116	9.3	173	289	116	1.45E+10
Shelton	0.17	64	115	9.2	24	139	115	7.91E+08
Salmon Creek	0.15	199	104	8.3	155	259	104	1.30E+10
Lakehaven Redondo	0.14	285	94	7.6	141	235	94	1.12E+10
Gig Harbor	0.03	35	22	1.8	33	56	22	7.17E+08
WA DOC McNeil Island	0.01	6.9	7.6	0.6	22	30	7.6	9.52E+08
Manchester	0.01	7.8	5.8	0.5	17	23	5.8	7.31E+08
Vashon	0.01	13	3.5	0.3	10	13	3.5	4.35E+08
Hartstene Pointe	0.004	2.5	2.5	0.2	7.3	10	2.5	3.17E+08
Rustlewood	0.002	5.4	1.7	0.1	4.8	6.5	1.7	2.09E+08
Boston Harbor	0.001	2.0	1.0	0.1	2.8	3.7	1.0	1.20E+08
Tamoshan	0.001	1.5	0.8	0.1	2.4	3.2	0.8	1.03E+08
Carlyon Beach	0.001	1.3	0.6	0.04	1.6	2.2	0.6	6.97E+07
Taylor Bay	0.001	0.3	0.4	0.04	1.3	1.7	0.4	5.58E+07
Seashore Villa	0.001	0.9	0.4	0.03	1.2	1.6	0.4	5.02E+07
WA Parks Blake Island	0.0005	1.3	0.3	0.03	1.0	1.3	0.3	4.23E+07
Beverly Beach	0.0001	0.1	0.1	0.01	0.2	0.3	0.1	1.02E+07
Industrial								
Simpson Tacoma Kraft	1.30	6629	50	3.4	49	99	42	8.63E+11
Aquaculture								
Global Aqua Viking/NW Sea Farms Fort Ward	-	77	20	4.3	27	46	6.0	-
NW Sea Farms Clam Bay/Orchard Rocks	-	215	55	12	74	129	17	-
NW Sea Farms Dana Passage/Hartstene	-	7.2	1.8	0.4	2.5	4.3	0.6	-
WDFW Fox Island	-	3.1	0.8	0.2	1.1	1.8	0.2	-
WDFW South Puget Sound Net Pens	-	11	2.7	0.6	3.7	6.5	0.8	-
Total Point Source Loads[13]	5.2	13,000	2,500	240	4,200	6,700	2,700	1.1E+11
Total Watershed Loads	280	180,000	3,300	1,900	10,000	12,000	2,300	5.4E+13

[11] Phase I did not include the 7.6 mgd (0.33 m^3/s) discharge from the Fort Lewis Solo Point wastewater treatment plant.
[12] Metro Alki discharge during the period of interest may not represent typical conditions.
[13] Loads do not include Metro Alki, which discharges near the grid boundary.

Atmospheric Loads

The total annual atmospheric deposition onto the surface area of southern Puget Sound (the area south of the Alki boundary) provides approximately 1,100 kg/year of total nitrogen and 110 kg/year of total phosphorus, significantly lower than the loads from point sources or watersheds. Atmospheric deposition of total organic carbon is approximately 10 times the loading rate for nitrogen, or 0.015 g/m^2/day. Atmospheric loads of nitrogen, phosphorus, and carbon were divided evenly into nutrient forms as a first approximation in the absence of partitioning data among the labile, refractive, and dissolved forms of nitrogen, phosphorus, and carbon.

Annual Loads to South Puget Sound

Figures 3-13, 3-14, and 3-15 combine the annual average loads of dissolved inorganic nitrogen, total organic carbon, and fecal coliform bacteria from tributaries and point sources. The figures illustrate the relative magnitude of watershed and point source loads.

Dissolved inorganic nitrogen loads are comparable among the largest point sources and major watershed loads, with significant point source DIN loads along the eastern shoreline. In Budd Inlet, the Deschutes River and LOTT wastewater discharge produce comparable annual DIN loads. From Table 3-6, total phosphorus loads from point sources exceed those from watershed loads, although point source orthophosphate loads are lower than watershed loads. Figure 3-14 shows that the Puyallup River and Nisqually River produce the largest organic carbon loads to South Puget Sound; however, these watershed load estimates are based on limited data.

From Figure 3-15, the four major tributaries (Puyallup River, Chambers Creek, Nisqually River, and Deschutes River) and two direct point source discharges (Simpson Tacoma Kraft and Metro Alki) produce comparable annual loads of fecal coliform bacteria. The Puyallup River is the single largest fecal coliform load to South Puget Sound. Watershed loads dominate direct point source loads of fecal coliform bacteria.

Summary and Conclusions

Site-specific regression coefficients developed from watershed-specific data provide appropriate estimates of regional daily loads tributary to South Puget Sound. The method requires a minimum of approximately 20 data points at any one site; a more robust and representative regression results from extensive representative data. While adjusted R^2 values ranged widely, the regression models capture sufficient variability to represent the load variation from the 71 watersheds.

Because limited additional sampling supported the development of watershed loads, the primary limitation of the regression approach is the availability and range of existing data. Fortunately, 89% of the South Puget Sound watershed has at least some water quality monitoring data available and 66% of the watershed area has continuous flow gaging. However, not all parameters of interest have been monitored at each site, and not all sites have monitoring data

available during the model calibration period. Data used in the regression were limited to the most recent decade. Many monitoring programs collect data at regular intervals and do not target high-flow events. Given that many parameter concentrations increase with increasing flow, annual loads are most sensitive to wet weather loads.

The daily load estimates can be used to prioritize watershed-based reductions, if necessary, to meet water quality standards in marine waterbodies. Load magnitude is one measure of impact on marine waters; however, larger tributaries generally produce larger loads and sources may be extensive. An alternative approach is the use of normalized loads, which are normalized by area and by differences in average annual rainfall as an indicator of discharge variations. Watersheds contributing higher-than-average normalized loads may be more efficient to target for load reductions due to more densely distributed sources.

Graphics of the normalized loads illustrate the overall pollutant loading patterns to South Puget Sound, and highlight areas of particular concern by parameter. These normalized loads may be used to prioritize pollutant-reduction efforts.

Direct atmospheric loads to the surface of Puget Sound are several orders of magnitude smaller than total freshwater inflows for both nitrogen and phosphorus. While direct point source inflow volumes represent 2% of the watershed inflows to South Puget Sound, loads of organic and inorganic nitrogen and phosphorus from point sources are of comparable magnitude to watershed loads. Point sources represent 36% of the total nitrogen load and 54% of the total phosphorus load to South Puget Sound, as well as 43% of the organic nitrogen load and 30% of the dissolved inorganic nitrogen load, neglecting the Metro Alki discharge. Point sources contribute 0.2% of the fecal coliform load to South Puget Sound. Point sources that discharge to freshwater are included with the watershed loads.

While the loads described herein represent the best estimates based on the best available data, they are not meant to be final or static. More recent or additional data collection may improve the regressions in certain bays of interest and for particular parameters. In particular, nitrogen loads should be more precisely quantified for direct point-source discharges through additional effluent monitoring.

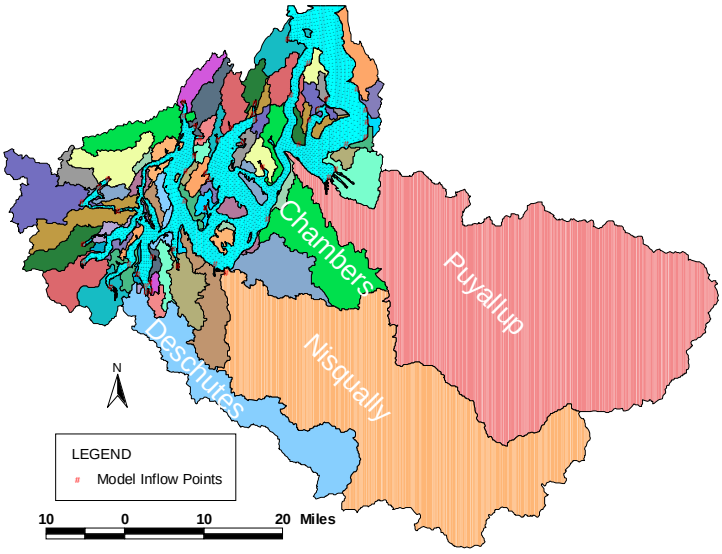

Figure 3-1. South Puget Sound watersheds and model inflow points.

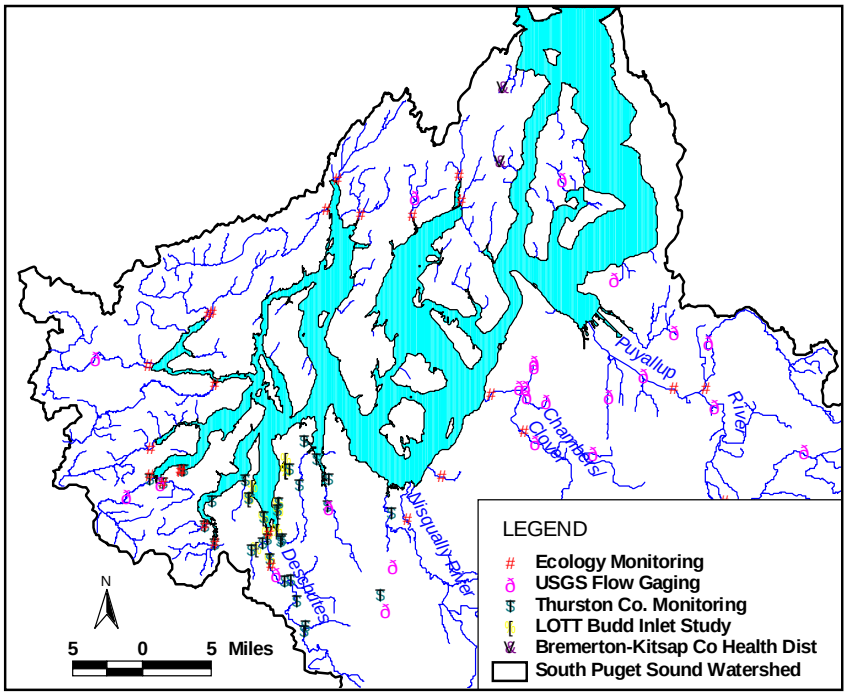

Figure 3-2. Existing monitoring stations.

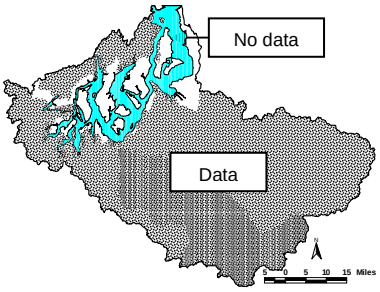

Figure 3-3. Existing monitoring data.

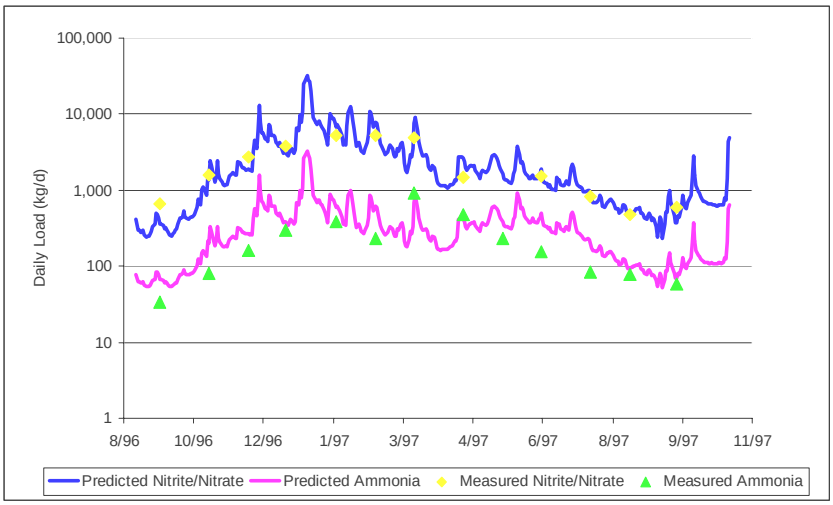

Figure 3-4. Predicted daily Puyallup River loads.

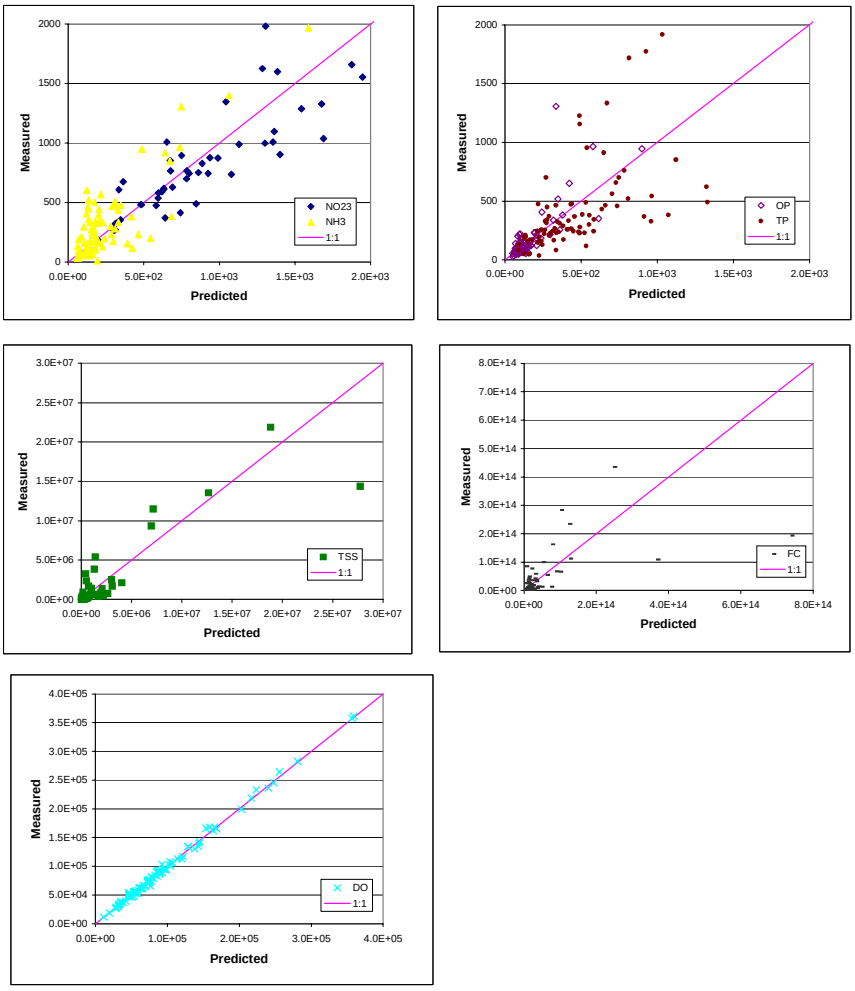

Figure 3-5. Comparison of predicted and measured loads in the Puyallup River.

Figure 3-6. Comparison of predicted and measured flows and loads for unmonitored locations. (Data later provided by Bremerton-Kitsap County Health District.)

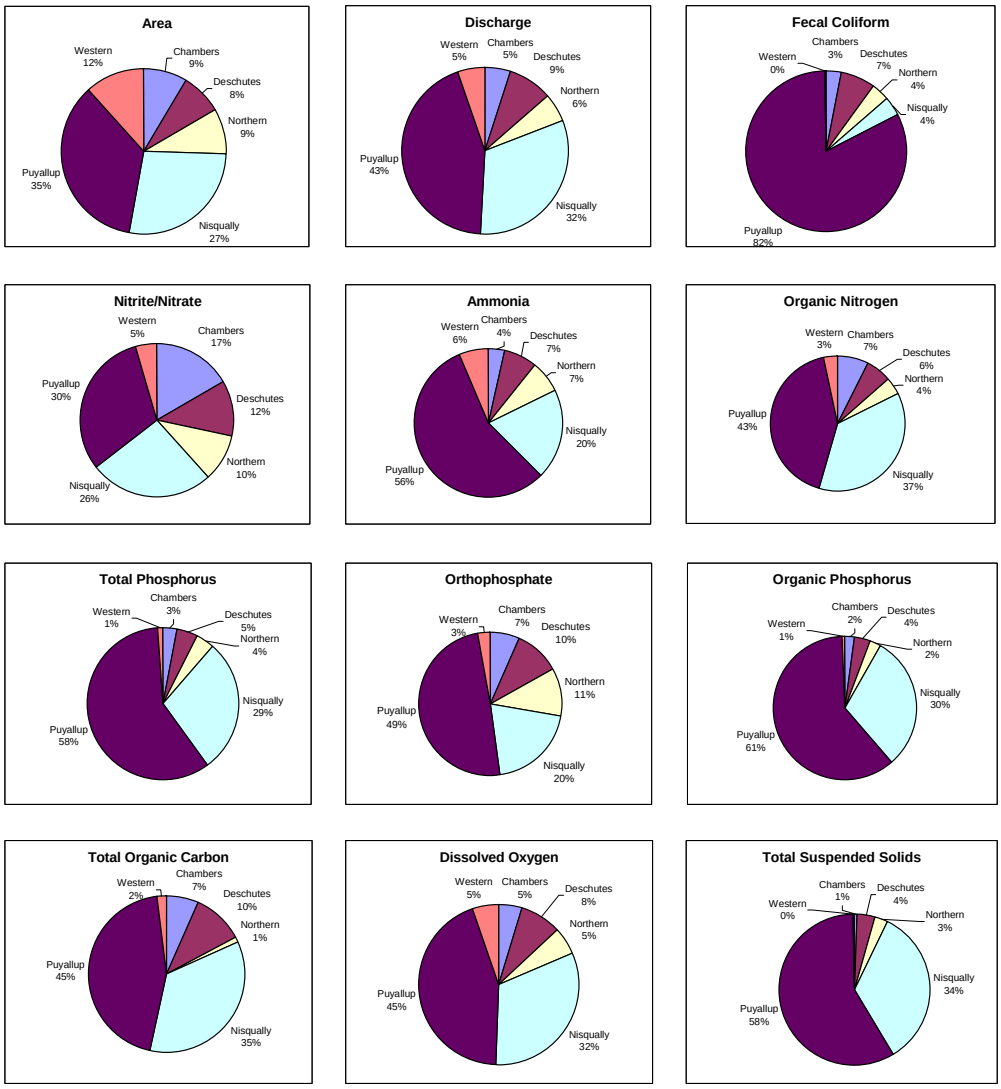

Figure 3-7. Percent total flows and loads by each region.

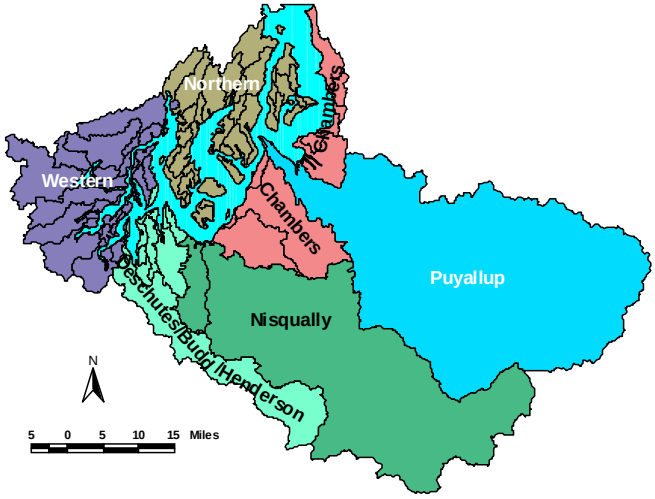

Figure 3-8. South Puget Sound regions.

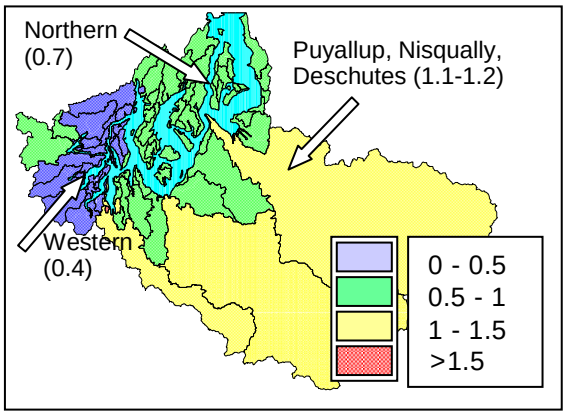

Figure 3-9. Comparison with average (1.0) discharge across South Puget Sounds regions.

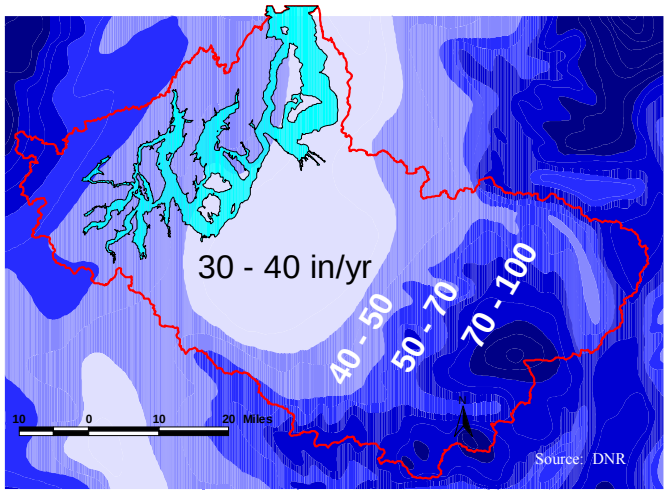

Figure 3-10. Annual average rainfall contours.

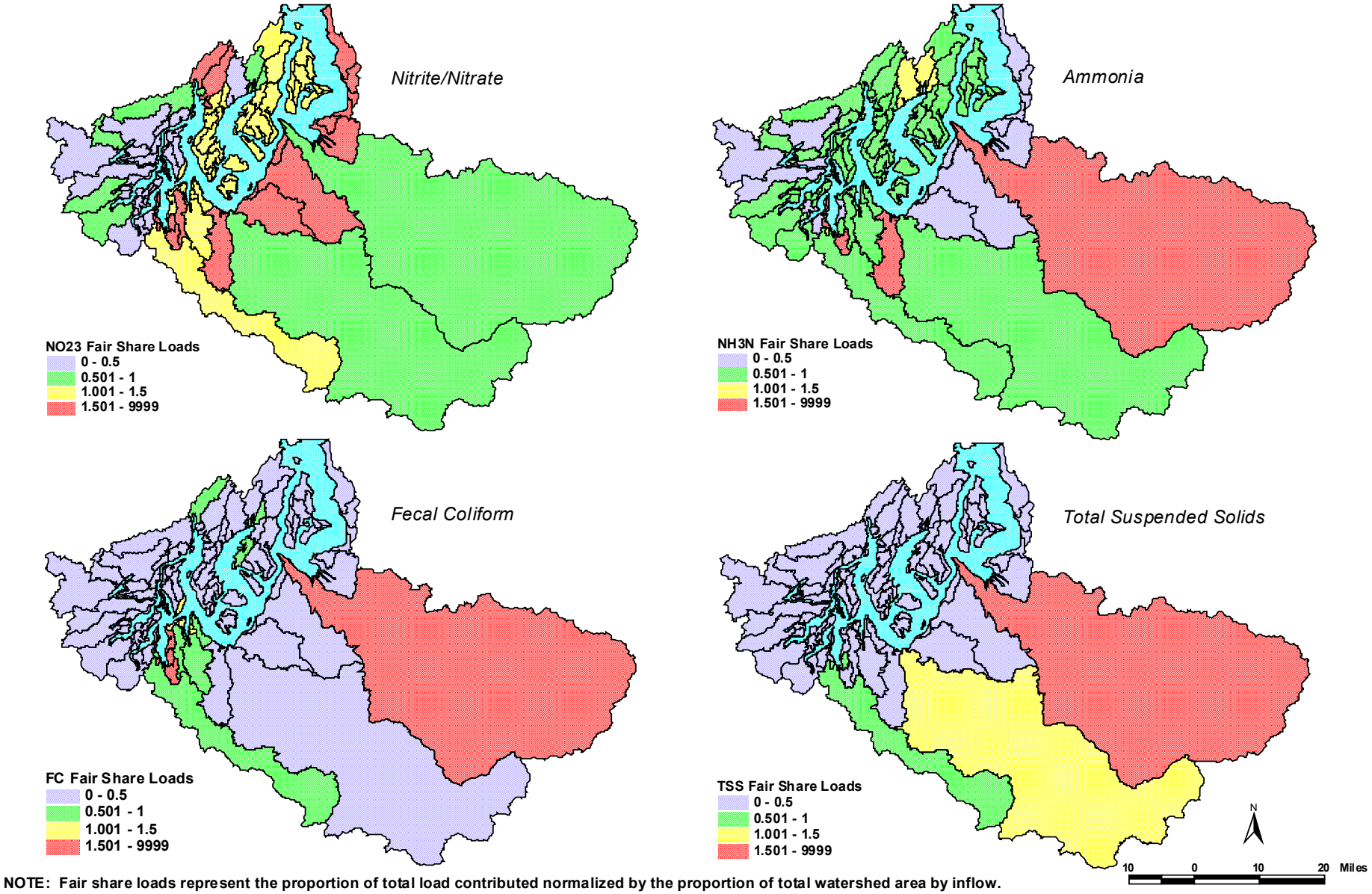

Figure 3-11. South Puget Sound normalized loads for nitrite/nitrate, ammonia, fecal coliform, and TSS.

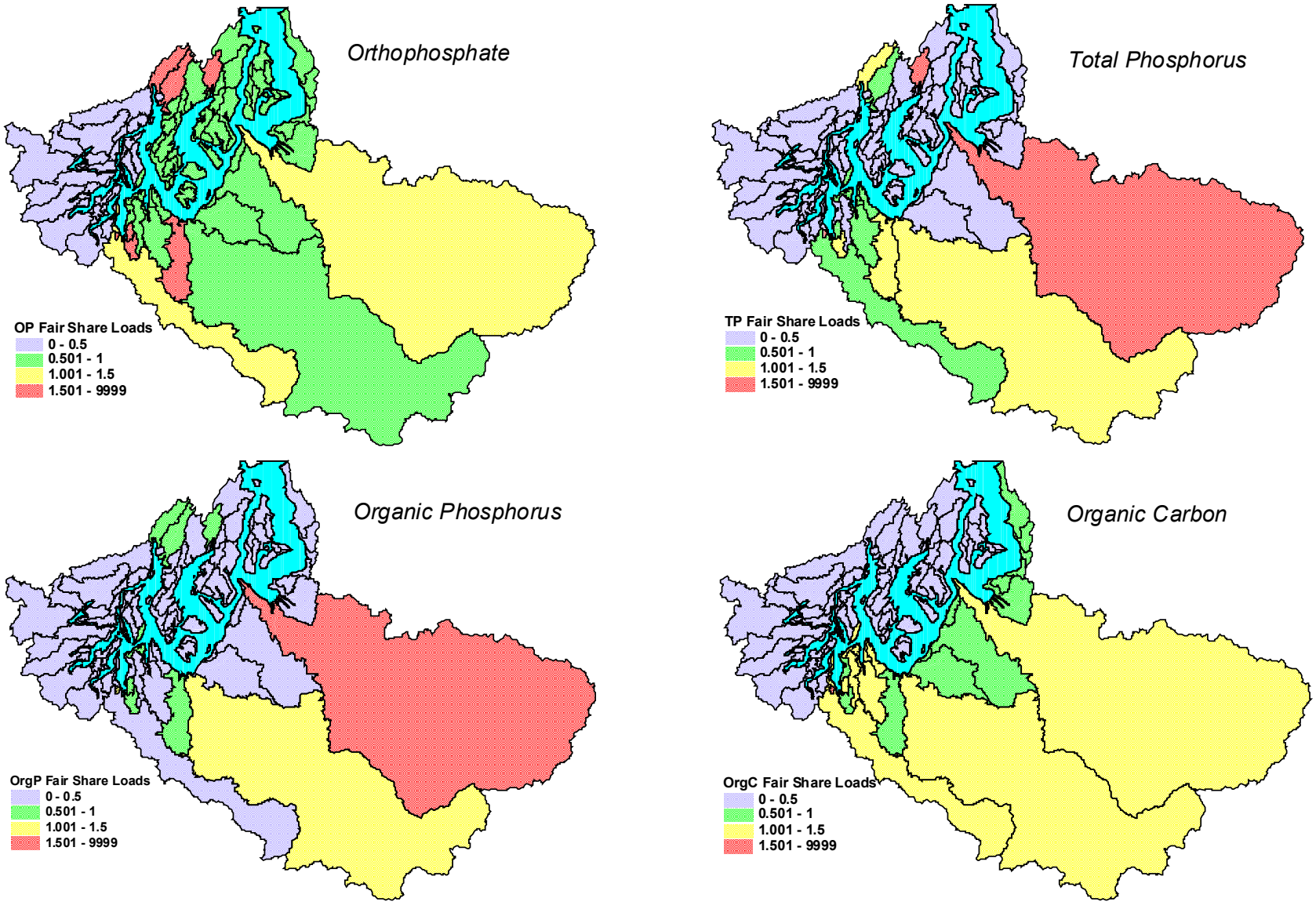

Figure 3-12. South Puget Sound normalized loads for orthophosphate, total phosphorus, organic phosphorus, and organic carbon.

This page is purposely blank for duplex printing

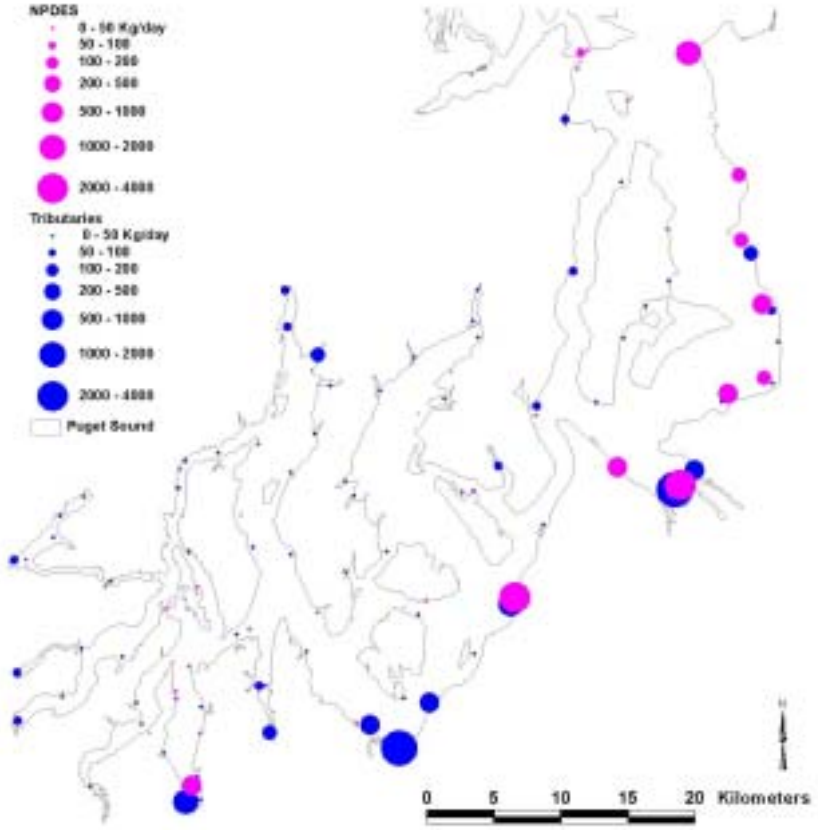

Figure 3-13. Annual DIN loads from watershed and point sources.

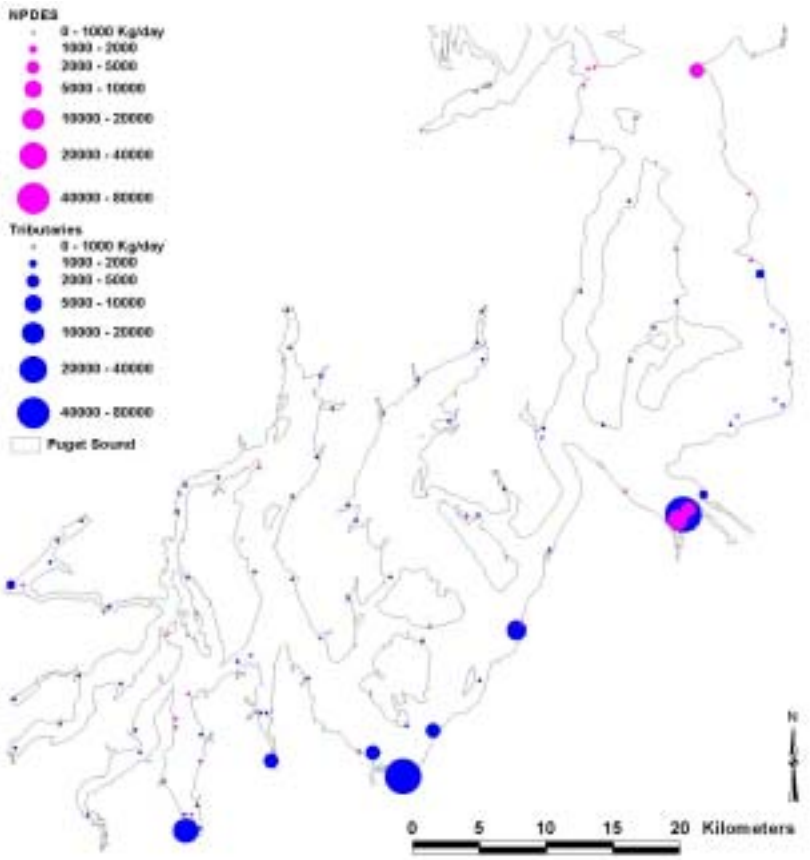

Figure 3-14. Annual organic carbon loads from watershed and point sources.

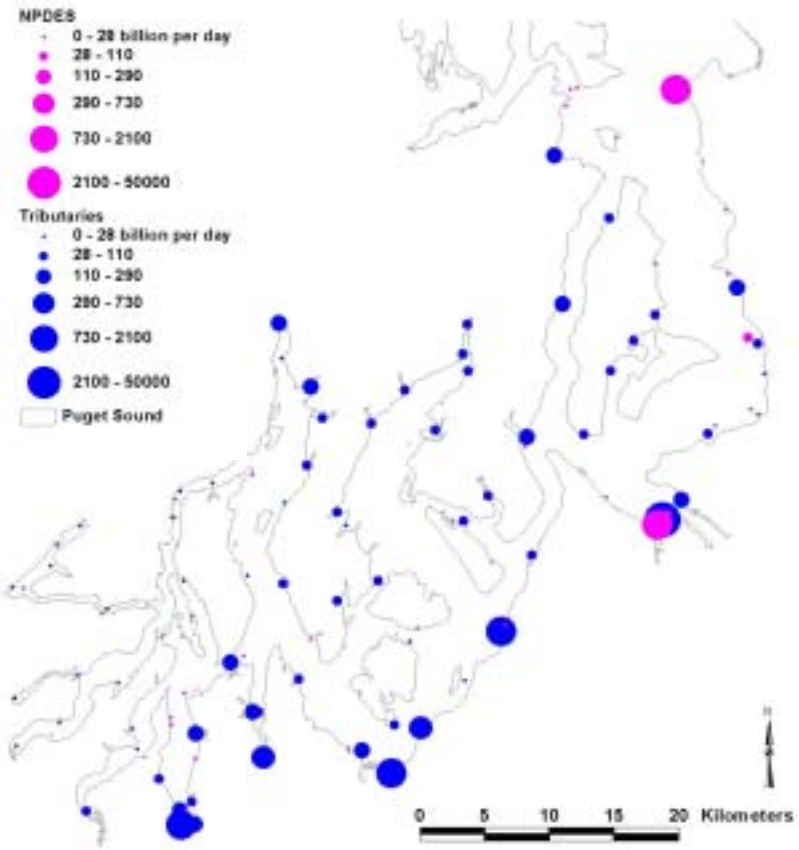

Figure 3-15. Annual fecal coliform loads from watershed and point sources.

This page is purposely blank for duplex printing

4. Hydrodynamic Model

by S.L. Albertson

Introduction

The South Puget Sound model uses the Environmental Fluid Dynamics Code (EFDC) (Hamrick, 1992a,b, 1994) to simulate hydrodynamics as well as biogeochemical transport for water quality issues. Section 5 of this report discusses water quality aspects of the model.

EFDC solves the three-dimensional, vertically hydrostatic, free surface, turbulent-averaged primitive equations of motion for a variable density fluid[14]. Thus, the model can represent the complex horizontal structure of South Puget Sound and its numerous inlets, as well as the vertical water column structure. EFDC uses the vertically hydrostatic assumption, which can potentially lead to an under-representation of real physical processes in high-flow regions over sills, such as those near the Tacoma Narrows. Tacoma Narrows itself has complexities that may not be well-represented (Seim and Gregg, 1997) in the model.

Reproducing the hydrodynamic conditions of Puget Sound is fundamental to representing the other chemical and biological processes appropriately, since advection of water from place to place strongly influences those processes. The model has now been calibrated to hydrodynamic forcing over the time scale of a few hours to several days. Integrated transports at a time scale of months or years will be discussed, and suggestions concerning them will be made for Phase 2 of this study.

A curvilinear orthogonal grid of 1,906 discrete cells represents the spatial domain of South Puget Sound, as shown in Figure 4-1. The average area of the grid cells is approximately 0.4 km^2, which corresponds to dimensions of approximately 630 by 630 meters. Each grid cell has four vertical layers in the stretched-sigma coordinate system used by the EFDC model. The sigma coordinates are defined in Figure 4-2 as

$$\sigma = (z - \eta) / (H + \eta)$$

where H (m) is bottom topography at Mean Lower Low Water (MLLW), η is the surface elevation (m) above this datum level, and z is the vertical dimension downward from the surface. Thus, σ ranges from $\sigma = 0$ at $z = \eta$ to $\sigma = -1$ at $z = -H$.

[14] EFDC solves the dynamically coupled transport equations for turbulent kinetic energy, turbulent length scale, salinity, and temperature. The turbulence parameter equations implement the Mellor-Yamada level 2.5 turbulence closure scheme as modified by Galperin et al (Hamrick, 1992b). Time integration of the momentum and continuity equations uses a second-order, semi-implicit, three-time-level, leap frog-trapezoidal method, with an insertion of a two-time level trapezoidal step to suppress the mode generated by the three-level scheme. The barotropic and baroclinic modes are split with a method that is implicit in the horizontal for the barotropic, and in the vertical for the baroclinic. Advection is handled with an upwind-difference technique described by Hamrick (1994)

The σ-based formulation for the underlying differential equations has computational advantages over Cartesian orthogonal (i.e., z-based) grids due to computational limitations. Fictitious velocities may develop around steep topography, which is a potential drawback for deep fjord-like systems with many vertical layers (Haney, 1991). These errors typically result from neglecting terms proportional to bottom slopes (i.e., $\partial h/\partial x$ and $\partial h/\partial y$ terms) and in estimating horizontal pressure gradients with sigma ($\partial\sigma/\partial x$, $\partial\sigma/\partial y$). Recent successful applications of sigma-based models to regions with steep topography and large density gradients exist (Pietrzak and Kleim, 1999). The present application restricts vertical discretization to four layers, which minimizes these types of error.

Hydrodynamic Model Development

The central issues in calibrating the hydrodynamic or circulation model of South Puget Sound involve adequately simulating the tides, currents, and density gradients. The pattern and motion of water in South Puget Sound influence the distribution of water quality parameters like dissolved oxygen. For example, stratification established by sunlight, fresh water inputs, and salty Pacific Ocean water inflows may limit the vertical exchange of dissolved oxygen and increase oxygen depletion in the bottom waters. Although much more complex, the circulation also affects algal productivity and the ultimate deposition and decomposition of the organic matter produced from algal blooms.

The terms validation, verification, and calibration have technically distinct meanings (Roache, 1998). Validation refers to solving the correctly formed differential equations in concept for each state variable. Verification is the mathematical confirmation that a model solves these written equations correctly once they have been coded into a computer language. Wu et al. (1997) discuss validation and verification for EFDC. The EFDC model is considered to be validated and verified as defined by Roache (1998) for the purpose of our study. Therefore, our study does not attempt to further validate or verify the EFDC model under these definitions.

Calibration involves the selection of model inputs and parameters that apply the model to a particular water body. The present study includes calibration of the EFDC model to southern Puget Sound. When a model is applied to a particular system, the modeler compares model output with measured quantities in the system being modeled. Calibration typically involves the selection of model parameters to minimize differences between measured and predicted values.

Calibration of the EFDC application to South Puget Sound focuses on the tidal forcing at the north boundary of the model, since real temperature and salinity data together with the turbulence closure will determine the density gradients. Wind forcing is also based on real data, although whether available data applied globally are acceptable is subject to debate. The final tidal forcing at the northern open boundary, shown in Table 4-1, was adjusted to best fit the model response to the observed tides based on five tidal constituent amplitudes and phase angles at nine tide gauge stations south of Tacoma Narrows.

Table 4-1. Result of the calibration; the tidal forcing at the open northern model boundary.

Constituent, Ω (deg/hr)	Elevation-specified amplitude (m)	Greenwich phase angle, G (deg)	Greenwich velocity, u (deg)	Greenwich offset, V_o (deg)	Radiative-separation amplitude (m)	Greenwich phase lag (s)
M2 (28.984)	1.107	11.5	117.83	0.65	0.536	43683
S2 (30.000)	0.258	37.9	0	0	0.133	15890
K1 (15.041)	0.22	277.3	9.94	3.94	0.099	11690
O1 (13.943)	0.742	255.4	-5.45	107.89	0.375	32220
N2 (28.440)	0.378	340.2	357.34	0.65	0.178	6279

* instantaneous values for 1/1/96, the start of the model run

Methods

October 1996 to September 1997 was selected as the calibration period for the model. Significant data were available for Budd Inlet, a critical model area, through studies associated with the LOTT wastewater discharge (Aura Nova Consultants et al., 1998). Monthly boundary conditions of temperature and salinity were interpolated from the mean value of two King County Department of Natural Resources stations. Stations LSNT01 (Dolphin Point, 47°32' N, 122°26' W) and KSBP01 (Point Jefferson, 47° 44'36" N, 122° 25'44" W) are located south and north of the model boundary. Historical tidal elevations were available from the National Ocean Service (NOS; part of the National Oceanic and Atmospheric Administration, or NOAA), Pacific Marine Environmental Laboratories (PMEL, also operated by NOAA), and the University of Washington (UW) for calibration. Figure 4-3 and Table 4-2 present the locations of these stations.

Table 4-2. Locations of NOS, PMEL, and UW tide gauge stations in South Puget Sound.

Station	Latitude (degree-minutes)	Longitude (degree-minutes)	Description	Source	Dates Available
0000	47 36.00	122 20.00	Seattle reference station	NOS	18-yr time series
0178	47 13.00	123 05.00	Oakland Bay near Shelton	UW	7-day time series (1954 only*)
6969	47 03.00	122 54.00	Budd Inlet near Olympia	NOS	29-day series
6800	47 08.50	122 54.20	Dofflemeyer Point, Boston Harbor, Budd Inlet	NOS	29-day series
6281	47 23.00	122 49.40	Case Inlet near Allyn	NOS	29-day series
6828	47 07.10	122 39.90	Nisqually	NOS	29-day series
6500	47 16.50	122 45.50	Carr Inlet – W (Von Geldern Cove)	NOS	29-day series
6451	47 18.10	122 40.90	Carr Inlet – E (Horsehead Bay)	NOS	29-day series
6539	47 15.40	122 38.90	Carr Inlet – Fox Island	NOS	29-day series
6486	47 16.30	122 33.10	Tacoma Narrows Bridge	NOS	29-day series

* Only the M2 tidal component can be derived, given the short time span.

As described in Section 2, Ecology conducted several cruises to obtain synoptic hydrography for the *South Puget Sound Water Quality Study*. The September 1997 cruise occurred during the calibration period; however, cruise data did not include synoptic current meter data, which would provide direct measurements of velocity for calibration purposes. Wind data from the Olympia Municipal Airport (National Climate Data Center station Olympia WSO AP, 456114) were applied to the entire model domain. Freshwater inputs are described in Section 3 of this report.

Area-wide Tidal Elevation Calibration

The first step in the calibration was the area-wide response to tidal forcing. The tidal forcing was adjusted at the north end of the model to best fit the observed tidal elevations at the nine tide gauge stations presented in Figure 4-3. Figure 4-4 illustrates that model tidal elevations are consistent with measured elevations. The largest differences between the modeled and measured tidal elevations occur at high tide, which the model underpredicts. This should be conservative in that the model underpredicts flushing in this regard. Model results support the finding by Mofjeld and Larsen (1984) that the phase relationships between the diurnal and semi-diurnal constituents in Puget Sound tides give rise to nearly equal high waters each day, but produce a distinct mean lower low water (MLLW) and mean higher low water (MHLW), except for the brief periods when the moon is near the equator.

Measured data at the nine tide gauge locations were transformed with a harmonic analysis of the time domain data. A simulation period of 29.5 days was used to calculate frequency domain transformations of amplitude and phase presented in Table 4-3 with a Fourier/harmonic analysis routine (Foreman, 1978).

The phase angles are derived from NOS, PMEL or UW tide gauge data, with the Greenwich phase lag, G (degrees), available from Lavelle and Mofjeld (1985) and adjusted for the current offsets due to position in the saros. A saros is the roughly 19-year period over which the Earth, Sun, and Moon return to approximately the same relative position with respect to each other. Tide phases are relative to January 1, 1985 with times given in GMT. The conversion from Greenwich phase lag to the model start time (January 1, 1996), theta (Θ) is given by:

$$\Theta = G - u - V_o$$

where u is Greenwich velocity (deg) and V_o is Greenwich offset (deg). For example, the lunar semidiurnal (M2) tide = $11.5^o - 117.83^o - 0.65^o = -106.98^o = +253.02^o$. With a frequency for the M2 component of 28.984 deg/hr, this represents a lag of 8.7296 hr, or 31427 s. The lag reported in Table 4-1 differs from this because a radiation-separation scheme was used rather than an elevation specified one (Hamrick, Ibid). Local time (PST) is eight hours behind Universal Coordinated Time, formerly known as Greenwich Mean Time. Schureman (1958) provides a complete description on tidal formulations.

Table 4-3. Observed and modeled amplitude (m) and Greenwich phase angle (degree) for each constituent in the barotropic tide.

Station/ Component	Amplitude (m)		Phase Angle (deg)		Difference (m, deg)	
	Observed	Simulated	Observed	Simulated	Amplitude	Phase
TN (6486)	1.225	1.193	21.4	17.5	-0.03	-3.9
M2	0.896	0.911	282.9	279.7	0.02	-3.2
K1	0.298	0.285	49.3	44.0	-0.01	-5.3
S2	0.502	0.496	258.8	255.8	-0.01	-3.0
O1	0.238	0.202	-1.6	351.9	-0.04	-6.5
N2	1.225	1.193	21.4	17.5	-0.03	-3.9
FX (6539)						
M2	1.33	1.354	27.2	23.29	0.02	-3.9
K1	0.927	0.934	285	282.62	0.01	-2.4
S2	0.324	0.320	55.2	52.73	0.00	-2.5
O1	0.479	0.459	257.1	255.44	-0.02	-1.7
N2	0.249	0.229	-1.6	1.19	-0.02	2.8
CE (6451)						
M2	1.318	1.358	22.3	23.76	0.04	1.5
K1	0.927	0.937	284.5	282.59	0.01	-1.9
S2	0.324	0.322	57.9	53.09	0.00	-4.8
O1	0.479	0.462	258.3	255.33	-0.02	-3.0
N2	0.249	0.231	-1.6	2.1	-0.02	3.7
CW (6500)						
M2	1.333	1.357	27.2	23.66	0.02	-3.5
K1	0.876	0.937	283.7	282.71	0.06	-1.0
S2	0.321	0.321	57.9	53.03	0.00	-4.9
O1	0.437	0.462	261.6	255.48	0.02	-6.1
N2	0.267	0.230	8.5	1.81	-0.04	-6.7
NQ (6828)						
M2	1.34	1.360	27	25.02	0.02	-2.0
K1	0.92	0.933	284.8	283.36	0.01	-1.4
S2	0.321	0.322	56.5	54.55	0.00	-1.9
O1	0.464	0.458	257.8	256.2	-0.01	-1.6
N2	0.253	0.230	1.8	2.71	-0.02	0.9
AL (6281)						
M2	1.412	1.449	30	26.63	0.04	-3.4
K1	0.867	0.955	288.1	284.25	0.09	-3.9
S2	0.33	0.344	57.9	56.63	0.01	-1.3
O1	0.435	0.466	261	257.03	0.03	-4.0
N2	0.265	0.245	8.5	5.33	-0.02	-3.2
OB (0178)						
M2	1.49	1.382	58	62.01	-0.11	4.0
K1	NA	0.924	NA	309.3	NA	NA
S2	NA	0.277	NA	94.8	NA	NA
O1	NA	0.380	NA	282.54	NA	NA
N2	NA	0.227	NA	52.09	NA	NA
DP (6800)						
M2	1.44	1.444	32.2	31.08	0.00	-1.1
K1	0.945	0.952	287.7	287.09	0.01	-0.6
S2	0.354	0.339	61.5	62.12	-0.01	0.6
O1	0.483	0.458	259.1	259.57	-0.03	0.5
N2	0.262	0.243	0.8	10.85	-0.02	10.1
BI (6969)						
M2	1.464	1.467	29.9	31.23	0.00	1.3
K1	0.849	0.957	288.7	287.12	0.11	-1.6
S2	0.348	0.345	62.4	62.29	0.00	-0.1
O1	0.463	0.460	265.1	259.53	0.00	-5.6
N2	0.275	0.247	3.2	11.14	-0.03	7.9

NA = Not available from a 7-day time series

A sixth constituent, P1, accounts for a known seasonal variation in tidal flushing. An important low-frequency change between the equinoxes (lower mixing) and the solstices (higher mixing) results from an interaction between the P1 and K1 constituents. The frequency of P1 (0.99726 cycle/day) is extremely close to that of K1 (1.00274 cycle/day), inducing a lower "beat" frequency inversely proportional to the difference between K1 and P1 with a period of about 180 days. This may be important because wind forcing is often low in late September, and phytoplankton are dying and decaying. Phytoplankton levels often peak in the spring, decline in July, then peak again in the fall (Newton et al., 1998). All this contributes to the low dissolved oxygen levels observed in the late summer and early fall. Several cruises, discussed in Section 2, were scheduled to evaluate the annual minima in dissolved oxygen in particular inlets of interest. Interannual fluctuations modulate the magnitude of dissolved oxygen depletion during a given year.

Since the frequencies of the P1 and K1 components are so close, they are difficult to separate with Fourier analysis. The present application can assume a ratio in the amplitudes and an offset in the phases from the Seattle 19-year station, located outside of the model domain, and applies it throughout Puget Sound (Mofjeld, 2000).

Tidal Exchange vs. Mean Flow

Tidal exchange and mean flow represent two distinct considerations. Puget Sound south of the Tacoma Narrows has a volume at mean high water of 1.58×10^{10} m^3. The mean intertidal volume is 1.66×10^9 m^3, implying an apparently short residence time of about 10 tidal cycles, or five days by tidal (prism) exchange. The fluid is stratified, however, and the effective residence time should be based on the tidally averaged[15] mean flow, calculated by summing the absolute value of the flow in each layer over a synodic month (709 hours) and dividing by the number of layers.

For example, consider a system of two equal-depth layers with flows of 400 m^3/s moving outward in the upper layer, and 300 m^3/s moving inward in the bottom layer. The vertically-averaged net outward flow of 100 m^3/s (400 m^3/s – 300 m^3/s) corresponds to riverine input. The tidally-averaged mean (exchange) flow, however, is (ABS(400 m^3/s) + ABS(-300m^3/s)) / 2 layers = 350 m^3/s (the average of the absolute values of the two flows). Of course, the actual flows will vary throughout the year with changing winds and other factors that affect mixing. The surface typically flushes quicker than the bottom waters. These flows are important when evaluating pollutant fate and transport. If a buoyant particle of pollution is tracked, it feels a net outward flow of 400 m^3/s; a heavy pollutant would presumably be advected inward to the estuary head at net 300 m^3/s, upwelled, and recirculated out. That assumes that it is not too dense or insoluble to mix.

The average flood tide pushes a water parcel into South Puget Sound and the average ebb draws it out again, plus a small transport out. This steady progress seaward, the incremental transport beyond the ebb, is most important to the transport of pollution. It is important to note, however,

[15] The residual mean flow consists of baroclinic components only. Baroclinic circulation results from motions induced internally by density stratification (e.g., differences in temperature and salinity).

that if the mean flows are small relative to ebb and flood, that it will not take long for a specific particle to leave the zone with a small mean flow and enter a different zone with a larger one. For this reason Eulerian mean flows are only one aspect to consider. They do suggest much longer residence times, on the order of two months rather than five days. There are very few field measurements of these mean flows (Albertson et al, 2001), and more are needed to test the calibration of this model on monthly to annual time scales. Tidal gauge heights are relatively insensitive to freshwater inflows, and to a lesser extent the wind patterns, but mean flow is most sensitive to these and is one reason that a specific year is being simulated.

Comparison of Model Output with Current Meter Data in Budd Inlet

No domain-wide measurements of water velocity were available for model calibration. Some prior current data are available for Budd Inlet from the LOTT Budd Inlet study (Aura Nova Consultants et al., 1998). Tidal ellipses provide a means of comparing observed and simulated results by plotting velocity components against each other. Figure 4-5 defines tidal ellipse geometry, where the major axis (a) defines the primary flow direction and magnitude, and the minor axis (b) defines orthogonal current components. The orientation (θ) is the angle between the major axis and the east compass direction. The tidal current arrows form tidal ellipses for each constituent of the tidal cycle.

Figure 4-6 compares model results from northeastern Budd Inlet with current meter[16] data from Budd Inlet station BE-1 (47° 7.79' N, –122° 54.42' W). Model output data are presented as a scatterplot of orthogonal velocities. The orientation of this ellipse ($\theta = 99.8°$) is similar to many of the individual constituents from a spectral decomposition shown in Table 4-4. The South Puget Sound model uses three grid cells to cover the width of Budd Inlet at this location, as compared with seven grid cells in the LOTT model application (Aura Nova Consultants et al., 1998), which may account for the slight differences. Overall, however, model output for Budd Inlet from the present model application agrees with the detailed Budd Inlet model application.

Table 4-4. Spectral decomposition of simulated and observed tidal ellipse components.

Constituent	Period	Simulated			Observed		
		A	B	θ	a	b	θ
M2	12.42	14.55	0.05	99.5	15.68	0.12	106.9
S2	12	10.86	0.04	99.5	4.38	0.05	103.8
N2	12.66	14.36	0.05	99.5	2.46	0.24	114.1
K1	23.93	5.8	0.01	98.8	2.02	0.09	117.2
O1	25.82	3.38	0.00	95.7	0.91	0.04	166.4

Test of Sigma Coordinate System

When the sigma coordinate system is used in the Navier Stokes equations, the $\partial/\partial z$ terms give rise to $\partial/\partial\theta$ terms as well as extra terms which may lead to fictitious velocities. Running the

[16] Aanderaa (rotor-type current meter useful for moderate to high flows) and Acoustic Doppler Current Profiler (ADCP)

model with no forcing identifies the magnitude and location of these fictitious velocities. Figure 4-7 compares the fictitious velocities (A) with velocities typical of a flood tide (B). Fictitious velocities are significantly less than those associated with typical flood tides except near the Tacoma Narrows and Colvos Passage, which are outside of the primary area of model interest. Thus, the use of the sigma coordinate system seems appropriate for South Puget Sound.

Salinity and Temperature Time Series Comparisons in Budd Inlet

The velocity calibration discussed above indicates that the parameterization for tidal forcing and wind effects is appropriate for South Puget Sound, and the barotropic[17] and daily tidal forcing are correct. In addition, the sunlight representation is consistent with standard approaches. The thermodynamics do not affect barotropic tidal velocities but will influence water quality and mean flow.

Temperature and salinity time series produced from a one-year simulation using a 30-second time step yielded significantly different results than measured data. Figure 4-8 compares model results with measured time series in western Budd Inlet. Temperature is overpredicted up to 4°C, although the model adequately represents the seasonal pattern. Salinity, however, is higher than measured, with peaks of 40 psu compared with measured peaks of 27 psu. Salinity also exhibits an upward trend as the simulation progresses. Decreasing the time step to 15 s produced little change in the temperature and salinity results. Thus, the model does not adequately represent thermodynamics in its present state and will need to be investigated in Phase 2 of the project. That this problem does not occur in a sub-model of Budd Inlet provides a clue into the origin of the cause for the next phase.

Summary and Conclusions

In general, hydrodynamic model simulations show good agreement with measured tide gauge data available at nine stations in South Puget Sound. Adjustments to the tidal forcing at the open north boundary was required to match the response at nine NOS and PMEL tide gauge stations south of the Tacoma Narrows. However, a small advancement of phase lag over the observed values from seaward to landward indicates that slightly too much friction is present in the model. This is conservative in that it predicts slightly longer flushing times with the model than actual conditions due to elevated friction. Specific bottom substrates are not well represented in the model and could be adjusted in the future. An evaluation of mean flow against measured data may lead to some modifications in the grid itself.

Determining the cause of the temperature and salinity differences should be a priority for Phase 2 of the project. Many state variables depend on temperature and salinity, and these must be represented correctly. In addition, field measurements of mean flow and current velocities (e.g., drifters, current meters, and dye studies) will improve model calibration.

---

[17] Barotropic flows include motions induced externally by water surface slope, induced by tides or atmospheric pressure gradients

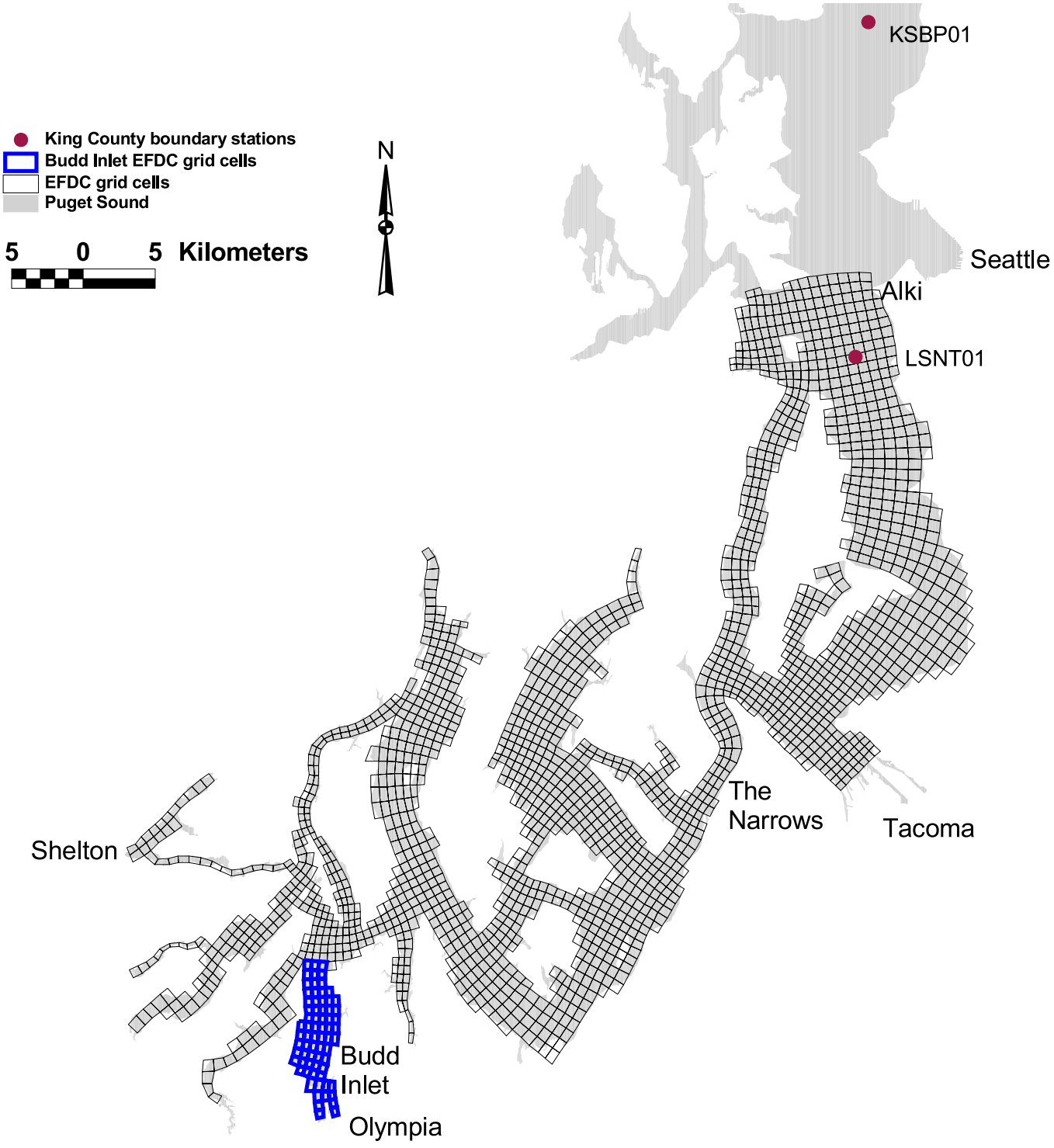

Figure 4-1. Computational grid for the South Puget Sound Model.

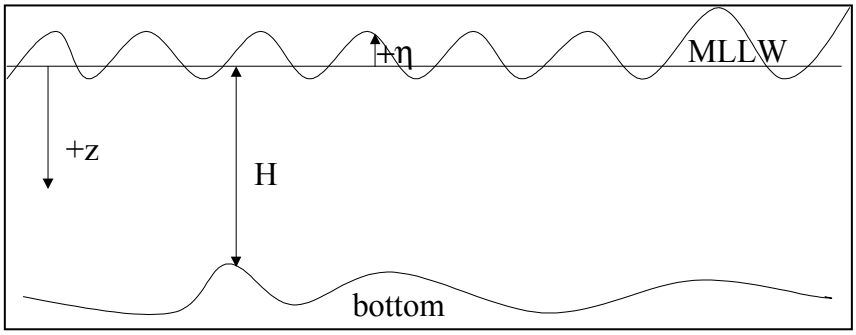

Figure 4-2. Definition sketch for sigma coordinate system.

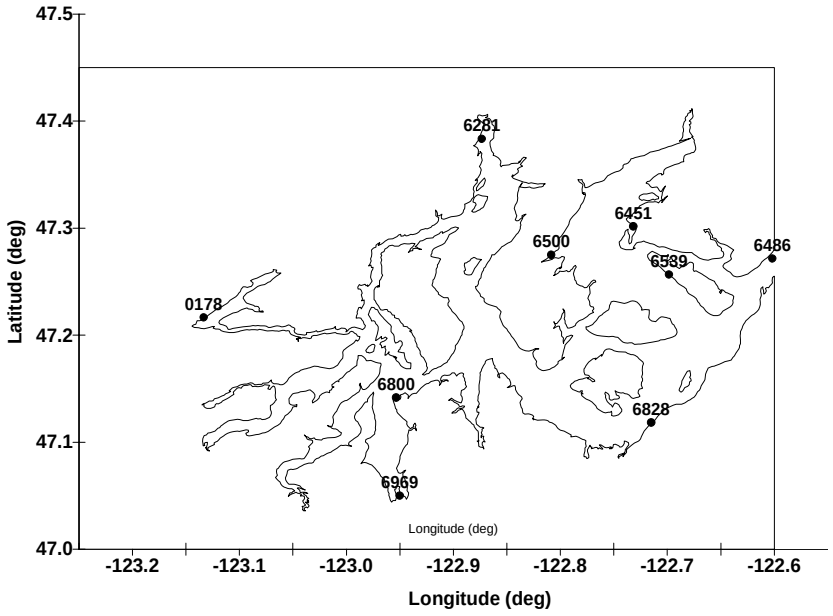

Figure 4-3. Location of nine tide gauge stations used to calibrate the hydrodynamic model of South Puget Sound.

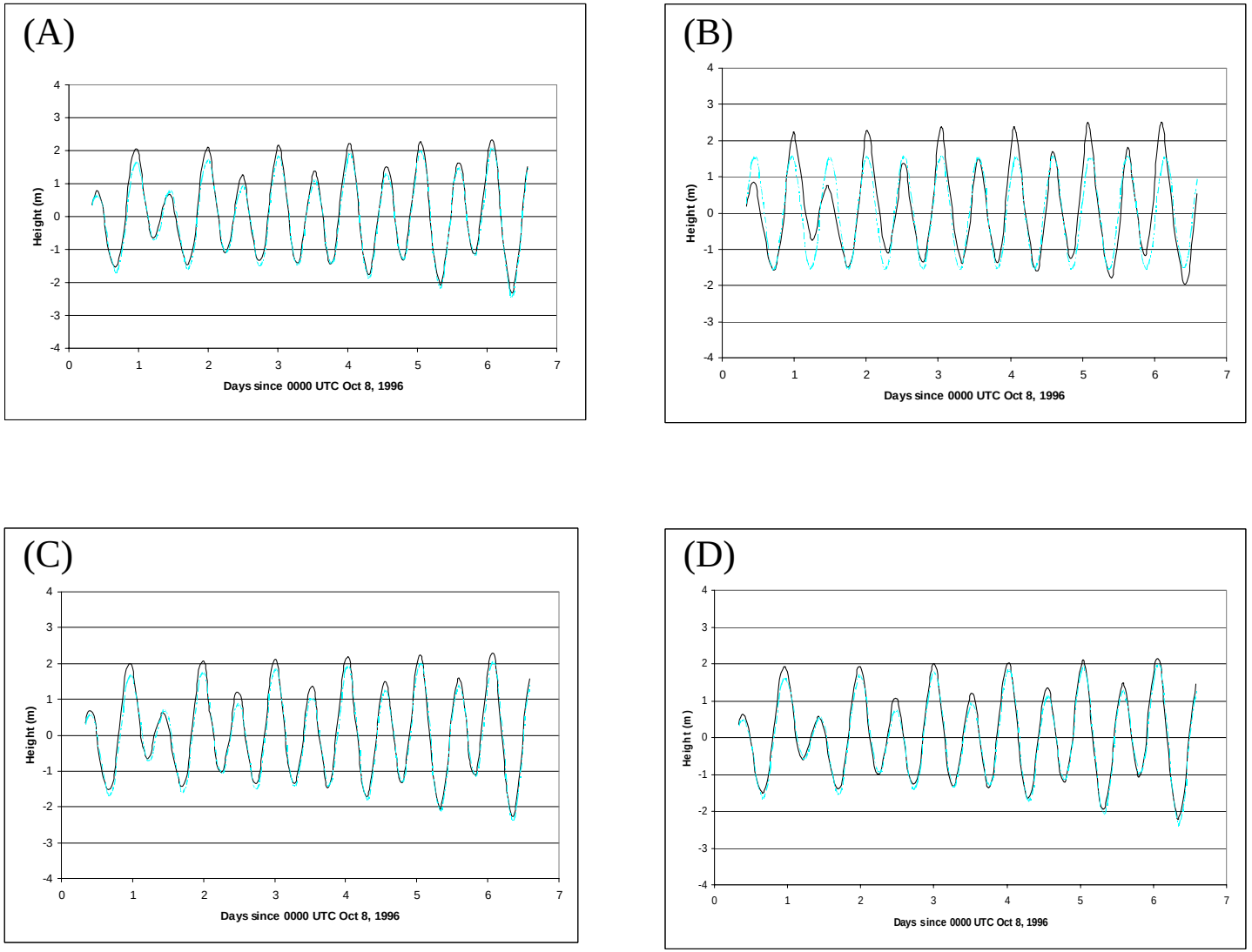

Figure 4-4. Time series for observed tides with no wind (light gray lines) with model output (solid black lines) at (A) Budd Inlet (6969), (B) Oakland Bay, Shelton (0178), (C) Port of Allyn in Case Inlet (6281) and (D) Carr Inlet (6451).

Due to the short duration of the time series at Oakland Bay (1 week), only an M2 constituent is typically available, which is responsible for the large discrepancy.

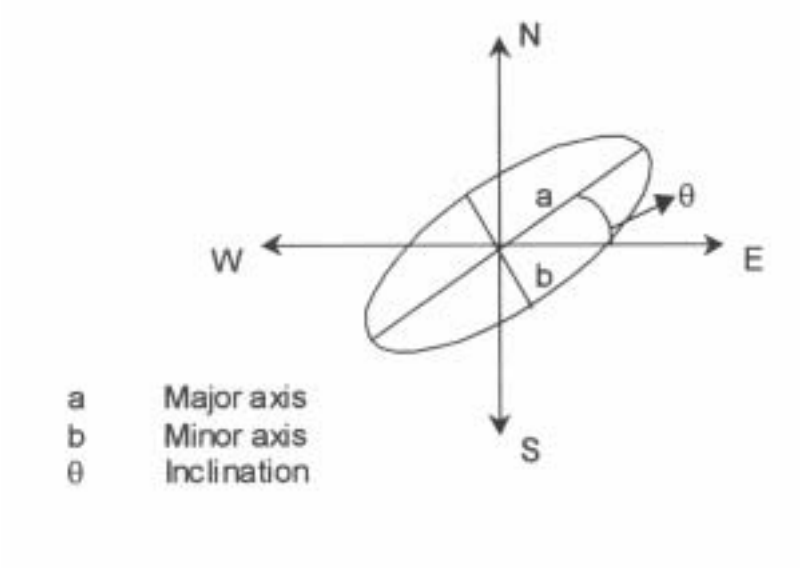

Figure 4-5. Major and minor axes (cm/s) and inclination of tidal current ellipses of major harmonic constituents for Budd Inlet stations.

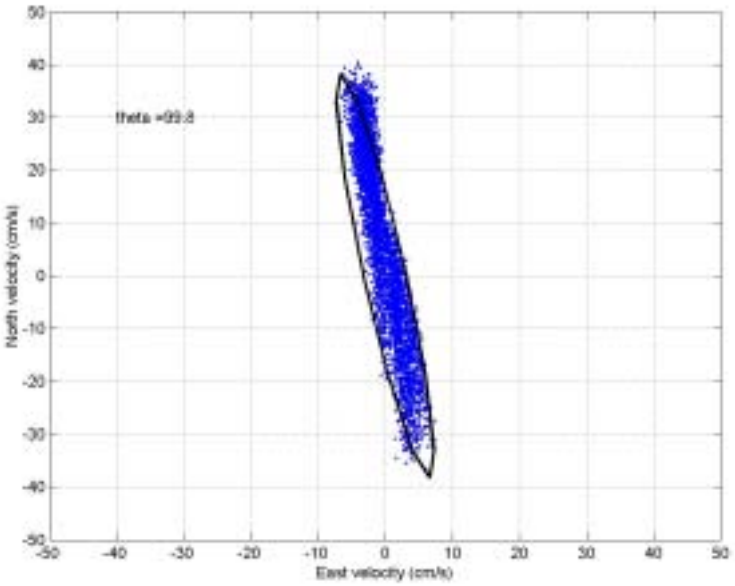

Figure 4-6. Comparison of modeled (dots) and measured (black ellipse) tidal current components at Budd Inlet station BE-1. Data were collected using Aanderaa meters deployed for 74 days from January 21, 1997 to April 5, 1997.

(A)

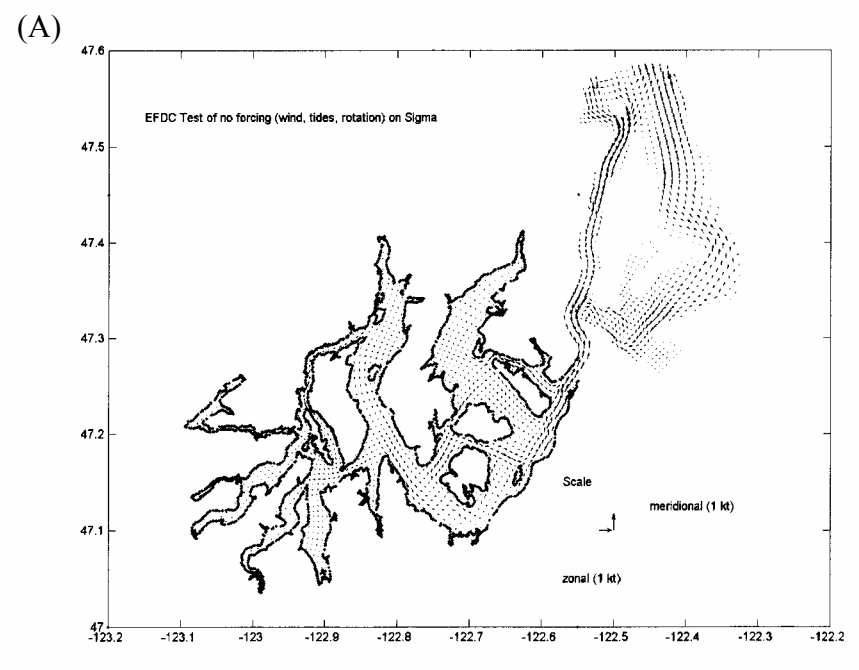

(B)

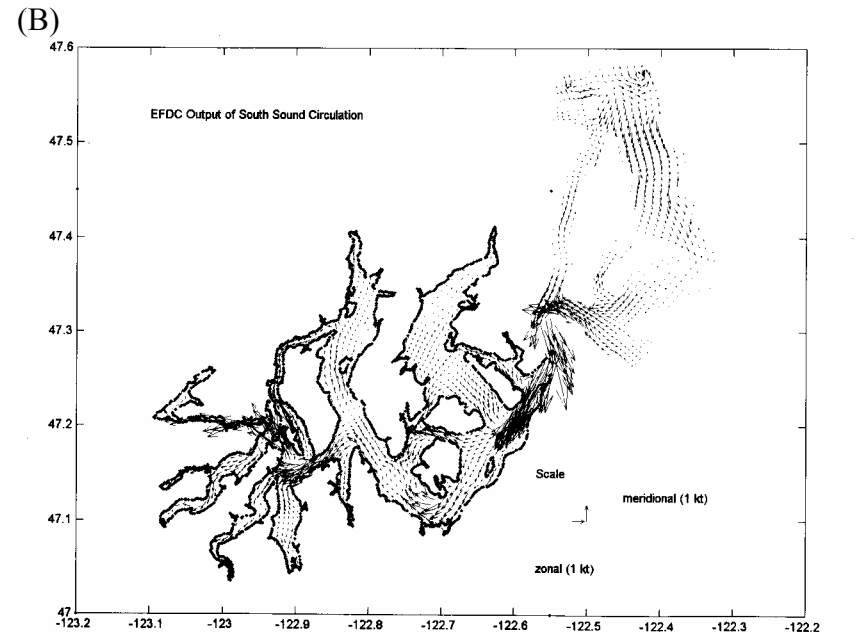

Figure 4-7. (A) Fictitious velocities that occur when no forcing is applied with sigma coordinates, and (B) a typical flood tide for comparison. Both are surface velocities.

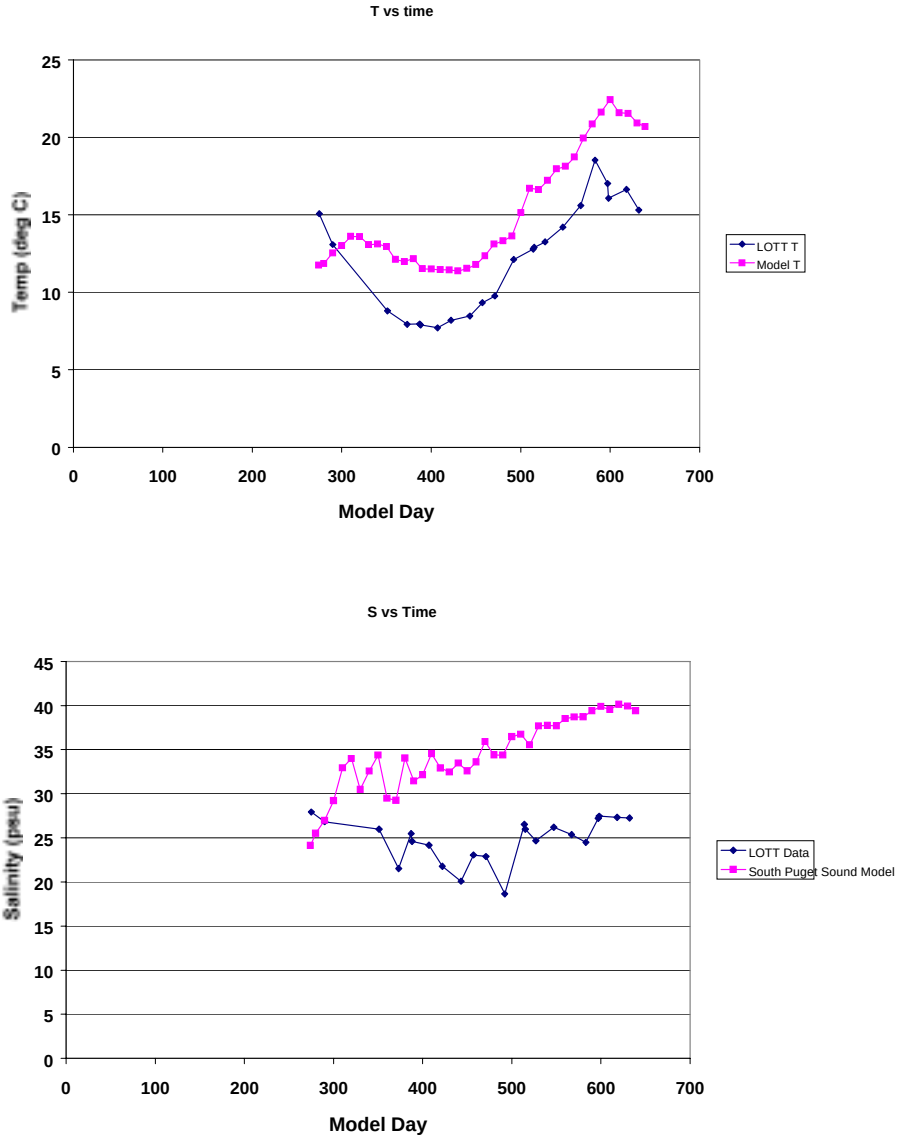

Figure 4-8. Temperature and salinity from a one-year simulation vs. measured data in the lowest water column layer in the west bay of Budd Inlet.

5. Water Quality Model

by G. Pelletier

Introduction

The water quality model simulates the concentration of dissolved oxygen (DO) in response to primary production of phytoplankton, oxidation of organic material, and sediment flux (Figure 5-1, Table 5-1, and Appendix B). Of the 21 possible state variables in EFDC, the model of South Puget Sound includes the following: two phytoplankton groups, three forms of organic carbon, three forms of organic phosphorus and nitrogen, dissolved reactive phosphorus, ammonia nitrogen, nitrate plus nitrite nitrogen, chemical oxygen demand, and dissolved oxygen. Fecal coliform bacteria was also included.

Table 5-1. EFDC model water quality state variables.

EFDC variable number	EFDC variable name	Symbol	Included in South Puget Sound model
1	cyanobacteria	Bc	no
2	diatom algae	Bd	yes
3	green algae	Bg	yes
4	refractory particulate organic carbon	RPOC	yes
5	labile particulate organic carbon	LPOC	yes
6	dissolved organic carbon	DOC	yes
7	refractory particulate organic phosphorus	RPOP	yes
8	labile particulate organic phosphorus	LPOP	yes
9	dissolved organic phosphorus	DOP	yes
10	total reactive phosphorus	TPO4	yes
11	refractory particulate organic nitrogen	RPON	yes
12	labile particulate organic nitrogen	LPON	yes
13	dissolved organic nitrogen	DON	yes
14	ammonia nitrogen	NH4	yes
15	nitrate + nitrite nitrogen	NO23	yes
16	particulate biogenic silica	SU	no
17	dissolved available silica	SA	no
18	chemical oxygen demand	COD	yes
19	dissolved oxygen	DO	yes
20	total active metal	TAM	no
21	fecal coliform bacteria	FCB	yes
22	macroalgae	Bm	no

A sediment process model is coupled with the water column model (Appendix C). The sediment model incorporates depositional flux of particulate organic matter (POM), diagenesis of POM, and the resulting sediment flux.

The water quality model also was calibrated to limited data collected between October 1996 and September 1997, as was the hydrodynamic model described in Section 4.

Because of the relative scarcity of data, the model is roughly calibrated at this time. Rigorous evaluations of model accuracy were not conducted during this phase of the project. Subsequent phases of the project will incorporate additional data collection to increase the rigor of evaluations of goodness-of-fit and model acceptability and uncertainty.

Methods

The computational grid for water quality modeling was identical to the grid used for hydrodynamic modeling, described in Section 4 and presented in Figure 4-1. Each of the cells comprises four layers in the sigma coordinate system to represent vertical profiles. The portion of the computational grid that represents Budd Inlet was extracted from the full grid to create a separate sub-model to facilitate model calibration using data from Budd Inlet.

The mass balance equations in the EFDC model are solved using the finite-difference method. A computational time step of 15 seconds or less was required for stability of the hydrodynamic model for the full grid. The water quality time step[18] was twice the hydrodynamic time step. The Budd Inlet sub-grid was extracted from the full grid to allow more practical use of the model with faster simulation performance[19]. This allowed for numerous simulations to test the results of the model using various calibration parameters, and to perform sensitivity analyses.

Boundary Conditions

The concentrations of water quality state variables at the saltwater boundary of the model grid represent boundary conditions. Boundary conditions for salinity, temperature, algae, organic carbon, dissolved oxygen, nitrogen, phosphorus, and fecal coliform bacteria were based on monitoring data collected near the open boundaries. For the full model grid, King County monitoring stations KSBP01 and LSNT01 (Figure 4-1) were selected to provide the best estimate of boundary conditions near Alki Point, used as the northern model boundary. For the Budd Inlet sub-grid, the data collected by LOTT from the four stations that cross the entrance to Budd Inlet were used to characterize the boundary (Figure 5-2; stations BF-1, BF-2, BF-3, and BF-4 described in Aura Nova Consultants et al. [1998]). A time series of the boundary concentrations of each model variable was interpolated from the data for the simulation period of October 1, 1996 through September 30, 1997.

The freshwater inflows and loads to the model domain are described in Section 3. In summary, daily flows and loads were calculated for 71 watershed inflows and 30 point sources.

[18] The required time steps resulted in fairly slow model simulations. Using a dual-processor Pentium-III 733 MHz workstation, the run-time required for a 12-month simulation was over 9 days. Simulations using the full grid were limited to periods of 7 months, which still required over 5 days to run.

[19] A computational time step of 300 seconds was sufficient for stability of the hydrodynamic model. The combination of a longer time step and few computational grid cells resulted in fast performance of less than half an hour to complete a 12-month simulation.

Climatology Data

Meteorological data for South Puget Sound were obtained from two primary sources:

- EarthInfo databases of the U.S. National Oceanographic and Atmospheric Administration (NOAA) National Climate Data Center (NCDC) surface airways and hourly precipitation (EarthInfo, Inc., Boulder CO, http://www.csn.net/~jacke/); and

- University of Washington Internet distribution of NCDC and UW climate data from the UW web site (http://www-k12.atmos.washington.edu/k12/grayskies/ nw_weather.html).

Data were obtained for four climate stations:

- Olympia Municipal Airport (NCDC WBAN station 24227)
- SeaTac Airport (NCDC WBAN station number 24233)
- Boeing Field (National Weather Service station BFI)
- University of Washington Atmospheric Sciences building

Available hourly climate data include barometric pressure, air temperature, relative humidity, precipitation, and cloud cover.

The EFDC model also requires a time series of solar short wave radiation for estimating photosynthesis and other processes that are dependent on light intensity. A FORTRAN program, based on Spencer (1971), generated time series of solar declinations, angles above horizon, and intensities for any specified latitude and longitude from functions. The program was calibrated to measurements of solar radiation at the UW Atmospheric Sciences building roof and cloud data from Boeing Field to estimate time series of actual short wave radiation onto the ground or water surface, accounting for shading from clouds. The program was then applied to generate time series of effective short wave radiation for locations where cloud cover data were available.

Model Calibration Parameters

The central issues in calibrating the water quality model is simulating the primary production by algae, decomposition of oxygen containing material, and the concentration of dissolved oxygen. Understanding the planktonic organisms, the effects of nutrient enrichment, and the rates and pathways of organic matter production and decomposition will determine the precision and accuracy of the model to predict dissolved oxygen concentrations.

Calibration of the water quality model consists of selecting of values to represent the kinetics and constants of the model equations. Model parameter selection is an iterative process, where parameters are adjusted within a range of feasible values to obtain the best agreement between predicted and observed values of the state variables. There may not be a unique combination of parameter values that would be representative of the conditions in Puget Sound. Several possible sets of parameters may produce similar agreement between predicted and observed conditions.

Two sets of parameters were evaluated for the model of South Puget Sound. Table 5-2 and Appendix D present the estimated parameters for both sets. The first set represents calibration parameters for Chesapeake Bay and the Peconic estuary (Cerco and Cole, 1994; Tetra Tech, 1998). The Chesapeake Bay parameters generally represent estuarine conditions based on experience in modeling studies on the East Coast of the United States. The second set of parameters considered was developed for a modeling study of Budd Inlet (Aura Nova Consultants et al., 1998; Boatman and Edinger, 1999). Calibration of the EFDC model to South Puget Sound was evaluated by comparing the model results with observed concentrations using the two sets of model parameters. A sensitivity analysis of model was conducted for various ranges of key parameters.

Table 5-2. Rates and constants for water column parameters in South Puget Sound application of the EFDC model.

Description	Units	Chesapeake/ Peconic Study	LOTT Study	Range of reported values
Card 8: Algae				
Nitrogen half saturation for algae group 2/d	g/m^3	0.01	0.006	0.001-0.14
Nitrogen half saturation for algae group 3/g	g/m^3	0.01	0.02	0.001-0.14
Phosphorus half saturation for algae group 1/d	g/m^3	0.001	0.001	0.001-0.05
Phosphorus half saturation for algae group 1/g	g/m^3	0.001	0.001	0.001-0.05
Card 9: Algae				
Carbon:chlorophyll for algae group 2/d	g-C/mg-Chl	0.05	0.07	0.02-0.2
Carbon:chlorophyll for algae group 3/g	g-C/mg-Chl	0.1	0.07	0.02-0.2
Card 15: Carbon and Denitrification				
Half saturation of oxygen for oxic respiration	$g\text{-}O/m^3$	0.5	0.1	
Card 22: Nitrogen, Hydrolysis/Mineralization of Organic Nitrogen				
Minimum hydrolysis rate for OrgN (labile)	1/day	0.075	0.075	
Minimum hydrolysis rate for OrgN (dissolved)	1/day	0.02	0.025	
Card 40: Algae				
Maximum algae growth rate for group 2/d	1/day	2.5	4	0.2-5.0
Maximum algae growth rate for group 3/g	1/day	2.5	1.2	0.2-5.0
Basal metabolism rate for group 2/d	1/day	0.05	0.25	0.02-0.36*
Basal metabolism rate for group 3/g	1/day	0.06	0.25	0.02-0.36*
Predation rate for group 2/d	1/day	0.25	0.21	0.01-1.0*
Predation rate for group 3/g	1/day	0.28	0.12	0.01-1.0*
Card 41: Settling Velocities				
Settling rate for algae group 2/d	m/day	0.35	0.5	
Settling rate for algae group 3/g	m/day	0.25	0.25	
Settling rate for labile particulate organic matter	m/day	1.5	0.5	0.5-1.5*

* Cerco and Cole (1994)

Results and Discussion

Results for the Budd Inlet Grid

Figures 5-3 through 5-6 compare predicted and observed chlorophyll, dissolved inorganic nitrogen (DIN), and dissolved oxygen in Budd Inlet. Figures 5-3 and 5-4 show surface- and bottom-layer conditions in the central region of Budd Inlet (station BUD005). Figures 5-5 and 5-6 show surface and bottom conditions in the inner West Bay region of Budd Inlet (stations BI-5 and BI-6).

In general both sets of parameters provide model results that describe many of the seasonal patterns of the observed data. The model results show increases in chlorophyll during the April to September season. Concentrations of DIN were predicted to decline during the same period, which is consistent with observed patterns caused by algal uptake. Concentrations in the bottom layer were predicted to decrease during the summer, although the model tends to over-predict the dissolved oxygen in the bottom layer. This could result from the action of dinoflagellates, which settle at night and take up oxygen; alternatively, the sediment oxygen demand may be too low.

The results for Budd Inlet suggest that each of the two parameter sets (Chesapeake/Peconic merged data set and LOTT parameters) provides a reasonable starting point for calibrating the EFDC model to South Puget Sound.

Results for the Full Grid

The full model grid shown in Figure 5-2 was applied using the Chesapeake parameters. Fewer simulations were possible using the full grid compared with the Budd Inlet grid because of the longer run-times required. Also, the model simulations for the full grid were limited to a duration of seven months. Evaluation of other parameter sets or sensitivity analysis and calibration using the full grid will occur in subsequent phases of the project.

Comparisons of predicted and observed water quality constituents in the surface layers at the four ambient monitoring stations in South Puget Sound are shown in Figures 5-7 through 5-10. Ecology's ambient monitoring of Puget Sound includes sampling of the upper 30 meters of the water column (sampling depths of 0, 10, and 30 meters). The model sufficiently represents the observed conditions in the surface layer, especially considering that Chesapeake parameters were used and there was no attempt made to calibrate the water quality model other than using actual boundary conditions, flows, and loads.

Available sampling data for the bottom layer are relatively sparse compared with the surface layer. Figures 5-11 through 5-13 compare predicted and observed water quality in the bottom layers at three of the ambient monitoring stations. Dissolved oxygen is well represented in Dana Passage and central Budd Inlet, but near-bottom dissolved oxygen is overpredicted in spring and early summer at Oakland Bay. DIN is overpredicted in Dana Passage, close to monitoring data in central Budd Inlet, and underpredicted in Oakland Bay. Chlorophyll *a* is significantly underpredicted in Budd Inlet.

Sensitivity Analysis

A sensitivity analysis was conducted to evaluate the changes in model predictions for various ranges of key parameters. Parameters were selected one at a time and varied within a reasonable range with all other parameters held constant. The Chesapeake Bay parameters were used as the baseline to conduct the sensitivity analysis. Figures 5-14 through 5-19 present the results of the analysis for bottom-layer dissolved oxygen in the inner West Bay region of Budd Inlet.

The following parameters were selected for the sensitivity analysis, in approximately decreasing order of sensitivity of the predicted bottom layer dissolved oxygen:

- Sediment oxygen demand multiplier (Figure 5-14)
- Settling rates of phytoplankton and particulate organic matter (Figure 5-15)
- Algal basal metabolism rates (Figure 5-16)
- Maximum algal growth rates (Figure 5-17)
- Zooplankton algal predation rates (Figure 5-18)
- Nitrogen half-saturation concentration (Figure 5-19)

The results of the sensitivity analysis suggest that proper calibration of the sediment model will be a key to water column model calibration. Sediment flux and concentration data are either very limited or nonexistent in most areas of South Puget Sound; this is an important data requirement for refinement of the calibration. Sediment flux studies should be designed according to methods that are recommended for calibration of water quality models (e.g., Di Toro and Fitzpatrick, 1993). The limited available data are *in situ* measurements from Budd Inlet. Di Toro and Fitzpatrick (1993) generally recommend *in vitro* measurements for model calibration. A study plan for further studies of sediment flux should include a review of available literature on calibration of sediment diagenesis models and the types of *in vitro* or *in situ* experiments that would be most useful.

Field studies for other key parameters, especially settling rates for phytoplankton and particulate organic matter and algal basal metabolism rates also would be useful for further refinement of the model calibration.

In addition to special studies to aid in estimation of key parameters, the available sampling data for concentrations of state variables in the water column and loading from tributaries are limited. Detailed spatial and temporal data are only available for Budd Inlet during the LOTT study. Ecology and the University of Washington are currently sampling an expanded spatial network of stations annually. Further refinement of the model calibration could be accomplished if the temporal frequency of sampling at the expanded network of stations increases to a monthly sampling interval for a year. Ideally this would coincide with increased spatial and temporally intensive sampling of the tributary loading sources.

Fecal Coliform Bacteria Simulation

The predicted and observed fecal coliform bacteria concentrations in Budd Inlet are presented in Figure 5-20. A fecal coliform die-off rate of 0.5 day^{-1} at 20 degrees C was assumed, based on Mancini (1978). In general, the model adequately represents fecal coliform in the outer part of the inlet. The model tends to under-predict the fecal coliform bacteria in the innermost regions, possibly because the loads of fecal coliform may have been underestimated, especially during the summer months. Possible sources that were not accounted for could include discharge from boats in the marinas in the inner inlet and feces of marine mammals.

Summary and Conclusions

The available sampling data for estimating state variables in the water column are limited. Detailed spatial and temporal data are only available for Budd Inlet during the LOTT study in 1996-97. Further refinement of the model calibration could be accomplished if the temporal frequency at an expanded network of stations was increased to approximately monthly sampling intervals for a one-year period. Ideally this would coincide with increased spatial and temporally intensive sampling of the loads from tributary sources.

Results of the EFDC model compare reasonably well with the limited available sampling data. The results for Budd Inlet suggest that each of the parameter sets for both the Chesapeake Bay and LOTT's Budd Inlet studies provides a reasonable starting point for calibrating the EFDC model to South Puget Sound.

Sensitivity analyses suggest that prediction of dissolved oxygen in the bottom layer is most sensitive to calibration of the sediment model, especially to sediment oxygen demand. Settling rates of phytoplankton and particulate organic matter, and basal metabolism rates of phytoplankton were also found to be particularly sensitive parameters for prediction of bottom dissolved oxygen.

Sensitivity to oxygen demand, settling rates, and algal metabolism rates show that dissolved oxygen is affected more by nutrient-driven processes than by direct biochemical oxygen demand (BOD) loading.

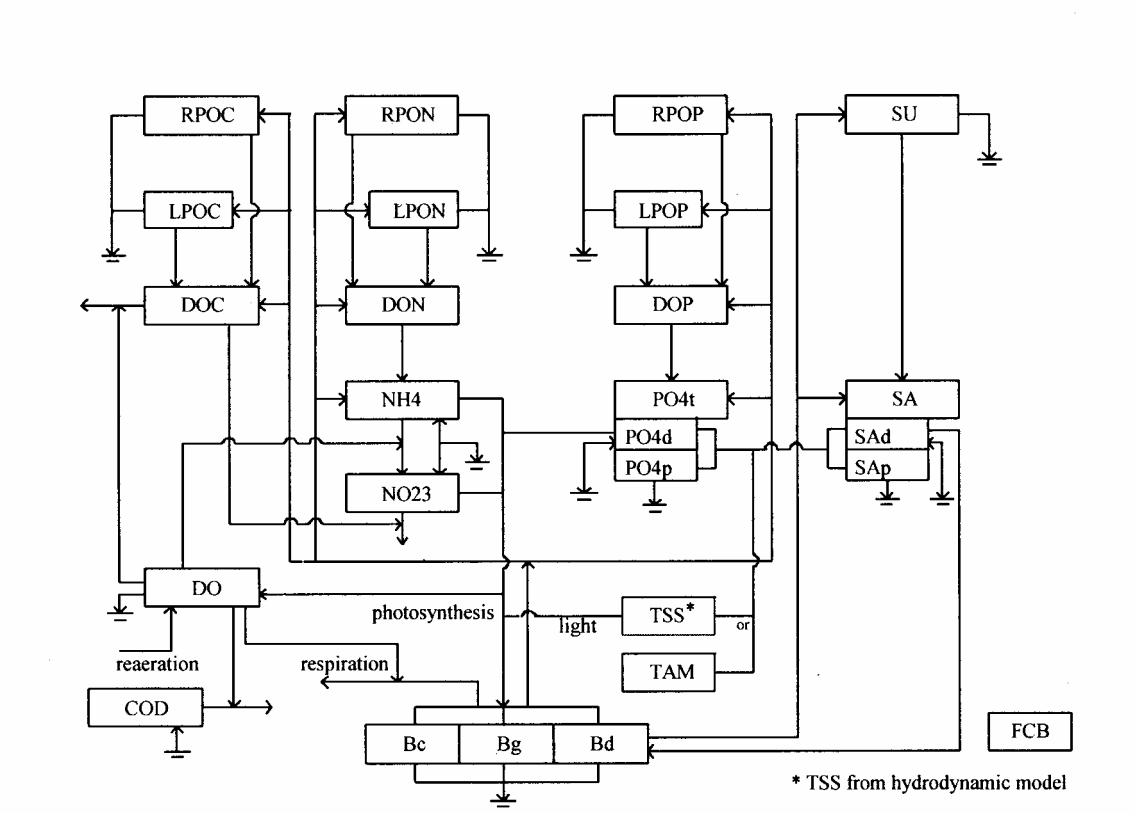

Figure 5-1. Schematic diagram of water column water quality model components of EFDC.

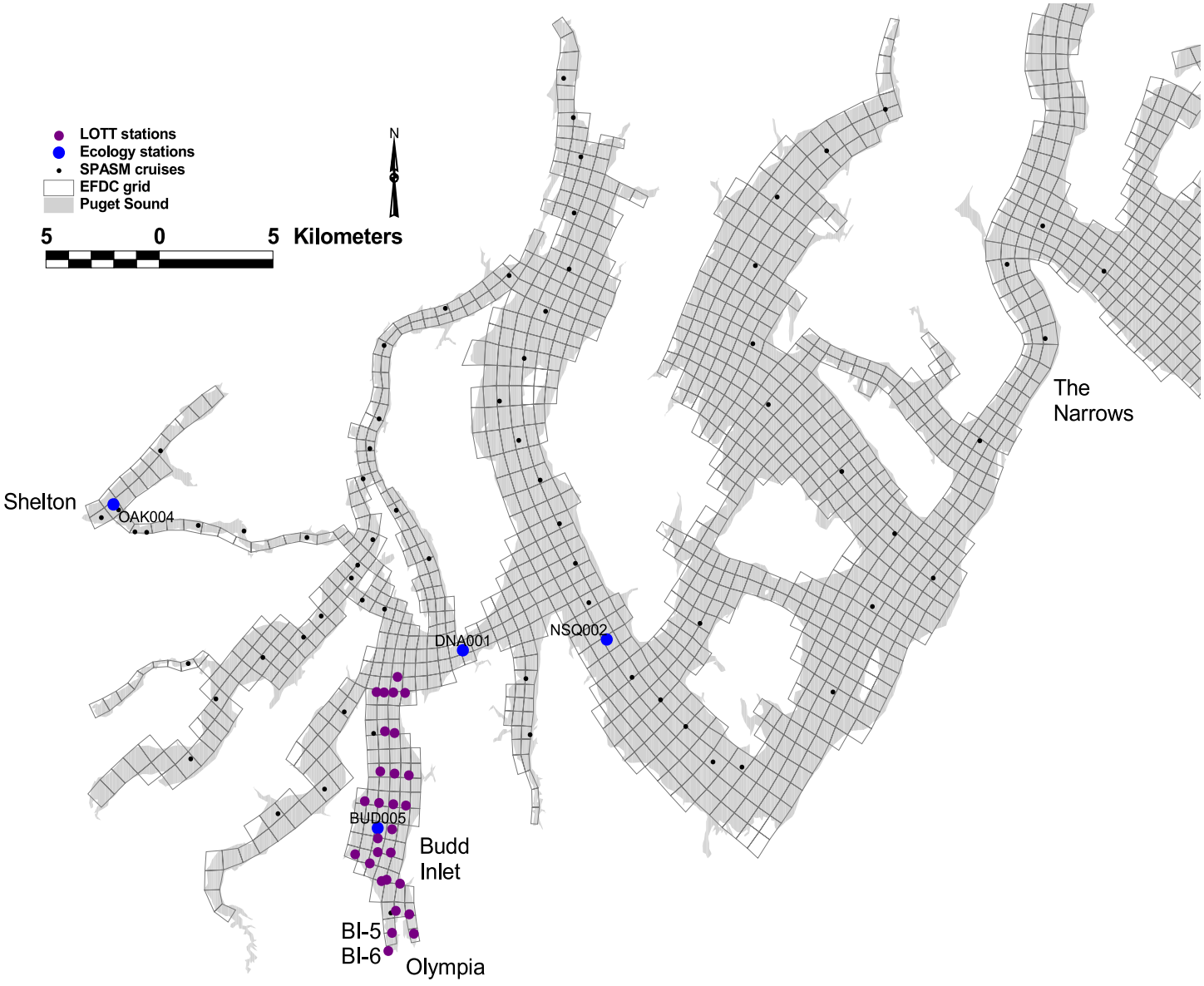

Figure 5.2. Marine sampling stations in South Puget Sound, 10/1/96 - 9/30/97.

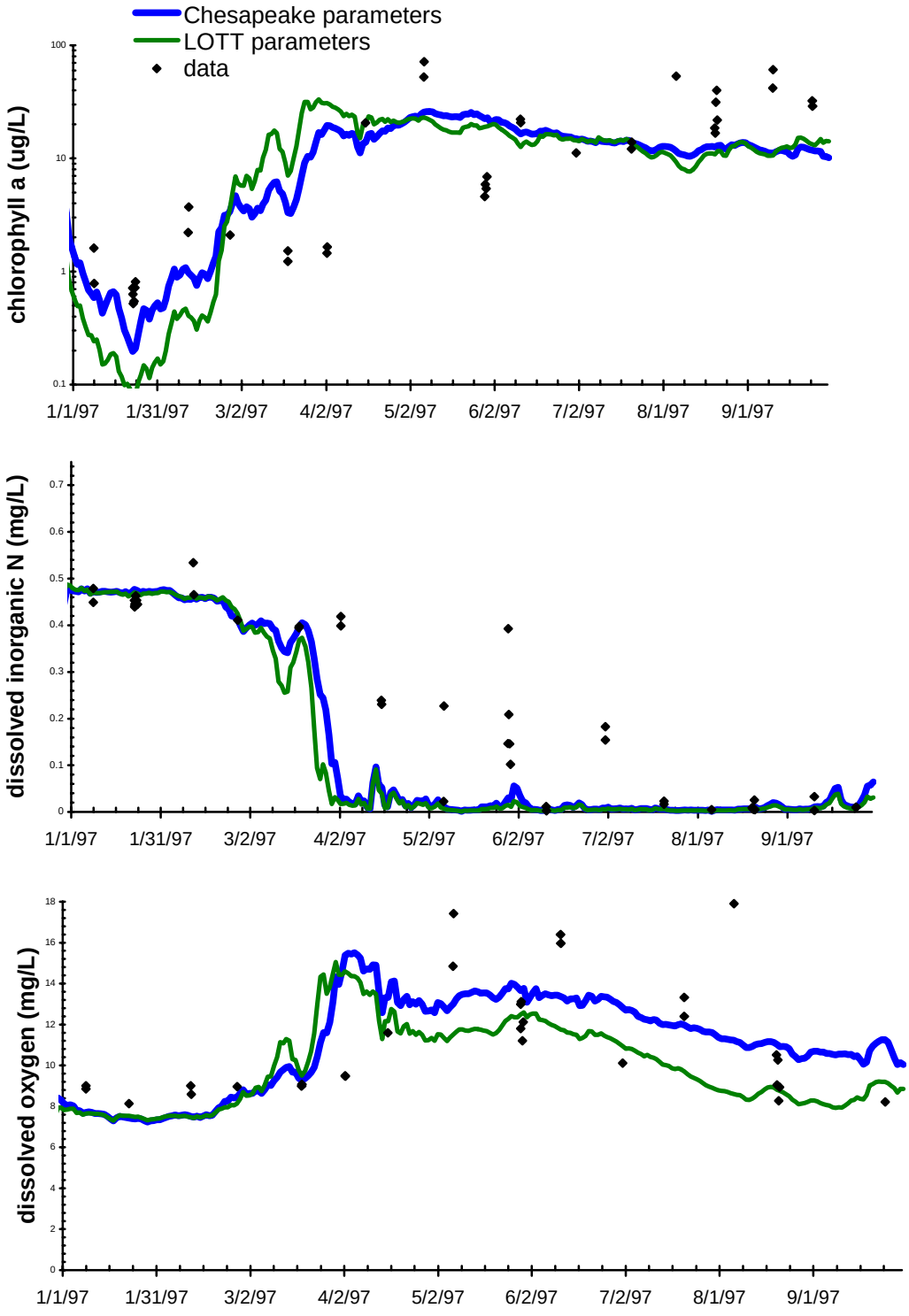

Figure 5-3. Model results for the surface layer of central Budd Inlet, station BUD005.

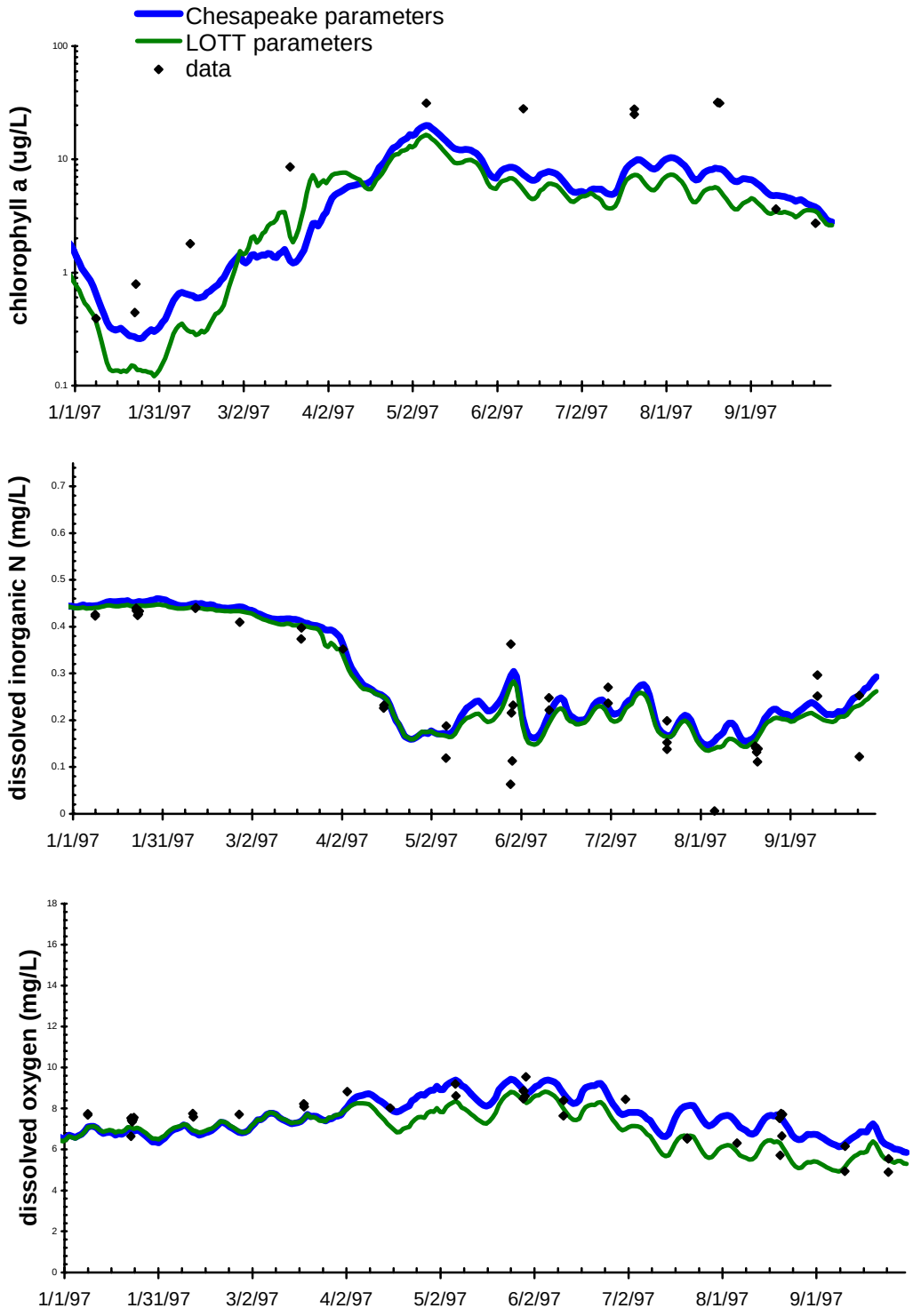

Figure 5-4. Model results for the bottom layer of central Budd Inlet, station BUD005.

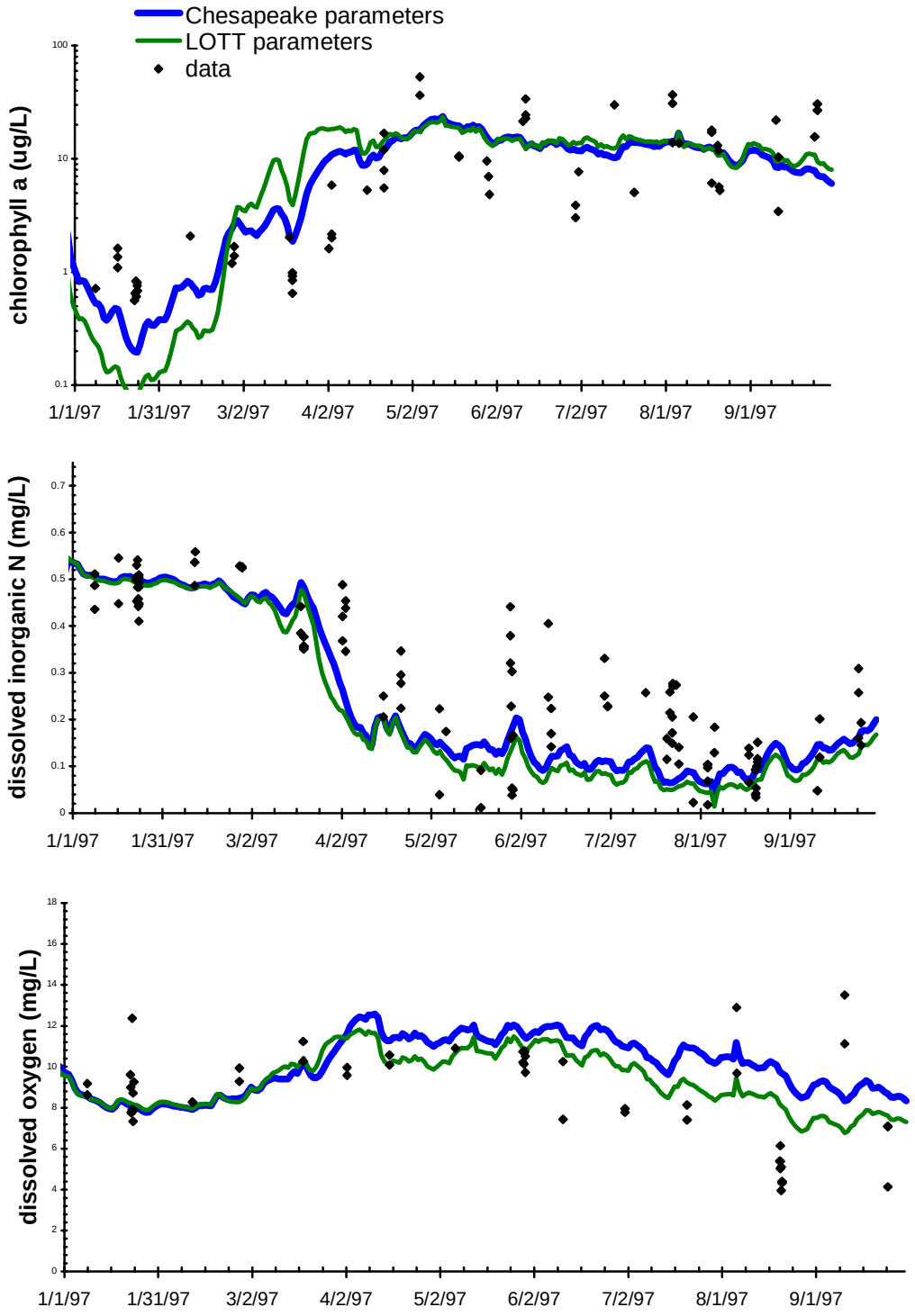

Figure 5-5. Model results for the surface layer of inner Budd Inlet, station BI-5/6.

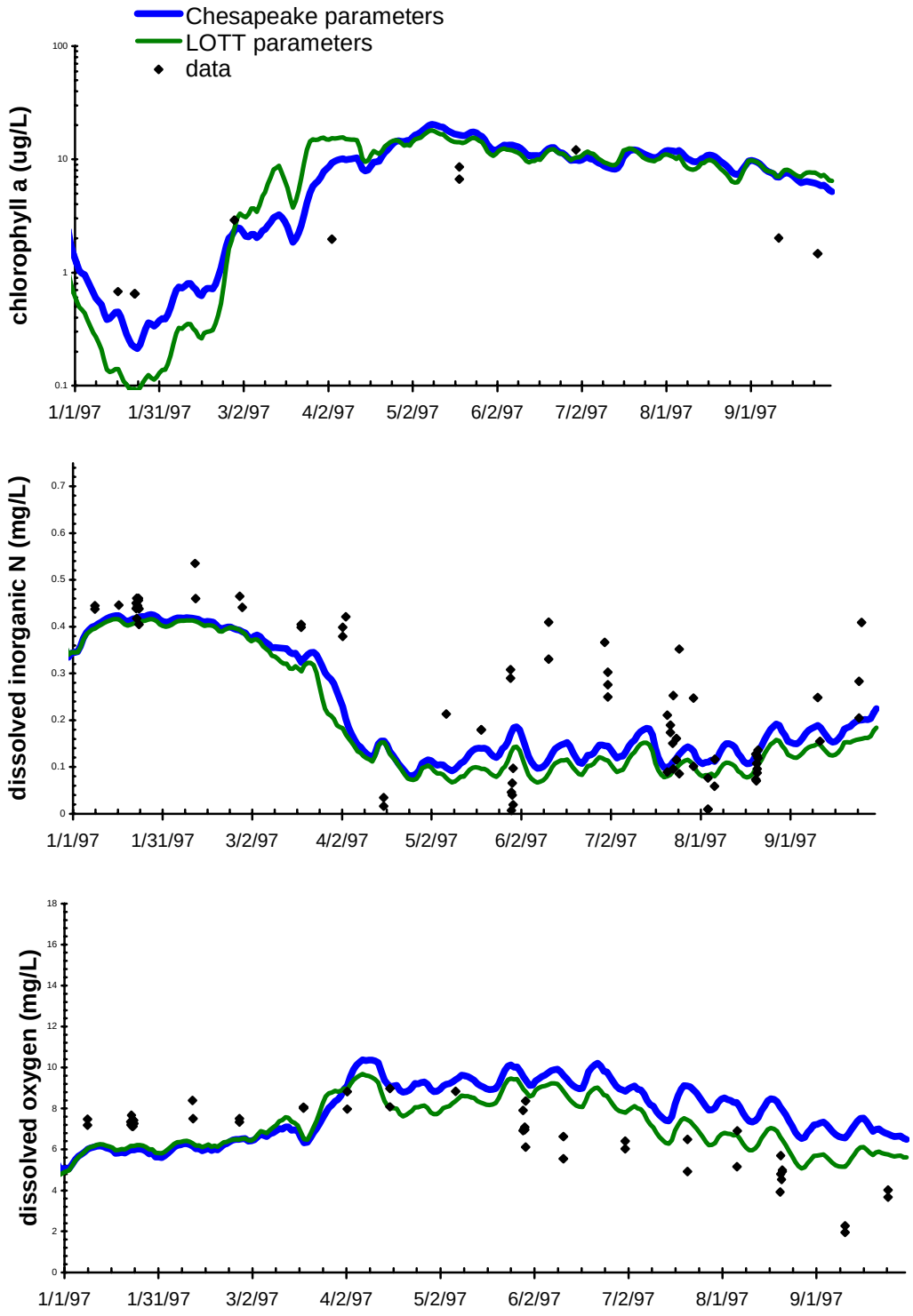

Figure 5-6. Model results for the bottom layer of inner Budd Inlet, station BI-5/6.

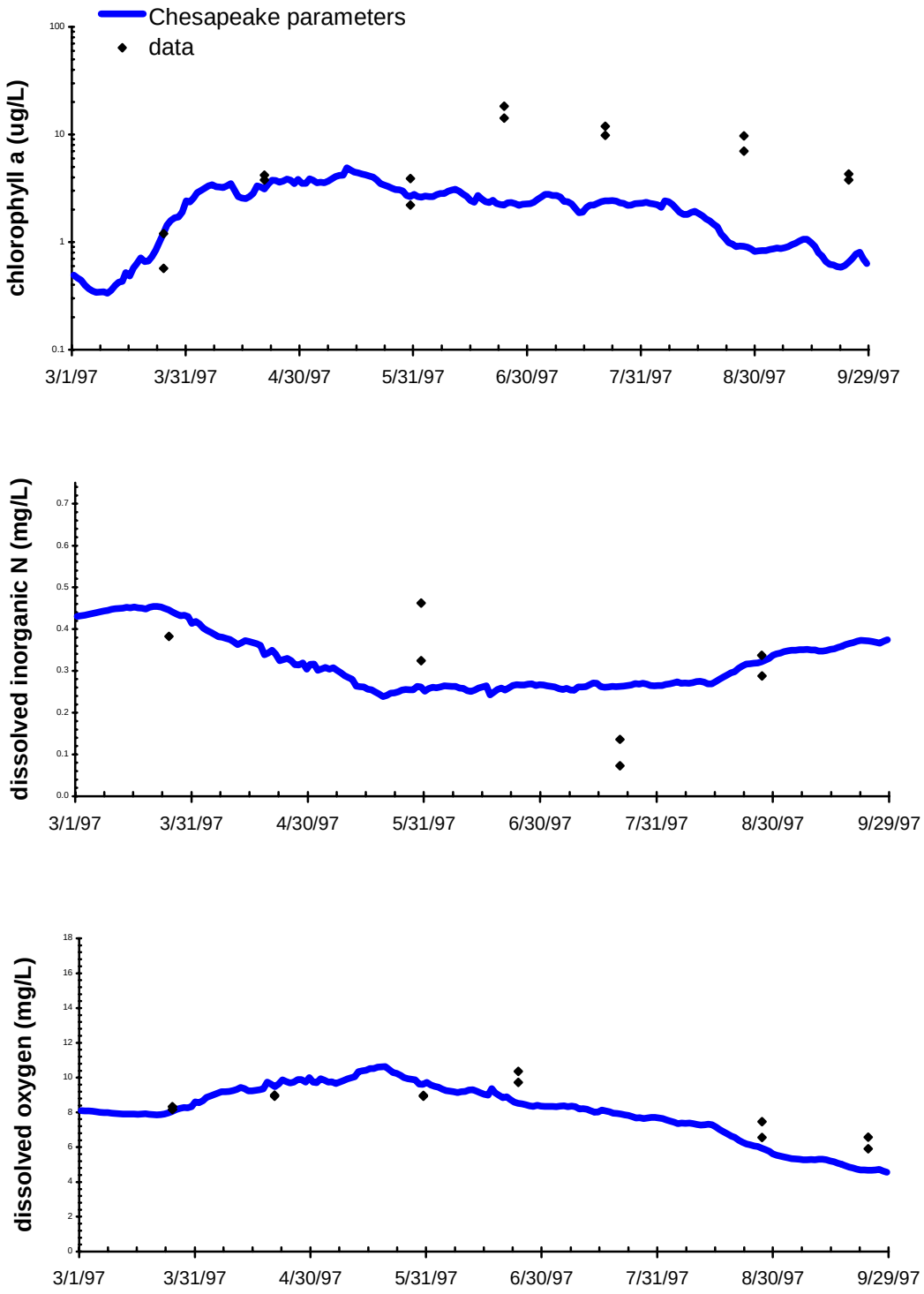

Figure 5-7. Model results for the surface layer of Nisqually Reach, station NSQ002 (full grid from Alki boundary).

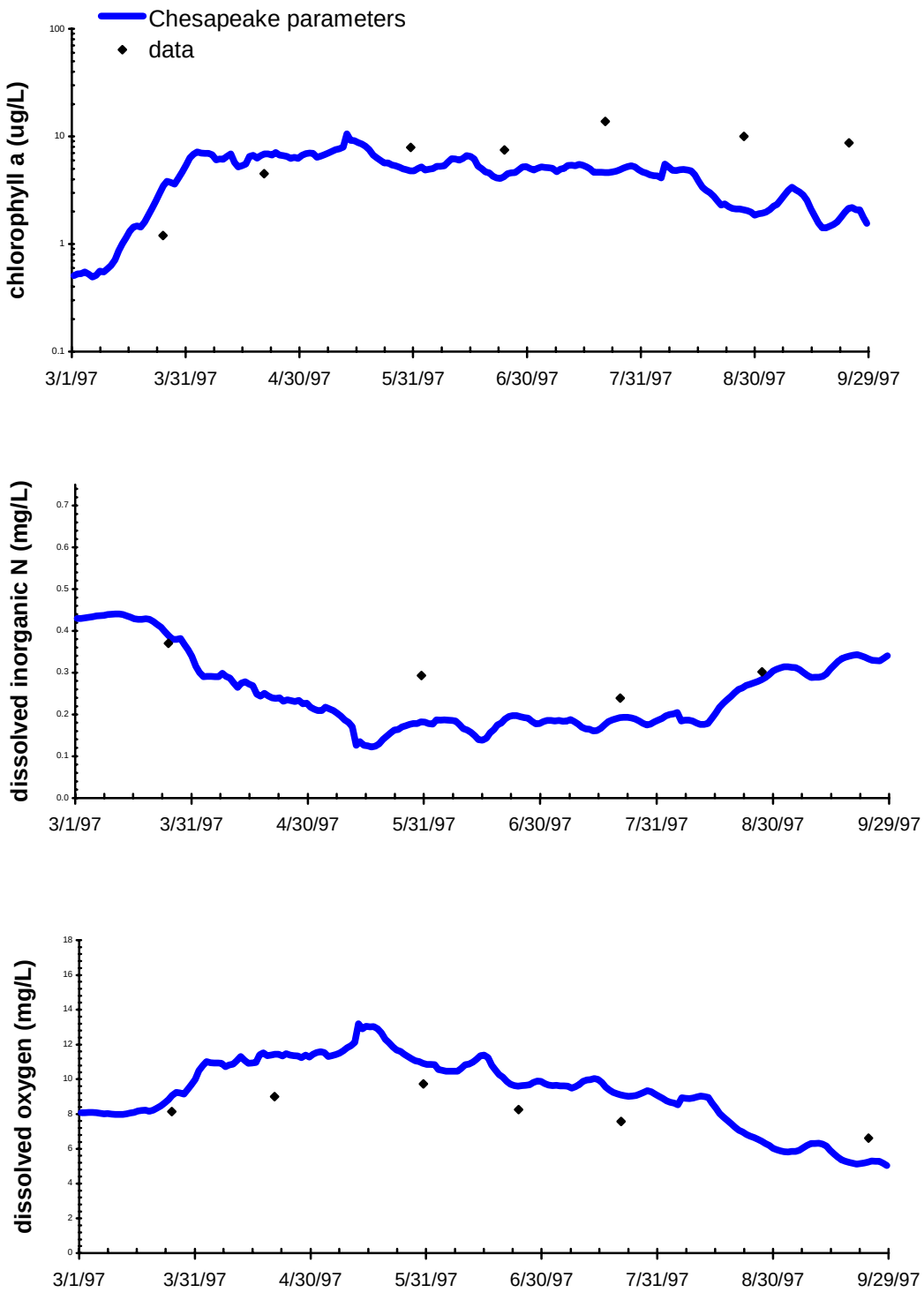

Figure 5-8. Model results for the surface layer of Dana Passage, station DNA001 (full grid from Alki boundary).

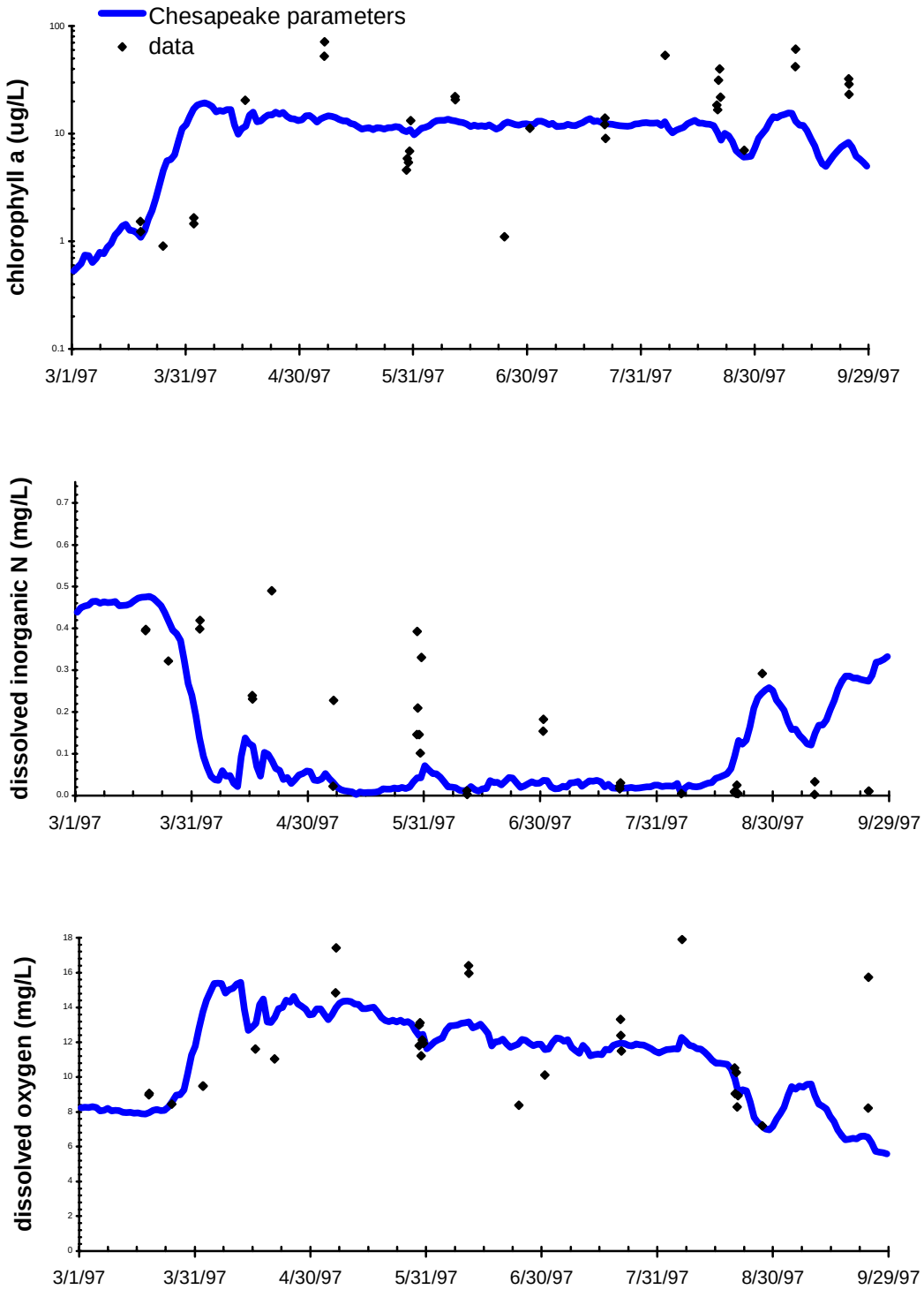

Figure 5-9. Model results for the surface layer of central Budd Inlet, station BUD005 (full grid from Alki boundary).

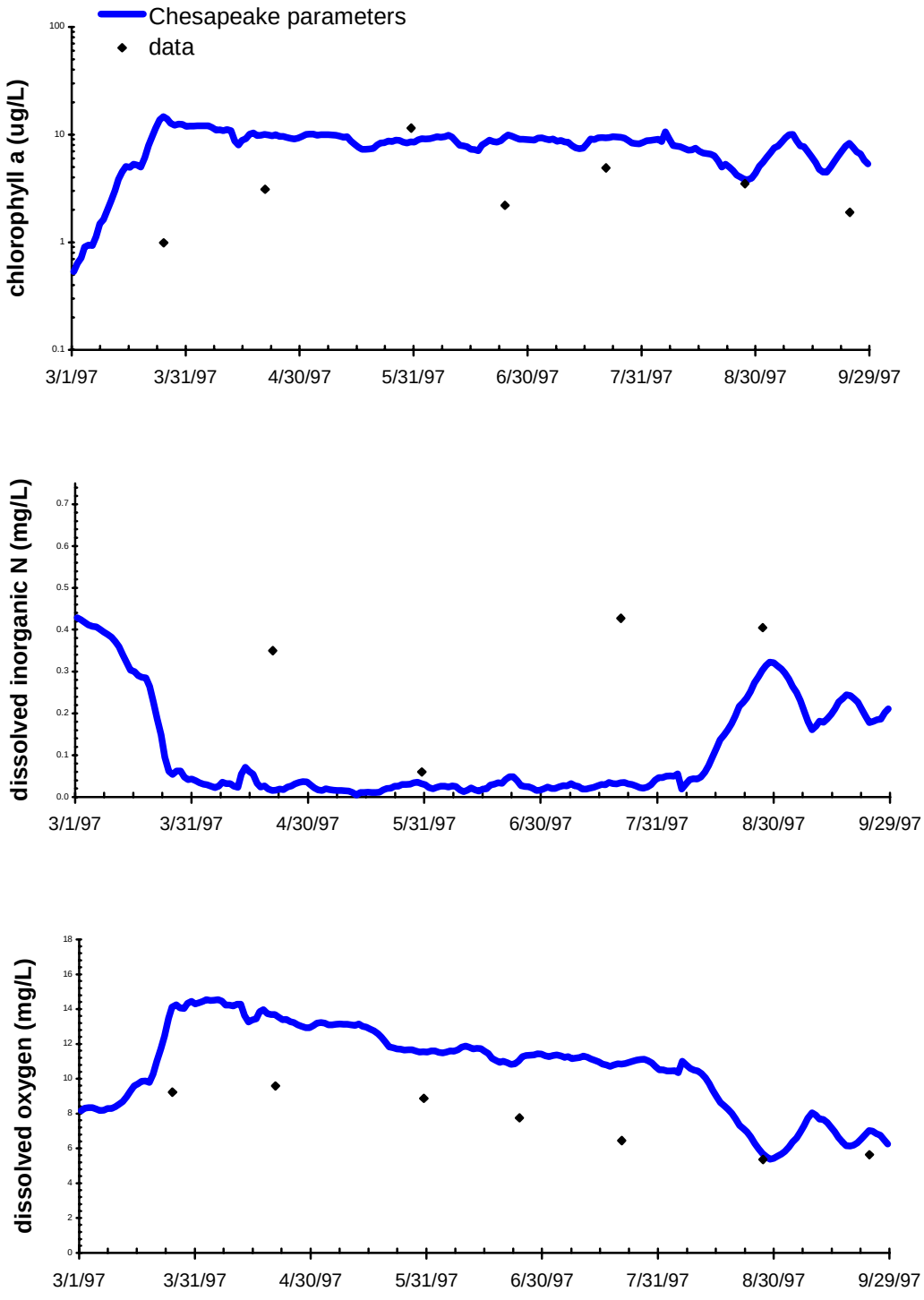

Figure 5-10. Model results for the surface layer of Oakland Bay, station OAK004 (full grid from Alki boundary).

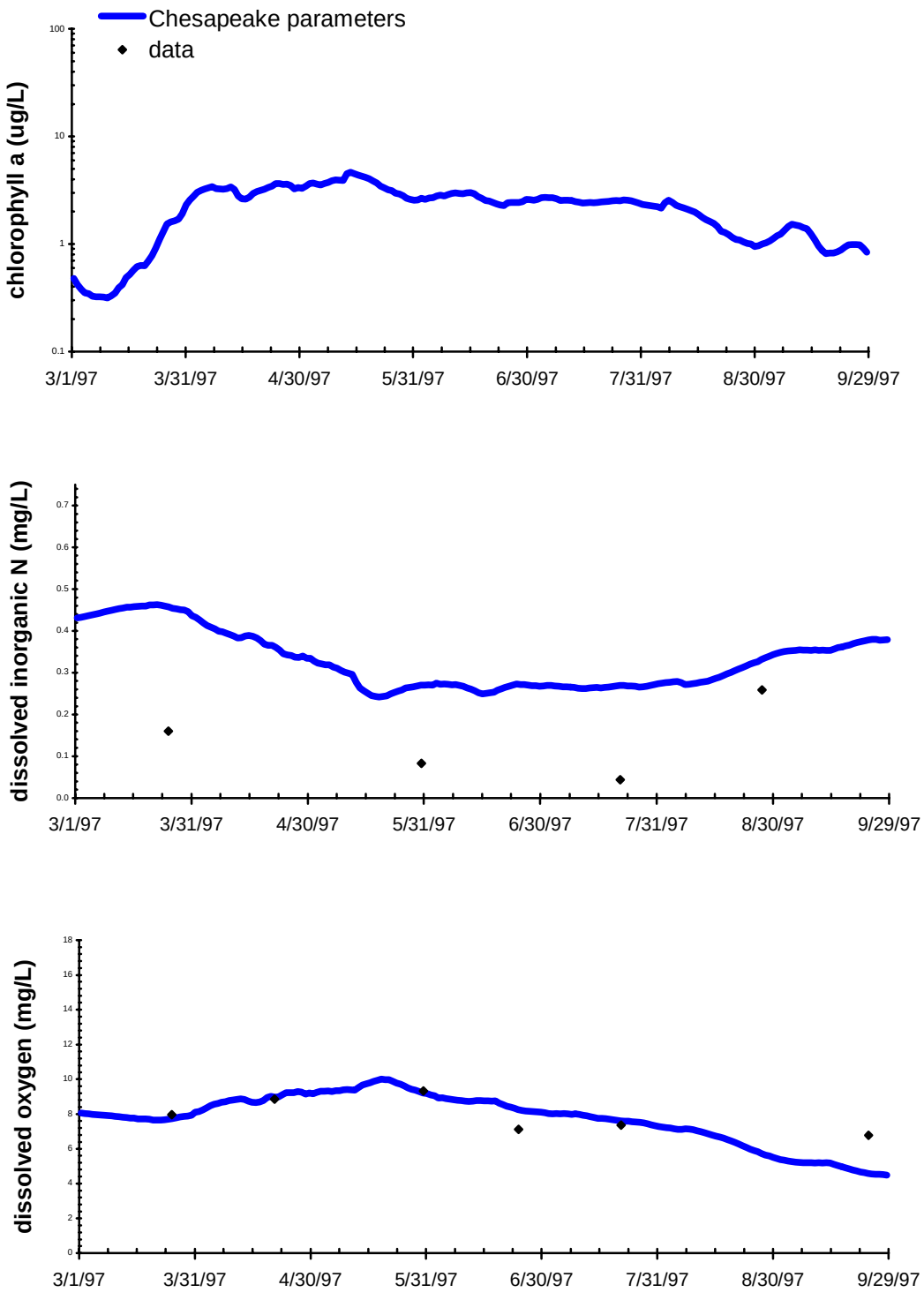

Figure 5-11. Model results for the bottom layer of Dana Passage, station DNA001 (full grid from Alki boundary).

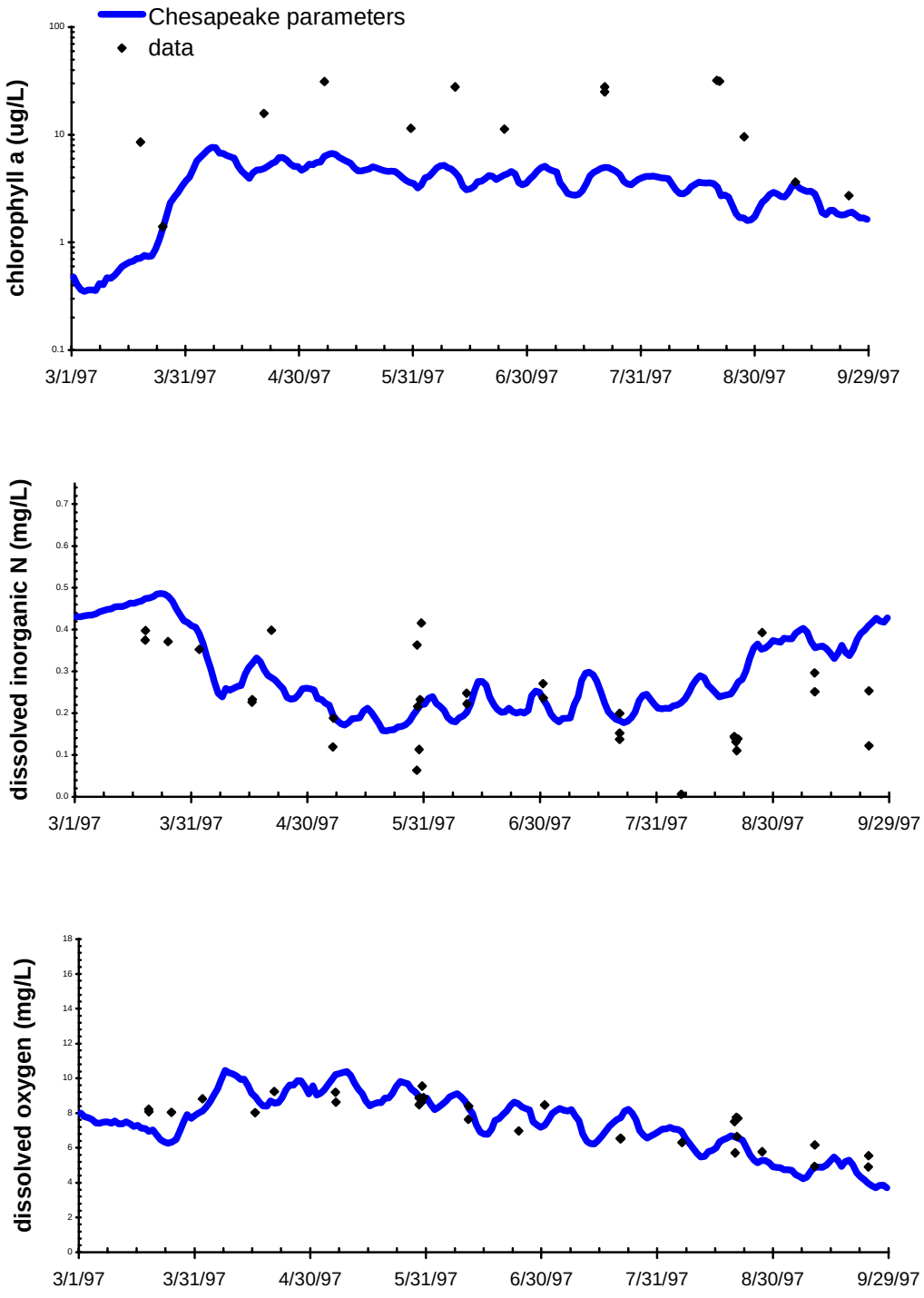

Figure 5-12. Model results for the bottom layer of central Budd Inlet, station BUD005 (full grid from Alki boundary).

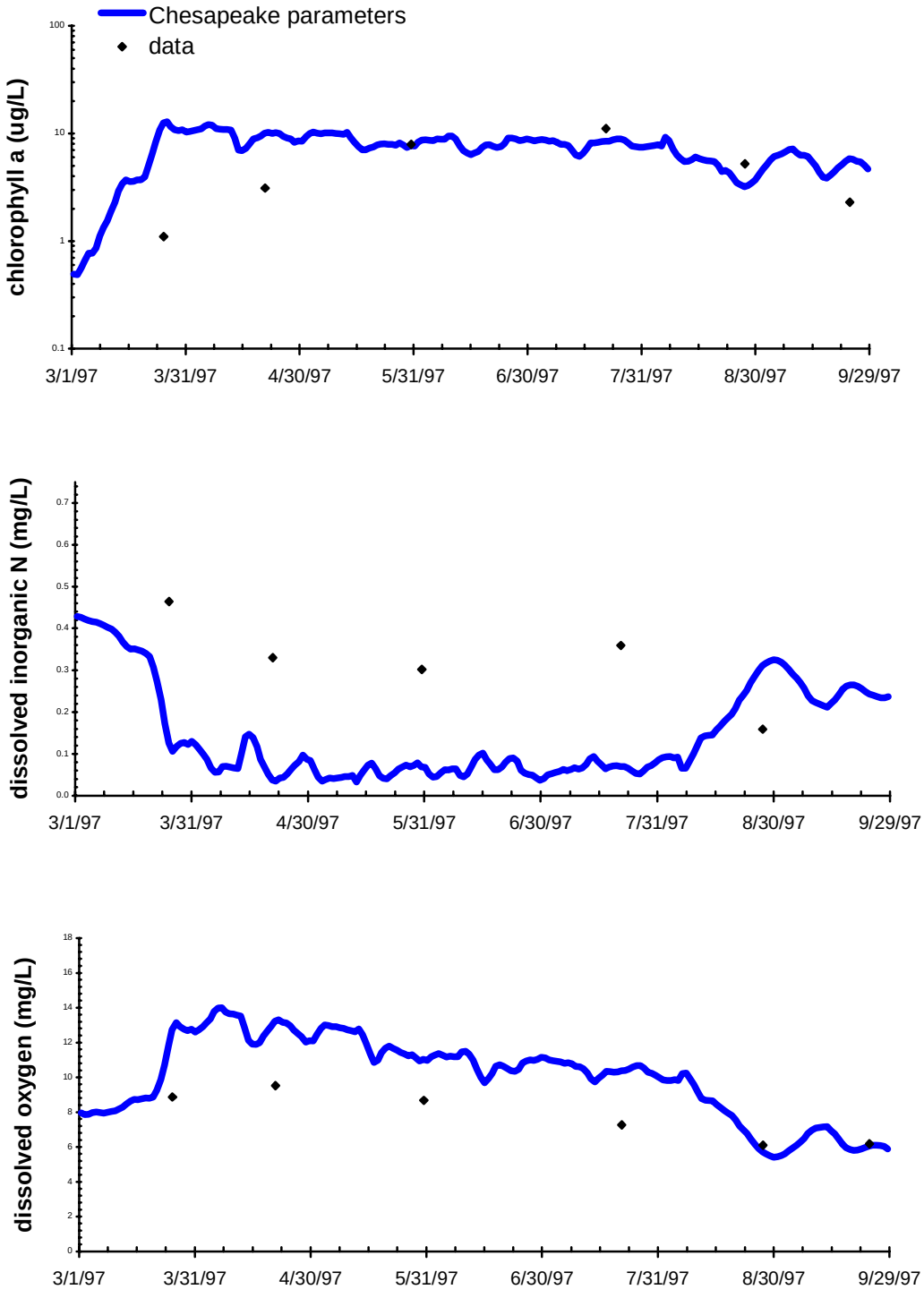

Figure 5-13. Model results for the bottom layer of Oakland Bay, station OAK004 (full grid from Alki boundary).

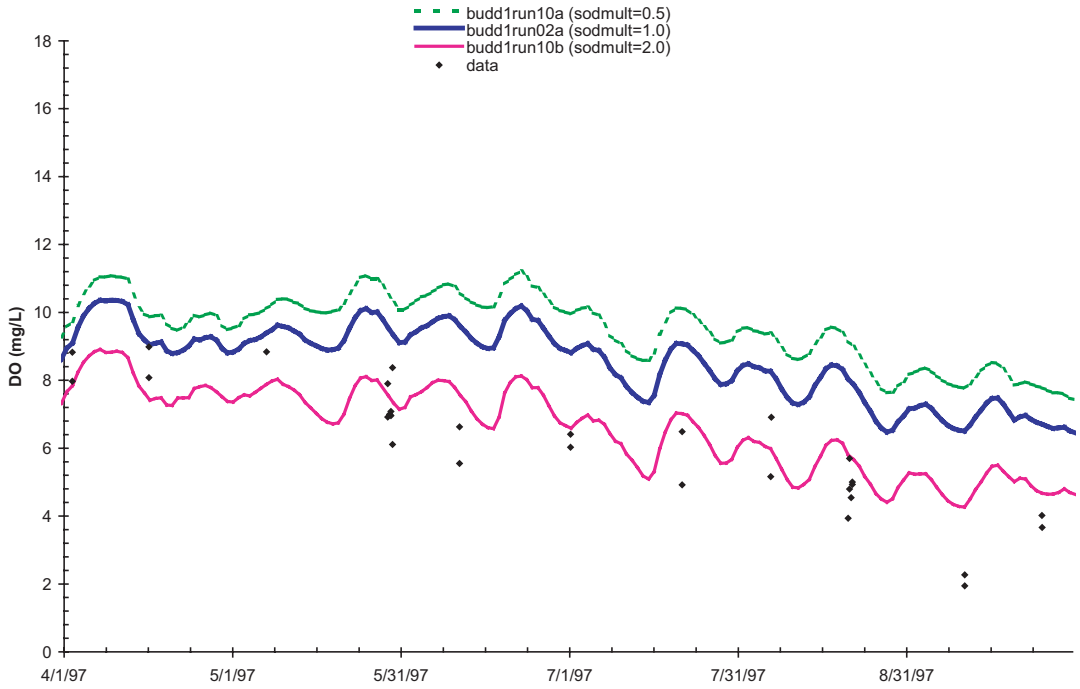

Figure 5-14. Sensitivity of bottom DO in inner Budd Inlet (BI-5/6) to changes in the sediment oxygen demand multiplier (sodmult, dimensionless).

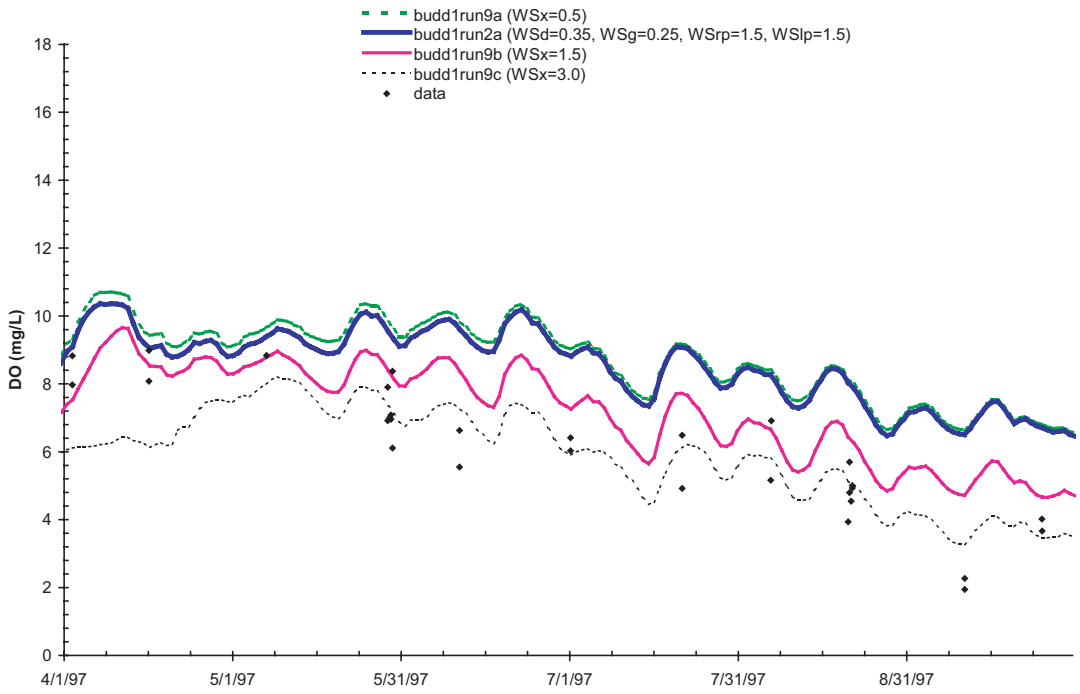

Figure 5-15. Sensitivity of bottom DO in inner Budd Inlet (BI-5/6) to changes in settling rates of phytoplankton and particulate organic matter (WSx, m/d).

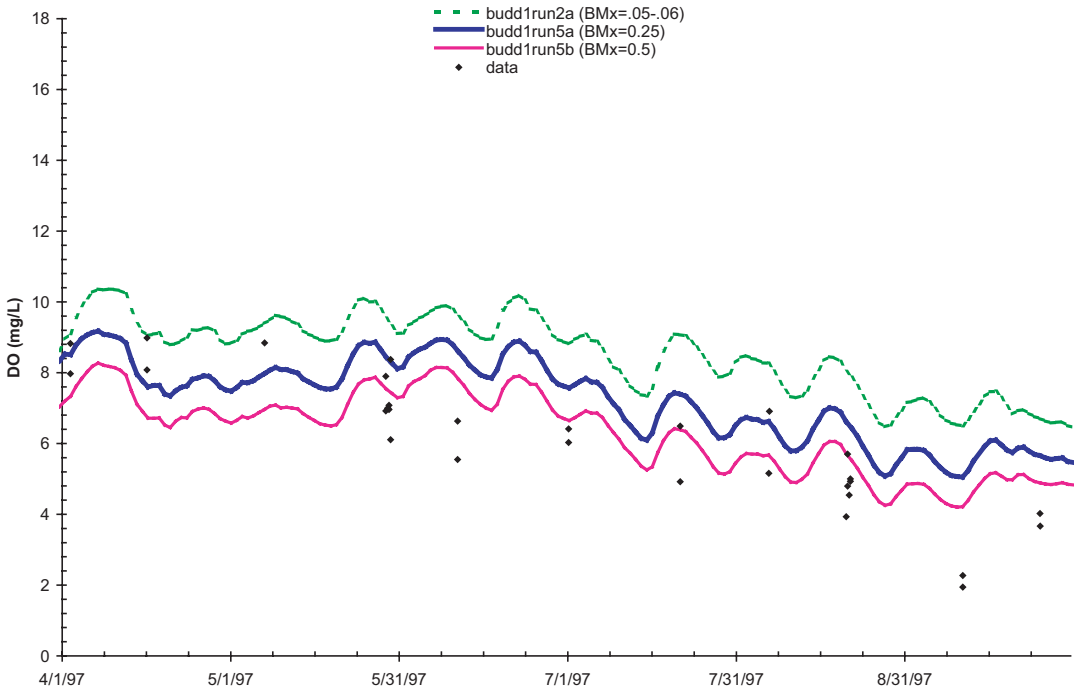

Figure 5-16. Sensitivity of DO in inner Budd inlet (stations BI-5/6) to algal basal metabolism (BMx, per day).

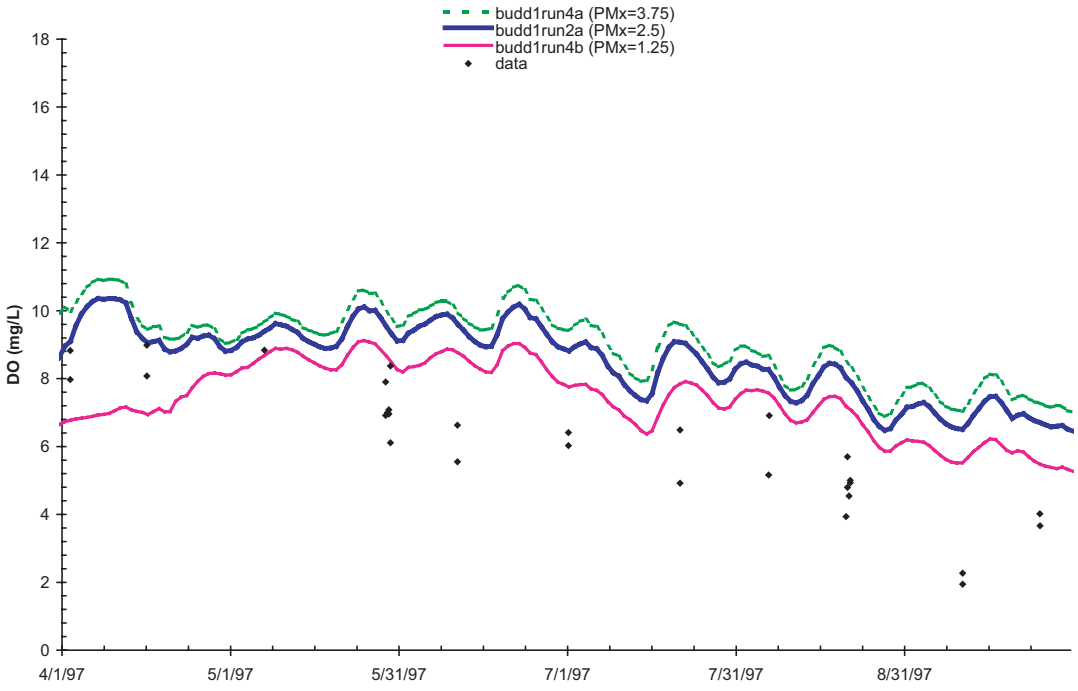

Figure 5-17. Sensitivity of bottom DO in inner Budd Inlet (stations BI-5/6) to maximum algal growth rates (PMx, per day).

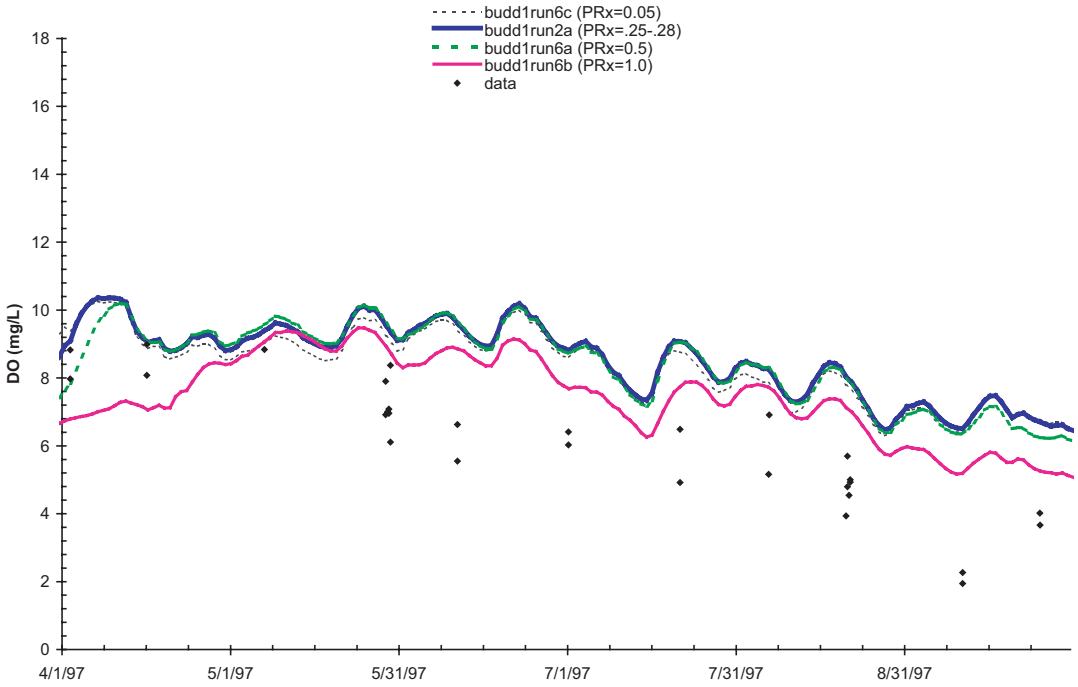

Figure 5-18. Sensitivity of bottom DO in inner Budd Inlet (BI-5/6) to changes in zooplankton algal predation rates (PRx, per day).

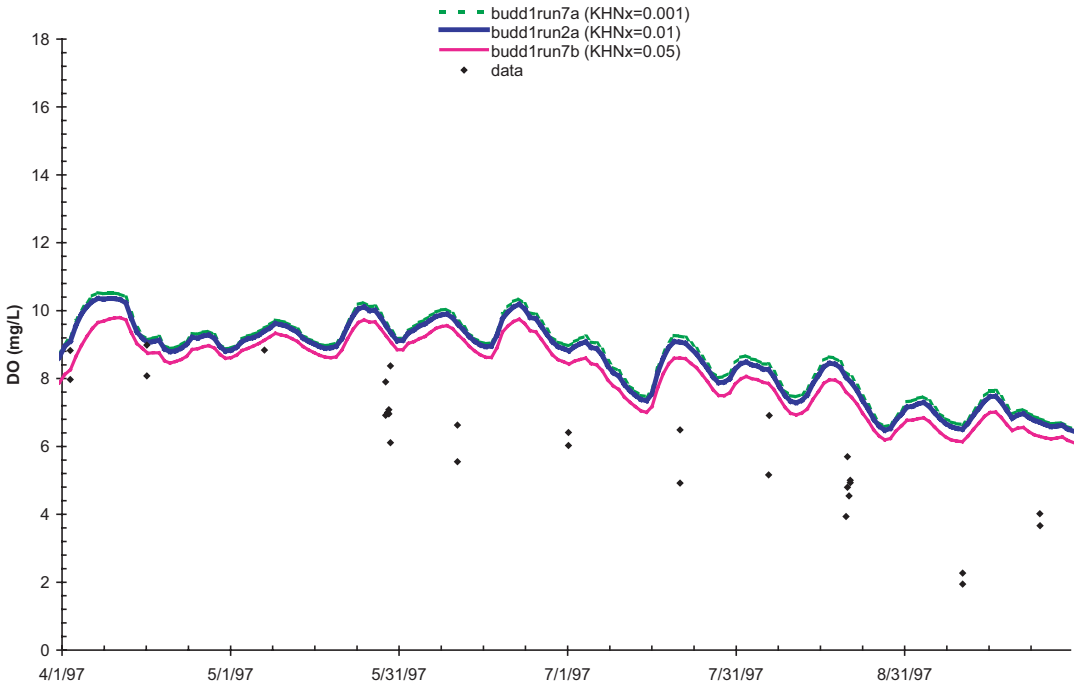

Figure 5-19. Sensitivity of bottom DO in inner Budd Inlet (BI-5/6) to changes in the nitrogen half-saturation concentration (KHNx, mg/L).

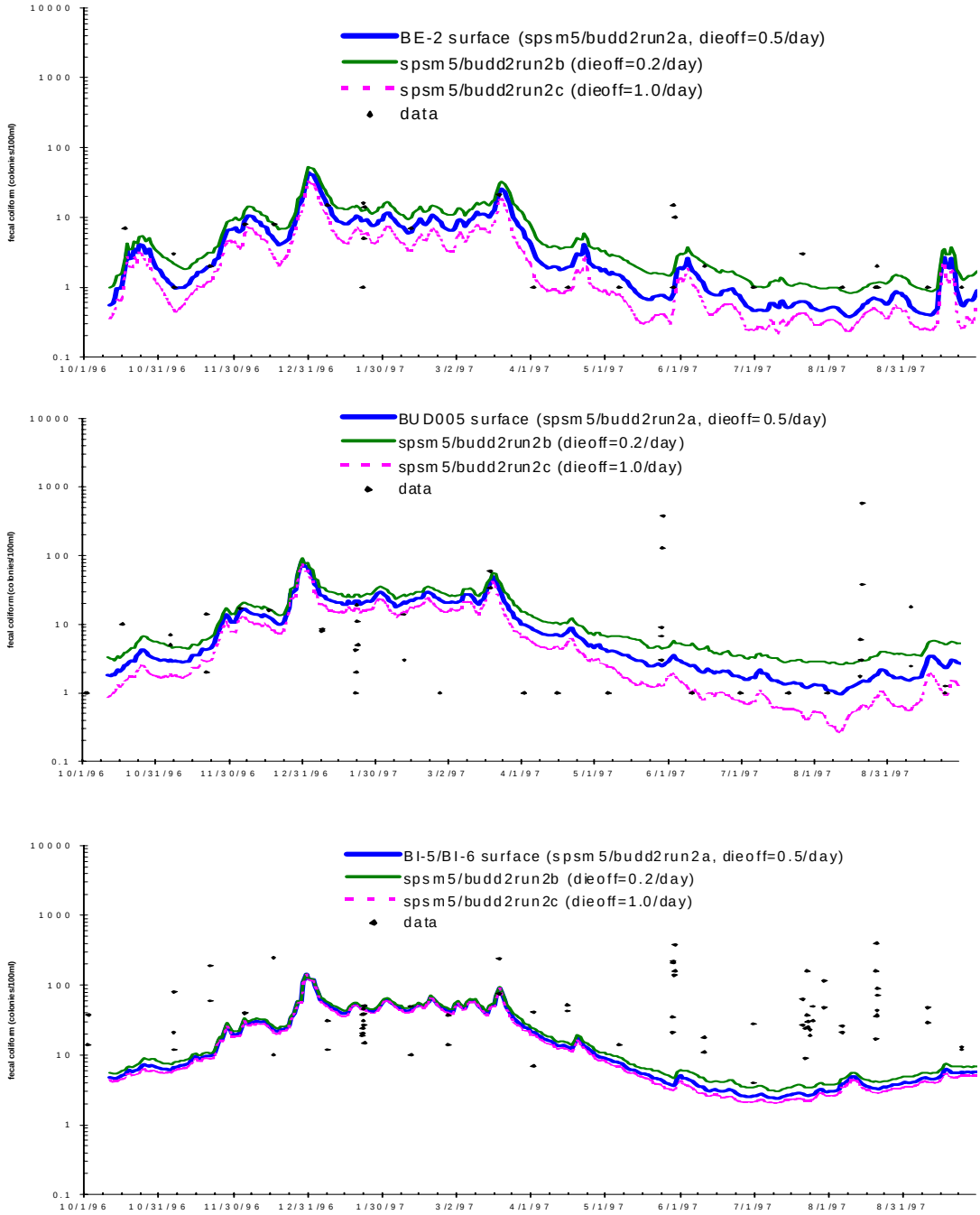

Figure 5-20. Comparison of predicted and observed fecal coliform in Budd Inlet.

6. Conclusions and Recommendations

Phase 1 Conclusions

- Based on field observations and experimental measurements, South Puget Sound appears to be sensitive to nutrient addition. This report confirms the potential for serious water quality degradation due to increased nutrient loads.

- Case, Carr, and Budd inlets appear to have the lowest dissolved oxygen levels within South Puget Sound, and may be the most sensitive areas to increased nutrient loads. Whereas Budd Inlet has already been studied in detail, additional focus on Case and Carr inlets is warranted.

- While point sources discharging directly to South Puget Sound contribute 2% of the total inflows, point sources contribute 30% of the dissolved inorganic nitrogen load and 54% of the total phosphorus load. Fecal coliform loads from watershed inflows are two orders of magnitude greater than point sources.

- Water quality modeling shows that dissolved oxygen is more sensitive to nutrient-driven processes than direct biochemical oxygen demand (BOD) loading.

- A coupled hydrodynamic and water quality model has been successfully developed for South Puget Sound that can be applied to evaluate the sensitivity of dissolved oxygen levels to increased nutrient loading. However, the model requires further refinement and testing before the results can be used for management decisions. Additional monitoring data will be needed for model calibration and verification.

Recommendations

The next phase of the study should focus on the following three areas:

- Improving flushing rate estimates by refining model hydrodynamics (addressing the salinity problem in particular) and by collecting current data for direct model calibration.

- Collecting additional marine water quality data and conducting field studies to enable model calibration to spatial and temporal patterns, with special attention to the sediment model.

- Refining point-source loading estimates through additional effluent data collection.

Phase 2 recommendations are discussed in more detail below.

Watershed

1. Future efforts should refine direct point-source nutrient loads to South Puget Sound through additional effluent data collection.

2. Watershed flows and nutrient load regression models should be updated to reflect more recent monitoring data throughout South Puget Sound. The Phase 1 load estimates provide the first detailed load summary to South Puget Sound, based on monitoring data collected by a variety of agencies, through 1998. However, the period was wetter than average and not representative of typical hydrologic conditions. Many of the larger rivers have been monitored regularly since 1998. Future load estimates should consider a range of conditions.

3. A limited water quality monitoring program should focus on areas of interest within Carr and Case inlets to develop better site-specific estimates for small and moderate inflows, including a representative subset of direct inflows. The program would include stream gaging, dissolved oxygen, and nutrient samples.

4. Uncertainty in watershed load estimates should be evaluated quantitatively, in conjunction with water quality model sensitivity analyses. While the existing watershed inflow loads are based on the best information available, error analysis would provide an indication of natural variation in the system. This should be conducted for the overall South Puget Sound model estimates as well as the focused Carr/Case inlet monitoring proposed for the next phase.

Hydrodynamics

1. The flushing of South Puget Sound is critical to the present assessment of nutrient loading. At present, flushing estimates are being estimated based solely on the hydrodynamic model calculations. Current meter data would improve the assessment of physical flushing in South Puget Sound inlets. Measuring current velocity as a function of depth should be done with instruments such as an ADCP (acoustic doppler current profiler). The model should be validated with currents measured directly in the field.

2. There are two areas where the current hydrodynamic model shows major uncertainties that should be addressed:

    - In the hydrodynamic model, bottom friction may be higher than actual, resulting in a phase lag in the observed and predicted sea surface elevations. We do not yet know the influence of bottom substrate on the calculated flushing rate obtained using this model. This effect is presently being investigated by King County; future work should include their findings. This factor should be evaluated further in Phase 2, which may require refinement of the model grid.

    - Thermodynamic properties were not well described by the model over long time scales (e.g., year). There is a directional increase in some properties (e.g., salinity) that is unrealistic. Thermodynamics will influence water quality simulations.

Water Quality

1. A time-series of water quality measurements for the entire *South Puget Sound Water Quality Study* grid should be conducted annually in the fall, at a minimum, to document the critical time of year for water quality. Occupation of the full grid is recommended due to the extremely high degree of spatial heterogeneity in water quality variables from the 80-station grid, as opposed to Ecology's Puget Sound Ambient Monitoring Program (PSAMP) long-term monitoring which only maintains five stations in South Puget Sound and neglects many of the inlets. A time-series is critical to document current conditions and to create a sufficient database to help separate anthropogenic from natural (e.g., variation in river flow, sunlight) sources of variability for water quality.

2. Improvements must be made in documenting water quality properties on finer temporal and spatial resolution in South Puget Sound. Observations from this study clearly show that water properties such as oxygen or chlorophyll can have very high variability over time-scales of a day or more and within several kilometers. Because the mechanism driving the variation is not known (e.g., tidal advection versus local processes), this introduces strong uncertainty into environmental assessment. Also, the accuracy of annual budgets of key attributes (e.g., nutrient sensitivity) is poor when based on monthly or semi-annual observations. Alternative monitoring methods will be required to improve understanding of spatial and temporal variability in phytoplankton and nutrients within South Puget Sound.

    - Ecology and the PSAMP are currently investigating the use of satellite remote sensing and other optical-based modeling approaches to improve spatial assessment of phytoplankton. This approach would have high payoff for South Puget Sound due to the high spatial variation of chlorophyll observed in Phase 1.

    - Ecology recommends an approach similar to the UW-Ecology CISNet profiling mooring to resolve water quality variables with high temporal resolution. The profiling mooring resolves some of the variation in water quality variables due, for instance, to tidal or diel cycles. This information will be highly useful for interpreting monthly monitoring data.

    - Cross-channel variation has been observed in Budd Inlet and other inlets in Puget Sound and has been hypothesized to influence near-shore community structure (Schoch et al., 2000). Additional fieldwork should focus on cross-channel spatial variation in a few selected inlets.

3. The degree to which natural vs. anthropogenic mechanisms contribute to interannual variation should be assessed. Non-anthropogenic mechanisms that contribute to interannual variation, such as climate or oceanic variation, should be assessed with respect to the time series of South Puget Sound water quality. For instance, factors related to weather, such as sunlight and river flows, and variation in water properties from oceanic waters (e.g., dissolved oxygen) that enter Puget Sound should be assessed relative to the variation in South Puget Sound water quality properties.

4. The South Puget Sound EFDC model application should be used to investigate questions not easily addressed by observational monitoring programs. Examples include studies on the response of the ecosystem to fluctuations in climate (e.g., El Niño-Southern Oscillation [ENSO]) or examining the impacts on water quality resulting from perturbations in the biological community structure (e.g., phytoplankton species shifts due to species invasions or altered nutrient regimes).

5. The following parameters are listed in approximately decreasing order of sensitivity of the predicted bottom layer dissolved oxygen based on the results of Phase 1:
   - Sediment oxygen demand
   - Settling rates for phytoplankton and particulate organic matter
   - Algal basal metabolism rates
   - Maximum algal growth rates
   - Zooplankton algal predation rates
   - Nitrogen half-saturation

   Therefore, calibration of the sediment model will be very important. Sediment flux and concentration data for South Puget Sound are either limited or nonexistent in most areas of South Puget Sound, so this is an important data requirement for refinement of the calibration.

   Field studies for other key parameters, especially settling rates for phytoplankton and particulate organic matter, as well as algal basal metabolism and maximum growth rates would also be useful for further refinement of the model calibration.

6. The coupled water quality/hydrodynamic model could be used to perform additional sensitivity analyses to determine the magnitude of response of dissolved oxygen in South Puget Sound to hypothetical increases in nutrient (nitrogen and carbon) loading. The sensitivity analyses would probably focus on the regions of most intensive continuous monitoring in Case and Carr inlets.

7. The coupled model should be further calibrated using the existing databases (Budd Inlet and project cruises) and new data collected during Phase 2 (profiling mooring). Further calibration of the model during Phase 2 will probably focus on the areas with the most temporally continuous new data such as Case and Carr inlets. Improvements in calibration of the model in other regions of South Puget Sound may not be possible during Phase 2 because of the scarcity of data.

8. Evaluations of model goodness-of-fit and uncertainty for water quality variables should be incorporated in subsequent phases of the project.

References

Albertson, S. L., C. Ebbesmeyer, J. Newton, R. Reynolds. 2001. *Investigation of the Mean Flow in a Complex Multi-Connected Estuary: South Puget Sound*. PSRC 2001 Proceedings.

Aura Nova Consultants, Brown and Caldwell, Inc., Evans-Hamilton, Inc., J.E. Edinger and Associates, Washington State Department of Ecology, and Dr. Alan Devol, University of Washington Department of Oceanography. 1998. *Budd Inlet Scientific Study Final Report.* Prepared for the Lacey, Olympia, Tumwater, Thurston County Partnership (LOTT), Olympia, WA. 2 volumes. August.

Barber, R.T. 1992. *In situ* primary productivity protocol. Joint Global Ocean Flux Study Equatorial Pacific Protocols, National Science Foundation, Washington, DC.

Boatman, C. and J.E. Edinger. 1999. *LOTT NPDES Permit Modifications Modeling Interim Report*. Prepared for the Lacey, Olympia, Tumwater, Thurston County Partnership (LOTT), Olympia, WA. Prepared by Aura Nova Consultants and J.E. Edinger and Associates.

Carpenter, J.H. 1964. The Accuracy of the Winkler Method for Dissolved Oxygen Analysis. *Limnol. Oceanogr.,* 10: 135-140.

Cerco, C.F., and T.M. Cole. 1994. *Three-dimensional eutrophication model of Chesapeake Bay.* Volume I: Main Report. Technical Report EL-94-4. U.S. Army Corps of Engineers Waterways Experiment Station, Vicksburg, MS.

Cohn, T.A., D.L. Caulder, E.J. Gilroy, L.D. Zynjuk, and R.M. Summers. 1992. The validity of a simple statistical model for estimating fluvial constituent loads – an empirical study involving nutrient loads entering Chesapeake Bay. *Water Resources Research,* v. 28, no. 9, p. 2353-2363.

Cohn, T.A., L.L. DeLong, E.J. Gilroy, R.M. Hirsch, and D.K. Wells. 1989. Estimating constituent loads. *Water Resources Research*, v. 25, no. 5, p. 937-942.

Cokelet, E.D. and R.J. Stewart. 1985. The exchange of water in fjords: The efflux/reflux theory of advective reaches separated by missing zones. *Jour. Geophy. Res*. 90, p. 7287-7306.

Collias, E.E., N. McGary, And C.A. Barnes. 1974. *Atlas of Physical and Chemical Properties of Puget Sound and Approaches.* Washington Sea Grant 74-1, Seattle, WA.

Di Toro, D.M. and J.J Fitzpatrick. 1993. *Chesapeake Bay Sediment Flux Model*. Contract Report EL-93-2. U.S. Army Corps of Engineers, Waterways Experiment Station, Vicksburg, MS.

Eisner, L.B. and J.A. Newton. 1997. *Budd Inlet Focused Monitoring Report for 1992, 1993 and 1994.* Washington State Department of Ecology, Environmental Investigations and Laboratory Services Program, Olympia, WA. Publication No. 97-327.

Eisner, L.B., C.A. Janzen, S.L. Albertson, S.A. Bell, and J.A. Newton. 1994. *1992 Budd Inlet Seasonal Monitoring Report*. Washington State Department of Ecology, Environmental Investigations and Laboratory Services Program, Olympia, WA. Publication No. 94-132.

Embrey, S.S. and E.L. Inkpen. 1998. *Water-Quality Assessment of the Puget Sound Basin, Washington, Nutrient Transport in Rivers, 1980-93*. USGS Water-Resources Investigations Report 97-4270, Tacoma, WA.

Fitzwater, S.E., G.A. Knauer, and J.H. Martin. 1982. Metal contamination and its effect on primary production measurement. *Limnol. Oceanogr*., 27: 544-551.

Foreman, M.G.G. 1978. *Manual for Tidal Currents Analysis and Prediction*. Pacific Marine Science Report 78-6, Institute of Ocean Sciences, Patricia Bay, Sidney, B.C., 57 p.

Hamrick, J.M. 1992a. Estuarine environmental impact assessment using a three-dimensional circulation and transport model. *Estuarine and Coastal Modeling*. Proceedings of the 2nd International Conference. M.L. Spaulding, K. Bedford, A. Blumberg, R. Cheng, and S. Swanson (eds.), American Society of Civil Engineers, NY, p. 292-303.

Hamrick, J. M. 1992b. A three-dimensional environmental fluid dynamics computer code, William Mary, Virginia Institute of Marine Science, special report in *Applied Marine Science and Ocean Engineering*, No. 317.

Hamrick, J.M. 1994. Linking hydrodynamic and biogeochemical transport models for estuarine and coastal waters. *Estuarine and Coastal Modeling*. Proceedings of the 3rd International Conference. M.L. Spaulding et al (eds.), American Society of Civil Engineers, NY, p. 591-608.

Haney, R.L. 1991. On the pressure gradient force over steep topography in sigma coordinate ocean models. *Journal of Physical Oceanography*, 21: 610-619.

Harrison, P.J, D.L. Mackas, B.W. Frost, R.W. Macdonald, and E.A. Crecelius. 1994. An assessment of nutrients, plankton and some pollutants in the water column of Juan de Fuca Strait, Strait of Georgia and Puget Sound, and their transboundary transport. *Canadian Technical Report of Fisheries and Aquatic Sciences*, No. 1948: 138-174.

Hasle, G.R. 1978. Using the inverted microscope. *In* A. Sournia (ed.), Phytoplankton Manual. Monographs on Oceanographic Methodology 6, UNESCO, Paris.

Heffner, M. 1992. *Simpson Tacoma Kraft Company February 1991 Class II Inspection Report*. Washington State Department of Ecology, Olympia, WA. Publication No. 92-e38.

Janzen, C.D. 1992. *Marine Water Column Ambient Monitoring Plan: Final Report.* Washington State Department of Ecology, Environmental Investigations and Laboratory Services Program, Olympia, WA. Publication No. 92-23.

Lavelle J.W., H.O. Mofjeld et al. 1985. A Multiply-Connected Channel Model of Tides and Tidal Currents in Puget Sound, Washington, and a Comparison with Updated Observations. NOAA Technical Memorandum ERL PMEL-84.

Lorenzen, C.J. 1966. A method for the continuous measurement of in vivo chlorophyll concetnration. *Deep Sea Research,* v. 13, p. 223-227.

Lung, W.S. 1993. *Water Quality Modeling: Applications to Estuaries*. CRC Press. ISBN 0849 369738.

Mancini, John L. 1978. Numerical estimates of coliform mortality rates under various conditions. *Journal Water Pollution Control Federation,* November, p. 2477-2484.

Metcalf and Eddy. 1991. *Wastewater Engineering: Treatment, Disposal and Reuse*. Third Edition. McGraw-Hill, Inc.

Mofjeld, H.O. 2000. Personal communication. Pacific Marine Environmental Laboratory, National Oceanographic and Atmospheric Administration - Sandpoint, Seattle, WA.

Mofjeld, H.O. and L.H. Larsen. 1984. Tides and Tidal Currents in the Inland Waters of Western Washington, NOAA Technical Memorandum ERL PMEL-56, Seattle, WA, 52 p.

Newton, J.A. 1995. *Marine Water Column Ambient Monitoring Program Water Year 1995 Long-Term Monitoring Implementation Plan*. Washington State Department of Ecology, Environmental Investigations and Laboratory Services Program, Olympia, WA. Publication No. 95-324.

Newton, J.A., S.L. Albertson, K. Nakata, and C. Clishe. 1998. *Washington State Marine Water Quality in 1996 and 1997.* Washington State Department of Ecology, Environmental Assessment Program, Olympia, WA. Publication No. 98-338.

Newton, J.A., S.L. Albertson, and A.L. Thomson. 1997. *Washington State Marine Water Quality in 1994 and 1995.* Washington State Department of Ecology, Environmental Investigations and Laboratory Services Program, Olympia, WA. Publication No. 97-316.

Olympian, The. 2001. *Red tide closes shellfish beaches*. Olympia, WA, July 31, pp. B1-B2.

Pelletier, G. 1994. *Addendum to the 1993 Puyallup River TMDL Report* (Pub. No. 96-326). Washington State Department of Ecology, Olympia, WA. Publication No. 94-e36.

Pietrzak, J. D., and N. Kleim. 1999. On the Pressure Gradient Error in Sigma Coordinate Ocean Models, Sigma Modeling Conf., Maine.

Poole, H.H. and W.R.G. Atkins. 1929. Photo-electric measurements of sub-marine illumination throughout the year. *Marine Biol. Assn. U.K. Jour*, 16: 297-324.

Puget Sound Estuary Program. 1997. Recommended Protocols for Measuring Selected Environmental Variables in Puget Sound. U.S. Environmental Protection Agency, Region 10, Seattle, WA, and Puget Sound Water Quality Action Team, Olympia, WA.

Rensel, J. 1999. Lake Roosevelt trophic status and net-pen studies. Prepared for Colville Confederated Tribes, Nespelem, WA.

Rensel and PTI. 1991. *Puget Sound Estuary Program: Nutrients and Phytoplankton in Puget Sound.* Prepared for U.S. Environmental Protection Agency, Region 10, Seattle, WA. Prepared by Rensel Associates, Bellevue, WA. and PTI Environmental Services, Bellevue, WA.

Roache, P.J. 1998. *Verification and Validation in Computational Science and Engineering*, Hermosa Publishers, Albuquerque, NM.

Schoch, G.C., M.N. Dethier, H. Berry, B. Bookheim, and A. Sewell. 2000. *Puget Sound Intertidal Biodiversity: Scales of variability for gravel beach communities.* Pacific Estuarine Research Society 2000 Abstract.

Schureman, P. 1958. *Manual of Harmonic Analysis and Prediction of Tides*. Spec. Pub. No. 98, U.S. Gov. Printing Office, 317 p. (reprinted 1976).

Seim, H.E. and M.C. Gregg. 1997. The importance of aspiration and channel curvature in producing strong vertical mixing over a sill. *Journal of Geophysical Research*, 102:3451-3472.

Spaulding, M.L. et al., (eds). 1994. American Society of Civil Engineers, NY.

Spencer, J.W. 1971. Fourier series representation of the position of the sun. *Search* 2, 172.

Steeman-Neilson, E. 1952. The use of radioactive carbon (C14) for measuring organic production in the sea. *J. Cons. Int. Explor. Mer*. 18:117-140.

Strickland, J.D.H. and T.R. Parsons. 1968. *A Practical Handbook of Seawater Analysis.* Bulletin 167, Fisheries Research Board of Canada, Ottawa.

Tetra Tech, Inc. 1988. *Puget Sound Estuary Program, Budd Inlet Action Plan: Initial Data Summaries and Problem Identification*. Prepared for U.S. Environmental Protection Agency, Region 10, Seattle, WA. Prepared by Tetra Tech, Bellevue, WA. TC-3338-27.

Tetra Tech, Inc. 1998. *Three-dimensional hydrodynamic and water quality model of Peconic Estuary*. Prepared for Peconic Estuary Program, County of Suffolk, Department of Health Services, Office of Ecology, Riverhead, NY. Prepared by Tetra Tech, Fairfax, VA.

Tetra Tech, Inc. 1999. *Hydrodynamic and water quality model of Christina River Basin.* Prepared for the U.S. Environmental Protection Agency. Prepared by Tetra Tech, Fairfax, VA.

Thurston County Planning Council. 1996. Personal communication.

UNESCO. 1994. Protocols for the Joint Global Ocean Flux Study (JGOFS) Core Measurements IOC Manual and Guides 29. United Nations Educational, Scientific, and Cultural Organization.

URS. 1985. *Discharge Zone Classification System, Southern Puget Sound.* Prepared for Washington State Department of Ecology, Olympia, WA. Prepared by URS Corporation, Seattle, WA.

URS. 1986a. *Circulation and flushing in South Puget Sound, Final Report.* Prepared for Washington State Department of Ecology, Olympia, WA. Prepared by URS Corporation, Seattle, WA.

URS. 1986b. *Southern Puget Sound Water Quality Assessment Study, Final Report: Comprehensive Circulation and Water Quality Study of Budd Inlet*. Prepared for Washington State Department of Ecology, Olympia, WA. Prepared by URS Corporation, Seattle, WA.

U.S. Geological Survey. 2000. ADAPS database. Results for the Puyallup River (site ID 12101500).

Washington State. 1997. *Water Quality Standards for Surface Waters of the State of Washington.* Chapter 173-201A of the Washington Administrative Code.

West Consultants, Inc. 1996. *Evaluating Hydrodynamic and Contaminant Transport Computer Models for Application to Duwamish River and Elliott Bay.* Prepared for King County Department of Natural Resources.

WRE. 1975. *Ecological modeling of Puget Sound and adjacent waters.* Prepared for the Environmental Protection Agency, in cooperation with the U.S. Department of Interior Office of Water Resource Research. Prepared by Water Resources Engineers, Inc., Walnut Creek, CA.

Wu, T.S., J.M. Hamrick, S.C. McCutcheon, and R.B. Ambrose. 1997. Benchmarking the EFDC/HEM3D Surface-Water Hydrodynamic and Eutrophication Models and Computational Methods. Siam Proceedings. ISBN: 0-89871-378-1.

This page is purposely blank for duplex printing

Appendices

Appendix A

1996 and 1998 Section 303(d) List of Impaired Waterbodies

Appendix A. 1996 and 1998 Section 303(d) List of Impaired Waters*

WBID	Waterbody	Parameter	Basis	Remarks	1998 List?	Medium	Action Needed	1996 List?
WA-13-0010	**Henderson Inlet**	Fecal Coliform	Department of Health Conditionally Approved Commercial Shellfish Area of Henderson Inlet based partially on data from three stations that exceed the criterion (from the Annual Growing Area Review ending December 1996).		Yes	Water	TMDL	Yes
		Temperature	8 excursions beyond the criterion out of 19 samples (42%) at Ecology ambient monitoring station HND001 between 9/91 and 9/96.	1	No	Water	None	No
		Dissolved Oxygen	2 excursions beyond the criterion out of 19 samples (11%) at Ecology ambient monitoring station HND001 between 9/91 and 9/96.		Yes	Water	TMDL	No
WA-13-0020	**Budd Inlet (outer)**	Fecal Coliform	BUD002 shows no excursions beyond the criterion from monthly samples between 1991 and 1997; Department of Health Prohibited Commercial Shellfish Area is based on policy (not water quality sampling).	2	No	Water	None	Yes
		Dissolved Oxygen	Data collected by Ecology (summarized by Eisner and Newton, 1997) show multiple excursions beyond the criterion at six stations between 1992 and 1994.		Yes	Water	TMDL	No
		Total Nitrogen	URS, 1985; URS, 1986; URS and Evans-Hamilton, 1986.	3	No	Water	None	Yes
		pH	4 excursions beyond the criterion out of 60 samples (7%) at Ecology ambient monitoring station BUD005 between 9/91 and 9/96.	4	No	Water	None	Yes
		pH	Data collected by Ecology (summarized by Eisner and Newton, 1997) show multiple excursions beyond the upper criterion at nine stations between 1992 and 1994.		Yes	Water	TMDL	No
		Temperature	Data collected by Ecology (summarized by Eisner and Newton, 1997) show multiple excursions beyond the criterion at 14 stations between 1992 and 1994 and 13 excursions beyond the criterion out of 60 samples (22%) at Ecology ambient monitoring station BUD005 between 9/91 and 9/96.	5	No	Water	None	No
WA-13-0030	**Budd Inlet (inner)**	Dissolved Oxygen	Data collected by Ecology (summarized by Eisner and Newton, 1997) show multiple excursions beyond the criterion at five stations between 1992 and 1994.		Yes	Water	TMDL	No
		Dissolved Oxygen	2 excursions beyond the criterion out of 22 samples (9%) at Ecology ambient monitoring station BUD002 between 9/91 and 9/96; URS, 1985; URS, 1986; URS and Evans-Hamilton, 1986. 1 excursion beyond the criterion out of 60 samples (2%) at Ecology ambient monitoring station BUD005 between 9/91 and 9/96.	6	No	Water	None	Yes
		pH	Data collected by Ecology (summarized by Eisner and Newton, 1997) show multiple excursions beyond the upper criterion at three stations between 1992 and 1994.		Yes	Water	TMDL	No
		pH	0 excursions beyond the criterion out of 11 samples (0%) at Ecology ambient monitoring station BUD002 between 9/91 and 9/96. Listed in 1996 based on 3 excursions beyond the criterion at Ecology ambient monitoring station BUD002 in 1986.	7	No	Water	None	Yes
		Temperature	Data collected by Ecology (summarized by Eisner and Newton, 1997) show multiple excursions beyond the criterion at five stations between 1992 and 1994 and at BUD002 between 9/91 and 9/96.	5	No	Water	None	No
		Multiple metals and toxics	varies		Yes	Sediment	TMDL	Yes
		Total Nitrogen	URS, 1985; URS, 1986; URS and Evans-Hamilton, 1986.	3	No	Water	None	Yes
		Fecal Coliform	Data from Ecology ambient monitoring station BUD005 show no excursions beyond the criterion from monthly samples between 1991 and 1997. Department of Health Prohibited Commercial Shellfish Area is based on policy (not water quality sampling); URS, 1985; URS, 1986; URS and Evans-Hamilton, 1986.	8	No	Water	None	Yes
WA-14-0010	**Squaxin, Peale, and Pickering Passages**	Temperature	Data collected by Ecology (summarized by Eisner and Newton, 1997) show multiple excursions beyond the criterion at five stations between 1992 and 1994 and 6 excursions beyond the criterion out of 12 samples (50%) at Ecology ambient monitoring station PCK001 between 9/91 and 9/96.	5, 9	No	Water	None	No
		pH	Two excursions beyond the criterion at Ecology ambient monitoring station DNA001 on 5/6/91 and 8/10/92.		Yes	Water	TMDL	Yes
		Dissolved Oxygen	Data collected by Ecology (summarized by Eisner and Newton, 1997) show multiple excursions beyond the criterion at two stations between 1992 and 1994.		Yes	Water	TMDL	No

WA-14-0020	**Eld Inlet**	Fecal Coliform	Department of Health Conditionally Approved Commercial Shellfish Area covers part of the southern portion of this bay (used station 7 to identify grid ID location).	10	No	Water	None	Yes
		Temperature	5 excursions beyond the criterion out of 22 samples (23%) at Ecology ambient monitoring station ELD001 between 9/91 and 9/96. Four excursions beyond the criterion at Ecology ambient monitoring station ELD002 between 1989 and 1990.	1	No	Water	None	No
		pH	Two excursions beyond the criterion at Ecology ambient monitoring station ELD002 on 1/17/89 and 9/25/89.	11	No	Water	None	No
WA-14-0050	**Shelton Harbor (inner)**	Fecal Coliform	Michaud, 1987.		Yes	Water	TMDL	Yes
WA-14-0100	**Hammersley Inlet**	Fecal Coliform	Department of Health Approved Commercial Shellfish Area in Hammersley Inlet. Data sampled from near the mouth of Gosnell Creek at station 5 that exceed the criterion (from the Annual Growing Area Review ending December 1996).		Yes	Water	TMDL	Yes
WA-14-0110	**Oakland Bay**	Fecal Coliform	Department of Health Conditionally Approved Commercial Shellfish Area in Oakland Bay based partially on data collected at three stations that exceed the criterion (from the Annual Growing Area Review ending December 1996). Department of Health Prohibited Commercial Shellfish Area in Oakland Bay based partially on data collected at two stations that exceed the criterion (from the Annual Growing Area Review ending December 1996).		Yes	Water	TMDL	Yes
		Dissolved Oxygen	0 excursions beyond the criterion out of 56 samples (0%) at Ecology ambient monitoring station OAK004 between 9/91 and 9/96. Listed in 1996 based on 3 excursions beyond the criterion at Ecology ambient monitoring station OAK004 in 1987.	12	No	Water	None	Yes
		Temperature	21 excursions beyond the criterion out of 56 samples (38%) at Ecology ambient monitoring station OAK004 between 9/91 and 9/96.	1	No	Water	None	No

NOTES:

* Table also includes parameters and waterbodies submitted for consideration that were not included on the final lists.

1 These excursions beyond the criterion are a natural condition with no direct human caused influence due to solar heating of the surface water based on the 6/97 judgement of Jan Newton (Dept. of Ecology).

2 TMDL submitted on 3/9/92; EPA determined that the TMDL was incomplete on 2/12/93. Many areas are classified as "Prohibited" for commercial shellfish harvest by the Department of Health because of the proximity on a wastewater discharge, and not due to violations of the water quality standards. Without water quality data to show an actual impact, there is no basis for listing waters in these areas.

3 Excessive productivity in the bay is controlled by nitrogen, which has an effect on the dissolved oxygen in the bay. There are no numeric the criterion in the water quality standards to evaluate for total nitrogen. There is not any information on human-caused impacts to designated uses to support a listing based on the interpretation of the narrative water quality standards per the Water Quality Program Policy. TMDL submitted on 3/9/92; EPA determined that the TMDL was incomplete on 2/12/93. The old data (1985-1986) do not represent current conditions and the segment should not be listed based on these data per the 8/97 judgement of Dept. of Ecology SWRO staff. Recent data collected by Evans-Hamilton verify that the significant upgrades to sewage treatment plants have improved the water quality.

4 The information does not meet the Water Quality Program policy for listing this segment for this parameter.

5 These excursions beyond the criterion are a natural condition with no direct human caused influence due to solar heating of the surface water based on the 4/95 and 1/98 judgement of Jan Newton (Dept. of Ecology).

6 Using the most recently collected data, the information does not meet the Water Quality Program Policy for listing. TMDL submitted on 3/9/92. EPA determined that the TMDL was incomplete on 2/12/93. Previously listed based on the following reports: URS, 1985; URS, 1986; URS and Evans-Hamilton,

7 The segment now meets water quality standards for pH.

8 TMDL submitted on 3/9/92. EPA determined that the TMDL was incomplete on 2/12/93. The older data used for past listings (1985-1986) do not represent current conditions and the segment should not be listed based on these data per the 8/97 judgement of Dept. of Ecology SWRO staff. Many areas are classified as "Prohibited" for commercial shellfish harvest by the Department of Health because of the proximity on a wastewater discharge, and not due to violations of the water quality standards. Without water quality data to show an actual impact, there is no basis for listing waters in these areas.

9 Mistakenly listed entered into 1996 list decision matrix based on station DNA001. This station is on the segment WA-PS-0090 and does not represent conditions on segment WA-14-0010.

10 The latest Assessment by Department of Health (shows that standards are now being met at all stations and an upgrade in classification is being considered.

11 These excursions beyond the criterion have not been repeated and there is no evidence that a direct human caused influence is significant based on the 6/97 judgement of Jan Newton (Dept. of Ecology).

12 The segment now meets water quality standards for dissolved oxygen.

Appendix B

Methods for Oceanographic Field Studies

Appendix B

Methods for Oceanographic Field Studies

Measurement Protocols

The sampling and analysis protocols used in this project were those in use by Ecology's Environmental Monitoring and Trends Section for its Marine Water Monitoring program (Newton et al., 1998). All protocols used are in compliance with the USEPA Puget Sound Estuary Program Standard Protocols (PSEP, 1997).

Two types of data were obtained: *in situ* measurements (using a sensor deployed in the field) and discrete samples (collected in a sampling vessel for subsequent analyses in a laboratory).

Table B-1 lists *in situ* sensors and manufacturer. The conductivity-temperature-depth (CTD) unit was lowered through the water column to generate a depth profile. Sensors were equilibrated just below the sea surface, before the unit was lowered at a steady rate to a few meters above the sea bed and raised back to the sea surface. Data were averaged in 0.5-m vertical length bins and the downcast data were processed using manufacturer's software (Sea-Bird Electronics SEASOFT; versions used were those current for each sampling year).

Table B-1. *In situ* sensors used for South Puget Sound monitoring.

Parameter	*Manufacturer*
Conductivity (used to calculate salinity)	Sea-Bird Electronics®
Temperature	Sea-Bird Electronics®
Pressure (used to calculate depth)	Sea-Bird Electronics®
Density	(calculated from salinity and temperature)
Dissolved oxygen (DO)	Yellow Springs International® and Beckman®
Light transmission	Sea-Tech®
Chlorophyll *a* fluorescence	Sea-Tech®
Photosynthetically active radiation[1] (PAR)	LiCor®

In addition, a Secchi disk was lowered to the depth of its disappearance and that depth recorded. This depth was then used in standard equations (Poole and Atkins, 1929) to determine the euphotic zone depth and the light extinction coefficient (e.g., Newton et al., 1998).

[1] Integrated light intensity over the spectral region 400 to 700 nm, which is of greatest importance to primary productivity.

Accompanying the depth profiles, discrete samples of salinity, DO, and phytoplankton pigments (chlorophyll *a* and phaeopigments) were obtained as check samples for salinity and as calibration samples for DO and chlorophyll *a* for the *in situ* sensors. Salinity, DO, and pigments were sampled using a rosette of Niskin bottles around the CTD, closed remotely at the desired depth. Sampling procedures for these parameters followed Ecology protocols (Janzen, 1992; Newton et al., 1998).

UW's state-accredited School of Oceanography Marine Chemistry Laboratory analyzed salinity using the state-of-the-art Guildline Instruments, Inc. Autosal® salinometer with standard seawater as a reference. Analysis followed the UNESCO (Hasle, 1978) protocol. Results for salinity were recorded as PSU (practical salinity units)[2].

The titration of DO in seawater used the Carpenter method with a Beckmann Dosimat® microburet (Carpenter, 1964). This method is a refinement over the standard Winkler titrations, offering increased precision and accuracy for marine water samples[3]. The equations in Strickland and Parsons (1968) were used to calculate DO in mg L^{-1}.

Fluorometric determination of chlorophyll *a* and phaeopigments was conducted using a Turner model 10 fluorometer and the standard acidification method of Lorenzen (1966)[4]. The equations of Lorenzen (1966) were used to calculate chlorophyll *a* and phaeopigments in µg L^{-1}.

Other discrete marine samples were obtained for parameters for which there were no *in situ* sensors. These include inorganic nutrient concentrations, phytoplankton production, and plankton biomass.

Seawater samples for dissolved nutrients were filtered through 0.45-µm cellulose filters in the field at the time of collection. The filtrate was dispensed into acid-washed, deionized water (DI)-rinsed bottles and frozen immediately onboard the ship. The Marine Chemistry Laboratory analyzed frozen dissolved nutrient samples while Ecology monitored QC data and procedures. Nutrient concentrations (mg L^{-1} or µmolar) were determined for nitrate, nitrite, ammonium, silicate and orthophosphate.

Phytoplankton primary production was estimated from standard ^{14}C uptake experiments (Steeman-Neilson, 1952) following more recent protocols of Barber (1992). Some of the precautions regarding trace metal contamination and toxicity (Fitzwater et al., 1982) were

[2] Salinity determined from conductivity measurements is expressed in terms of practical salinity units (PSU).

[3] Samples were drawn into clean glass iodine flasks through tubing to prevent turbulence. The sample was fixed with MgCl and NaI-NaOH-azide, inverted to mix, and stored out of direct light or heat. After a second mixing, H_2SO_4 was added prior to analysis and samples were titrated with sodium thiosulfate. This analysis was conducted onboard the ship within 48 hrs of sample collection.

[4] Seawater was filtered onto Whatman GF/F filters, the filter immersed in 90% acetone, and extracted in a dark freezer (to prevent photo-oxidation). The extract was sonicated to promote chloroplast lysis, centrifuged to remove cell debris, and decanted into a cuvette for determination of fluorescence before and after addition of 2 drops 1N HCl. This analysis was conducted onboard the ship; samples were held in a freezer and analyzed within 48 hrs of collection.

followed, including contamination of stock, acid cleaning and rinsing of incubation bottles, and use of silicone tubing/o-rings on Niskin bottles. Samples for phytoplankton production[5] were collected from six depths at specified light levels within the euphotic zone, as determined from Secchi disk calculations.

Although no samples have been analyzed, samples for plankton biomass and species composition were taken following UNESCO (Hasle, 1978) protocols. At each productivity station, samples of plankton were collected in glass jars and preserved with 1% formalin. No funding was provided for analysis of these samples; however, if phytoplankton species abundance are desired, the samples will be retained for two years.

Data Reduction, Review, and Reporting

Digital data obtained using the CTD were logged internally, downloaded to a field laptop computer, processed, and stored in both raw and processed forms. Multiple backups were archived in paper and digital form. Software used in processing CTD data was the most recent version of SEASOFT® supplied by the CTD manufacturer, Sea-Bird Electronics, Inc. New software versions were tested for differences from calculated values and any changes noted in database documentation.

Data from lab instruments were maintained on printed sheets in notebooks. Sheets were copied and one copy filed with the CTD data from each survey. The originals are maintained in the notebooks stored at Ecology. Raw data from the hard copy sheets were transcribed into standard template Microsoft Excel® spreadsheets that have transformation equations entered. Units were recorded in all spreadsheets and data sheets, and are accounted for in all calculations. The data spreadsheet was then saved under a different file name. Calculations are checked for accuracy using previous known data.

Newton et al. (1998) describe data archiving procedures in more detail. Data are compiled into a Microsoft Access® database, following the format already in use by Ecology's Marine Waters Monitoring Unit.

[5] Samples were obtained with clean Niskin bottles and dispensed into clean, acid-washed polycarbonate bottles. Sample bottles were inoculated with sodium bicarbonate ($NaH^{14}CO_3$) stock of a known activity. Replicate bottles were incubated in screened bags to mimic the light level at which samples were obtained and one bottle was incubated in the dark. Incubation was on-deck in a running seawater incubator for 24 h, with ambient and nutrient-spike (nitrogen and phosphorus addition) treatments. At the conclusion of incubation, the sample was filtered, acidified to eliminate aqueous ^{14}C activity and placed in scintillation vials filled with 10 mL EcoLume® scintillation fluor. At the beginning of the incubation, samples for abiotic uptake and adsorption (T_o) were inoculated, filtered immediately, and treated as above. From the T_o samples, 1-mL aliquots were removed and injected into a scintillation vial with fluor to determine the total activity added to sample bottles. The specific activity in the scintillation vials was counted using a Beckmann Liquid Scintillation Counter. Disintegrations per minute (DPMs) were converted to photosynthetic carbon uptake (primary production) in mg-C m^3 d^{-1} using standard equations (Strickland and Parsons, 1968).

Quality Control Procedures

Quality assurance procedures and objectives for these cruises followed those in the Quality Assurance Project Proposal written for similar marine studies in Puget Sound by Newton et al. (1998).

CTD sensors were evaluated monthly for blank (zero) and standard (or known) readings when possible for conductivity, temperature, DO, light transmission, and pH. Voltage readings for the CTD fluorescence and PAR sensors were verified for blanks under dark conditions. Failure to meet these criteria prevents use of the sensors until servicing. The data obtained from the CTD were processed using the manufacturer's software, then the processed data are checked for accuracy in values and coefficients. Failure to obtain 100% agreement results in a complete re-processing.

Laboratory instruments were also checked for blank and standard readings. The DO titration was subjected to three standard determinations and one blank determination, following published protocols (Strickland and Parsons, 1968). Analysis was not conducted unless two of the three standard values agreed within 0.002 mL and the blank determination was less than 0.010 mL. A blank reading for the lab fluorometer was determined using a 90% acetone sample that was required to read below 0.5 fluorescence units (FU). Due to the stability of the fluorometer, standards were not run, but every 6 to 8 months the instrument was calibrated against a dilution series of known concentrations of chlorophyll *a*, as determined by spectrophotometric analysis. Drift in instrument response between calibrations was extremely low. The PAR sensor was checked for zero readings (dark) and reasonable output at the time of use. Failure to obtain reasonable values from either the fluorometer or PAR sensor prevented further analysis.

Instruments owned by the UW Marine Chemistry Laboratory (salinometer, nutrient auto-analyzer) have prescribed QC check procedures that were followed by the lab personnel. Results of the checks for the samples from this project were made available to Ecology. The liquid scintillation counter was first run with blank and standard ^{14}C vials. The values for these vials was verified before proceeding with sample vial counts.

Preventative maintenance was routinely performed on all instruments, as indicated in Newton et al. (1998). All meters were maintained in accordance with the manufacturer's recommendations. Critical equipment and supplies are listed on a check-sheet and are the responsibility of the field personnel.

Appendix C

EFDC Water Quality Model

(excerpt from Tetra Tech, 1999)

4 - EFDC WATER QUALITY MODEL

4.1 Introduction

The central issues in the water quality model are primary production of carbon by algae and concentration of dissolved oxygen. Primary production provides the energy required by the ecosystem to function. However, excessive primary production is detrimental since its decomposition in the water and sediments consumes oxygen. Dissolved oxygen is necessary to support the life functions of higher organisms and is considered an indicator of the health of estuarine systems. In order to predict primary production and dissolved oxygen, a large suite of model state variables is necessary (Table 4-1). The nitrate state variable in the model represents the sum of nitrate and nitrite nitrogen. The three variables (salinity, water temperature, and total suspended solids) needed for computation of the above 21 state variables are provided by the EFDC hydrodynamic model. The interactions among the state variables is illustrated in Figure 4-1. The kinetic processes included in the EFDC water quality model are mostly from the Chesapeake Bay three-dimensional water quality, model, CE-QUAL-ICM (Cerco & Cole 1994). The kinetic sources and sinks as well as the external loads for each state variable are described in Sections 4.3 to 4.11. The kinetic processes include the exchange of fluxes at the sediment-water interface, including sediment oxygen demand, which are explained in Section 5 (EFDC Sediment Process Model) of this report. The description of the EFDC water column water quality model in this section is from Park et al. (1995).

Table 4-1. EFDC Model Water Quality State Variables

1) cyanobacteria	12) labile particulate organic nitrogen
2) diatom algae	13) dissolved organic nitrogen
3) green algae	14) ammonia nitrogen
4) refractory particulate organic carbon	15) nitrate nitrogen
5) labile particulate organic carbon	16) particulate biogenic silica
6) dissolved organic carbon	17) dissolved available silica
7) refractory particulate organic phosphorus	18) chemical oxygen demand
8) labile particulate organic phosphorus	19) dissolved oxygen
9) dissolved organic phosphorus	20) total active metal
10) total phosphate	21) fecal coliform bacteria
11) refractory particulate organic nitrogen	22) macroalgae

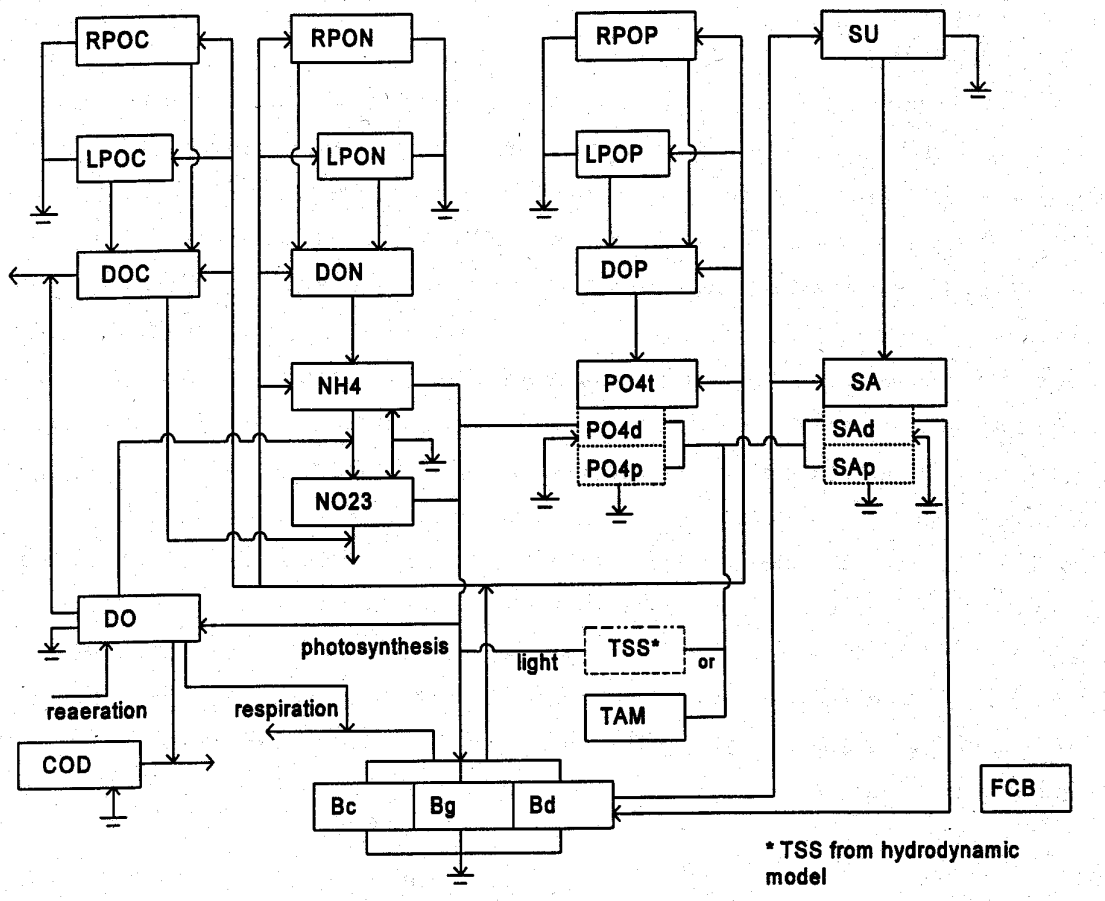

Figure 4-1. Schematic diagram for the EFDC water column water quality model.

4.1.1 Algae

Algae are grouped into three model classes: cyanobacteria, diatoms, and greens. The grouping is based upon the distinctive characteristics of each class and upon the significant role the characteristics play in the ecosystem. Cyanobacteria, commonly called blue-green algae, are characterized by their abundance (as picoplankton) in saline water and by their bloom-forming characteristics in fresh water. Cyanobacteria are unique in that some species fix atmospheric nitrogen although nitrogen fixers are not predominant in the Peconic Estuary system. The cyanobacteria distinguished in the model are a surrogate for the bloom-forming brown tide species found in the Peconic Estuary. They are characterized as having very 1ow settling velocity and their growth rates are specified such that they only grow in the brown-tide bloom years (i.e., 1991 and 1995). Diatoms are distinguished by their requirement of silica as a nutrient to form cell walls. Diatoms are large algae characterized by high settling velocities. Settling of spring diatom) blooms to the sediments may be a significant source of carbon for sediment oxygen

demand. Algae that do not fall into the preceding two groups are lumped into the heading of green algae. Green algae settle at a rate intermediate between cyanobacteria and diatoms and are subject to greater grazing pressure than cyanobacteria.

4.1.2 Organic Carbon

Three organic carbon state variables are considered: dissolved, labile particulate, and refractory particulate. Labile and refractory distinctions are based upon the time scale of decomposition. Labile organic carbon decomposes on a time scale of days to weeks while refractory organic carbon requires more time. Labile organic carbon decomposes rapidly in the water column or the sediments. Refractory organic carbon decomposes slowly, primarily in the sediments, and may contribute to sediment oxygen demand years after deposition.

4.1.3 Nitrogen

Nitrogen is first divided into organic and mineral fractions. Organic nitrogen state variables are: dissolved organic nitrogen, labile particulate organic nitrogen, and refractory particulate organic nitrogen. Two mineral nitrogen forms are considered: ammonium and nitrate. Both are utilized to satisfy algal nutrient requirements although ammonium is preferred from thermodynamic considerations. The primary reason for distinguishing the two is that ammonium is oxidized by nitrifying bacteria into nitrate. This oxidation can be a significant sink of oxygen in the water column and sediments. An intermediate in the complete oxidation of ammonium, nitrite, also exists. Nitrite concentrations are usually much less than nitrate and for modeling purposes nitrite is combined with nitrate. Hence the nitrate state variable actually represents the sum of nitrate plus nitrite.

4.1.4 Phosphorus

As with carbon and nitrogen, organic phosphorus is considered in three states: dissolved, labile particulate, and refractory particulate. Only a single mineral form, total phosphate, is considered. Total phosphate exists as several states within the model ecosystem: dissolved phosphate, phosphate sorbed to inorganic solids, and phosphate incorporated in algal cells. Equilibrium partition coefficients are used to distribute the total among the three states.

4.1.5 Silica

Silica is divided into two state variables: available silica and particulate biogenic silica. Available silica is primarily dissolved and can be utilized by diatoms. Particulate biogenic silica cannot be utilized. In the model, particulate biogenic silica is produced through diatom mortality. Particulate biogenic silica undergoes dissolution to available silica or else settles to the bottom sediments.

4.1.6 Chemical Oxygen Demand

In the context of this study, chemical oxygen demand is the concentration of reduced substances that are oxidizable by inorganic means. The primary component of chemical oxygen demand is sulfide released from sediments. Oxidation of sulfide to sulfate may remove substantial quantities of dissolved oxygen from the water column.

4.1.7 Dissolved Oxygen

Dissolved oxygen is required for the existence of higher life forms. Oxygen availability determines the distribution of organisms and the flows of energy and nutrients in an ecosystem. Dissolved oxygen is a central component of the water quality model.

4.1.8 Total Active Metal

Both phosphate and dissolved silica sorb to inorganic solids, primarily iron and manganese. Sorption and subsequent settling is one pathway for removal of phosphate and silica from the water column. Consequently, the concentration and transport of iron and manganese are represented in the model. Limited data do not allow a complete treatment of iron and manganese chemistry, however. Rather, a single state variable, total active metal, is defined as the total concentration of metals that are active in phosphate and silica transport. Total active metal is partitioned between particulate and dissolved phases by an oxygen-dependent partition coefficient.

4.1.9 Salinity

Salinity is a conservative tracer that provides verification of the transport component of the model and facilitates examination of conservation of mass. Salinity also influences the dissolved oxygen saturation concentration and is used in the determination of kinetics constants that differ in saline and fresh water.

4.1.10 Temperature

Temperature is a primary determinant of the rate of biochemical reactions. Reaction rates increase as a function of temperature although extreme temperatures result in the mortality of organisms.

4.2 Conservation Of Mass Equation

The governing mass-balance equation for each of the water quality state variables may be expressed as:

$$\frac{\partial \mathrm{C}}{\partial \mathrm{t}} + \frac{\partial (uC)}{\partial \chi} + \frac{\partial (\mathrm{v}C)}{\partial \gamma} + \frac{\partial (wC)}{\partial z} =$$

$$\frac{\partial}{\partial x}\left(\mathrm{K_x}\frac{\partial C}{\partial x}\right)+\frac{\partial}{\partial y}\left(\mathrm{K}_y\frac{\partial C}{\partial y}\right)+\frac{\partial}{\partial z}\left(\mathrm{K}_z\frac{\partial C}{\partial z}\right)+\mathrm{S}_C \qquad (4\text{-}1)$$

C = concentration of a water quality state variable

u, v & w = velocity components in the x-, y- and z-directions, respectively

K_x, K_y & K_z = turbulent diffusivities in the x-, y- and z-directions, respectively

S_c = internal and external sources and sinks per unit volume.

The last three terms on the left-hand side (LHS) of Eq. 4-1 account for the advective transport and the first three terms on the right-hand side (RHS) of Eq. 4-1 account for the diffusive transport. These six terms for physical transport are analogous to, and thus the numerical method of solution is the same as, those in the mass-balance equation for salinity in the hydrodynamic model (Hamrick 1992). The last term in Eq. 4-1 represents the kinetic processes and external loads for each of the state variables. The present model solves Eq. 4-1 after decoupling the kinetic terms from the physical transport terms. The solution scheme for both the physical transport (Hamrick 1992) and the kinetic equations is second-order accurate.

The governing mass-balance equation for water quality state variables (Eq. 4-1) consists of physical transport, advective and diffusive, and kinetic processes. When solving Eq. 4-1, the kinetic terms are decoupled from the physical transport terms. The mass-balance equation for physical transport only, which takes the same form as the salt-balance equation, is:

$$\frac{\partial \mathrm{C}}{\partial \mathrm{t}}+\frac{\partial(uC)}{\partial \chi}+\frac{\partial(\nu C)}{\partial \gamma}+\frac{\partial(wC)}{\partial z}=\frac{\partial}{\partial x}\left(\mathrm{K_x}\frac{\partial C}{\partial x}\right)+\frac{\partial}{\partial y}\left(\mathrm{K}_y\frac{\partial C}{\partial y}\right)+\frac{\partial}{\partial z}\left(\mathrm{K}_z\frac{\partial C}{\partial z}\right) \qquad (4\text{-}2)$$

The equation for kinetic processes only, which will be referred to as kinetic equation, is:

$$\frac{\partial C}{\partial t}=\mathrm{S_C} \qquad (4\text{-}3)$$

which may be expressed as:

$$\frac{\partial C}{\partial t}=K\cdot C+R \qquad (4\text{-}4)$$

where K is kinetic rate (time^{-1}) and R is source/sink term (mass volume^{-1} time^{-1}). Equation 4-4 is obtained by linearizing some terms in the kinetic equations, mostly Monod type expressions. Hence, K and R are known values in Eq. 4-4. Equation 4-2 is identical with, and thus its numerical method of solution is the same as, the mass-balance equation for salinity (Hamrick 1992).

The remainder of this chapter details the kinetics portion of the mass-conservation equation for each state variable. Parameters are defined where they first appear. All parameters are listed, in alphabetical order, in an appendix. For consistency with reported rate coefficients, kinetics are detailed using a temporal dimension of days. Within the CE-QUAL-ICM computer code, kinetics sources and sinks are converted to a dimension of seconds before employment in the mass-conservation equation.

4.3 Algae

Algae, which occupies a central role in the model (Fig. 4-1), are grouped into three model state variables: cyanobacteria (blue-green algae), diatoms and green algae. The subscript, **x**, is used to denote three algal groups: **c** for cyanobacteria, **d** for diatoms and **g** for green algae. Sources and sinks included in the model are

- growth (production)
- basal metabolism
- predation
- settling
- external loads

Equations describing these processes are largely the same for three algal groups with differences in the values of parameters in the equations. The kinetic equation describing these processes is:

$$\frac{\partial B_x}{\partial t} = (P_x - BM_x - PR_x)B_x + \frac{\partial}{\partial z}(WS_x \cdot B_x) + \frac{WB_x}{V} \qquad (4\text{-}5)$$

B_x = algal biomass of algal group x (g C m^{-3})

t = time (day)

P_x = production rate of algal group x (day^{-1})

BM_x = basal metabolism rate of algal group x (day^{-1})

PR_x = predation rate of algal group x (day^{-1})

WS_x = settling velocity of algal group x (m day^{-1})

WB_x = external loads of algal group x (g C day^{-1})

V = cell volume (m^3).

4.3.1 Production (Algal Growth)

Algal growth depends on nutrient availability, ambient light and temperature. The effects of these processes are considered to be multiplicative:

$$P_x = PM_x f_1(N) f_2(I) f_3(T) \qquad (4\text{-}6)$$

PM_x = maximum growth rate under optimal conditions for algal group x (day^{-1})

$f_1(N)$ = effect of suboptimal nutrient concentration ($0 \le f_1 \le 1$))

$f_2(I)$ = effect of suboptimal light intensity ($0 \leq f_2 \leq 1$)

$f_3(T)$ = effect of suboptimal temperature ($0 \leq f_3 \leq 1$).

The freshwater cyanobacteria may undergo rapid mortality in salt water, e.g., freshwater organisms in the Potomac River (Thomann et al. 1985). For the freshwater organisms, the increased mortality may be included in the model by retaining the salinity toxicity term in the growth equation for cyanobacteria:

$$P_c = PM_c f_1(N) f_2(I) f_3(T) f_4(S) \tag{4-7}$$

$f_4(S)$ = effect of salinity on cyanobacteria growth ($0 \leq f_4 \leq 1$).

Activation of the salinity toxicity term, f_4 (S), is an option in the source code.

4.3.2 Effect of Nutrients on Algal Growth

Using Liebig's "law of the minimum" (Odum 1971) that growth is determined by the nutrient in least supply, the nutrient limitation for growth of cyanobacteria and green algae is expressed as:

$$f_1(N) = minimum\left(\frac{NH4 + NO3}{KHN_x + NH4 + NO3}, \frac{PO4d}{KHP_x + PO4d}\right) \tag{4-8}$$

NH4 = ammonium nitrogen concentration (g N m^{-3})

NO3 = nitrate nitrogen concentration (g N m^{-3})

KHN_x = half-saturation constant for nitrogen uptake for algal group x (g N m^{-3})

PO4d = dissolved phosphate phosphorus concentration (g P m^{-3})

KHP_x = half-saturation constant for phosphorus uptake for algal group x (g P m^{-3}).

Some cyanobacteria, e.g., *Anabaena,* can fix nitrogen from atmosphere and thus is not limited by nitrogen. Hence, Eq. 4-8 is not applicable to the growth of nitrogen fixers.

Since diatoms require silica as well as nitrogen and phosphorus for growth, the nutrient limitation for diatoms is expressed as:

$$f_1(N) = minimum\left(\frac{NH4 + NO3}{KHN_d + NH4 + NO3}, \frac{PO4d}{KHP_d + PO4d}, \frac{SAd}{KHS + SAd}\right) \tag{4-9}$$

SAd = concentration of dissolved available silica (g Si m^{-3})

KHS = half-saturation constant for silica uptake for diatoms (g Si m^{-3}).

4.3.3 Effect of Light on Algal Growth

The daily and vertically integrated form of Steele's equation is:

$$f_2(I) = \frac{2.718 \cdot FD}{Kess \cdot \Delta_z} \left(e^{-\alpha_B} - e^{-\alpha_r}\right) \tag{4-10}$$

$$\alpha_B = \frac{I_o}{FD \cdot (I_s)_x} \cdot \exp(-Kess[H_T + \Delta z]) \tag{4-11}$$

$$\alpha_T = \frac{I_o}{FD \cdot (I_s)_x} \cdot \exp(-Kess \cdot H_T) \tag{4-12}$$

FD = fractional daylength ($0 \leq FD \leq 1$)

Kess = total light extinction coefficient (m^{-1})

Δz = layer thickness (m)

I_o = daily total light intensity at water surface (langleys day^{-1})

$(I_s)_x$ = optimal light intensity for algal group x (langleys day^{-1})

H_T= depth from the free surface to the top of the layer (m).

Light extinction in the water column consists of three fractions in the model: a background value dependent on water color, extinction due to suspended particles and extinction due to light absorption by ambient chlorophyll:

$$Kess = Ke_b + Ke_{Tss}.TSS + Ke_{Chl}. \sum_{x=c,d,g} \left(\frac{B_x}{CChl_x}\right) \tag{4-13}$$

Ke_b = background light extinction (m^{-1})

Ke_{TSS} = light extinction coefficient for total suspended solid (m^{-1} per g m^{-3})

TSS = total suspended solid concentration (g m^{-3}) provided from the hydrodynamic model

Ke_{Chl} = light extinction coefficient for chlorophyll 'a' (m^{-1} per mg Chl m^{-3})

$CChl_x$ = carbon-to-chlorophyll ratio in algal group x (g C per mg Chl).

For a model application that does not simulate TSS, the Ke_{TSS} term may be set to zero and Ke_b may be estimated to include light extinction due to suspended solid.

Optimal light intensity (I_s) for photosynthesis depends on algal taxonomy, duration of exposure, temperature, nutritional status and previous acclimation. Variations in I_s are largely due to adaptations by algae intended to maximize production in a variable environment. Steel (1962) noted the result of adaptations is that optimal intensity is a consistent fraction (approximately 50%) of daily intensity. Kremer & Nixon, (1978) reported an analogous finding that maximum algal growth occurs at a constant

depth (approximately 1 m) in the water column. Their approach is adopted so that optimal intensity is expressed as:

$$(I_s)_x = minimum \left\{ (I_o)_{avg} \cdot e^{-Kess \cdot Dopt)x} , (I_s)_{min} \right\} \quad (4\text{-}14)$$

$(D_{opt})_x$ = depth of maximum algal growth for algal group x (m)

$(I_o)_{avg}$ = adjusted surface light intensity (langleys day^{-1}).

A minimum, $(I_s)_{min}$, in Eq. 4-14 is specified so that algae do not thrive at extremely low light levels. The time required for algae to adapt to changes in light intensity is recognized by estimating $(I_s)_x$

$$(I_o)_{avg} = CI_a \cdot I_o + CI_b \cdot I_1 + CI_c \cdot I_2 \quad (4\text{-}15)$$

I_1 = daily light intensity one day preceding model day (langleys day^{-1})

1_2 = daily light intensity two days preceding model day (langleys day^{-1})

CI_a, CI_b & CI_c = weighting factors for I_o, I_1 and I_2, respectively: $CI_a + CI_b + CI_c = 1$.

4.3.4 Effect of Temperature on Algal Growth

A Gaussian probability curve is used to represent temperature dependency of algal growth:

$$f_3(T) = \exp(-KTGI_X [T - TM_x]^2) \quad if \quad T \leq TM_x$$
$$= \exp(-KTG2_x [TM_x - T]^2) \quad if \quad T > TM_x \quad (4\text{-}16)$$

T = temperature (°C) provided from the hydrodynamic model

TM_x = optimal temperature for algal growth for algal group x (°C)

$KTGl_x$ = effect of temperature below TM_x on growth for algal group x (°C^{-2})

$KTG2_x$ = effect of temperature above TM_x on growth for algal group x (°C^{-2}).

4.3.5 Effect of Salinity on Growth of Freshwater Cyanobacteria

The growth of freshwater cyanobacteria in salt water is limited by:

$$f_4(S) = \frac{STOX^2}{STOX^2 + S^2} \quad (4\text{-}17)$$

STOX = salinity at which Microcystis growth is halved (ppt)

S = salinity in water column (ppt) provided from the hydrodynamic model.

4.3.6 Algal Basal Metabolism

Algal biomass in the present model decreases through basal metabolism (respiration and excretion) and predation. Basal metabolism in the present model is the sum of all internal processes that

decrease algal biomass, and consists of two parts; respiration and excretion. In basal metabolism, algal matter (carbon, nitrogen, phosphorus and silica) is returned to organic and inorganic pools in the environment, mainly to dissolved organic and inorganic matter. Respiration, which may be viewed as a reversal of production, consumes dissolved oxygen. Basal metabolism is considered to be an exponentially increasing function of temperature:

$$BM_x = BMR_x \cdot \exp(KTB_x[T - TR_x]) \quad (4\text{-}18)$$

BMR_x = basal metabolism rate at TR_x for algal group x (day^{-1})
KTB_x = effect of temperature on metabolism for algal group x ($°C^{-1}$)
TR_x = reference temperature for basal metabolism for algal group x (°C).

4.3.7 Algal Predation

The present model does not include zooplankton. Instead, a constant rate is specified for algal predation, which implicitly assumes zooplankton biomass is a constant fraction of algal biomass. An equation similar to that for basal metabolism (Eq. 4-18) is used for predation:

$$PR_x = PRR_x \cdot \exp(KTB_x[T = TR_x]) \quad (4\text{-}19)$$

PRR_x = predation rate at TR_x for algal group x (day^{-1}).

The difference between predation and basal metabolism lies in the distribution of the end products of two processes. In predation, algal matter (carbon, nitrogen, phosphorus and silica) is returned to organic and inorganic pools in the environment, mainly to particulate organic matter.

4.3.8 Algal Settling

Settling velocities for three algal groups, WS_c, WS_d and WS_g, are specified as an input. Seasonal variations in setting velocity of diatoms can be accounted for by specifying time-varying WS_d.

4.4 Organic Carbon

The present model has three state variables for organic carbon: refractory particulate, labile particulate and dissolved.

4.4.1 Particulate Organic Carbon

Labile arid refractory distinctions are based on the time scale of decomposition. Labile particulate organic carbon with a decomposition time scale of days to weeks decomposes rapidly in the water column or in the sediments. Refractory particulate organic carbon with longer-than-weeks decomposition tine scale decomposes slowly, primarily in the sediments, and may contribute to sediment

oxygen demand years after decomposition. For labile and refractory particulate organic carbon, sources and sinks included in the model are (Fig. 4-1):

- algal predation
- dissolution to dissolved organic carbon
- settling
- external loads

The governing equations for refractory and labile particulate organic carbons are:

$$\frac{\partial RPOC}{\partial t} = \sum_{x+c,d,g} FCRP \cdot PR_x \cdot B_x - K_{RPOC} \cdot RPOC + \frac{\partial}{\partial z}(WS_{RP} \cdot RPOC) + \frac{WRPOC}{V} \qquad (4\text{-}20)$$

$$\frac{\partial LPOC}{\partial t} = \sum_{x+c,d,g} FCLP \cdot PR_x \cdot B_x - K_{LPOC} \cdot LPOC + \frac{\partial}{\partial z}(WS_{LP} \cdot LPOC) + \frac{WLPOC}{V} \qquad (4\text{-}20)$$

RPOC = concentration of refractory particulate organic carbon (g C m^{-3})

LPOC = concentration of labile particulate organic carbon (g C m^{-3})

FCRP = fraction of predated carbon produced as refractory particulate organic carbon

FCLP = fraction of predated carbon produced as labile particulate organic carbon

K_{RPOC} = dissolution rate of refractory particulate organic carbon (day^{-1})

K_{LPOC} = dissolution rate of labile particulate organic carbon (day^{-1})

WS_{RP} = settling velocity of refractory particulate organic matter (m day^{-1})

WS_{LP} = settling velocity of labile particulate organic matter (m day^{-1})

WRPOC = external loads of refractory particulate organic carbon (g C day^{-1})

WLPOC = external loads of labile particulate organic carbon (g C day^{-1}).

4.4.2 Dissolved Organic Carbon

Sources and sinks for dissolved organic carbon included in the model are (Fig. 4-1):

- algal excretion (exudation) and predation
- dissolution from refractory and labile particulate organic carbon
- heterotrophic respiration of dissolved organic carbon (decomposition)
- denitrification
- external loads

The kinetic equation describing these processes is:

$$\frac{\partial \mathrm{DOC}}{\partial \mathrm{t}} = \sum_{x=c,d,g} \left(\left[FCD_x + (1 = FCD_x) \frac{KHR_x}{KHR_x + DO} \right] BM_x + FCDP \cdot PR_x \right) \cdot B_x$$

$$+ K_{RPOC} \cdot RPOC + K_{LPOC} \cdot LPOC - K_{HR} \cdot DOC - Denit \cdot DOC + \frac{WDOC}{V} \qquad (4\text{-}22)$$

DOC = concentration of dissolved organic carbon (g C m^{-3})

FCD_x = fraction of basal metabolism exuded as dissolved organic carbon at infinite dissolved oxygen concentration for algal group x

KHR_x = half-saturation constant of dissolved oxygen for algal dissolved organic carbon excretion for group x (g O_2 m^{-3})

DO = dissolved oxygen concentration (g O_2 m^{-3})

FCDP = fraction of predated carbon produced as dissolved organic carbon

K_{HR} = heterotrophic respiration rate of dissolved organic carbon (day^{-1})

Denit = denitrification rate (day^{-1}) given in Eq. 4-34

WDOC = external loads of dissolved organic carbon (g C day^{-1}).

The remaining of this section explains each term in Equations 4-20 to 4-22.

4.4.3 Effect of Algae on Organic Carbon

The term s within summation (Σ) in Equations 4-20 to 4-22 account for the effects of algae on organic carbon through basal metabolism and predation.

4.4.3.1 Basal metabolism. Basal metabolism, consisting of respiration and excretion, returns algal matter (carbon, nitrogen, phosphorus and silica) back to the environment. Loss of algal biomass through basal metabolism is (Eq. 4-18):

$$\frac{\partial B_x}{\partial t} = -BM_x \cdot B_x \qquad (4\text{-}23)$$

which indicates that the total loss of algal biomass due to basal metabolism is independent of ambient dissolved oxygen concentration. In this model, it is assumed that the distribution of total loss between respiration and excretion is constant as long as there is sufficient dissolved oxygen for algae to respire. Under that condition, the losses by respiration and excretion may be written as:

$(1 - FCD_x) \cdot BM_x \cdot B_x$ due to respiration (4-24)

$FCD_x \cdot BM_x \, B_x$ due to excretion (4-25)

where FCD_x is a constant of value between 0 and 1. Algae cannot respire in the absence of oxygen, however. Although the total loss of algal biomass due to basal metabolism is oxygen-independent (Eq. 4-23), the distribution of total loss between respiration and excretion is oxygen-dependent. When oxygen level is high, respiration is a large fraction of the total. As dissolved oxygen becomes scarce, excretion becomes dominant. Thus, Eq. 4-24 represents the loss by respiration only at high oxygen levels. In general, Eq. 4-24 can be decomposed into two fractions as a function of dissolved oxygen availability:

$$(1 - FCD_x)\cdot\frac{DO}{KHR_x + DO} BM_x \cdot B_x \qquad \text{due to respiration} \qquad (4\text{-}26)$$

$$(1 - FCD_x)\frac{KHR_x}{KHR_x + DO} BM_x \cdot B_x \qquad \text{due to excretion} \qquad (4\text{-}27)$$

Equation 4-26 represents the loss of algal biomass by respiration and Eq. 4-27 represents additional excretion due to insufficient dissolved oxygen concentration. The parameter KHR_x, which is defined as the half-saturation constant of dissolved oxygen for algal dissolved organic carbon excretion in Eq. 4-22, can also be defined as the half-saturation constant of dissolved oxygen for algal respiration in Eq. 4-26.

Combining Equations 4-25 and 4-27, the total loss due to excretion is:

$$\left(FCD_x + (1 - FCD_x)\frac{KHR_x}{KHR_x + DO}\right) BM_x \cdot B_x \qquad (4\text{-}28)$$

Equations 4-26 and 4-28 combine to give the total loss of algal biomass due to basal metabolism, $BM_x \cdot B_x$ (Eq. 4-23). The definition of FCD_x in Eq. 4-22 becomes apparent in Eq. 4-28; i.e., fraction of basal metabolism exuded as dissolved organic carbon at infinite dissolved oxygen concentration. At zero oxygen level, 100% of total loss due to basal metabolism is by excretion regardless of FCD_x. The end carbon product of respiration is primarily carbon dioxide, an inorganic form not considered in the present model, while the end carbon product of excretion is primarily dissolved organic carbon. Therefore, Eq. 4-28, that appears in Eq. 4-22, represents the contribution of excretion to dissolved organic carbon, and there is no source term for particulate organic carbon from algal basal metabolism in Equations 4-20 and 4-21.

4.4.3.2 Predation. Algae produce organic carbon through the effects of predation. Zooplankton take up and redistribute algal carbon through grazing, assimilation, respiration and excretion. Since zooplankton are not included in the model, routing of algal carbon through zooplankton predation is simulated by empirical distribution coefficients in Equations 4-20 to 4-22; FCRP, FCLP and FCDP. The sum of these three predation fractions should be unity.

4.4.4 Heterotrophic Respiration and Dissolution

The second term on the RHS of Equations 4-20 and 4-21 represents dissolution of particulate to dissolved organic carbon and the third term in the second line of Eq. 4-22 represents heterotrophic respiration of dissolved organic carbon. The oxic heterotrophic respiration is a function of dissolved

oxygen: the lower the dissolved oxygen, the smaller the respiration term becomes. Heterotrophic respiration rate, therefore, is expressed using a Monod function of dissolved oxygen:

$$KHR = \frac{DO}{KHOR_{DO} + DO} K_{DOC} \quad (4\text{-}29)$$

$KHOR_{DO}$ = oxic respiration half-saturation constant for dissolved oxygen (g O_2 m^{-3})

K_{DOC} = heterotrophic respiration rate of dissolved organic carbon at infinite dissolved oxygen concentration (day^{-1}).

Dissolution and heterotrophic respiration rates depend on the availability of carbonaceous substrate and on heterotrophic activity. Algae produce labile carbon that fuels heterotrophic activity: dissolution and heterotrophic respiration do not require the presence of algae though, and may be fueled entirely by external carbon inputs. In the model, algal biomass, as a surrogate for heterotrophic activity, is incorporated into formulations of dissolution and heterotrophic respiration rates. Formulations of these rates require specification of algal-dependent and algal-independent rates:

$$K_{RPOC} = (K_{RC} + K_{RCalg} \sum_{x=c,d,g} B_x) \cdot \exp(KT_{HDR}[T - TR_{HDR}]) \quad (4\text{-}30)$$

$$K_{LPOC} = (K_{LC} + K_{LCalg} \sum_{x=c,d,g} B_x) \cdot \exp(KT_{HDR}[T - TR_{HDR}]) \quad (4\text{-}31)$$

$$K_{DOC} = (K_{DC} + K_{DCalg} \sum_{x=c,d,g} B_x) \cdot \exp(KT_{MNL}[T - TR_{MNL}]) \quad (4\text{-}32)$$

K_{RC} = minimum dissolution rate of refractory particulate organic carbon (day^{-1})

K_{LC} = minimum dissolution rate of labile particulate organic carbon (day^{-1})

K_{DC} = minimum respiration rate of dissolved organic carbon (day^{-1})

K_{RCalg} & K_{LCalg} = constants that relate dissolution of refractory and labile particulate organic carbon, respectively, to algal biomass (day^{-1} per g C m^{-3})

K_{DCalg} = constant that relates respiration to algal biomass (day^{-1} per g C m^{-3})

KT_{HDR} = effect of temperature on hydrolysis of particulate organic matter ($°C^{-1}$)

TR_{HDR} = reference temperature for hydrolysis of particulate organic matter (°C)

KT_{MNL} = effect of temperature on mineralization of dissolved organic matter ($°C^{-1}$)

TR_{MNL} = reference temperature for mineralization of dissolved organic matter (°C).

Equations 4-30 to 4-32 have exponential functions that relate rates to temperature.

In the present model, the term "hydrolysis" is defined as the process by which particulate organic matter is converted to dissolved organic form, and thus includes both dissolution of particulate carbon and hydrolysis of particulate phosphorus and nitrogen. Therefore, the parameters, KT_{HDR} and TR_{HDR}, are

also used for the temperature effects on hydrolysis of particulate phosphorus (Equations 4-28 and 4-29) and nitrogen (Equations 4-54 and 4-55). The term "mineralization" is defined as the process by which dissolved organic matter is converted to dissolved inorganic form, and thus includes both heterotrophic respiration of dissolved organic carbon and mineralization of dissolved organic phosphorus and nitrogen. Therefore, the parameters, KT_{MNL} and TR_{MNL}, are also used for the temperature effects on mineralization of dissolved phosphorus (Eq. 4-46) and nitrogen (Eq. 4-56).

4.4.5 Effect of Denitrification on Dissolved Organic Carbon

As oxygen is depleted from natural systems, organic matter is oxidized by the reduction of alternate electron acceptors. Thermodynamically, the first alternate acceptor reduced in the absence of oxygen is nitrate. The reduction of nitrate by a large number of heterotrophic anaerobes is referred to as denitrification, and the stoichiometry of this reaction is (Stumm & Morgan 1981):

$$4NO_3^- + 4H^+ + 5\,CH_2O \rightarrow 2N_2 + 7H_20 + 5C0_2 \tag{4-33}$$

The last term in Eq. 4-22 accounts for the effect of denitrification on dissolved organic carbon. The kinetics of denitrification in the model are first-order:

$$Denit = \frac{KHOR_{DO}}{KHOR_{DO} + DO}\,\frac{NO3}{KHDN_N + NO3}\,AANOX \cdot K_{DOC} \tag{4-34}$$

$KHDN_N$ = denitrification half-saturation constant for nitrate (g N m^{-3})
AANOX = ratio of denitrification rate to oxic dissolved organic carbon respiration rate.

In Eq. 4-34, the dissolved organic carbon respiration rate, K_{DOC}, is modified so that significant decomposition via denitrification occurs only when nitrate is freely available and dissolved oxygen is depleted. The ratio, AANOX, makes the anoxic respiration slower than oxic respiration. Note that K_{DOC}, defined in Eq. 4-32, includes the temperature effect on denitrification.

4.5 Phosphorus

The present model has four state variables for phosphorus: three organic forms (refractory particulate, labile particulate and dissolved) and one inorganic form (total phosphate).

4.5.1 Particulate Organic Phosphorus

For refractory and labile particulate organic phosphorus, sources and sinks included in the model are (Fig. 4-1):

- algal basal metabolism and predation
- dissolution to dissolved organic phosphorus
- settling

• external loads

The kinetic equations for refractory and labile particulate organic phosphorus are:

$$\frac{\partial RPOP}{\partial t} = \sum_{x=c,d,g}(FPR_x \cdot BM_x + FPRP \cdot PR_x)APC \cdot B_x - K_{RPOP} \cdot RPOP + \frac{\partial}{\partial z}(WS_{RP} \cdot RPOP) + \frac{WRPOP}{V} \quad (4\text{-}35)$$

$$\frac{\partial LPOP}{\partial t} = \sum_{x=c,d,g}(FPL_x \cdot BM_x + FPLP \cdot PR_x)APC \cdot B_x - K_{LPOP} \cdot LPOP + \frac{\partial}{\partial z}(WS_{LP} \cdot LPOP) + \frac{WLPOP}{V} \quad (4\text{-}36)$$

RPOP = concentration of refractory particulate organic phosphorus (g P m^{-3})

LPOP = concentration of labile particulate organic phosphorus (g P m^{-3})

FPR_x = fraction of metabolized phosphorus by algal group x produced as refractory particulate organic phosphorus

FPL_x = fraction of metabolized phosphorus by algal group x produced as labile particulate organic phosphorus

FPRP = fraction of predated phosphorus produced as refractory particulate organic phosphorus

FPLP = fraction of predated phosphorus produced as labile particulate organic phosphorus

APC = mean phosphorus-to-carbon ratio in all algal groups (g P per g C)

K_{RPOP} = hydrolysis rate of refractory particulate organic phosphorus (day^{-1})

K_{LPOP} = hydrolysis rate of labile particulate organic phosphorus (day^{-1})

WRPOP = external loads of refractory particulate organic phosphorus (g P day^{-1})

WLPOP = external loads of labile particulate organic phosphorus (g P day^{-1}).

4.5.2 Dissolved Organic Phosphorus

Sources and sinks for dissolved organic phosphorus included in the model are (Fig. 4-1):

• algal basal metabolism and predation

• dissolution from refractory and labile particulate organic phosphorus

• mineralization to phosphate phosphorus

• external loads

The kinetic equation describing these processes is:

$$\frac{\partial DOP}{\partial t} = \sum_{x=c,d,g}(FPD_x \cdot BM_x + FPDP \cdot PR_x)APC \cdot B_x$$

$$+ K_{RPOP} \cdot RPOP + K_{LPOP} \cdot LPOP - K_{DOP} \cdot DOP + \frac{WDOP}{V} \quad (4\text{-}37)$$

DOP = concentration of dissolved organic phosphorus (g P m^{-3})

FPD_x = fraction of metabolized phosphorus by algal group x produced as dissolved organic phosphorus

FPDP = fraction of predated phosphorus produced as dissolved organic phosphorus

K_{DOP} = mineralization rate of dissolved organic phosphorus (day^{-1})

WDOP = external loads of dissolved organic phosphorus (g P day^{-1}).

4.5.3 Total Phosphate

For total phosphate that includes both dissolved and sorbed phosphate (Section 4.5.4), sources and sinks included in the model are (Fig. 4-1):

- algal basal metabolism, predation, and uptake
- mineralization from dissolved organic phosphorus
- settling of sorbed phosphate
- sediment-water exchange of dissolved phosphate for the bottom layer only
- external loads

The kinetic equation describing these processes is:

$$\frac{\partial PO4t}{\partial t} = \sum_{x=c,d,g} (FPI_x \cdot BM_x + FPIP \cdot PR_x - P_x) APC \cdot B_x + K_{DOP} \cdot DOP$$

$$+ \frac{\partial}{\partial z}(WS_{TSS} \cdot PO4p) + \frac{BFPO4d}{\Delta_z} + \frac{WPO4t}{V} \quad (4\text{-}38)$$

PO4t = total phosphate (g P m^{-3}) = PO4d + PO4p (4-39)

PO4d = dissolved phosphate (g P m^{-3})

PO4p = particulate (sorbed) phosphate (g P m^{-3})

FPI_x = fraction of metabolized phosphorus by algal group x produced as inorganic phosphorus

FPIP = fraction of predated phosphorus produced as inorganic phosphorus

WS_{TSS} = settling velocity of suspended solid (m day^{-1}), provided by the hydrodynamic model

BFPO4d = sediment-water exchange flux of phosphate (g P m^{-2} day^{-1}), applied to the bottom layer only

WPO4t = external loads of total phosphate (g P day^{-1}).

In Eq. 4-38, if total active metal is chosen as a measure of sorption site, the settling velocity of total suspended solid, WS_{TSS}, is replaced by that of particulate metal, WS_s (Sections 4.5.4 and 4.10). The remainder of this section explains each term in Equations 4-35 to 4-38, except BFPO4d described in Chapter IV of Park et al. (1995).

4.5.4 Total Phosphate System

Suspended and bottom sediment particles (clay, silt and metal hydroxides) adsorb and desorb phosphate in river and estuarine waters. This adsorption-desorption process has been suggested to buffer phosphate concentration in water column and to enhance the transport of phosphate away from its external sources (Carritt & Goodgal 1954; Froelich 1988; Lebo 1991). To ease the computational complication due to the adsorption-desorption of phosphate, dissolved and sorbed phosphate are treated and transported as a single state variable. Therefore, the model phosphate state variable, total phosphate, is defined as the sum of dissolved and sorbed phosphate (Eq. 4-39), and the concentrations for each fraction are determined by equilibrium partitioning of their sum.

In CE-QUAL-ICM, sorption of phosphate to particulate species of metals including iron and manganese was considered based on phenomenon observed in the monitoring data from the mainstem of the Chesapeake Bay: phosphate was rapidly depleted from anoxic bottom waters during the autumn reaeration event (Cerco & Cole 1994). Their hypothesis was that reaeration of bottom waters caused dissolved iron and manganese to precipitate, and phosphate sorbed to newly-formed metal particles and rapidly settled to the bottom. One state variable, total active metal, in CE-QUAL-ICM was defined as the sum of all metals that act as sorption sites, and the total active metal was partitioned into particulate and dissolved fractions via an equilibrium partitioning coefficient (Section 4.10). Then, phosphate was assumed to sorb to only the particulate fraction of the total active metal.

In the treatment of phosphate sorption in CE-QUAL-ICM, the particulate fraction of metal hydroxides was emphasized as a sorption site in bottom waters under anoxic conditions. Phosphorus is a highly particle-reactive element, and phosphate in solution reacts quickly with a wide variety of surfaces, being taken up by and released from particles (Froelich 1988). The present model has two options, total suspended solid and total active metal, as a measure of a sorption site for phosphate, and dissolved and sorbed fractions are determined by equilibrium partitioning of their sum as a function of total suspended solid or total active metal concentration:

$$PO4p = \frac{K_{PO4p} \cdot TSS}{1 + K_{PO4p} \cdot TSS} PO4t \quad \text{or} \quad PO4p = \frac{K_{PO4p} \cdot TAMp}{1 + K_{PO4p} \cdot TAMp} PO4t \tag{4-40}$$

$$PO4d = \frac{1}{1 + K_{PO4p} \cdot TSS} PO4t \quad \text{or} \quad PO4d = \frac{1}{1 + K_{PO4p} \cdot TAMp} PO4t$$

$$= PO4t - PO4p \tag{4-41}$$

K_{PO4p} = empirical coefficient relating phosphate sorption to total suspended solid (per g m^{-3}) or particulate total active metal (per mol m^{-3}) concentration

TAMP = particulate total active metal (mol m^{-3}).

Dividing Eq. 4 0 by Eq. 4-41 gives:

$$K_{PO4p} = \frac{\text{PO4p}}{PO4d}\frac{1}{TSS} \qquad \text{or} \qquad K_{PO4p} = \frac{\text{PO4p}}{PO4d}\frac{1}{TAMp} \tag{4-42}$$

where the meaning of K_{PO4p} becomes apparent, i.e., the ratio of sorbed to dissolved phosphate per unit concentration of total suspended solid or particulate total active metal (i.e., per unit sorption site available).

4.5.5 Algal Phosphorus-to-Carbon Ratio (APC)

Algal biomass is quantified in units of carbon per volume of water. In order to express the effects of algal biomass on phosphorus and nitrogen, the ratios of phosphorus-to-carbon and nitrogen-to-carbon in algal biomass must be specified. Although global mean values of these ratios are well known (Redfield et al. 1963), algal composition varies especially as a function of nutrient availability. As phosphorus and nitrogen become scarce, algae adjust their composition so that smaller quantities of these vital nutrients are required to produce carbonaceous biomass (DiToro 1980; Parsons et al. 1984). Examining the field data from the surface of upper Chesapeake Bay, Cerco & Cole (1994) showed that the variation of nitrogen-to-carbon stoichiometry was small and thus used a constant algal nitrogen-to-carbon ratio, ANC_x. Large variations, however, were observed for algal phosphorus-to-carbon ratio indicating the adaptation of algae to ambient phosphorus concentration (Cerco & Cole 1994): algal phosphorus content is high when ambient phosphorus is abundant and is low when ambient phosphorus is scarce. Thus a variable algal phosphorus-to-carbon ratio, APC, is used in model formulation. A mean ratio for all algal group, APC, is described by an empirical approximation to the trend observed in field data (Cerco & Cole 1994):

$$APC = (CP_{\text{prml}} + CP_{prm2}\cdot\exp[\,-\,CP_{prm3}\cdot PO4d])^{-1} \tag{4-43}$$

CP_{prml} = minimum carbon-to-phosphorus ratio (g C per g P)
CP_{prm2} = difference between minimum and maximum carbon-to-phosphorus ratio (g C per g P)
CP_{prm3} = effect of dissolved phosphate concentration on carbon-to-phosphorus ratio (per g P m^{-3}).

4.5.6 Effect f Algae on Phosphorus

The terms within summation (Σ) in Equations 4-35 to 4-38 account for the effects of algae on phosphorus. Both basal metabolism (respiration and excretion) and predation are considered, and thus formulated, to contribute to organic and phosphate phosphorus. That is, the total loss by basal metabolism ($BM_x \cdot B_x$ in Eq. 4-5) is distributed using distribution coefficients; FPR_x, FPL_x, FPD_x and FPI_x.

The total loss by predation ($PR_x \cdot B_x$ in Eq. 4-5), is also distributed using distribution coefficients; FPRP, FPLP, FPDP and FPIP. The sum of four distribution coefficients for basal metabolism should be unity, and so is that for predation. Algae take up dissolved phosphate for growth, and algae uptake of phosphate is represented by ($- \Sigma P_x \cdot APC \cdot B_x$) in Eq. 4-38.

4.5.7 Mineralization and Hydrolysis

The third term on the RHS of Equations 4-35 and 4-36 represents hydrolysis of particulate organic phosphorus and the last term in Eq. 3-7 represents mineralization of dissolved organic phosphorus. Mineralization of organic phosphorus is mediated by the release of nucleotidase and phosphatase enzymes by bacteria (Chróst & Overbek 1987) and algae (Boni et al. 1989). Since the algae themselves release the enzymes and bacterial abundance is related to algal biomass, the rate of organic phosphorus mineralization is related to algal biomass in model formulation. Another mechanism included in model formulation is that algae stimulate production of an enzyme that mineralizes organic phosphorus to phosphate when phosphate is scarce (Chróst & Overbek 1987; Boni et al. 1989). The formulations for hydrolysis and mineralization rates including these processes are:

$$K_{RPOP} = (K_{RP} + \frac{KHP}{KHP + PO4d} K_{RPalg} \sum_{x=c,d,g} B_x) \cdot \exp(KT_{HDR}[T - TR_{HDR}]) \quad (4\text{-}44)$$

$$K_{LPOP} = (K_{LP} + \frac{KHP}{KHP + PO4d} K_{LPalg} \sum_{x=c,d,g} B_x) \cdot \exp(KT_{HDR}[T - TR_{HDR}]) \quad (4\text{-}45)$$

$$K_{DOP} = (K_{DP} + \frac{KHP}{KHP + PO4d} K_{DPalg} \sum_{x=c,d,g} B_x) \cdot \exp(KT_{MNL}[T - TR_{MNL}]) \quad (4\text{-}46)$$

K_{RP} =minimum hydrolysis rate of refractory particulate organic phosphorus (day^{-1})

K_{LP} = minimum hydrolysis rate of labile particulate organic phosphorus (day^{-1})

K_{DP} =minimum mineralization rate of dissolved organic phosphorus (day^{-1})

K_{RPalg} & K_{LPalg} = constants that relate hydrolysis of refractory and labile particulate organic phosphorus, respectively, to algal biomass (day^{-1} per g C m^{-3})

K_{DPalg} =constant that relates mineralization to algal biomass (day^{-1} per g C m^{-3})

KHP = mean half-saturation constant for algal phosphorus uptake (g P of m^{-3})

$$= \frac{1}{3} \sum_{x=c,d,g} KHP_x \quad (4\text{-}47)$$

When phosphate is abundant relative to KHP, the rates become to be close to the minimum values with little influence from algal biomass. When phosphate becomes scarce relative to KHP, the rates increase with the magnitude of increase depending on algal biomass. Equations 4-44 to 4-46 have exponential functions that relate rates to temperature.

4.6 Nitrogen

The present model has five state variables for nitrogen: three organic forms (refractory particulate, labile particulate and dissolved) and two inorganic forms (ammonium and nitrate). The nitrate state variable in the model represents the sum of nitrate and nitrite.

4.6.1 Particulate Organic Nitrogen

For refractory and labile particulate organic nitrogen, sources and sinks included in the model are (Fig. 4-1):

- algal basal metabolism and predation
- dissolution to dissolved organic nitrogen
- settling
- external loads

The kinetic equations for refractory and labile particulate organic nitrogen are:

$$\frac{\partial RPON}{\partial t} = \sum_{x=c,d,g} (FNR_x \cdot BM_x + FNRP \cdot PR_x) ANC \cdot B_x - K_{RPON} \cdot RPON + \frac{\partial}{\partial z}(WS_{RP} \cdot RPON) + \frac{WRPON}{V} \quad (4\text{-}48)$$

$$\frac{\partial LPON}{\partial t} = \sum_{x=c,d,g} (FNL_x \cdot BM_x + FNLP \cdot PR_x) ANC \cdot B_x - K_{RPON} \cdot RPON + \frac{\partial}{\partial z}(WS_{LP} \cdot LPON) + \frac{WLPON}{V} \quad (4\text{-}49)$$

RPON = concentration of refractory particulate organic nitrogen (g N m^{-3})

LPON = concentration of labile particulate organic nitrogen (g N m^{-3})

FNR_x = fraction metabolized nitrogen by algal group x as refractory particulate organic nitrogen

FNL_x = fraction of metabolized nitrogen by algal group x produced as labile particulate organic nitrogen

FNRP = fraction of predated nitrogen produced as refractory particulate organic nitrogen

FNLP = fraction of predated nitrogen produced as labile particulate organic nitrogen

ANC_x = nitrogen-to-carbon ratio in algal group x (g N per g C)

K_{RPON} = hydrolysis rate of refractory particulate organic nitrogen (day^{-1})

K_{LPON} = hydrolysis rate of labile particulate organic nitrogen (day^{-1})

WRPON = external loads of refractory particulate organic nitrogen (g N day^{-1})

WLPON = external loads of labile particulate organic nitrogen (g N day^{-1}).

4.6.2 Dissolved Organic Nitrogen

Sources and sinks for dissolved organic nitrogen included in the model are (Fig. 4-1):

- algal basal metabolism and predation
- dissolution from refractory and labile particulate organic nitrogen
- mineralization to ammonium
- external loads

The kinetic equation describing these processes is:

$$\frac{\partial DON}{\partial t} = \sum_{x=c,d,g}(FND_x \cdot BM_x + FNDP \cdot PR_x)ANC_x \cdot B_x$$

$$+ K_{RPON} \cdot RPON + K_{LPON} \cdot LPON - K_{DON} \cdot DON + \frac{WDON}{V} \qquad (4\text{-}50)$$

DON = concentration of dissolved organic nitrogen (g N m^{-3})

FND_x = fraction of metabolized nitrogen by algal group x produced as dissolved organic nitrogen

FNDP = fraction of predated nitrogen produced as dissolved organic nitrogen

K_{DON} = mineralization rate of dissolved organic nitrogen (day^{-1})

WDON = external loads of dissolved organic nitrogen (g N day^{-1}).

4.6.3 Ammonium Nitrogen

Sources and sinks for ammonia nitrogen included in the model are (Fig. 4-1):

- algal basal metabolism, predation, and uptake
- mineralization from dissolved organic nitrogen
- nitrification to nitrate
- sediment-water exchange for the bottom layer only
- external loads

The kinetic equation describing these processes is:

$$\frac{\partial NH4}{\partial t} = \sum_{x=c,d,g}(FNI_x \cdot BM_x + FNIP \cdot PR_x - PN_x \cdot P_x)ANC_x \cdot B_x + K_{DON} \cdot DON$$

$$- Nit \cdot NH4 + \frac{BFNH4}{\Delta z} + \frac{WHN4}{V} \qquad (4\text{-}51)$$

FNI_x = fraction of metabolized nitrogen by algal group x produced as inorganic nitrogen

FNIP = fraction of predated nitrogen produced as inorganic nitrogen

PN_x = preference for ammonium uptake by algal group x ($0 \le PNx \le 1$)

Nit = nitrification rate (day^{-1}) given in Eq. 4-59

BFNH4 = sediment-water exchange flux of ammonium (g N m^{-2} day^{-1}), applied to the bottom layer only

WNH4 = external loads of ammonium (g N day^{-1}).

4.6.4 Nitrate Nitrogen

Sources and sinks for nitrate nitrogen included in the model are (Fig. 4-1):

- algal uptake
- nitrification from ammonium
- denitrification to nitrogen gas
- sediment-water exchange for the bottom layer only
- external loads

The kinetic equation describing these processes is:

$$\frac{\partial NO3}{\partial t} = \sum_{x=c,d,g}(1 - \mathrm{PNx})P_x \cdot ANC_x \cdot B_x + Nit \cdot NH4 - ANDC \cdot Denit \cdot DOC + \frac{BFN03}{\Delta z} + \frac{WN03}{V} \quad (4\text{-}52)$$

ANDC = mass of nitrate nitrogen reduced per mass of dissolved organic carbon oxidized (0.933 g N per g C from Eq. 4-33)

BFNO3 = sediment-water exchange flux of nitrate (g N m^{-2} day^{-1}), applied to the bottom layer only

WNO3 = external loads of nitrate (g N day^{-1}).

The remainder of this section explains each term in Equations 4-48 to 4-52, except BFNH4 and BFNO3 described in Chapter IV of Park et al. (1995).

4.6.5 Effect of Algae on Nitrogen

The terms within summation (Σ) in Equations 4-48 to 4-52 account for the effects of algae on nitrogen. As in phosphorus, both basal metabolism (respiration and excretion) and predation are considered, and thus formulated, to contribute to organic and ammonium nitrogen. That is, algal nitrogen released by both basal metabolism and predation are represented by distribution coefficients; FNR_x, FNL_x, FND_x, FNI_x, FNRP, FNLP, FNDP and FNIP. The sum of four distribution coefficients for basal metabolism should be unity, and so is that for predation.

Algae take up ammonium and nitrate for growth, and ammonium is preferred from thermodynamic considerations. The preference of algae for ammonium is expressed as:

$$PN_x = NH4\frac{NO3}{(KHN_x + NH4)(KHN_x + NO3)} + NH4\frac{KHN_x}{(NH4 + NO3)(KHN_x + NO3)} \quad (4\text{-}53)$$

This equation forces the preference for ammonium to be unity when nitrate is absent, and to be zero when ammonium is absent.

4.6.6 Mineralization and Hydrolysis

The third term on the RHS of Equations 4-48 and 4-49 represents hydrolysis of particulate organic nitrogen and the last term in Eq. 4-50 represents mineralization of dissolved organic nitrogen. Including a mechanism for accelerated hydrolysis and mineralization during nutrient-limited conditions (Section 4.5.7), the formulations for these processes are:

$$K_{RPON} = (K_{RN} + \frac{KHN}{KHN + \mathrm{NH4} + \mathrm{N03}} K_{RNalg} \sum_{x=c,d,g} B_x) \cdot \exp(KT_{HDR}[T - TR_{HDR}]) \quad (4\text{-}54)$$

$$K_{LPON} = (K_{LN} + \frac{KHN}{KHN + \mathrm{NH4} + \mathrm{N03}} K_{LNalg} \sum_{x=c,d,g} B_x) \cdot \exp(KT_{HDR}[T - TR_{HDR}]) \quad (4\text{-}55)$$

$$K_{DON} = (K_{DN} + \frac{KHN}{KHN + \mathrm{NH4} + \mathrm{N03}} K_{DNalg} \sum_{x=c,d,g} B_x) \cdot \exp(KT_{MNL}[T - TR_{MNL}]) \quad (4\text{-}56)$$

K_{RN} = minimum hydrolysis rate of refractory particulate organic nitrogen (day^{-1})

K_{LN} = minimum hydrolysis rate of labile particulate organic nitrogen (day^{-1})

K_{DN} = minimum mineralization rate of dissolved organic nitrogen (day^{-1})

K_{RNalg} & K_{LNa1g} = constants that relate hydrolysis of refractory and labile particulate organic nitrogen, respectively, to algal biomass (day^{-1} per g C m^{-3})

K_{DNalg} = constant that relates mineralization to algal biomass (day^{-1} per g C m^{-3})

KHN = mean half-saturation constant for algal nitrogen uptake (g N m^{-3})

$$= \frac{1}{3} \sum_{x=c,d,g} KHN_x \quad (4\text{-}57)$$

Equations 4-54 to 4-56 have exponential functions that relate rates to temperature.

4.6.7 Nitrification

Nitrification is a process mediated by autotrophic nitrifying bacteria that obtain energy through the oxidation of ammonium to nitrite and of nitrite to nitrate. The stoichiometry of complete reaction is (Bowie et al. 1985):

$$NH_4^+ + 2O_2 \rightarrow NO_3^- + H_2O + 2H^+ \quad (4\text{-}58)$$

The first term in the second line of Eq. 4-51 and its corresponding term in Eq. 4-52 represent the effect of nitrification on ammonium and nitrate, respectively. The kinetics of complete nitrification process are formulated as a function of available ammonium, dissolved oxygen and temperature:

$$\text{Nit} = \frac{DO}{KHNit_{DO} + DO} \frac{1}{KHNit_N + NH4} Nit_m \cdot f_{NIT}(T) \tag{4-59}$$

$$f_{Nit}(T) = \exp(-KNit1[T - Tnit]^2) \quad if \quad T \leq TNit$$
$$= \exp(-KNit2[TNit - T]^2) \quad if \quad T > TNit \tag{4-60}$$

$KHNit_{DO}$ = nitrification half-saturation constant for dissolved oxygen (g O_2 m^{-3})

$KHNit_N$ = nitrification half-saturation constant for ammonium (g N m^{-3})

Nit_m = maximum nitrification rate at TNit (g N m^{-3} day^{-1})

TNit = optimum temperature for nitrification (°C)

KNitl = effect of temperature below TNit on nitrification rate ($°C^{-2}$)

KNit2 = effect of temperature above TNit on nitrification rate ($°C^{-2}$).

The Monod function of dissolved oxygen in Eq. 4-59 indicates the inhibition of nitrification at low oxygen level. The Monod function of ammonium indicates that when ammonium is abundant, the nitrification rate is limited by availability of nitrifying bacteria. The effect of suboptimal temperature is represented using Gaussian form.

4.6.8 Denitrification

The effect of denitrification on dissolved organic carbon was described in Section 4.4.5. Denitrification removes nitrate from the system in stoichiometric proportion to carbon removal as determined by Eq. 4-33. The last term in the first line of Eq. 4-52 represent this removal of nitrate.

4.7 Silica

The present model has two state variables for silica: particulate biogenic silica and available silica.

4.7.1. Particulate Biogenic Silica

Source and sinks for particulate biogenic silica included in the model are (Fig. 4-1):

- diatom basal metabolism and predation
- dissolution to available silica
- settling
- external loads

The kinetic equation describing these processes is:

$$\frac{\partial SU}{\partial t} = (FSP_d \cdot BM_d + FSPP \cdot PR_d) ASC_d \cdot B_d - K_{SUA} \cdot SU + \frac{\partial}{\partial z}(WS_d \cdot SU) + \frac{WSU}{V} \tag{4-61}$$

SU = concentration of particulate biogenic silica (g Si m^{-3}).

FSP_d = fraction of metabolized silica by diatoms produced as particulate biogenic silica

FSPP = fraction of predated diatom silica produced as particulate biogenic silica

ASC_d = silica-to-carbon ratio of diatoms (g Si per g C)

K_{SUA} = dissolution rate of particulate biogenic silica (day^{-1})

WSU = external loads of particulate biogenic silica (g Si day^{-1}).

4.7.2 Available Silica

Sources and sinks for available silica included in the model are (Fig. 4-1):

- diatom basal metabolism, predation, and uptake
- settling of sorbed (particulate) available silica
- dissolution from particulate biogenic silica
- sediment-water exchange of dissolved silica for the bottom layer only
- external loads

The kinetic equation describing these processes is:

$$\frac{\partial SA}{\partial t} = (FSI_d \cdot BM_d + FSIP \cdot PR_d - P_d) ASC_d \cdot B_d + K_{SUA} \cdot SU + \frac{\partial}{\partial z}(WS_{TSS} \cdot Sap) + \frac{BFSAd}{\Delta z} + \frac{WSA}{V} \quad (4\text{-}62)$$

SA = concentration of available silica (g Si m^{-3}) = SAd + SAp (4-63)

SAd = dissolved available silica (g Si m^{-3})

SAp = particulate (sorbed) available silica (g Si m^{-3})

FSI_d = fraction of metabolized silica by diatoms produced as available silica

FSIP = fraction of predated diatom silica produced as available silica

BFSAd = sediment-water exchange flux of available silica (g Si m^{-2} day^{-1}), applied to bottom layer only.

WSA = external loads of available silica (g Si day^{-1}).

In Eq. 4-62, if total active metal is chosen as a measure of sorption site, the settling velocity of total suspended solid, WS_{TSS}, is replaced by that of particulate metal, WS_s (Sections 4.7.3 and 4.10).

4.7.3 Available Silica System

Analysis of Chesapeake Bay monitoring data indicates that silica shows similar behavior as phosphate in the adsorption-desorption process (Cerco & Cole 1994). As in phosphate, therefore, available silica is defined to include both dissolved and sorbed fractions (Eq. 4-63). Treatment of

available silica is the same as total phosphate and the same method to partition dissolved and sorbed phosphate is used to partition dissolved and sorbed available silica:

$$SAp = \frac{K_{SAp} \cdot TSS}{1 + K_{SAp} \cdot TSS} SA \quad \text{or} \qquad SAp = \frac{K_{SAp} \cdot TAMp}{1 + K_{SAp} \cdot TAMp} SA \tag{4-64}$$

$$SAd = \frac{1}{1 + K_{SAp} \cdot TSS} SA \quad \text{or} \qquad SAd = \frac{1}{1 + K_{SAp} \cdot TAMp} SA$$

$$= SA - SAp \tag{4-65}$$

K_{SAP} = empirical coefficient relating available silica sorption to total suspended solid (per g m^{-3}) or particulate total active metal (per mol m^{-3}) concentration.

As in K_{PO4p} in Section 4.5.4, K_{SAp} is the ratio of sorbed to dissolved available silica per unit sorption site available.

4.7.4 Effect of Diatoms on Silica

In Equations 4-62 and 4-63, those terms expressed as a function of diatom biomass (B_d) account for the effects of diatoms on silica. As in phosphorus and nitrogen, both basal metabolism (respiration and excretion) and predation are considered, and thus formulated, to contribute to particulate biogenic and available silica. That is, diatom silica released by both basal metabolism and predation are represented by distribution coefficients; FSP_d, FSI_d, FSPP and FSIP. The sum of two distribution coefficients for basal metabolism should be unity, and so is that for predation. Diatoms require silica as well as phosphorus and nitrogen, and diatom uptake of available silica is represented by (- $P_d \cdot ASC_d \cdot B_d$) in Eq. 4-63.

4.7.5 Dissolution

The term (- K_{SUA}.SU) in Eq. 4-62 and its corresponding term in Eq. 4-63 represent dissolution of particulate biogenic silica to available silica. The dissolution rate is expressed as an exponential function of temperature:

$$K_{SUA} = K_{SU} \cdot \exp\left(KT_{SUA}\,[T - TR_{SUA}]\right) \tag{4-66}$$

K_{SU} = dissolution rate of particulate biogenic silica at TR_{SUA} (day^{-1})

KT_{SUA} = effect of temperature on dissolution of particulate biogenic silica ($°C^{-1}$)

TR_{SUA} = reference temperature for dissolution of particulate biogenic silica (°C).

4.8 Chemical Oxygen Demand

In the present model, chemical oxygen demand is the concentration of reduced substances that are oxidizable though inorganic means. The source of chemical oxygen demand in saline water is sulfide released from sediments. A cycle occurs in which sulfate is reduced to sulfide in the sediments and reoxidized to sulfate in the water column. In freshwater, methane is released to the water column by the sediment process model. Both sulfide and methane are quantified in units of oxygen demand and are treated with the same kinetic formulation. The kinetic equation including external loads, if any, is:

$$\frac{\partial COD}{\partial t} = -\frac{DO}{KH_{COD} + DO} KCOD \cdot COD + \frac{BFCOD}{\Delta z} + \frac{WCOD}{V} \quad (4\text{-}67)$$

COD = concentration of chemical oxygen demand (g O_2-equivalents of m^{-3})

KH_{COD} = half-saturation constant of dissolved oxygen required for oxidation of chemical oxygen demand (g O_2 m^{-3})

KCOD = oxidation rate of chemical oxygen demand (day^{-1})

BFCOD = sediment flux of chemical oxygen demand (g O_2-equivalents M^{-2} day^{-1}), applied to bottom layer only

WCOD = external loads of chemical oxygen demand (g O_2-equivalents day^{-1}).

An exponential function is used to describe the temperature effect on the oxidation rate of chemical oxygen demand:

$$KCOD = K_{CD} \cdot \exp\left(KT_{COD}\left[T - TR_{COD}\right]\right) \quad (4\text{-}68)$$

K_{CD} = oxidation to of chemical oxygen demand at TR_{COD} (day^{-1})

KT_{COD} = effect of temperature on oxidation of chemical oxygen demand ($°C^{-1}$)

TR_{COD} = reference temperature for oxidation of chemical oxygen demand (°C).

4.9 Dissolved Oxygen

Sources and sinks of dissolved oxygen in the water column included in the model are (Fig. 4-1):

- algal photosynthesis and respiration
- nitrification
- heterotrophic respiration of dissolved organic carbon
- oxidation of chemical oxygen demand
- surface reaeration for the surface layer only
- sediment oxygen demand for the bottom layer only
- external loads

The kinetic equation describing these processes is:

$$\frac{\partial DO}{\partial t} = \sum_{x=c,d,g} \left((1.3 - 0.3 \cdot PN_x) P_x - (1 - FCD_x) \frac{DO}{KHR_x + DO} BM_x \right) AOCR \cdot B_x$$

$$- AONT \cdot Nit \cdot NH4 - AOCR \cdot K_{HR} \cdot DOC - \frac{DO}{KH_{COD} + DO} KCOD \cdot COD$$

$$+ K_r (DO_s - DO) + \frac{SOD}{\Delta z} + \frac{WDO}{V} \qquad (4\text{-}69)$$

AONT = mass of dissolved oxygen consumed per unit mass of ammonium nitrogen nitrified (4.33 g O_2 per g N; see Section 4.9.2)

AOCR = dissolved oxygen-to-carbon ratio in respiration (2.67 g O_2 per g C; see Section 4.9.1)

K_I = reaeration coefficient (day^{-1}): the reaeration term is applied to the surface layer only

DO_S = saturate concentration of dissolved oxygen (g O_2 m^{-3})

SOD = sediment oxygen demand (g O_2 m^{-2} day^{-1}), applied to the bottom layer only; positive is to the water column

WDO = external loads of dissolved oxygen (g O_2 day^{-1}).

The two sink terms in Eq. 4-69, heterotrophic respiration and chemical oxygen demand, are explained in Section 4.4.4 (Eq. 4-29) and Section 4.8 (Eq. 4-67), respectively. The remainder of this section explains the effects of algae, nitrification and surface reaeration.

4.9.1 Effect of Algae on Dissolved Oxygen

The first line on the RHS of Eq. 4-69 accounts for the effects of algae on dissolved oxygen. Algae produce oxygen through photosynthesis and consume oxygen through respiration. The quantity produced depends on the form of nitrogen utilized for growth. Equations describing production of dissolved oxygen are (Morel 1983):

$$106\ C0_2 + 16\ NH_4^+ + H_2P0_4^- + 106\ H_20 \rightarrow protoplasm + 106 0_2 + 15H^+ \qquad (4\text{-}70)$$

$$106\ C0_2 + 16\ N0_3 + H_2P0_4^- + 122\ H_20 + 17H^+ \rightarrow protoplasm + 138 0_2 \qquad (4\text{-}71)$$

When ammonium is the nitrogen source, one mole of oxygen is produced per mole of carbon dioxide fixed. When nitrate is the nitrogen source, 1.3 moles of oxygen are produced per mole of carbon dioxide fixed. The quantity, $(1.3 - 0.3 \cdot PN_x)$, in the first term of Eq. 4-69 is the photosynthesis ratio and represents the molar quantity of oxygen produced per mole of carbon dioxide fixed. It approaches unity as the algal preference for ammonium approaches unity.

The last term in the first line of Eq. 4-69 accounts for the oxygen consumption due to algal respiration (Eq. 4-26). A simple representation of respiration process is:

$$CH_20 + 0_2 = C0_2 + H_20 \tag{4-72}$$

from which, AOCR = 2.67 g O_2 per g C.

4.9.2 Effect of Nitrification on Dissolved Oxygen

The stoichiometry of nitrification reaction (Eq. 4-58) indicates that two moles of oxygen are required to nitrify one mole of ammonium into nitrate. However, cell synthesis by nitrifying bacteria is accomplished by the fixation of carbon dioxide so that less than two moles of oxygen are consumed per mole ammonium utilized (Wezemak & Gannon 1968), i.e., AONT = 4.33 g O_2 per g N.

4.9.3 Effect of Surface Reaeration on Dissolved Oxygen

The rearation rate of dissolved oxygen at the air-water interface is proportional to the oxygen gradient across the interface, (DO_s - DO), when assuming the air is saturated with oxygen. The saturated concentration of dissolved oxygen, which decreases as temperature and salinity increase, is specified using an empirical formula (Genet et al. 1974):

$$DO_S = 14.532 - 0.38217 \cdot T + 5.4258\text{x}10^{-3} \cdot T^2 - CL \cdot (1.665\text{x}10^{-4} - 5.866\text{x}10^{-6} \cdot T + 9.796 \text{ x } 10^{-8} \cdot T^2) \tag{4-73}$$

CL = chloride concentration (mg/L) = S/1.80655.

The reaeration coefficient includes the effect of turbulence generated by bottom friction (O'Connor & Dobbins 1958) and that by surface wind stress (Banks & Herrera 1977):

$$K_r = \left(K_{ro} \sqrt{\frac{u_{eq}}{h_{eq}}} + W_{rea} \right) \frac{1}{\Delta z} \cdot KT_r^{T-20} \tag{4-74}$$

K_{ro} = proportionality constant = 3.933 in MKS unit

U_{eq} = weighted velocity over cross-section (m sec^{-1}) = $\Sigma(u_k V_k)/\Sigma(V_k)$

h_{eq} = weighted depth over cross-section (m) = $\Sigma(V_k)/B_\eta$

B_η = width at the free surface (m)

W_{rea} = wind-induced reaeration (m day^{-1})

$$= 0.728\ U_w^{\frac{1}{2}} - 0.317\ U_w + 0.0372\ U_w^2 \tag{4-75}$$

U_w = wind speed (m sec^{-1}) at the height of 10 m above surface

KT_r = constant for temperature adjustment of DO reaeration rate.

4.10 Total Active Metal

The present model requires simulation of total active metal for adsorption of phosphate and silica if that option is chosen (Fig. 4-1). The total active metal state variable is the sum of iron and manganese concentrations both particulate and dissolved. In the model, the origin of total active metal is benthic sediments. Since sediment release of metal is not explicit in the sediment model (Chapter IV of Park et al. 1995), release is specified in the kinetic portion of the water column model. The only other term included is setting of the particulate fraction. Then, the kinetic equation for total active metal including external loads, if any, may be written as:

$$\frac{\partial TAM}{\partial t} = \frac{KHbmf}{KHbmf + DO}\frac{BFTAM}{\Delta z}e^{Ktam(T - Ttam)} + \frac{\partial}{\partial z}(WS_s \cdot TAMp) + \frac{WTAM}{V} \quad (4\text{-}76)$$

TAM = total active metal concentration (mol m^{-3}) = TAMd + TAMp (4-77)

TAMd = dissolved total active metal (mol m^{-3})

TAMp = particulate total active metal (mol m^{-3})

KHbmf = dissolved oxygen concentration at which total active metal release is half the anoxic release rate (g O_2 m^{-3})

BFTAM = anoxic release rate of total active metal (mol m^{-2} day^{-1}), applied to the bottom layer only

Ktam = effect of temperature on sediment release of total active metal ($°C^{-1}$)

Ttam = reference temperature for sediment release of total active metal (°C).

WS_s = settling velocity of particulate metal (m day^{-1})

WTAM = external loads of total active metal (mol day^{-1}).

In estuaries, iron and manganese exist in particular and dissolved forms depending on dissolved oxygen concentration. In the oxygenated water, most of iron and manganese exist as particulate while under anoxic conditions, large fractions are dissolved although solid-phase sulfides and carbonates exist and may predominate. The partitioning between particulate and dissolved phases is expressed using a concept that total active metal concentration must achieve a minimum level, which is a function of dissolved oxygen, before precipitation occurs:

$$TAMd = minimum\{TAMdmx \cdot \exp(-Kdotam \cdot DO)\ ,\ TAM\} \quad (4\text{-}78)$$

$$TAMp = TAM - TAMd \quad (4\text{-}79)$$

TAMdmx = solubility of total active metal under anoxic conditions (mol m^{-3})

Kdotam = constant that relates total active metal solubility to dissolved oxygen (per g O_2 m^{-3}).

4.11 Fecal Coliform Bacteria

Fecal coliform bacteria are indicative of organisms from the intestinal tract of humans and other animals and can be used as an indicator bacteria as a measure of public health (Thomann & Mueller 1987). In the present model, fecal coliform bacteria have no interaction with other state variables, and have only one sink term, die-off. The kinetic equation including external loads may be written as:

$$\frac{\partial \mathrm{FCB}}{\partial \mathrm{t}} = - KFCB \cdot TFCB^{\mathrm{T}-20} \cdot FCB + \frac{WFCB}{V} \tag{4-80}$$

FCB = bacteria concentration (MPN per 100 ml)

KFCB = first order die-off rate at 20°C (day^{-1})

TFCB = effect of temperature on decay of bacteria ($°C^{-1}$)

WFCB = external loads of fecal coliform bacteria (MPN per 100 ml m^3 day^{-1}).

4.12 Method of Solution

The kinetic equations for the 21 state variables in the EFDC water column water quality model can be expressed in a 21x21 matrix after linearizing some terms, mostly Monod type expressions:

$$\frac{\partial}{\partial \mathrm{t}} [C] - [K] \cdot [C] + [R] \tag{4-8l}$$

where [C] is in mass $volume^{-1}$, [K] is in $time^{-1}$ and [R] is in mass $volume^{-1}$ $time^{-1}$. Since the settling of particulate matter from the overlying cell acts as an input for a given cell, when Eq. 4-81 is applied to a cell of finite volume, it may be expressed as:

$$\frac{\partial}{\partial \mathrm{t}} [C]_k = [\mathrm{K}I]_k \cdot [C]_k + \lambda \cdot [K2]_k \cdot [C]_{k+1} + [R]_k \tag{4-82}$$

where the four matrices [C], [Kl], [K2] and [R] are defined in Appendix A of Park et al. (1995). The subscript k designates a cell at the k^{th} vertical layer. The layer index k increases upward with KC vertical layers, k = 1 is the bottom layer and k = KC is the surface layer. Then, $\lambda = 0$ for k = KC, otherwise $\lambda = 1$. The matrix [K2] is a diagonal matrix, and the non-zero elements account for the settling of particulate matter from the overlying cell.

Equation 4-82 is solved using a second-order accurate trapezoidal scheme over a time step of θ, which may be expressed as:

$$[C]_{\mathrm{k}}^{\mathrm{N}} = \left([I] - \frac{\theta}{2} [KI]_{\mathrm{k}}^{\mathrm{O}} \right)^{-1} \cdot \left([\mathrm{C}]_{\mathrm{k}}^{\mathrm{O}} + \frac{\theta}{2} \left\{ [KI]_{\mathrm{k}}^{\mathrm{O}} \cdot [C]_{\mathrm{k}}^{\mathrm{O}} + \lambda [K2]_{\mathrm{k}}^{\mathrm{O}} \cdot [C]_{\mathrm{k+1}}^{\mathrm{A}} \right\} + \theta [R]_{\mathrm{k}}^{\mathrm{O}} \right) \tag{4-83}$$

where $\theta = 2 \cdot m \cdot \Delta t$ is the time step for the kinetic equations; [I] is a unit matrix; $[C]^A = [C]^N + [C]^\circ$; the superscripts O and N designate the variables before and after being adjusted for the relevant kinetic processes. Since Eq. 4-83 is solved from the surface layer downward, the term with $[C]_{k+1}^A$ is known for the k^{th} layer and thus placed on the RHS. In Eq. 4-83, inversion of a matrix can be avoided if the 21 state variables are solved in a proper order. The kinetic equations are solved in the order of the variables in the matrix [C] defined in Appendix A of Park et al. (1995).

Appendix D

EFDC Sediment Process Model

(excerpt from Tetra Tech, 1999)

5 - EFDC SEDIMENT PROCESS MODEL

A sediment process model developed by DiToro & Fitzpatrick (1993; hereinafter referred to as D&F) and was coupled with CE-QUAL-ICM for Chesapeake Bay water quality modeling (Cerco & Cole 1994). The sediment process model was slightly modified and incorporated into the EFDC water quality model for the Peconic Estuary application to simulate the processes in the sediment and at the sediment-water interface. The description of the EFDC sediment process model in this section is from Park et al. (1995). The sediment process model has 27 water quality related state variables and fluxes (Table 5-1).

Table 5-1. EFDC Sediment Process Model State Variables and Flux Terms

1) particulate organic carbon G1 class in layer 2	15) nitrate nitrogen in layer 1
2) particulate organic carbon G2 class in layer 2	16) nitrate nitrogen in layer 2
3) particulate organic carbon G3 class in layer 2	17) phosphate phosphorus in layer 1
4) particulate organic nitrogen G1 class in layer 2	18) phosphate phosphorus in layer 2
5) particulate organic nitrogen G2 class in layer 2	19) available silica in layer 1
6) particulate organic nitrogen G3 class in layer 2	20) available silica in layer 2
7) particulate organic phosphorus G1 class in layer 2	21) ammonia nitrogen flux
8) particulate organic phosphorus G2 class in layer 2	22) nitrate nitrogen flux
9) particulate organic phosphorus G3 class in layer 2	23) phosphate phosphorus flux
10) particulate biogenic silica in layer 2	24) silica flux
11) sulfide/methane in layer 1	25) sediment oxygen demand
12) sulfide/methane in layer 2	26) release of chemical oxygen demand
13) ammonia nitrogen in layer 1	27) sediment temperature
14) ammonia nitrogen in layer 2	

The nitrate state variables, (15), (16) and (22), in the model represent the sum of nitrate and nitrite nitrogen. The three G classes for particulate organic matter (POM) in Layer 2, and the two layers for inorganic substances are described below.

In the sediment model, benthic sediments are represented as two layers (Fig. 5-1). The upper layer (Layer 1) is in contact with the water column and may be oxic or anoxic depending on dissolved oxygen concentration in the overlying water. The lower layer (Layer 2) is permanently anoxic. The upper layer depth, which is determined by the penetration of oxygen into the sediments, is at its maximum only a small fraction of the total depth. Because H_1 (~ 0.1 cm) « H_2,

$$H = H_1 + H_2 = H_2 \quad (5\text{-}1)$$

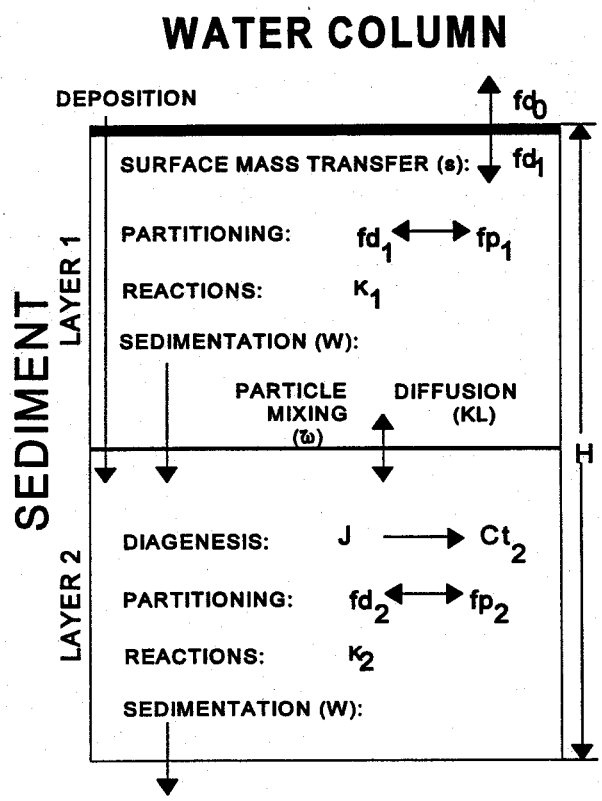

Figure 5-1. Sediment layers and processes included in sediment process model.

where H is the total depth (approximately 10 cm), H_1 is the upper layer depth and H_2 is the lower layer depth.

The model incorporates three basic processes (Fig. 5-2): (1) depositional flux of POM, (2) the diagenesis of POM, and (3) the resulting sediment flux. The sediment model is driven by net settling of particulate organic carbon, nitrogen, phosphorus and silica from the overlying water to the sediments (**depositional flux**). Because of the negligible thickness of the upper layer (Eq. 5-1), deposition is considered to be proceeded from the water column directly to the lower layer. Within the lower layer, the model simulates the diagenesis (mineralization or decay) of deposited POM, which produces oxygen demand and inorganic nutrients (**diagenesis flux**). The third basic process is the flux of substances produced by diagenesis **(sediment flux).** Oxygen demand, as sulfide (in saltwater) or methane (in freshwater), takes three paths out of the sediments: (1) oxidation at the sediment-water interface as sediment oxygen demand, (2) export to the water column as chemical oxygen demand, or (3) burial to

deep, inactive sediments. Inorganic nutrients produced by diagenesis takes two paths out of the sediments: (1) release to the water column or (2) burial to deep, inactive sediments (Fig. 5-2).

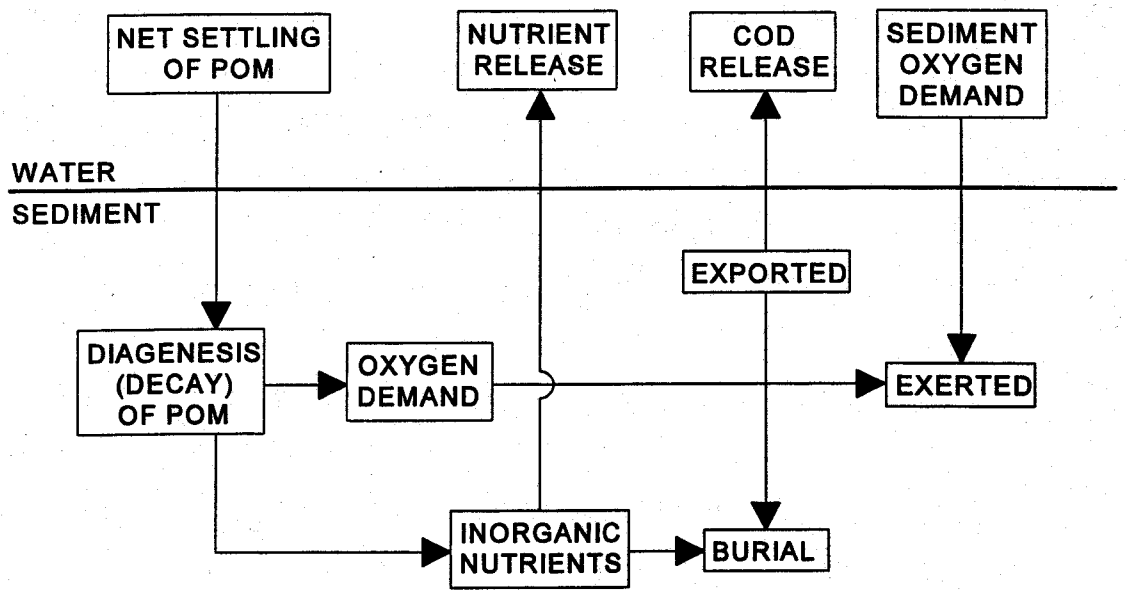

Figure 5-2. Schematic diagram for sediment process model.

This section describes the three basic processes with reactions and sources/sinks for each state variable. The method of solution including finite difference equations, solution scheme, boundary and initial conditions. Complete model documentation can be found in D&F (1993).

5.1 Depositional Flux

Deposition is one process that couples the water column model with the sediment model. Consequently, deposition is represented in both the water column and sediment models. In the water column model, the governing mass-balance equations for the following state variables contain settling terms, which represent the depositional fluxes:

- three algal groups, cyanobacteria, diatoms and green algae (Eq. 4-5)
- refractory and labile particulate organic carbon (Equations 4-20 and 4-21)
- refractory and labile particulate organic phosphorus (Equations 4-35 and 4-36) and total phosphate (Eq. 4-38)
- refractory and labile particulate organic nitrogen (Equations 4-48 and 4-49)
- particulate biogenic silica (Eq. 4-61) and available silica (Eq. 4-62)

The sediment model receives these depositional fluxes of particulate organic carbon (POC), particulate organic nitrogen (PON), particulate organic phosphorus (POP) and particulate biogenic silica (PSi). Because of the negligible thickness of the upper layer (Eq. 5-1), deposition is considered to proceed from the water column directly to the lower layer. Since the sediment model has three G classes of POM, G_1 (i = 1, 2 or 3), depending on the time scales of reactivity (Section 5.2), the POM fluxes from the water column should be mapped into three G classes based on their reactivity. Then, the depositional fluxes for the i^{th} G class (i = 1, 2 or 3) may be expressed as:

$$J_{POC,i} = FCLP_i \cdot WS_{LP} \cdot LPOC^N + FCRP_i \cdot WS_{RP} \cdot RPOC^N + \sum_{x=c,d,g} FCB_{x,i} \cdot WS_x \cdot B_x^N \quad (5\text{-}2)$$

$$J_{PON,i} = FNLP_i \cdot WS_{LP} \cdot LPON^N + FNRP_i \cdot WS_{RP} \cdot RPON^N + \sum_{x=c,d,g} FNB_{x,i} \cdot ANC_x \cdot WS_x \cdot B_x^N \quad (5\text{-}3)$$

$$J_{POP,i} = FPLP_i \cdot WS_{LP} \cdot LPOP^N + FPRP_i \cdot WS_{RP} \cdot RPOP^N + \sum_{x=c,d,g} FPB_{x,i} \cdot APC \cdot WS_x \cdot B_x^N \quad (5\text{-}4)$$

$$+ \gamma_i \cdot WS_{TSS} \cdot PO4p^N \quad (5\text{-}4)$$

$$J_{PSi} = WS_d \cdot SU^N + ASC_d \cdot WS_d \cdot B_d^N + WS_{TSS} \cdot SAp^N \quad (5\text{-}5)$$

$J_{POM,i}$ = depositional flux of POM (M = C, N or P) routed into the i^{th} G class (g m^{-2} day^{-1})

J_{PSi} = depositional flux of PSi (g Si m^{-2} day^{-1})

$FCLP_i$, $FNLP_i$ & $FPLP_i$ = fraction of water column labile POC, PON and POP, respectively, routed into the i^{th} G class in sediment

$FCRP_i$, $FNRP_i$ & $FPRP_i$ = fraction of water column refractory POC, PON and POP, respectively, routed into the i^{th} G class in sediment

$FCB_{x,i}$, $FNB_{x,i}$ & $FPB_{x,i}$ = fraction of POC, PON and POP, respectively, in the algal group x routed into the i^{th} G class in sediment

γ_i = 1 for i = 1

0 for i= 2or3.

In the source code, the sediment process model is solved after the water column water quality model, and the calculated fluxes using the water column conditions at $t = t_n$ are used for the computation of the water quality variables at $t = t_n+\theta$. The superscript N indicates the variables after being updated for the kinetic processes, as defined in Eq. 4-82.

The settling of sorbed phosphate is considered to contribute to the labile G_1 pool in Eq. 5-4, and settling of sorbed silica contributes to J_{PSi} in Eq. 5-5 to avoid creation of additional depositional fluxes

for inorganic particulates. The sum of distribution coefficients should be unity: $\Sigma_i FCLP_i = \Sigma_i FNLP_i = \Sigma_i FPLP_i = \Sigma_i FCRP_i = \Sigma_i FNRP_i = \Sigma_i FPRP_i = \Sigma_i FCB_{x,i} = \Sigma_i FNB_{x,i} = \Sigma_i FPB_{x,i} = 1$. The settling velocities, WS_{LP}, WS_{RP}, WS_x and WS_{TSS}, as defined in the EFDC water column model (Section 4), are net settling velocities. If total active metal is selected as a measure of sorption site, WS_{TSS} is replaced by WS_s in Equations 5-4 and 5-5 (see Sections 4.5 and 4.7).

5.2 Diagenesis Flux

Another coupling point of the sediment model to the water column model is the sediment flux, which is described in Section 5.3. The computation of sediment flux requires that the magnitude of the diagenesis flux be known. The diagenesis flux is explicitly computed using mass-balance equations for deposited POC, PON and POP. (Dissolved silica is produced in the sediments as the result of the dissolution of PSi. Since the dissolution process is different from the bacterial-mediated diagenesis process, it is presented separately in Section 5.4.) In the mass-balance equations, the depositional fluxes of POM are the source terms and the decay of POM in the sediments produces the diagenesis fluxes. The integration of the mass-balance equations for POM provides the diagenesis fluxes that are the inputs for the mass-balance equations for ammonium, nitrate, phosphate and sulfide/methane in the sediments (Section 5.3).

The difference in decay rates of POM is accounted for by assigning a fraction of POM to various decay classes (Westrisch & Berner 1984). POM in the sediments is divided into three G classes, or fractions, representing three scales of reactivity. The G_1 (labile) fraction has a half life of 20 days, and the G_2 (refractory) fraction has a half life of one year. The G_3 (inert) fraction is non-reactive, i.e., undergoes no significant decay before burial into deep, inactive sediments. The varying reactivity of the G classes controls the time scale over which changes in depositional flux will be reflected in changes in diagenesis flux. If the G_1 class would dominate the POM input into the sediments, then there would be no significant time lag introduced by POM diagenesis and any changes in depositional flux would be readily reflected in diagenesis flux.

Because the upper layer thickness is negligible (Eq. 5-1) and thus depositional flux is considered to proceed directly to the lower layer (Equations 5-2 to 5-5), diagenesis is considered to occur in the lower layer only. The mass-balance equations are similar for POC, PON and POP, and for different G classes. The mass-balance equation in the anoxic lower layer for the i^{th} G class (i = 1, 2 or 3) may be expressed as:

$$H_2 \frac{\partial G_{POM,i}}{\partial t} = - K_{POM,i} \cdot \theta_{POM,i}^{T-20} \cdot G_{POM,i} \cdot H_2 - W \cdot G_{POM,i} + J_{POM,i} \quad (5\text{-}6)$$

$G_{POM,i}$ – concentration of POM (M = C, N or P) in the i^{th} G class in Layer 2 (g m^{-3})

K_{POMi} = decay rate of the i^{th} G class POM at 20°C in Layer 2 (day^{-1})

$\theta_{POM,i}$ = constant for temperature adjustment for $K_{POM,i}$

T = sediment temperature (°C)

W = burial rate (m day^{-1}).

Since the G_3 class is inert, $K_{POM,3} = 0$.

Once the mass-balance equations for $G_{POM,1}$ and $G_{POM,2}$ are solved, the diagenesis fluxes are computed from the rate of mineralization of the two reactive G classes:

$$J_M = \sum_{i-1}^{2} K_{POM,i} \cdot \theta_{POM,i}^{T-20} \cdot GPOM,i \cdot H_2 \quad (5\text{-}7)$$

J_M = diagenesis flux (g m^{-2} day^{-1}) of carbon (M = C), nitrogen (M = N) or phosphorus (M = P).

5.3 Sediment Flux

The mineralization of POM produces soluble intermediates, which are quantified as diagenesis fluxes in the previous section. The intermediates react in the oxic and anoxic layers, and portions are returned to the overlying water as sediment fluxes. Computation of sediment fluxes requires mass-balance equations for ammonium, nitrate, phosphate, sulfide/methane and available silica. This section describes the flux portion for ammonium, nitrate, phosphate and sulfide/methane of the model. Available silica is described in Section 5.4.

In the upper layer, the processes included in the flux portion are (Fig. 5-1)

- exchange of dissolved fraction between Layer 1 and the overlying water
- exchange of dissolved fraction between Layer 1 and 2 via diffusive transport
- exchange of particulate fraction between Layer 1 and 2 via particle mixing
- loss by burial to the lower layer (Layer 2)
- removal (sink) by reaction
- internal sources.

Since the upper layer is quite thin, $H_1 \sim 0.1$ cm (Eq. 5-1) and the surface mass transfer coefficient (s) is on the order of 0.1 m day^{-1}, then the residence time in the upper layer is: $H_1/s \sim 10^{-2}$ days. Hence, a

steady-state approximation is made in the upper layer. Then, the mass-balance equation for ammonium, nitrate, phosphate or sulfide/methane in the upper layer is:

$$H_1 \frac{\partial Ct1}{\partial t} = 0 = s(fd_0 \cdot Ct_0 - fd_1 \cdot Ct_1) + KL(fd_2 \cdot Ct_2 - fd_1 \cdot Ct_1)$$

$$+ \varpi(fp_2 \cdot Ct_2 - fp_1 \cdot Ct_1) - W \cdot Ct_1 - \frac{K1}{S}^2 Ct_1 + J_1 \qquad (5\text{-}8)$$

Ct_1 & Ct_2 = total concentrations in Layer 1 and 2, respectively (g m^{-3})

Ct_o = total concentration in the overlying water (g m^{-3})

s = surface mass transfer coefficient (m day^{-1})

KL = diffusion velocity for dissolved fraction between Layer l and 2 (m day^{-1})

ϖ = particle mixing velocity between Layer 1 and 2 (m day^{-1})

fd_o = dissolved fraction of total substance in the overlying water ($0 \leq fd_o \leq 1$)

fd_1 = dissolved fraction of total substance in Layer 1 ($0 \leq fd_l s \leq 1$)

fp_1 = particulate fraction of total substance in Layer 1 ($= 1 - fd_1$)

fd_2 = dissolved fraction of total substance in Layer 2 ($0 \leq fd_2 \leq 1$)

fp_2 = particulate fraction of total substance in Layer 2 ($= 1 - fd_2$)

κ_1 = reaction velocity in Layer 1 (m day^{-1})

J_1 = sum of all internal sources in Layer 1 (g m^{-2} day^{-1}).

The first term on the RHS of Eq. 5-8 represents the exchange across sediment-water interface. Then, the sediment flux from Layer 1 to the overlying water, which couples the sediment model to the water column model, may be expressed as:

$$J_{aq} = s\,(fd_1 \cdot Ct_1 - fd_o \cdot Ct_o) \qquad (5\text{-}9)$$

J_{aq} = sediment flux of ammonium, nitrate, phosphate or sulfide/methane to the overlying water (g m^{-2} day^{-1}).

The convention used in Eq. 5-9 is that positive flux is from the sediment to the overlying water.

In the 1ower layer, the processes included in the flux portion are (Fig. 5-1)

- exchange of dissolved fraction between Layer 1 and 2 via diffusive transport
- exchange of particulate fraction between Layer 1 and 2 via particle mixing
- deposition from Layer 1, and burial to the deep inactive sediments
- removal (sink) by reaction
- internal sources including diagenetic source.

The mass-balance equation for ammonium, nitrate, phosphate or sulfide/methane in the lower layer is:

$$H_2 \frac{\partial Ct_2}{\partial t} = - KL(fd_2 \cdot Ct_2 - fd_1 \cdot Ct_1) - \varpi(fp_2 \cdot Ct_2 - fp_1 \cdot Ct_1)$$

$$+ W(Ct_1 = Ct_2) = \kappa_2 \cdot Ct_2 + J_2 \qquad (5\text{-}10)$$

κ_2 = reaction velocity in Layer 2 (m day^{-1})

J_2 = sum of all internal sources including diagenesis in Layer 2 (g m^{-2} day^{-1}).

The substances produced by mineralization of POM in sediments may be present in both dissolved and particulate phases. This distribution directly affects the magnitude of the substance that is returned to the overlying water. In Equations 5-8 to 5-10, the distribution of a substance between the dissolved and particulate phases in a sediment is parameterized using a linear partitioning coefficient. The dissolved an particulate fractions are computed from the partitioning equations:

$$fd_1 = \frac{1}{1 + m_1 \cdot \pi_1} \qquad fp_1 = 1 - fd_1 \qquad (5\text{-}11)$$

$$fd_2 = \frac{1}{1 + m_2 \cdot \pi_2} \qquad fp_2 = 1 - fd_2 \qquad (5\text{-}12)$$

m_1 & m_2 = solid concentrations in Layer l and 2, respectively (kg L^{-1})

π_1 & π_2 = partition coefficients in Layer 1 and 2, respectively (per kg L^{-1}).

The partition coefficient is the ratio of particulate to dissolved fraction per unit solid concentration (i.e., per unit sorption site available).

All terms, except the last two terms, in Equations 5-8 and 5-10 are common to all state variables and are described in Section 5.3.1. The last two terms represent the reaction and source/sink terms, respectively. These terms, which take different mathematical formulations for different state variables, are described in Sections 5.3.2 to 5.3.5 for ammonium, nitrate, phosphate and sulfide/methane, respectively.

5.3.1 Common Parameters for Sediment Flux

Parameters that are needed for the sediment fluxes are s, ϖ, KL, W, H_2, m_1, m_2, π_1, π_2, κ_1, κ_2, J_1 and J_2 in Equations 5-8 to 5-12. Of these, κ_1, κ_2, J_1 and J_2 are variable-specific. Among the other common parameters, W, H_2, m_1 and m_2, are specified as input. The modeling of the remaining three parameters, s, ϖ, KL,, are described in this section.

5.3.1.1 Surface mass transfer coefficient. Owing to the observation that the surface mass transfer coefficient, *s*, can be related to the sediment oxygen demand, SOD (DiToro et al. 1990), *s* can be estimated from the ratio of SOD and overlying water oxygen concentration:

$$s = \frac{D_1}{H_1} = \frac{SOD}{DO_0} \tag{5-13}$$

D_1 = diffusion coefficient in Layer 1 (m^2 day^{-1}).

Knowing *s*, it is possible to estimate the other model parameters.

5.3.1.2 Particulate phase mixing coefficient: The particle mixing velocity between Layer 1 and 2 is parameterized as:

$$\varpi = \frac{D_p \cdot \theta_{Dp}^{T-20}}{H_2} \frac{G_{POC,1}}{G_{POC,R}} \frac{DO_0}{KM_{Dp} + DO_0} \tag{5-14}$$

D_p = apparent diffusion coefficient for particle mixing (m^2 day^{-1})

θ_{Dp} = constant r temperature adjustment for D_p

$G_{POC,R}$ = reference concentration for $G_{POC,1}$ (g C m^{-3})

KM_{Dp} = particle mixing half-saturation constant for oxygen (g O_2 m^{-3}).

The enhanced mixing of sediment particles by macrobenthos (bioturbation) is quantified by estimating D_p. The particle mixing appears to be proportional to the benthic biomass (Matisoff 1982), which is correlated to the carbon input to the sediment (Robbins et al. 1989). This is parameterized by assuming that benthic biomass is proportional to the available labile carbon, $G_{POC,1}$ and $G_{POC,R}$ is the reference concentration at which the particle mixing velocity is at its nominal value. The Monod-type oxygen dependency accounts for the oxygen dependency of benthic biomass.

It has been observed that a hysteresis exists in the relationship between the bottom water oxygen and benthic biomass. Benthic biomass increases as the summer progresses. However, the occurrence of anoxia/hypoxia reduces the biomass drastically and also imposes stress on benthic activities. After full overturn, the bottom water oxygen increases but the population does not recover immediately. Hence, the particle mixing velocity, which is proportional to the benthic biomass, does not increase in response to the increased bottom water oxygen. Recovery of benthic biomass following hypoxic events depends on many factors including severity and longevity of hypoxia, constituent species and salinity (Diaz & Rosenberg 1995).

This phenomenon of reduced benthic activities and hysteresis is parameterized based on the idea of stress that low oxygen imposes on the benthic population. It is analogous to the modeling of the toxic effect of chemicals on organisms (Mancini 1983). A first order differential equation is employed, in which the benthic stress 1) accumulates only when overlying oxygen is below KM_{Dp} and 2) is dissipated at a first order rate (Fig. 5-3a):

$$\frac{\partial ST}{\partial t} = - K_{ST} \cdot ST + \left(1 - \frac{DO_0}{KM_{Dp}}\right) \qquad if\ DO_0 < KM_{DP}$$

$$\frac{\partial ST}{\partial t} = - K_{ST} \cdot ST + \qquad if\ DO_0 < KM_{DP} \tag{5-15}$$

ST = accumulate benthic stress (day)

K_{ST} = first order decay rate for ST (day^{-1}).

The behavior of this formulation can be understood by evaluating the steady-state stresses at two extreme conditions of overlying water oxygen, DO_o:

as $DO_0 = 0$	$K_{ST} \cdot ST = 1$	$f(ST) = (1 - K_{ST} \cdot ST) = 0$
as $DO_0 \geq KM_{Dp}$	$K_{ST}\ ST = 0$	$f(ST) = (1 - K_{ST}\ ST) = 1$

The dimensionless expression, $f(ST) = 1 - K_{ST} \cdot ST$, appears to be the proper variable to quantify the effect of benthic stress on benthic biomass and thus particle mixing (Fig. 5-3b).

The final formulation for the particle mixing velocity including the benthic stress is:

$$\varpi = \frac{D_p \cdot \theta_{Dp}^{T-20}}{H_2} \frac{G_{POC,1}}{G_{POC,R}} \frac{DO_0}{KM_{Dp} + DO_0} f(ST) + \frac{Dp_{\min}}{H_2} \tag{5-16}$$

Dp_{min} = minimum diffusion coefficient for particle mixing ($m^2\ day^{-1}$).

The reduction in particle mixing due to the benthic stress, f(ST), is estimated by employing the following procedure. The stress, ST, is normally calculated with Eq. 5-15. Once DO_0 drops below a critical concentration, $DO_{ST,c}$, for $NC_{hypoxia}$ consecutive days or more, the calculated stress is not allowed to decrease until t_{MBS} days of $DO_0 > DO_{ST,c}$. That is, only when hypoxic days are longer than critical hypoxia days ($NC_{hyposia}$), the maximum stress, or minimum ($1 - K_{ST} \cdot ST$), is retained for a specified period (t_{MBS} days) after DO_0 recovery (Fig. 5-3). No hysteresis occurs if DO_0 does not drop below $DO_{ST,c}$ or if hypoxia lasts shorter than $NC_{hypoxia}$ days. When applying maximum stress for t_{MBS} days, the subsequent hypoxic days are not included in t_{MBS}. This parameterization of hysteresis essentially assumes seasonal

hypoxia, i.e., one or two major hypoxic events during summer, and might be unsuitable for systems with multiple hypoxic events throughout a year.

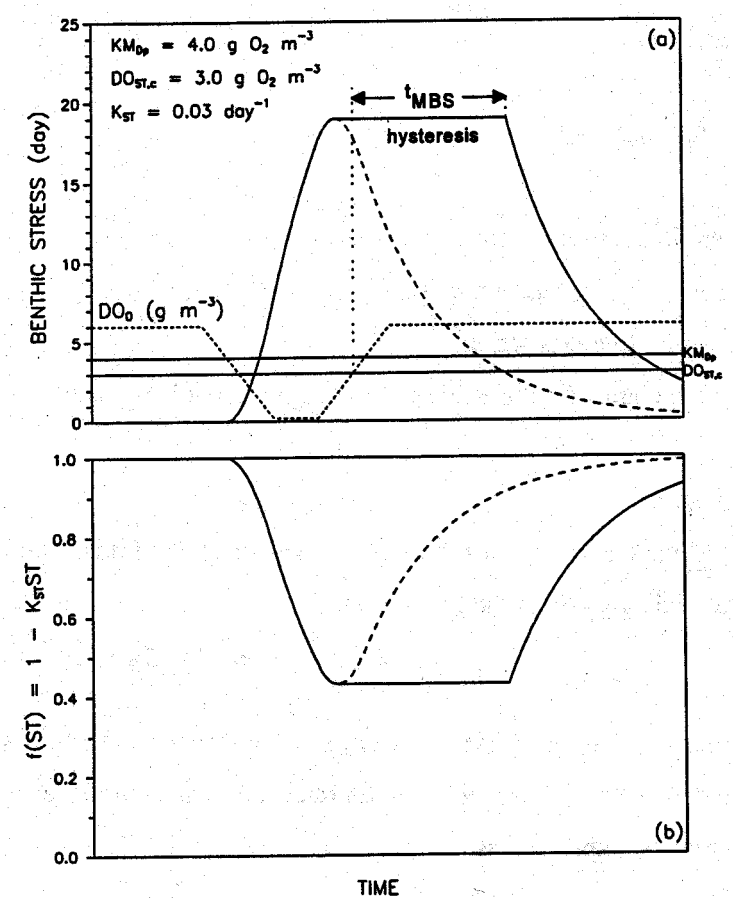

Figure 5-3. Benthic stress (a) and its effect on particle mixing (b) as a function of overlying water column dissolved oxygen concentration.

Three parameters relating to hysteresis, $DO_{ST,c}$, $NC_{hypoxia}$ and t_{MBS}, are functions of many factors including severity and longevity of hypoxia, constituent species and salinity, and thus have site-specific variabilities (Diaz & Rosenberg 1995). The critical overlying oxygen concentration, $DO_{ST,c}$, also depends on the distance from the bottom of the location of DO_0. The critical hypoxia days, $NC_{hypoxia}$, depends on tolerance of benthic organisms to hypoxia and thus on benthic community structure (Diaz & Rosenberg 1995). The time lag for the recovery of benthic biomass following hypoxic events, t_{MBS}, tends to be longer for higher salinity. The above three parameters are considered to be spatially constant input parameters.

5.3.1.3 Dissolved phase mixing coefficient. Dissolved phase mixing between Layer 1 and 2 is via passive molecular diffusion, which is enhanced by the mixing activities of the benthic organisms

(bio-irrigation). This is modeled by increasing the diffusion coefficient relative to the molecular diffusion coefficient:

$$KL = \frac{D_d \cdot \theta_{Dd}^{T-20}}{H_2} + R_{BI,BT} \cdot \varpi$$

D_d = diffusion coefficient in pore water (m^2 day^{-1})

θ_{Dd} = constant for temperature adjustment for D_d

$R_{BI,BT}$ = ratio of bio-irrigation to bioturbation.

The last term in Eq. 5-17 accounts for the enhanced mixing by organism activities.

5.3.2 Ammonia Nitrogen

Diagenesis is assumed not to occur in the upper layer because of its shallow depth, and ammonium is produced by diagenesis in the lower layer:

$$J_{1,NH4} = 0 \qquad J_{2,NH4} = J_N \quad (\textit{from Eq. 5-7}) \tag{5-18}$$

Ammonium is nitrified to nitrate in the presence of oxygen. A Monod-type expression is used for the ammonium and oxygen dependency of the nitrification rate. Then, the oxic layer reaction velocity in Eq. 5-8 for ammonium may be expressed as:

$$K_{1,NH4}^2 = \frac{DO_0}{2 \cdot KM_{NH4,02} + DO_0} \frac{KM_{NH4}}{KM_{NH4} + NH4_1} K_{NH4}^2 \cdot \theta_{NH4}^{T-20} \tag{5-19}$$

and then the nitrification flux becomes:

$$J_{Nit} = \frac{K_{1,NH4}^2}{s} \cdot NH4_1 \tag{5-20}$$

$KM_{NH4,O2}$ = nitrification half-saturation constant for dissolved oxygen (g O_2 m^{-3})

$NH4_1$ = total ammonium nitrogen concentration in Layer 1 (g N m^{-3})

KM_{NH4} = nitrification half-saturation constant for ammonium (g N m^{-3})

K_{NH4} = optimal reaction velocity for nitrification at 20°C (m day^{-1})

θ_{NH4} = constant for temperature adjustment for κ_{NH4}

J_{Nit} = nitrification flux (g N m^{-2} day^{-1}).

Nitrification doe not occur in the anoxic lower layer:

$$\kappa_{2,NH4} = 0 \tag{5-21}$$

Once Equations 5-8 and 5-10 are solved for $NH4_1$ and $NH4_2$, the sediment flux of ammonium to the overlying water, $J_{aq,NH4}$, can be calculated using Eq. 5-9. Note that it is not $NH4_1$ and $NH4_2$ that determine the magnitude of $J_{aq,NH4}$ (Section X-B-2 in D&F 1993). The magnitude is determined by (1) the diagenesis flux, (2) the fraction that is nitrified, and (3) surface mass transfer coefficient (*s*) that mixes the remaining portion.

5.3.3 Nitrate Nitrogen

Nitrification flux is the only source of nitrate in the upper layer, and there is no diagenetic source for nitrate in both layers:

$$J_{1,N03} = J_{Nit} \ \ (from\ Eq.\ 5\text{-}19) \qquad\qquad J_{2,N03} = 0 \qquad (5\text{-}22)$$

Nitrate is present in sediments as dissolved substance, i.e., $\pi_{1,NO3} - \pi_{2,NO3} = 0$, making $fd_{1,NO3} = fd_{2,NO3} = 1$ (Equations 5-11 and 5-12): it also makes ϖ meaningless, hence $\varpi = 0$. Nitrate is removed by denitrification in both oxic and anoxic layers with the carbon required for denitrification supplied by carbon diagenesis. The reaction velocities in Equations 5-8 and 5-10 for nitrate may be expressed as:

$$K^2_{1,NO3} = K^2_{NO3,1} \cdot \theta^{T-20}_{NO3} \qquad (5\text{-}23)$$

$$K_{1,NO3} = K_{NO3,2} \cdot \theta^{T-20}_{NO3} \qquad (5\text{-}24)$$

and the denitrification flux out of sediments as a nitrogen gas becomes:

$$JN2(g) = \frac{K^2_{1,NO3}}{s} NO3_1 + K_{2,NO3} \cdot NO3_2 \qquad (5\ 25)$$

$\kappa_{NO3,1}$ = reaction velocity for denitrification in Layer 1 at 20°C (m day^{-1})
$\kappa_{NO3,2}$ = reaction velocity for denitrification in Layer 2 at 20°C (m day^{-1})
θ_{NO3} = constant or temperature adjustment for $\kappa_{NO3,1}$ and $\kappa_{NO3,2}$
$J_{N2(g)}$ - denitrification flux (g N M^{-2} day^{-1})
$NO3_1$ = total nitrate nitrogen concentration in Layer 1 (g N m^{-3})
$NO3_2$ = total nitrate nitrogen concentration in Layer 2 (g N m^{-3}).

Once Equations 5-8 and 5-10 are solved for $NO3_1$ and $NO3_2$, the sediment flux of nitrate to the overlying water $J_{aq,NO3}$, can be calculated using Eq. 5-9. The steady-state solution for nitrate showed that the nitrate flux is a linear function of $NO3_o$ (Eq. III-15 in D&F 1993): the intercept quantifies the amount of ammonium in the sediment that is nitrified but not denitrified (thus releases as $J_{aq,NO3}$), and the slope quantifies the extent to which overlying water nitrate is denitrified in the sediment. It also revealed that

if the internal production of nitrate is small relative to the flux of nitrate from the overlying water, the normalized nitrate flux to the sediment, $- J_{aq,NO3}/NO3_o$, is linear in *s* for small *s* and constant for large *s* (Section III-C in D&F 1993). For small *s* (~ 0.01 m day^{-1}), H_1 is large (Eq. 5-13) so that oxic layer denitrification predominates and $J_{aq,NO3}$ is essentially zero independent of $NO3_o$ (Fig. III-4 in D&F 1993).

5.3.4 Phosphate Phosphorus

Phosphate is produced by the diagenetic breakdown of POP in the lower layer:

$$J_{1,P04} = 0 \qquad J_{2,PO4} - J_p \quad (from\ Eq.\ 5\text{-}7) \tag{5-26}$$

A portion of the liberated phosphate remains in the dissolved form and a portion becomes particulate phosphate, either via precipitation of phosphate-containing minerals (Troup 1974), e.g., vivianite, $Fe_3(PO_4)_2(s)$, or by partitioning to phosphate sorption sites (Lijklema 1980; Barrow 1983; Giordani & Astorri 1986). The extent of particulate formation is determined by the magnitude of the partition coefficients, $\pi_{1,PO4}$ and $\pi_{2,PO4}$, in Equations 5-11 and 5-12. Phosphate flux is strongly affected by DO_o, the overlying water oxygen concentration. As DO_o approaches zero, the phosphate flux from the sediments increases. This mechanism is incorporated by making $\pi_{1,PO4}$ larger, under oxic conditions, than $\pi_{2,PO4}$. In the model, when DO_o exceeds a critical concentration, $(DO_o)_{crit,PO4}$, sorption in the upper layer is enhanced by amount $\Delta\pi_{PO4,1}$:

$$\pi_{1,PO4} = \pi_{2,PO4} \cdot (\Delta\pi_{PO4,1}) \qquad DO_0 > (DO_0)_{crit,PO4} \tag{5-27}$$

When oxygen falls below $(DO_0)_{crit,PO4}$, then:

$$\pi_{1,PO4} = \pi_{2,PO4} \cdot (\Delta\pi_{PO4,1})^{DO_0 - 1(DO_0)_{crit,PO4}} \qquad DO_0 > (DO_0)_{crit,PO4} \tag{5-28}$$

which smoothly reduces $\pi_{1,PO4}$ to $\pi_{2,PO4}$ as DO_0 goes to zero. There is no removal reaction for phosphate in both layers:

$$\kappa_{1,PO4} = \kappa_{2,PO4} = 0 \tag{5-29}$$

Once Equations 5-8 and 5-10 are solved for $PO4_1$ and $PO4_2$, the sediment flux of phosphate to the overlying water, $J_{aq,PO4}$, can be calculated using Eq. 5-9.

5.3.5 Sulfide/methane and Oxygen Demand

5.3.5.1 Sulfide. No diagenetic production of sulfide occurs in the upper layer. In the lower layer, sulfide is produced by carbon diagenesis (Eq. 5-7) decremented by the organic carbon consumed by denitrification (Eq. 5-25). Then:

$$J_{1,H2S} = 0 \qquad J_{2,H2S} = a_{02,C} \cdot J_C - a_{02,N03} \cdot J_{N2(g)} \qquad (5\text{-}30)$$

$a_{O2,C}$ = stoichiometric coefficient for carbon diagenesis consumed by sulfide oxidation (2.6667 g O_2-equivalents per g C)

$a_{O2,NO3}$ = stoichiometric coefficient for carbon diagenesis consumed by denitrification (2.8571 g O_2-equivalents per g N).

A portion of the dissolved sulfide that is produced in the anoxic layer reacts with the iron to form particulate iron monosulfide, FeS(s) (Morse et al. 1987). The particulate fraction is mixed into the oxic layer where it can be oxidized to ferric oxyhydroxide, Fe_2O_3(s). The remaining dissolved fraction also diffuses into the oxic layer where it is oxidized to sulfate. Partitioning between dissolved and particulate sulfide in the model represents the formation of FeS(s), which is parameterized using partition coefficients, $\pi_{1,H2S}$ and $\pi_{2,H2S}$, in Equations 5-11 and 5-12.

The present sediment model has three pathways for sulfide, the reduced end product of carbon diagenesis: (1) sulfide oxidation, (2) aqueous sulfide flux, and (3) burial. The distribution of sulfide among the three pathways is controlled by the partitioning coefficients and the oxidation reaction velocities (Section V-E in D&F 1993). Both dissolved and particulate sulfide are oxidized in the oxic layer, consuming oxygen in the process. In the oxic upper layer, the oxidation rate that is linear in oxygen concentration is used (Cline & Richards 1969; Millero 1986; Boudreau 1991). In the anoxic lower layer, no oxidation can occur. Then, the reaction velocities in Equations 5-8 and 5-10 may be expressed as:

$$K^2_{1,H2S} = \left(K^2_{H2S,d1} \cdot fd_{1,H2S} + K^2_{H2S,p1} \cdot fp_{1,H2S}\right)\theta^{T-20}_{H2S} \frac{DO_0}{2 \cdot KM_{H2S,02}} \qquad (5\text{-}31)$$

$$\kappa_{2,H2S} = 0 \qquad (5\text{-}32)$$

$\kappa_{H2S,d1}$ = reaction velocity for dissolved sulfide oxidation in Layer 1 at 20°C (m day^{-1})

$K_{H2S,Pl}$ = reaction velocity for particulate sulfide oxidation in Layer 1 at 20°C (m day^{-1})

θ_{H2S} = constant for temperature adjustment for $\kappa_{H2S,d1}$ and $K_{H2S,Pl}$

$KM_{H2S,O2}$ = constant to normalize the sulfide oxidation rate for oxygen (g O_2 m^{-3}).

The constant, $KM_{H2S,O2}$, which is included for convenience only, is used to scale the oxygen concentration in the overlying water. At $DO_0 = KM_{H2S,O2}$, the reaction velocity for sulfide oxidation rate is at its nomina1 value.

The oxidation reactions in the oxic upper layer cause oxygen flux to the sediment, which exerts SOD. By convention, SOD is positive: SOD = $-J_{aq,O2}$. The SOD in the model consists of two components, carbonaceous sediment oxygen demand (CSOD) due to sulfide oxidation and nitrogenous sediment oxygen demand (NSOD) due to nitrification:

$$SOD = CSOD + NSOD = \frac{K_{1,H2S}^2}{s} H2S_1 + a_{02,NH4} J_{Nit} \quad (5\text{-}33)$$

$H2S_1$ = total sulfide concentration in Layer 1 (g O_2 equivalents m^{-3})
$a_{O2,NH4}$= stoichiometric coefficient for oxygen consumed by nitrification (4.33 g O_2 per g N).

Equation 4-29 is nonlinear for SOD because the RHS contains *s* (= SOD/DO_0) so that SOD appears on both sides of the equation: note that J_{Nit} (Eq. 5-20) is also a function of *s*. A simple back substitution method is used, as explained in Section 5.6.1.

If the overlying water oxygen is low, then the sulfide that is not completely oxidized in the upper layer can diffuse into the overlying water. This aqueous sulfide flux out of the sediments, which contributes to the chemical oxygen demand in the water column model, is modeled using

$$J_{aq,H2S} = s(fd_{1,H2S} H2S_1 - COD) \quad (5\text{-}34)$$

The sulfide released from the sediment reacts very quickly in the water column when oxygen is available, but can accumulate in the water column under anoxic conditions. The COD, quantified as oxygen equivalents, is entirely supplied by benthic release in the water column model (Eq. 3-16). Since sulfide also is quantified as oxygen equivalents, COD is used as a measure of sulfide in the water column in Eq. 5-34.

5.3.5.2 Methane: When sulfate is used up, methane can be produced by carbon diagenesis and methane oxidation consumes oxygen (DiToro et al. 1990). Owing to the abundant sulfate in the saltwater, only the aforementioned sulfide production and oxidation are considered to occur in the saltwater. Since the sulfate concentration in the freshwater is generally insignificant, methane production is considered to place sulfide production in the freshwater. In the freshwater, methane is produced by carbon diagenesis in the lower layer decremented by the organic carbon consumed by denitrification, and no diagenetic production of methane occurs in the upper layer (Eq. 5-30):

$$J_{1,CH4} = 0 \qquad J_{2,CH4} = a_{02,C} J_C - a_{02,N03} J_{N2(g)} \quad (5\text{-}35)$$

The dissolved methane produced takes two pathways: (1) oxidation in the oxic upper layer causing CSOD or (2) escape from the sediment as aqueous flux or as gas flux:

$$J_{2,CH4} = CSOD + J_{aq,CH4} + J_{CH4(g)} \quad (5\text{-}36)$$

$J_{aq,CH4}$ = aqueous methane flux (g O_2-equivalents m^{-2} day^{-1})

$J_{CH4(g)}$ = gaseous methane flux (g O_2-equivalents m^{-2} day^{-1}).

A portion of dissolved methane that is produced in the anoxic layer diffuses into the oxic layer where it is oxidized. This methane oxidation causes CSOD in the freshwater sediment (DiToro et al. 1990):

$$CSOD = CSOD_{max} \cdot \left(1 = sech[\frac{K_{CH4} \cdot \theta_{CH4}^{T-20}}{s} \right) \quad (5\text{-}37)$$

$$CSOD_{\max} = minimum \left\{ \sqrt{2 \cdot KL \cdot CH4_{sat} \cdot J_{2,CH4}}, J_{2,CH4} \right\} \quad (5\text{-}38)$$

$$\text{CH4sat} = 100 \left(1 + \frac{h + H_2}{10} \right) 1.024^{20 - T} \quad (5\text{-}39)$$

$CSOD_{max}$ = maximum CSOD occurring when all the dissolved methane transported to the oxic layer is oxidized

K_{CH4} = reaction velocity for dissolved methane oxidation in Layer 1 at 20°C (m day^{-1})

θ_{CH4} = constant or temperature adjustment for κ_{CH4}

$CH4_{sat}$ = saturation concentration of methane in the pore water (g O_2-equivalents m^{-3}).

The term, $(h + H_2)/10$ where h and H_2 are in meters, in Eq. 5-39 is the depth from the water surface that corrects for the in situ pressure. Equation 5-39 is accurate to within 3% of the reported methane solubility between 5 and 20°C (Yamamoto et al. 1976).

If the overlying water oxygen is low, the methane that is not completely oxidized can escape the sediment into the overlying water either as aqueous flux or as gas flux. The aqueous methane flux, which contributes to the chemical oxygen demand in the water column model, is modeled using (DiToro et al. 1990):

$$J_{aq,CH4} = CSOD_{max} \cdot sech[\frac{K_{CH4} \cdot \theta_{CH4}^{T-20}}{s}] \; CSOD_{max} - CSOD \quad (5\text{-}40)$$

Methane is only lightly soluble in water. If its solubility, $CH4_{sat}$ given by Eq. 5-39, is exceeded in the pore water, it forms a gas phase that escapes as bubbles. The loss of methane as bubbles, i.e., the gaseous methane flux, is modeled using Eq. 5-36 with $J_{2,CH4}$ from Eq. 5-35, CSOD from Eq. 5-37 and $J_{aq,CH4}$ from Eq. 5-40 (DiToro et al. 1990).

5.4 Silica

The production of ammonium, nitrate and phosphate in sediments is the result of the mineralization of POM by bacteria. The production of dissolved silica in sediments is the result of the dissolution of particulate biogenic or opaline silica, which is thought to be independent of bacterial processes.

The depositional flux of particulate biogenic silica from the overlying water to the sediments is modeled using Eq. 5-5. With this source, the mass-balance equation for particulate biogenic silica may be written as:

$$H_2 \frac{\partial PSi}{\partial t} = - S_{Si} \cdot H_2 - W \cdot PSi + J_{PSi} + J_{DSi} \qquad (5\text{-}41)$$

PSi = concentration of particulate biogenic silica in the sediment (g Si m^{-3})

S_{Si} = dissolution rate of PSi in Layer 2 (g Si m^{-3} day^{-1})

J_{PSi} = depositional flux of PSi (g Si m^{-2} day^{-1}) given by Eq. 5-5

J_{DSi} = detrital flux of PSi (g Si m^{-2} day^{-1}) to account for PSi settling to the sediment that is not associated with the algal flux of biogenic silica.

The processes included in Eq. 5-41 are dissolution (i.e., production of dissolved silica), burial, and depositional and detrital fluxes from the overlying water. Equation 5-41 can be viewed as the analog of the diagenesis equations for POM (Eq. 5-6). The dissolution rate is formulated using a reversible reaction that is first order in silica solubility deficit and follows a Monod-type relationship in particulate silica:

$$S_{Si} = K_{Si} \cdot \theta_{Si}^{T-20} \frac{PSi}{PSi + KM_{PSi}} (Si_{sat} - Fd_{2,Si} \cdot Si_2) \qquad (5\text{-}42)$$

K_{Si} = first order dissolution rate for PSi at 20°C in Layer 2 (day^{-1})

θ_{Si}= constant for temperature adjustment for K_{Si}

KM_{PSi} = silica dissolution half-saturation constant for PSi (g Si m^{-3})

Si_{sat} = saturation concentration of silica in the pore water (g Si m^{-3}).

The mass-balance equations for mineralized silica can be formulated using the general forms, Equations 5-8 and 5-10. There is no source/sink term and no reaction in the upper layer:

$$J_{1,Si} = \kappa_{1,Si} = 0 \tag{5-43}$$

In the lower layer, silica is produced by the dissolution of particulate biogenic silica, which is modeled using Eq. 5-42. The two terms in Eq. 5-42 correspond to the source term and reaction term in Eq. 5-10:

$$J_{2,Si} = K_{si} \cdot \theta_{\mathrm{Si}}^{\mathrm{T}-20} \frac{PSi}{PSi + KM_{PSi}} Si_{sat} \cdot H_2 \tag{5-44}$$

$$\kappa_{2,Si} = K_{si} \cdot \theta_{\mathrm{Si}}^{\mathrm{T}-20} \frac{PSi}{PSi + KM_{PSi}} f_{d2,Si} \cdot H_2 \tag{5-45}$$

A portion of silica dissolved from particulate silica sorbs to solids and a portion remains in the dissolved form. Partitioning using the partition coefficients, $\pi_{1,Si}$ and $\pi_{2,Si}$, in Equations 5-11 and 5-12 controls the extent to which dissolved silica sorbs to solids. Since silica shows similar behavior as phosphate in adsorption-desorption process, the same partitioning method as applied to phosphate (Section 5.3.4) is used for silica. That is, when DO_0 exceeds a critical concentration, $(DO_0)_{crit,Si}$, sorption in the upper layer is enhanced by an amount $\Delta\pi_{1,Si}$:

$$\pi_{1,Si} = \pi_{2,Si} \cdot (\Delta\pi_{Si,1}) \qquad DO_0 > (DO_0)_{crit,Si} \tag{5-46}$$

When oxygen falls below $(DO_0)_{crit,Si}$, then:

$$\pi_{1,Si} = \pi_{2,Si} \cdot (\Delta\pi_{Si,1})^{DO_0/(DO_0)_{crit,Si}} \qquad DO_0 \leq (DO_0)_{crit,Si} \tag{5-47}$$

which smoothly reduces $\pi_{1,Si}$ to $\pi_{2,Si}$ as DO_0 goes to zero.

Once Equations 5-8 and 5-10 are solved for Si_1 and Si_2, the sediment flux of silica to the overlying water, $J_{aq.Si}$, can be calculated using Eq. 5-9.

5.5 Sediment Temperature

All rate coefficients in the aforementioned mass-balance equations are expressed as a function of sediment temperature, T. The sediment temperature is modeled based on the diffusion of heat between the water column and sediment:

$$\frac{\partial T}{\partial t} = \frac{D_T}{H^2}(T_W - T) \tag{5-48}$$

D_T = heat diffusion coefficient between the water column and sediment (m^2 sec^{-1})

T_W = temperature in the overlying water column (°C) calculated by Eq. 4-82.

The model application in D&F and Cerco & Cole (1994) used $D_T = 1.8 \times 10^{-7}$ m^2 sec^{-1}.

5.6 Method f Solution

5.6.1 Finite-Difference Equations and Solution Scheme

An implicit integration scheme is used to solve the governing mass-balance equations. The finite difference form of Eq. 5-8 may be expressed as:

$$0 = s(fd_0 \cdot Ct_0' - fd_1 \cdot Ct_1') + KL(fd_2 \cdot Ct_2' - fd_1 \cdot Ct_1') + \varpi(fp_2 \cdot Ct_2' - fp_1 \cdot Ct_1')$$
$$- W \cdot Ct_1' - \frac{K_1^2}{s} Ct_1' + J_1' \qquad (5\text{-}49)$$

where the prime variables designate the values evaluated at t+θ and the unprimed variables are those at *t*, where θ is defined in Eq. 4-82. The finite difference form of Eq. 5-10 may be expressed as:

$$0 = -KL(fd_2 \cdot Ct_2' - fd_1 \cdot Ct_1') - \varpi(fp_2 \cdot Ct_2' - fp_1 \cdot Ct_1') + W(Ct_1' - Ct_2'$$
$$- (K_2 + \frac{H_2}{\theta})Ct_2' + \left(J_2' + \frac{H_2}{\theta} Ct_2\right) \qquad (5\text{-}50)$$

The two terms, $-(H_2/\theta)Ct_2'$ and $(H_2/\theta)Ct_2$, are from the derivative term, $H_2(\partial Ct_2/\partial t)$ in Eq. 5-10, each of which simply adds to the Layer 2 removal rate and the forcing function, respectively. Setting these two terms equal to zero results in the steady-state model. The two unknowns, Ct_1' and Ct_2', can be calculated at every time step using:

$$\begin{pmatrix} s \cdot fd_1 + a_1 + \frac{K_1^2}{s} & -a_2 \\ -a_1 & a_2 + W + K_2 + \frac{H_2}{\theta} \end{pmatrix} \begin{pmatrix} Ct_1' \\ Ct_2' \end{pmatrix} = \begin{pmatrix} J_1' + s \cdot fd_0 \cdot Ct_0' \\ J_2' + \frac{H_2}{\theta} Ct_2 \end{pmatrix} \qquad (5\text{-}51)$$

$$a_1 = KL \cdot fd_1 + \varpi \cdot fp_1 + W \qquad a_2 = KL \cdot fd_2 + \varpi \cdot fp_2 \qquad (5\text{-}52)$$

The solution of Eq. 5-51 requires an iterative method since the surface mass transfer coefficient, s, is a function of the SOD (Eq. 5-13), which also is a function of s (Eq. 5-33). A simple back substitution method is used:

(1) Start wit an initial estimate of SOD: for example, SOD = $a_{o2,C} \cdot J_C$ or the previous time step SOD.

(2) Solve Eq. 5-51 for ammonium, nitrate and sulfide/methane.

(3) Compute the SOD using Eq. 5-33.

(4) Refine the estimate of SOD: a root finding method (Brent's method in Press et al. 1986) is used to make the new estimate.

(5) Go to (2) if no convergence.

(6) Solve Eq. 5-51 for phosphate and silica.

For the sake of symmetry, the equations for diagenesis, particulate biogenic silica and sediment temperature are also solved in implicit form. The finite difference form of the diagenesis equation (Eq. 5-6) may b expressed as:

$$G'_{POM,i} = \left(G_{POM,i} + \frac{\theta}{H2} \; J_{POM,I} \right) \left(1 + \theta \cdot K_{POM,i} \cdot \theta_{POM,i}^{T-20} + \frac{\theta}{H_2} W \right)^{-1} \tag{5-53}$$

The finite difference form of the PSi equation (Eq. 5-41) may be expressed as:

$$PSi' = \left(PSi + \frac{\theta}{H2} (J_{PSi} + J_{DSi}) \right) \left(1 + \theta \cdot K_{S,i} \cdot \theta_{Si}^{T-20} \; \frac{Si_{sat} - F_{d2,Si} \cdot Si_2}{PSi + KM_{PSi}} + \frac{\theta}{H_2} W \right)^{-1} \tag{5-54}$$

using Eq. 5-36 for the dissolution term, in which PSi in the Monod-type term has been kept at time level *t* to simplify the solution. The finite difference form of the sediment temperature equation (Eq. 5-48) may be expressed as.

$$T' = \left(T + \frac{\theta}{H_2} D_T \cdot T_W \right) \left(1 + \frac{\theta}{H_2} D_T \right)^{-1} \tag{5-55}$$

5.6.2 Boundary and Initial Conditions

The above finite difference equations constitute an initial boundary-value problem. The boundary conditions are the depositional fluxes ($J_{POM,i}$ and J_{Psi}) and the overlying water conditions (Ct_o and T_W) as a function of time, which are provided from the water column water quality model. The initial conditions are the concentrations at $t = 0$, $G_{POM,i}(0)$, PSi(0), $Ct_1(0)$, $Ct_2(0)$ and T(0), to start the computations. Strictly speaking, these initial conditions should reflect the past history of the overlying water conditions and depositional fluxes, which often is impractical because of lack of field data for these earlier years.

Appendix E

Water Quality Model Rates and Constants

(water column and sediment parameters)

Appendix E. List of rates and constants used for water column parameters for the southern Puget Sound application of the EFDC model.

Input File	Description	Notation	Units	Chesapeake/Pec onic parameters: model run spsm5/ budd1run 2a. (based on model run spsm3 budd2run10)	LOTT Paramaters: approximate comparable parameters from LOTT's revised Budd Inlet model, Boatman, 1999	Value used in Peconic model (Tetra Tech, 1998)	Range of reported values [EPA 1985 or 1995 except where noted]	
Water Quality Model Rates and Constants								
wq3dwc.inp								
	Card 8: constant parameters for algae							
	nitrogen half saturation for algae group 1/c	KHNc	g/m^3	0.01		0.01	NA	
	nitrogen half saturation for algae group 2/d	KHNd	g/m^3	0.01	0.006	0.01	0.001 – 0.14	
	nitrogen half saturation for algae group 3/g	KHNg	g/m^3	0.01	0.02	0.01	0.001 – 0.14	
	nitrogen half saturation for macroalgae	KHNm	g/m^3	0.02			NA	
	phosphorus half saturation for algae group 1/c	KHPc	g/m^3	0.001		0.001	NA	
	phosphorus half saturation for algae group 1/d	KHPd	g/m^3	0.001	0.001	0.001	0.001 – 0.05	
	phosphorus half saturation for algae group 1/g	KHPg	g/m^3	0.001	0.001	0.001	0.001 – 0.05	
	phosphorus half saturation for macroalgae group	KHPm	g/m^3	0.002			NA	
	silica half saturation for algal group 2/d	KHS	g/m^3	0.035		0.035	NA	
	salinity at which Microsystis growth is halved	STOX	ppt?	1		1	NA	
	Card 9: constant parameters for algae							
	light extinction TSS	KeTSS	m^-1 per g/m^3	0.015		0	NA	
	light extinction total suspended chlorophyll	KeChl	m^-1 per mg/m^3	0.017		0.017	0.014 – .031	Cerco and Cole (1994)
	carbon to chlorophyll ratio for algae group 1/c	CChlc	g C per mg Chl	0.06		0.06	0.02 – 0.2	
	carbon to chlorophyll ratio for algae group 2/d	CChld	g C per mg Chl	0.05	0.07	0.05	0.02 – 0.2	
	carbon to chlorophyll ratio for algae group 3/g	CChlg	g C per mg Chl	0.1	0.07	0.1	0.02 – 0.2	
	carbon to chlorophyll ratio for macroalgae group 3/g	CChlm	g C per mg Chl	0.1			NA	
	depth of maximum algal growth for group 1/c	DOPTc	m	1		1		Cerco and Cole (1994)
	depth of maximum algal growth for group 2/d	DOPTd	m	1		1		
	depth of maximum algal growth for group 3/g	DOPTg	m	1		1		
	depth of maximum macroalgal growth	DOPTm	m	1				
	Card 10: constant parameters for algae							
	initial to at water surface	IO	langley/day	175		175		
	minimum optimum solar radiation	IsMIN	langley/day	40		40		
	fractional daylength	FD	fraction (0-1)	0.5		0.5		
	weighting factor for radiation at current day	Cla	fraction (Cla+Clb+Clc=1)	0.7		0.7		
	weighting factor for radiation at previous day	Clb	fraction (Cla+Clb+Clc=1)	0.2		0.2		
	weighting factor for radiation at 2 days before current day	Clc	fraction (Cla+Clb+Clc=1)	0.1		0.1		
	???	Cim	?	0.7				
	???	Rea	?	1				
	Card 11: constant parameters for algae							
	lower optimum temperature for algal growth for group 1/c	TMc1	degrees C	20		20		
	upper optimum temperature for algal growth for group 1/c	TMc2	degrees C	27		27		
	optimum temperature for algal growth for group 2/d	TMd1	degrees C	3		3		
	upper optimum temperature for algal growth for group 2/d	TMd2	degrees C	12		12		
	optimum temperature for algal growth for group 3/g	TMg1	degrees C	4		4		
	upper optimum temperature for algal growth for group 3/g	TMg2	degrees C	18		18		
	lower optimum temperature for macroalgal growth	TMm1	degrees C	14				
	upper optimum temperature for macroalgal growth	TMm2	degrees C	18				
	???	TMp1	degrees C	2				
	???	TMp2	degrees C	29				
	suboptimal temperature effect for algal growth for group 1/c	KTG1c	deg C ^-2	0.003		0.003		
	superoptimal temperature effect for algal growth for group 1/c	KTG2c	deg C ^-2	0.003		0.003		
	suboptimal temperature effect for algal growth for group 2/d	KTG1d	deg C ^-2	0.003		0.003		
	superoptimal temperature effect for algal growth for group 2/d	KTG2d	deg C ^-2	0.0005		0.0005		
	suboptimal temperature effect for algal growth for group 3/g	KTG1g	deg C ^-2	0.0015		0.0015		
	superoptimal temperature effect for algal growth for group 3/g	KTG2g	deg C ^-2	0.0004		0.0004		
	suboptimal temperature effect for macroalgal growth?	KTG1m	deg C ^-2	0.0007				

Appendix E. List of rates and constants used for water column parameters for the southern Puget Sound application of the EFDC model.

Input File	Description	Notation	Units	Chesapeake/Peconic parameters: model run spsm5/budd1run 2a. (based on model run spsm3 budd2run10)	LOTT Paramaters: approximate comparable parameters from LOTT's revised Budd Inlet model, Boatman, 1999	Value used in Peconic model (Tetra Tech, 1998)	Range of reported values [EPA 1985 or 1995 except where noted]
	superoptimal temperature effect for macroalgal growth?	KTG2m	deg C ^-2	0.003			
	???	KTG1p	deg C ^-2	0.05			
	???	KTG2p	deg C ^-2	0.0001			
	Card 12: constant parameters for algae						
	reference temperature for algal metabolism for group 1/c	TRc	deg C	20		20	
	reference temperature for algal metabolism for group 2/d	TRd	deg C	20		20	
	reference temperature for algal metabolism for group 3/g	TRg	deg C	20		20	
	reference temperature for macroalgae?	TRm	deg C	20			
	temperature efect for algal metabolism for group 1/c	KTBc	deg C ^-1	0.069		0.069	
	temperature efect for algal metabolism for group 2/d	KTBd	deg C ^-1	0.069		0.069	
	temperature efect for algal metabolism for group 3/g	KTBg	deg C ^-1	0.069		0.069	
	temperature efect for macroalga3 metabolism	KTBm	deg C ^-1	0.069			
	Card 13: constant parameters for carbon						
	carbon distribution coefficient for algal predation: refractory	FCRP	fcrp+fclp+fcdp=1	0.1		0.1	
	carbon distribution coefficient for algal predation: labile	FCLP	fcrp+fclp+fcdp=1	0.2		0.2	
	carbon distribution coefficient for algal predation: dissolved	FCDP	fcrp+fclp+fcdp=1	0.7		0.7	
	fraction of basal metabolism exuded as DOC at high DO, algal group 1/c	FCDc		0		0	
	fraction of basal metabolism exuded as DOC at high DO, algal group 2/d	FCDd		0		0	
	fraction of basal metabolism exuded as DOC at high DO, algal group 3/g	FCDg		0		0	
	half-saturation constant dissolved oxygen for algal DOC excretion, group 1/c	KHRc	g O /m^3	0.5		0.5	
	half-saturation constant dissolved oxygen for algal DOC excretion, group 2/d	KHRd	g O /m^3	0.5		0.5	
	half-saturation constant dissolved oxygen for algal DOC excretion, group 3/g	KHRb	g O /m^3	0.5		0.5	
	Card 13a: constant parameters for carbon, macroalgae						
	carbon distribution coefficient for macroalgal predation: refractory	FCRPm	fcrp+fclp+fcdp=1	0.3			
	carbon distribution coefficient for macroalgal predation: labile	FCLPm	fcrp+fclp+fcdp=1	0.5			
	carbon distribution coefficient for macroalgal predation: dissolved	FCDPm	fcrp+fclp+fcdp=1	0.1			
	fraction of basal metabolism exuded as DOC at high DO, macroalgae	FCDm		0			
	half-saturation constant dissolved oxygen for algal DOC excretion, macroalgae	KHRm	g O /m^3	0.5			
	Card 14: constant parameters for carbon						
	minimum dissolution rate of organic C: refractory	KRC	day^-1	0.01		0.01	
	minimum dissolution rate of organic C: labile	KLC	day^-1	0.09		0.09	
	minimum dissolution rate of organic C: dissolved	KDC	day^-1	0.04		0.04	
	constant relating dissolution rate to algae: refractory	KRCalg	day^-1 per g C m^-3	0		0	
	constant relating dissolution rate to algae: labile	KLCalg	day^-1 per g C m^-3	0		0	
	constant relating dissolution rate to algae: dissolved	KDCalg	day^-1 per g C m^-3	0		0	
	constant relating dissolution rate to macroalgae: dissolved?	KDCalgm	day^-1 per g C m^-3	0		0	
	Card 15: constant parameters for carbon and denitrification						
	reference temperature for hydrolysis	TRHDR	deg C	20		20	
	reference temperature for mineralization	TRMNL	deg C	20		20	
	temperature effect on hydrolysis	KTHDR	deg C ^-1	0.069		0.069	
	temperature effect on mineralization	KTMNL	deg C ^-1	0.069		0.069	
	half saturation constant of oxygen for oxic respiration	KHORDO	g O m^3	0.5	0.1	0.5	
	half saturation constant of nitrate required for denitrification	KHDNN	g N m^3	0.1		0.1	
	ratio of denitrification to oxic DOC respiration	AANOX	0 <= AANOX <= 1	0.5		0.5	
	Card 16: constant parameters for phosphorus, effect of algae						
	phosphorus distribution coefficients for algal predation: refractory	FPRP	fprp+fplp+fpdp+fpip=1	0.02		0.02	
	phosphorus distribution coefficients for algal predation: labile	FPLP	fprp+fplp+fpdp+fpip=1	0.13		0.13	
	phosphorus distribution coefficients for algal predation: dissolved	FPDP	fprp+fplp+fpdp+fpip=1	0.35		0.35	
	phosphorus distribution coefficients for algal predation: inorganic	FPIP	fprp+fplp+fpdp+fpip=1	0.5		0.5	
	phosphorus distribution coefficient of RPOP for algal metabolism, group 1/c	FPRc	FPRc+FPLc+FPDc+FPIc=1	0.02		0.02	

Appendix E. List of rates and constants used for water column parameters for the southern Puget Sound application of the EFDC model.

Input File	Description	Notation	Units	Chesapeake/Pec onic parameters: model run spsm5/ budd1run 2a. (based on model run spsm3 budd2run10)	LOTT Paramaters: approximate comparable parameters from LOTT's revised Budd Inlet model, Boatman, 1999	Value used in Peconic model (Tetra Tech, 1998)	Range of reported values [EPA 1985 or 1995 except where noted]
	phosphorus distribution coefficient of RPOP for algal metabolism, group 2/d	FPRd	FPRd+FPLd+FPDd+FPId=1	0.02		0.02	
	phosphorus distribution coefficient of RPOP for algal metabolism, group 3/g	FPRg	FPRg+FPLg+FPDg+FPlg=1	0.02		0.02	
	phosphorus distribution coefficient of LPOP for algal metabolism, group 1/c	FPLc	FPRc+FPLc+FPDc+FPlc=1	0.13		0.13	
	phosphorus distribution coefficient of LPOP for algal metabolism, group 2/d	FPLcl	FPRd+FPLd+FPDd+FPld=1	0.13		0.13	
	phosphorus distribution coefficient of LPOP for algal metabolism, group 3/b	FPLg	FPRg+FPLg+FPDg+FPlg=1	0.13		0.13	
	Card 16a: constant parameters for phosphorus, macroalgae						
	phosphorus distribution coefficients for macroalgae, refractory?	FPRPM	fprpm+fplpm+fpdpm+fpipm=1	0.3			
	phosphorus distribution coefficients for macroalgae, labile?	FPLPM	fprpm+fplpm+fpdpm+fpipm=1	0.3			
	phosphorus distribution coefficients for macroalgae, dissolved?	FPDPM	fprpm+fplpm+fpdpm+fpipm=1	0.2			
	phosphorus distribution coefficients for macroalgae, inorganic?	FPIPM	fprpm+fplpm+fpdpm+fpipm=1	0.2			
	phosphorus distribution coefficient of RPOP for macroalgae metabolism?	FPRm	FPRm+FPLm+FPDm+FPIm=1	0.1			
	phosphorus distribution coefficient of LPOP for macroalgae metabolism?	FPLm	FPRm+FPLm+FPDm+FPlm=1	0.1			
	coefficient to modify phosphorus-to-carbon (APC) ratio for macroalgae	APCM	?	0.5			
	Card 17: constant parameters for phosphorus, effect of algae						
	phosphorus distribution coefficient of DOP for algal metabolism, group 1/c	FPDc	FPRc+FPLc+FPDc+FPIc=1	0.35		0.35	
	phosphorus distribution coefficient of DOP for algal metabolism, group 2/d	FPDd	FPRd+FPLd+FPDd+FPId=1	0.35		0.35	
	phosphorus distribution coefficient of DOP for algal metabolism, group 3/g	FPDg	FPRg+FPLg+FPDg+FPlg=1	0.35		0.35	
	phosphorus distribution coefficient of DOP for macroalgae	FPDm	FPRm+FPLm+FPDm+FPlm=1	0.6			
	phosphorus distribution coefficient of PO4T for algal metabolism, group 1/c	FPIc	FPRO+FPLc+FPDc+FPlc=t	0.5		0.5	
	phosphorus distribution coefficient of PO4T for algal metabolism, group 2/d	FPId	FPRd+FPLd+FPDd+FPId=1	0.5		0.5	
	phosphorus distribution coefficient of PO4T for algal metabolism, group 3/g	FPIg	FPRg+FPLg+FPDg+FPlg=1	0.5		0.5	
	phosphorus distribution coefficient of PO4T for macroalgae	FPIm	FPRm+FPLm+FPDm+FPlm=1	0.2			
	coefficient relating PO4 sorption to TSS (per g m^-3) or TAM (per mol m^-3)	KPO4p	per g m^-3 or per mol m^-3	0.04		0.04	
	Card 18: constant parameters for phosphorus: hydrolysis of organic P and algal P/C ratio						
	minimum hydrolysis rate of organic P: refractory	KRP	day^-1	0.01		0.01	
	minimum hydrolysis rate of organic P: labile	KLP	day^-1	0.085		0.085	
	minimum hydrolysis rate of organic P: dissolved	KDP	day^-1	0.1		0.1	
	constant relating hydrolysis rate to algae: refractory	KRPalg	day^-1 per g C m^-3	0		0	
	constant relating hydrolysis rate to algae: labile	KLPalg	day^-1 per g C m^-3	0		0	
	constant relating hydrolysis rate to algae: dissolved	KDPalg	day^-1 per g C m^-3	0.5		0.5	
	minimum carbon-to-phosphorus ratio to calculate APC	CPprm1	g C per g P	42		42	
	difference between min and max carbon-to-phosphorus ratio for APC	CPprm2	g C per g P	85		85	
	effect of dissolved phosphate on carbon-to-phosphorus ratio for APC	CPprm3	per g P m^-3	200		200	
	Card 19: constant parameters for nitrogen, effect of algae						
	nitrogen distribution coefficients for algal predation: refractory	FNRP	fnrp+fnlp+fndp+fnip=1	0.1		0.1	
	nitrogen distribution coefficients for algal predation: labile	FNLP	fnrp+fnlp+fndp+fnip=1	0.3		0.3	
	nitrogen distribution coefficients for algal predation: dissolved	FNDP	fnrp+fnlp+fndp+fnip=1	0.25		0.25	
	nitrogen distribution coefficients for algal predation: inorganic	FNIP	fnrp+fnlp+fndp+fnip=1	0.35		0.35	
	nitrogen distribution coefficient of RPON for algal metabolism, group 1/c	FNRc	FNRc+FNLc+FNDc+FNlc=1	0.1		0.1	
	nitrogen distribution coefficient of RIPON for algal metabolism, group 2/d	FNRd	FNRd+FNLd+FNDd+FNId=1	0.1		0.1	
	nitrogen distribution coefficient of RPON for algal metabolism, group 3/g	FNRg	FNRg+FNLg+FNDg+FNlg=1	0.1		0.1	
	nitrogen distribution coefficient of LPON for algal metabolism, group 1/c	FNLc	FNRc+FNLc+FNDc+FNlc=1	0.3		0.3	
	nitrogen distribution coefficient of LPON for algal metabolism, group 2/d	FNLd	FNRd+FNLd+FNDd+FNld=1	0.3		0.3	
	nitrogen distribution coefficient of LPON for algal metabolism, group 3/g	FNLg	FNRg+FNLg+FNDg+FNlg=1	0.3		0.3	
	Card 19a: constant parameters for nitrogen, macroalgae						
	nitrogen distribution coefficients for macroalgae, refractory?	FNRPM	fnrpm+fnlpm+fndpm+fnipm=1	0.4			
	nitrogen distribution coefficients for macroalgae, labile?	FNLPM	fnrpm+fnlpm+fndpm+fnipm=1	0.5			
	nitrogen distribution coefficients for macroalgae, dissolved?	FNDPM	fnrpm+fnlpm+fndpm+fnipm=1	0.1			
	nitrogen distribution coefficients for macroalgae, inorganic?	FNIPM	fnrpm+fnlpm+fndpm+fnipm=1	0			
	nitrogen distribution coefficient of RPON for macroalgae metabolism?	FNRm	FNRm+FNLm+FNDm+FNlm=1	0.2			
	nitrogen distribution coefficient of LPON for macroalgae metabolism?	FNLm	FNRm+FNLm+FNDm+FNIm=1	0.4			

Appendix E. List of rates and constants used for water column parameters for the southern Puget Sound application of the EFDC model.

Input File	Description	Notation	Units	Chesapeake/Peconic parameters: model run spsm5/budd1run 2a. (based on model run spsm3 budd2run10)	LOTT Paramaters: approximate comparable parameters from LOTT's revised Budd Inlet model, Boatman, 1999	Value used in Peconic model (Tetra Tech, 1998)	Range of reported values [EPA 1985 or 1995 except where noted]
Card 20: constant parameters for nitrogen, effect of algae							
	nitrogen distribution coefficient of DON for algal metabolism, group 1/c	FNDc	FNRc+FNLc+FNDc+FNlc=1	0.25		0.25	
	nitrogen distribution coefficient of DON for algal metabolism, group 2/d	FNDd	FNRd+FNLd+FNDd+FNld=1	0.25		0.25	
	nitrogen distribution coefficient of DOn for algal metabolism, group 3/g	FNDg	FNRg+FNLg+FNDg+FNlg=1	0.25		0.25	
	nitrogen distribution coefficient of DON for macroalgae	FNDm	FNRm+FNLm+FNDm+FNlm=1	0.2		0	
	nitrogen distribution coefficient of NH4 for algal metabolism, group 1/c	FNIc	FNRc+FNLc+FNDc+FNlc=1	0.35		0.35	
	nitrogen distribution coefficient of NH4 for algal metabolism, group 2/d	FNId	FNRd+FNLd+FNDd+FNId=1	0.35		0.35	
	nitrogen distribution coefficient of NH4 for algal metabolism, group 3/g	FNIg	FNRg+FNLg+FNDg+FNlg=1	0.35		0.35	
	nitrogen distribution coefficient of NH4 for macroalgae	FNIm	FNRm+FNLm+FNDm+FNlm=1	0.2			
	nitrogen-to-carbon ratio for algal group 1/c	ANCc	g N per g C	0.167		0.167	
	nitrogen-to-carbon ratio for algal group 2/d	ANCd	g N per g C	0.176		0.176	
	nitrogen-to-carbon ratio for algal group 3/g	ANCg	g N per g C	0.176		0.176	
	nitrogen-to-carbon ratio for macroalgae	ANCm	g N per g C	0.176			
Card 21: constant parameters for nitrogen, nitrification							
	mass NO3 reduced per DOC oxidized	ANDC	g N per g C	0.933		0.933	
	maximum nitrification rate	rNitM	g N m^-3 day^-1	0.05		0.05	
	nitrification half saturation for dissolved oxygen	KHNitDO	g O2 m^-3	1		1	
	nitrification half saturation for ammonium	KHNitN	g N m^-3	1		1	
	optimum temperature for nitrification	TNit	degrees C	20		20	
	sub-optimum temperature effect on nitrification	Knit1	degrees C ^-2	0.0045		0.0045	
	super-optimum temperature effect on nitrification	KNit2	degrees C ^-2	0.0045		0.0045	
Card 22: constant parameters for nitrogen, hydrolysis/mineralization of organic N							
	minimum hydrolysis rate of organic nitrogen: refractory	KRN	day^-1	0.005		0.005	
	minimum hydrolysis rate of organic nitrogen: labile	KLN	day^-1	0.075	0.075	0.075	
	minimum mineralization rate of organic nitrogen: dissolved	KDN	day^-1	0.02	0.025	0.02	
	constant relating hydrolysis rate to algae: refractory	KRNalg	day^-l per g C m^-3	0		0	
	constant relating hydrolysis rate to algae: labile	KLNalg	day^-l per g C m^-3	0		0	
	constant relating mineralization rate to algae: refractory	KDNalg	day^-1 per g C m^-3	0		0	
Card 23: constant parameters for silica							
	silica distribution for diatom predation	FSPP	FSPP+FSIP=1	1		1	
	silica distribution for diatom predation	FSIP	FSPP+FSIP=1	0		0	
	silica distribution for diatom metabolism	FSPd	FSPd+FSld=1	1		1	
	silica distribution for diatom metabolism	FSId	FSPd+FSld=1	0		0	
	silica-to-carbon ratio in diatoms	ASCd	g Si per g C	0.36		0.36	
	partition coefficient for sorbed/dissolved silica	KSAp		0.16		0.16	
	dissolution rate for PSi	KSU	day^-1	0.05		0.05	
	reference temperature for PSi dissolution	TRSUA	degrees C	20		20	
	temperature effect on PSi dissolution	KTSUA	deg C^-1	0.092		0.092	
Card 24: constant parameters for COD and DO							
	DO-to-carbon ratio in respiration	AOCR	g O2 per g C	2.67		2.67	
	mass DO consumed per NH4 nitrified	AONT	g O2 per g N	4.33		4.33	
	constant of proportionality for DO-reaeration (mks) (kro=3.933?)	KRO		3.933		3.933	
	temperature effect on DO-reaeration	KTR		1.024		1.024	
	half-saturation constant of DO for COD	KHCOD	g O2 m^-3	1.5		1.5	
	oxidation rate of COD at TRCOD	KCD	day^-l	20		20	
	reference temperature for COD oxidation	TRCOD	degrees C	20		20	
	temperature effect on COD oxidation	KTCOD	deg C^-1	0.041		0.041	
Card 25: constant parameters for total active mental and fecal coliform bacteria							
	DO where TAM release is one-half anoxic release	KHbmf	g O2 m^-3	0.5		0.5	
	anoxic release of TAM	BFTAM	mol m^-2 day^-1	0.1		0.1	
	reference temperature for TAM release	Ttam	deg C	20		20	

Appendix E. List of rates and constants used for water column parameters for the southern Puget Sound application of the EFDC model.

Input File	Description	Notation	Units	Chesapeake/Peconic parameters: model run spsm5/budd1run 2a. (based on model run spsm3 budd2run10)	LOTT Paramaters: approximate comparable parameters from LOTT's revised Budd Inlet model, Boatman, 1999	Value used in Peconic model (Tetra Tech, 1998)	Range of reported values [EPA 1985 or 1995 except where noted]	
	temperature effect on TAM release	Ktam	deg C^-1	0.2		0.2		
	TAM solubility at anoxic conditions	TAMdmx	mol m^-3	0.015		0.015		
	constant relating TAM solubility to DO	Kdotam	per g O2 m^-3	1		1		
	fecal coliform die-off rate at 20 degrees C	KFCB	day^-1	0.5		2.5		
	temperate effect on fecal coliform die-off	TFCB	deg C^-1	1.07		1.07		
	Card 40: spatially/temporally constant algal parameters day^-1 except Keb m^-1)							
	maximum algal growth rate for algae group 1/c	PMc	day^-1	2.5		3.4		
	maximum algal growth rate for algae group 2/d	PMd	day^-1	2.5	4	2.8	0.2 - 5.0	
	maximum algal growth rate for algae group 3/g	PMg	day^-1	2.5	1.2	3.0	0.2 - 5.0	
	maximum macroalgal growth rate	PMm	day^-1	2.0				
	basal metabolism rate for algae group 1/c	BMRc	day^-1	0.05		0.05		
	basal metabolism rate for algae group 2/d	BMRd	day^-1	0.05	0.25	0.05	0.02 - 0.36	Cerco and Cole (1994)
	basal metabolism rate for algae group 3/g	BMRg	day^-1	0.06	0.25	0.06	0.02 - 0.36	Cerco and Cole (1994)
	basal metabolism rate for macroalgae	BMRm	day^-1	0.1				
	predation rate for algae group 1/c	PRRc	day^-1	0.25		0.25	0.01 - 1	
	predation rate for algae group 2/d	PRRd	day^-1	0.25	0.21	0.25	0.01 - 1	Cerco and Cole (1994)
	predation rate for algae group 3/g	PRRg	day^-1	0.28	0.12	0.28	0.01 - 1	Cerco and Cole (1994)
	predation rate for macroalgae	PRRm	day^-1	0.33				
	background light extinction coefficient	Keb	m^-1	0.51		1		
	?	WOSDcoef	day^-1	1.7				
	Card 41: spatially/temporally constant settling velocities (m/d)							
	settling rate for algae group 1/c	WSc		0.15		0.15	0.02 -4.0	
	settling rate for algae group 2/d	WSd		0.35	0.5	0.35		
	settling rate for algae group 3/g	WSg		0.25	0.25	0.25		
	settling rate for refractory particulate organic matter	WSrp		1.5		1.5	0.5 - 1.5	Cerco and Cole (1994)
	settling rate for labile particulate organic matter	WSlp		1.5	0.5	1.5	0.5- 1.5	Cerco and Cole (1994)
	settling rate for particulate metal	WSs		0.5		0.5	0.5 - 1.5	Cerco and Cole (1994)
	?	WSM		0				
	Card 41+: constant benthic flux (g/m2/d)							
		PO4		0		0.002		
		NH4		0		0.02		
		NO3		0		0.004		
		SA		0		0.048		
		COD		0		2		
		DO		0		-1.75		
	Card 41+: constant atmospheric deposition (g/m2/d, MPN/m2/d)							
	based on typical atmospheric deposition to Puget Sound	DSQ	?	0.000				
	in Embrey and Inkpen 1997	Bc	g C/m2/d	0.000				
	total N = 0.001 to 0.002 g/m2/d	Bd	g C/m2/d	0.000				
	total P = 0.0001 to 0.0002 g/m2/d	Bg	g C/m2/d	0.000				
	total C assumed to be 10X total N	RPOC	g C/m2/d	0.005				
	evenly split C, N, and P to various forms	LPOC	g C/m2/d	0.005				
		DOC	g C/m2/d	0.005				
		RPOP	g P/m2/d	0.0000375				
		LPOP	g P/m2/d	0.0000375				
		DOP	g P/m2/d	0.0000375				
		PO4t	g P/m2/d	0.0000375				
		RPON	g N/m2/d	0.0003				
		LPON	g N/m2/d	0.0003				
		DON	g N/m2/d	0.0003				
		NH4	g N/m2/d	0.0003				
		NO3	g N/m2/d	0.0003				

Appendix E. List of rates and constants used for water column parameters for the southern Puget Sound application of the EFDC model.

Input File	Description	Notation	Units	Chesapeake/Peconic parameters: model run spsm5/budd1run 2a. (based on model run spsm3 budd2run10)	LOTT Paramaters: approximate comparable parameters from LOTT's revised Budd Inlet model, Boatman, 1999	Value used in Peconic model (Tetra Tech, 1998)	Range of reported values [EPA 1985 or 1995 except where noted]
		SU	g Si/m2/d	0.000			
		SA	g Si/m2/d	0.000			
		COD	g/m2/d	0.000			
		DO	g/m2/d	0.000			
		TAM	g/m2/d	0.000			
		FCB	MPN/m2/d	0.000			
	Card 41+: constant wet atmospheric deposition (mg/L, MPN/L)						
		Bc	mg/L as C	0.000			
		Bd	mg/L as C	0.000			
		Bg	mg/L as C	0.000			
		RPOC	mg/L as C	0.000			
		LPOC	mg/L as C	0.000			
		DOC	mg/L as C	0.000			
		RPOP	mg/L as P	0.000			
		LPOP	mg/L as P	0.000			
		DOP	mg/L as P	0.000			
		PO4t	mg/L as P	0.000			
		RPON	mg/L as N	0.000			
		LPON	mg/L as N	0.000			
		DON	mg/L as N	0.000			
		NH4	mg/L as N	0.000			
		NO3	mg/L as N	0.000			
		SU	mg/L as Si	0.000			
		SA	mg/L as Si	0.000			
		COD	mg/L	0.000			
		DO	mg/L	0.000			
		TAM	mg/L	0.000			
		FCB	MPN/L	0.000			
wq3dsd.inp	**also see spsm4_rates_and oonstants.xlstsed**						
	Card 18: factor to enhance magnitude of sediment oxygen demand	SODmult	unitless	1			
wqpsl.inp	RMULADJ (factor to increase magnitude of loads for sensitivity analysis)	RMULADJ		1			
efdc.inp	tidal amplitude						

Appendix E. List of rates and constants for the sediment model, input file WQ3DSD.INP

Description	Notation	Units	Parameter values used for spsm4 and spsm5 model runs
Card 1: program control switches			
number of zones for spatially varying parameters IN SPM	iSMZ		1
ICs constant (iICl=0), or from wqsdici.inp (iICI=1) or wqsdrst.inp (iICI=2)	iIcl		0
write spatial distributions to restart file wqsdrst.out (iRST=1)	iRST		1
activate hysteresis in benthic mixing (iHyst=1)	iHyst		1
activate diagnostic output for FUNC ZBRENT (zbrent.log)	iZB		1
this global SODmult factor is no longer used, see Card 18	sodmult		1
Card 2: program control parameters			
Number of time series output locations, ISMTS should be <= NWQTS	ISMTS		20
Begin writing output time-series data on this day	TSMTSB	day	0
End writing output time-series data on this day	TSMTSE	day	1000
Write to output time-series file at this interval	SMTSDT	hour	12
Activate binary output file of benthic flux rates (isSDBIN > O)	isSDBIN		0
Card 3: locations of output cells (number of locations should equal ISMTS)			
Card 4:			
Diffusion coefficient for sediment temperature	DifT	m^2/sec	1.80E-07
Card 5: spatially constant parameters to split depositional fluxes to Gi classes			
fraction of PON from Cyanobacteria routed to G1 class	FNBci	fnbcl+fnbc2+fnbc3=1	0.65
fraction of PON from Cyanobacteria routed to G2 class	FNBc2		0.28
fraction of PON from Cyanobacteria routed to G3 class	FNBc3		0.07
fraction of PON from diatom algae group routed to G1 class	FNBdt	fnbdi+fnbd2+fnbd3=1	0.65
fraction of PON from diatom algae group routed to G2 class	FNBd2		0.28
fraction of PON from diatom algae group routed to G3 class	FNBd3		0.07
fraction of PON from green algae group routed to G1 class	FNBgi	fnbgt+fnbg2+fnbg3=1	0.65
fraction of PON from green algae group routed to G2 class	FNBg2		0.28
fraction of PON from green algae group routed to G3 class	FNBg3		0.07
Card 6:			
fraction of POP from Cyanobacteria routed to G1 class	•FPBci	fpbci+fpbc2+fpbc3=1	0.65
fraction of POP from Cyanobacteria routed to G2 class	FPBc2		0.255
fraction of POP from Cyanobacteria routed to G3 class	FPBc3		0.095
fraction of POP from diatom algae group routed to G1 class	,FPBdt	fpbdl+fpbd2+fpbd3=1	0.65
fraction of POP from diatom algae group routed to G2 class	FPBd2		0.255
fraction of POP from diatom algae group routed to G3 class	FPBd3		0.095
fraction of POP from green algae group routed to G1 class	FPBg1	fpbgi+fpbg2+fpbg3=1	0.65
fraction of POP from green algae group routed to G2 class	FPBg2		0.255
fraction of POP from green algae group routed to G3 class	FPBg3		0.095
Card 7:			
fraction of POC from Cyanobacteria routed to G1 class	FCBci	fcbcl+fcbc2+fcbc3=1	0.65
fraction of POC from Cyanobacteria routed to G2 class	FCBc2		0.255
fraction of POC from Cyanobacteria routed to G3 class	FCBc3		0.095
fraction of POC from diatom algae group routed to GI class	FCBd1	fcbdi+fcbd2+fcbd3=1	0.65
fraction of POC from diatom algae group routed to G2 class	FCBd2		0.255
fraction of POC from diatom algae group routed to G3 class	FCBd3		0.095
fraction of POC from green algae group routed to GI class	FCBgI	fcbgi+fcbg2+fcbg3=1	0.65
fraction of POC from green algae group routed to G2 class	FCBg2		0.255
fraction of POC from green algae group routed to G3 class	FCBg3		0.095
Card 8: spatially constant parameters for diagenesis			
Decay rate of PON at 20oC in Layer 2 for G1 class	KPON1	1/day	0.035
Decay rate of PON at 20oC in Layer 2 for G2 class	KPON2	1/day	0.0018
Decay rate of PON at 20oC in Layer 2 for G3 class	KPON3	1/day	0
Decay rate of POP at 20oC in Layer 2 for G1 class	KPOPi	1/day	0.035
Decay rate of POP at 20oC in Layer 2 for G2 class	KPOP2	1/day	0.0018
Decay rate of POP at 20oC in Layer 2 for G3 class	KPOP3	1/day	0
Decay rate of POC at 20oC in Layer 2 for G1 class	KPOC1	1/day	0.035
Decay rate of POC at 20oC in Layer 2 for G2 class	KPOC2	1/day	0.0018
Decay rate of POC at 20oC in Layer 2 for G3 class	KPOC3	1/day	0
Card 9:			
Constant for temperature adjustment for KPON1	ThKNi	unitless	1.1
Constant for temperature adjustment for KPON2	ThKN2	unitless	1.15
Constant for temperature adjustment for KPON3	ThKN3	unitless	1
Constant for temperature adjustment for KPOP1	ThKPi	unitless	1.1
Constant for temperature adjustment for KPOP2	ThKP2	unitless	1.15
Constant for temperature adjustment for KPOP3	ThKP3	unitless	1
Constant for temperature adjustment for KPOC1	ThKCt	unitless	1.1
Constant for temperature adjustment for KPOC2	ThKC2	unitless	1.15
Constant for temperature adjustment for KPOC3	ThKC3	unitless	1
Card 10: spatially constant parameters common to sediment flux			
Solid concentrations in Layer 1	rMl	Kg/L	0.5
Solid concentrations in Layer 2	rM2	Kg/L	0.5
Constant for temperature adjustment for Dd	ThDd	unitless	1.08
Constant for temperature adjustment for Dp	ThDp	unitless	1.117
Reference concentration for GPOC(1)	GPOCr	gC/m3	100
Particle mixing half-saturation constant for oxygen	KMDp	mg/L	4
First-order decay rate for accumulated benthic stress	KST	1/day	0.03
Minimum diffusion coefficient for particle mixing	DpMIN	m^2/d	3.00E-06
Ratio of bio-irrigation to bioturbation	RBIBT	unitless	0

Description	Notation	Units	Parameter values used for spsm4 and spsm5 model runs
Card 11			
Critical overlying oxygen cone. below which benthic hysteresis occurs	02BSc	mg/L	3
Time duration for which the maximum or minimum stress is retained	TDMBS	days	90
Critical hypoxia duration; if less than this value, no hysteresis occurs	TCMBS	days	7
Card 12: Spatially constant parameters for NH4, NO3, and PO4 flux			
Partition coefficient, ratio of particulate to dissolved NH4 in layer 1	P1NH4	L/Kg	1
Partition coefficient, ratio of particulate to dissolved NH4 in layer 2	P2NH4	LKg	1
Nitrification half-saturation constant for ammonium	KMNH4	gN/m^3	1.5
Nitrification half-saturation constant for dissolved oxygen	KMNH4O2	gO2/m^3	1
Constant for temperature adjustment for KNH4	ThNH4	unitless	1.08
Constant for temperature adjustment for KNO31 and KNO32	ThNO3	unitless	1.08
Partition coefficient, ratio of particulate to dissolved PO4 in layer 2	P2PO4	L/Kg	100
Critical dissolved oxygen for PO4 sorption	DOcPO4	mg/L	2
Card 13: Spatially constant parameters for H2S/CH4 flux and SOD			
Partition coefficient for H2S in Layer 1	P1H2S	UKg	100
Partition coefficient for H2S in Layer 1	P2H2S	UKg	100
Reaction velocity for dissolved sulfide oxidation in Layer 1 at 20 degC	KH2Sd1	m/day	0.2
Reaction velocity for particulate sulfide oxidation in Layer 1 at 20 degC	KH2Sp1	m/day	0.4
Constant for temperature adjustment for KH2Sd1 and KH2Sp1	ThH2S	unitless	1.08
Constant to normalize the sulfide oxidation rate for oxygen	KMH2S	mg O2/L	4
Reaction velocity for methane oxidation in layer 1 at 20 degC	KCH4	m/day	0.2
Constant for temperature adjustment for KCH4	ThCH4	unitless	1.08
Critical salinity; below this value CH4 is produced, above H2S is produced	cSHSCH	g/L	1
Card 14			
Stoichiometric coefficient for carbon diagenesis consumed by H2S oxidation	aO2C	gO2/gC	2.66667
Stoichiometric coefficient for carbon diagenesis consumed by denitritrification	aO2NO3	gO2/gN	2.85714
Stoichiometric coefficient for carbon diagenesis consumed by nitrification	aO2NH4	gO2/gN	4.33
Card15: spatially constant parameters for silica			
First order dissolution rate for particulate biogenic silica (PSi) at 20 degC in layer 2	KSi	1/day	0.5
Constant for temperature adjustment of KSi	ThSi		1.1
Silica dissolution half-saturation constant for PSi	KMPSi	g Si/m^3	5.00E+04
Saturation concentration of silica in pore water	SiSat	g Si/m^3	40
Partition coefficient for Si in Layer 2, controls sorption of dissolved silica to solids	P2Si	L/Kg	100
factor that enhances sorption of silica in layer 1 when DO exceeds DOcSi	DP1 Si	unitless	10
Critical dissolved oxygen for silica sorption in layer 1	DOcSi	mg/L	1
Detrital flux of particulate biogenic silica from sources other than diatom algae	DetFPSi	gSi/m^2/d	0.1
Card 16: spatially constant ICs			
Cone. Particulate Org. Nitrogen in G-class 1	CPON1	g/m3	50
Cone. Particulate Org. Nitrogen in G-class 2	CPON2	g/m3	150
Cone. Particulate Org. Nitrogen in G-class 3	CPON3	g/m3	250
Cone. Particulate Org. Phosphorus in G-class 1	CPOP1	g/m3	20
Cone. Particulate Org. Phosphorus in G-class 2	CPOP2	g/m3	100
Cone. Particulate Org. Phosphorus in G-class 3	CPOP3	g/m3	150
Conc. Particulate Org. Carbon in G-class 1	CPOC1	g/m3	1000
Conc. Particulate Org. Carbon in G-class 2	CPOC2	g/m3	3000
Conc. Particulate Org. Carbon in G-class 3	CPOC3	g/m3	5000
Card 17: spatially constant ICs			
Conc. NH4-N in layer 1	C1NH4	g/m3	2
Conc. NH4-N in layer 2	C2NH4	g/m3	4
Conc. NO3-N in layer 2	C2NO3	g/m3	1
Conc. PO4-P in layer 2	C2PO4	g/m3	250
Conc. Sulfide (H2S) in layer 2	C2H2S	g/m3	250
Conc. Particulate biogenic silica in layer 2	CPSi	g/m3	5000
Conc. Dissolved available silica in layer 2	C2Si	g/m3	500
Initial accumulated benthic stress	CBSt	days	20
Initial sediment temperature	GT	degC	20
Card 18: spatially varying parameters: physical and rate velocity			
zone for spatially variable parameters IN SPM	ISMz		1
Layer 1 sediment thickness	Hsed	meters	0.1
sediment burial rate	W2	cm/year	0.5
diffusion coefficient in pore water	Dd	m2/day	0.001
apparent diffusion coefficient for particle mixing	Dp	m2/day	1.20E-04
optimal reaction velocity for nitrification at 20 degC	KNH4	m/day	0.14
reaction velocity for denitrification in layer 1 at 20 degC	KNO31	m/day	0.125
reaction velocity for denitrification in layer 2 at 20 degC	KNO32	m/day	0.25
factor to enhance sorption of PO4 in layer 1 when DO is greater than DOcPO4	DP1PO4	unitless	300
factor to enhance magnitude of sediment oxygen demand	SODmult	unitless	1
Card 19: spatially varying parameters: distribution coefficients for RPOM			
zone for spatially variable parameters IN SPM	ISMz		1
fraction of water column refractory PON routed to G-class 1	FNRPi	fnrpl+fnrp2+fnrp3=1	0
fraction of water column refractory PON routed to G-class 2	FNRP2		0.82
fraction of water column refractory PON routed to G-class 3	FNRP3		0.18
fraction of water column refractory POP routed to G-class 1	FPRPi	fprpl+fprp2+fprp3=1	0
fraction of water column refractory POP routed to G-class 2	FPRP2		0.73
fraction of water column refractory POP routed to G-class 3	FPRP3		0.27
fraction of water column refractory POC routed to G-class 1	FCRPi	fcrpl+fcrp2+fcrp3=1	0
fraction of water column refractory POC routed to G-class 2	FCRP2		0.73
fraction of water column refractory POC routed to G-class 3	FCRP3		0.27